Addressing the complexity of Notch-induced cancer

Molecular mechanisms of the microRNA miR-7 and the BTB-transcription factor Pipsqueak

Memoria de tesis presentada por
Irene Gutiérrez Pérez

Thesis Director:
María Domínguez Castellano, PhD

CSIC
Consejo Superior de Investigaciones Científicas
UNIVERSITAS Miguel Hernández
INSTITUTO DE NEUROCIENCIAS

UNIVERSITAS
Miguel
Hernández

INSTITUTO DE NEUROCIENCIAS

Consejo Superior de Investigaciones Científicas
Universidad Miguel Hernández
Instituto de Neurociencias

Prof. Juan Lerma
Director

A QUIEN CORRESPONDA:

Prof. Juan Lerma Gómez, Director del Instituto de Neurociencias, centro mixto de la Universidad Miguel Hernández (UMH) y el Consejo Superior de Investigaciones Científicas,

CERTIFICA:

Que la Tesis Doctoral titulada "Addressing the complexity of Noch-induced cancer. Molecular Mechanisms of the microRNAmiR-7 and the BTB-transcription factor Pipsqueak" ha sido realizada por Doña Irene Gutiérrez Pérez (NIF 48621177M) bajo la dirección de la Prof.ª. María Domínguez Castellano y da su conformidad para que sea presentada a la Comisión de Doctorado de la Universidad Miguel Hernández.

Para que así conste a los efectos oportunos, firma el presente certificado en San Juan de Alicante a 18 de mayo de 2015

Juan Lerma
Director

direccion.in@umhc.es
director.in@umh.es
www.ina.umh.es

Tel: +34 965-919221(d)
+34 965-919220 (s)
Fax: +34 965 919561

Av Ramón y Cajal s/n
Campus de San Juan
03550 SAN JUAN DE ALICANTE– ESPAÑA

UNIVERSITAS
Miguel
Hernández

Consejo Superior de Investigaciones Científicas
Universidad Miguel Hernández
Instituto de Neurociencias

María Domínguez Castellano
Profesora de Investigación del CSIC

INSTITUTO DE NEUROCIENCIAS

D.ª María Domínguez Castellano, Profesora de Investigación del Consejo Superior de Investigaciones Científicas, en el Instituto de Neurociencias de Alicante, centro mixto CSIC-UMH,

AUTORIZA la presentación de la Tesis Doctoral titulada: "Addressing the complexity of Notch-induced cancer. Molecular mechanisms of the microRNA miR-7 and the BTB-transcription factor Pipsqueak", realizada por D.ª Irene Gutiérrez Pérez con DNI 48621177M, bajo mi inmediata dirección y supervisión en el Instituto de Neurociencias (CSIC-UMH) y que presenta para la obtención del grado de Doctor Internacional por la Universidad Miguel Hernández.

Y para que conste, y a los efectos oportunos, firma el presente Certificado en San Juan de Alicante, a cuatro de Junio de dos mil quince.

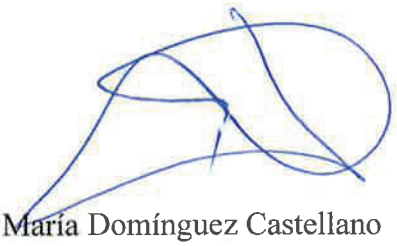

Fdo.: María Domínguez Castellano

m.dominguez@umh.es
www.ina.umh.es

Tel : +34 965 919346

Av Ramón y Cajal, s/n
03550 SAN JUAN DE ALICANTE – ESPAÑA

UNIVERSITAS
Miguel
Hernández

AGRADECIMIENTOS

UNIVERSITAS
Miguel
Hernández

A MIS PADRES

UNIVERSITAS
Miguel
Hernández

Por fin ha llegado el día. Nunca hubiera podido imaginar que iba a ser una larga carrera de fondo de la que salgo reforzada y acompañada de gente maravillosa sin la que no podría haberlo conseguido.

En primer lugar me gustaría darles las gracias a mis padres. Siempre os estaré profundamente agradecida por vuestra abnegada dedicación, por apoyarme y por hacer todo lo posible para darme la mejor educación y formación. Estoy muy orgullosa de tener a mi lado a unos padres como vosotros, os quiero. Quiero dar también las gracias a toda mi familia por su apoyo, echando de menos a una persona muy importante para mí y que seguro está muy orgullosa esté donde esté. Gracias a mis amigas Anna, Mariola y Laura por estar siempre ahí a pesar del tiempo y la distancia y a mis compañeras de baile por ayudarme a terminar el día con una sonrisa.

Por otro lado, me gustaría agradecerle a mi directora de tesis, María Domínguez, la oportunidad que me dio al elegirme a mí para disfrutar de una beca FPI y el proyecto que me asignó. Gracias por darme la libertad necesaria para desarrollarme y crecer a nivel profesional. Ha resultado ser un proyecto multidisciplinar con el que no sólo he adquirido una completa formación, sino que además me ha dado la oportunidad de viajar y conocer a gente extraordinaria:

-The laboratory of Professor Tilman Borggrefe in Giessen is full of wonderful people and brilliant scientists who made me fully enjoy my stay in Germany.

-The laboratory of Arts & Sciences Distinguished Professor Victor Corces gave me the opportunity to learn directly from a leading scientist as well as a great person and his amazing research group. I have no words to express my gratitude to them for their help.

Dentro del laboratorio he encontrado una segunda familia, no sólo por las horas que pasamos juntos. Compañeros siempre dispuestos a ayudarme y facilitarme mucho el trabajo. Por ello, les estoy muy agradecida en general a TODOS. Y en especial:

Me gustaría hacer mención primero a aquellos que se fueron del laboratorio y sin los que no podría haber llegado hasta aquí: Andrés, gracias por tu apoyo y paciencia para enseñarme todo lo que sé del trabajo con *Drosophila*, no olvidándome de mi tocaya de nombre y apellido Irene Gutiérrez, Dolors y Gabriela. Gracias Vanina por incluirme en un proyecto del que he aprendido no solo nuevas técnicas, sino también lo que realmente significa hacer ciencia. Muchísimas gracias Vero por enseñarme, ayudarme, apoyarme y por los buenos momentos dentro y fuera del laboratorio que, por otro lado, sin Zeus no habrían sido lo mismo. Mil gracias Alisson por contagiarme tu ilusión por la ciencia. Almudena, gracias simplemente por ser tú, esa magnífica persona que eres. Esther B., estoy muy orgullosa de tener como compañera y amiga a una persona y profesional tan extraordinaria como tú. Espero que a la rubia y a la morena les queden muchas más sevillanas por bailar juntas. Dianilla, muchas gracias por ayudarme en todo lo que he necesitado y por mostrarme un ejemplo de esfuerzo y dedicación, acompañado de una profesionalidad y discreción envidiables. Esther C., te debo mucho por darme la oportunidad de participar en las prácticas de la universidad y por ofrecerte a ayudarme en todo lo que he necesitado a pesar de tu apretadísima agenda. Vales muchísimo y ojalá te den mil premios más. Sergio y Nahuel, gracias por alegrarnos la vida todos los días. De Sergio voy a poder disfrutar un poco más en el laboratorio, pero a ti Nahuel te vamos a echar mucho de menos. Gracias por haberme ayudado tanto y por dejarnos disfrutar de tus asados

argentinos. Gracias Tobi por ayudarme a mejorar los puntos flacos de mi investigación. Mucha suerte en tu nueva etapa. Gracias Pol por recordarme una canción que se ajuste a cada situación. No pierdas nunca ese buen humor. Mi Lucisan, ha sido un placer trabajar contigo estos meses. Te mando mucha fuerza para superar los nuevos retos que se te presentan. No tengo ninguna duda de que lo harás con creces, vales muchísimo. Gracias Laura por contagiarme tu positividad, no la pierdas nunca porque lo bueno llama a lo bueno y eso es lo que yo te deseo, lo mejor. Gracias Irene O. por tu buen humor y por abrirme las puertas al mundo de la dieta saludable. Espero que seas muy feliz, te lo mereces. Mil gracias Rosa por ser tan atenta conmigo y por tus Werther's Original. Eres encantadora. Gracias Noelia por compartir con nosotros tu faceta repostera y endulzarnos los almuerzos, me ha encantado conocerte. Gracias Mari por ser tan atenta conmigo y sacar lo mejor de mí. Hemos tenido mucha suerte de tenerte en el laboratorio.

Gracias también a Rafael Susín y a Jorge Bolívar por ayudarme con la proteómica del proyecto y a José López, Luís García Alonso y Hugo Cabedo por estar siempre dispuestos a resolverme cualquier duda.

No quiero olvidarme de toda la gente que me ha acompañado en el camino dentro del instituto: durante el doctorado (Nuria, Belén, Ana, Edu, Adri, Jose, Clara, Rebeca, Danny, etc), durante las rotaciones (laboratorio de Hugo Cabedo y Ana Carmena por el buen recibimiento), ayudándome en el confocal invertido (Giovanna) o solucionando cualquier problema administrativo (Maite, Ruth, Gisela, Mª Luísa, Jesús, etc), muchas gracias por todo.

No puedo terminar sin hablar de quien ha estado a mi lado durante casi 9 años, pase lo que pase y apoyándome a cada paso que he dado. El karate ha sido mi forma de vida durante más de 17 años y no sólo me ha aportado mucho a nivel personal, sino que ha puesto en mi camino a una gran persona. David, gracias por tu paciencia y por entender los sacrificios que conlleva dedicarse a la investigación. Has sido y eres un pilar fundamental en mi vida y estoy deseando emprender contigo todos los proyectos que aún nos quedan por construir juntos.

"There should be no boundaries to human endeavour.
We are all different.
However bad life may seem,
there is always something you can do, and succeed at.
While there's life, there is hope."

Stephen Hawking

INDEX

UNIVERSITAS
Miguel
Hernández

ABBREVIATIONS

µg	microgram
A	Alanine
A/P	Anterior-Posterior
anti-luc	antibody against Luciferase protein
BL	Bloomington *Drosophila* Stock Center
boi	brother of ihog
Bdx-Gal4	Beadex-Gal4
BR-C	Broad-Complex
BRD	Bromodomain-containing
BTB	Broad-Complex/Tramtack/Bric à Brac
CBP	CREB-binding protein
ChIP-seq	Chromatin Immunoprecipitation sequencing
Chro	Chromator
ci	cubitus interruptus
CP190	Centrosome-associated zinc finger protein
Ct	Cut
CTCF	CCCTC-binding factor
CTD	C-terminal domain
D/V	Dorsal-Ventral
Dac	Dacshund
DE-cad	DE-cadherin
Dl	Delta
dpp	decapentaplegic gene
DSL	Delta/Serrate/LAG-2
dsRNA	double stranded RNA
E(z)	Enhancer of zeste
EcR	Ecdysone Receptor
eGFP	Enhanced Green Fluorescent Protein
EGFR	Epidermal Growth Factor-like Receptor
Eip	Ecdysone-induced protein
Elav	Embryonic lethal abnormal visual system
EMT	Epithelial to Mesenchimal Transition
en-Gal4	engrailed-Gal4
Enhan.	Enhancers
Eq-Z	Equatorial (eyegone)-lacZ
eRNA	enhancer RNA
ey-Flp	eyeless-Flippase
ey-Gal4	eyeless-Gal4
fng-Z	fringe-lacZ
FRT	Flippase Recognition Target
G	Glycine
GAF	GAGA Factor
H	Histone
HDAC	Histone Deacetylase

Hh	Hedgehog
hsp70-Flp	heat shock promoter 70-Flippase
HTH	Helix-Turn-Helix
IGV	Interactive Genomic Viewer
ihog	interference hedgehog
IR	Interference RNA
K	Lysine
Kb	Kilobase
Kuz	ADAM metalloprotease Kuzbanian
LI, LII, LIII	Larval stages I, II and III
Lola	Longitudinals Lacking
Lolal	Lola Like
MAM	Master Mind
me	methyl
MET	Mesenchimal to epithelial transition
MF	Morphogenetic Furrow
miRNA	microRNA
mirr-Z	mirror-lacZ
mM	miliMolar
mod(mdg4)2.2 /Mod2.2	Modifier of mdg4 isoform 2.2
mut	mutated
NECD	Notch Extracellular Domain
NICD	Notch Intracellular Domain
O-Fuc	O-fucosylation
ORF	Open Reading Frame
pb	paired bases
Pc	Polycomb
PG	Prothoracic Gland
PH3	Phospho histone H3
PI	Pausing Index
Pol II	Polymerase II
PTSSs	Pol II levels at Transcription Start Sites
Pbody	Pol II levels in the gene body
POZ	Pox virus/ Zinc finger
PRC	Polycomb Repressor Complex
PRE	Polycomb Response Element
pre-miRNA	precursor miRNAs
pri-miRNA	primary miRNAs
Prom.	Promoters
Psq	Pipsqueak
Ptc-Z	Patched-lacZ
Q	Glutamine
qRT-PCR	quantitative Reverse Transcription Polymerase Chain Reaction
RISCs	RNA-Induced Silencing Complexes
RNAi	RNA interference
s.e.m.	standard error of the mean

S/G	Serine/Glycine
Ser	Serine
Ser-Z	Serrate-lacZ
siRNA	short interference RNA
smo	smoothened
Su(Hw)	Suppressor of Hairy Wing
T	Threonine
TAD	Topologically Associated Domain
T-All	Acute Lymphoblastic Leukaemia
TRE	Trithorax Response Elements
trxG	Trithorax group
TSS	Transcription Start Sites
Tub-Gal4	αTubulin84B promoter -Gal4
Tub-Gal80	αTubulin84B promoter -Gal80
UAS	Upstream Activation Sequences
UAS	Upstream Activating Sequence
Usp	Ultraspiracle
UTR	Untraslated Region
VDRC	Vienna *Drosophila* RNAi Centre
VS	versus
WB	Western Blot
Wg	Wingless
wt	wild type

SUMMARY

Cancer and development are often considered two sides of the same coin, as they both involve the same processes with the goal to expand cell populations. For that, they probably require common genes with the crucial difference that during normal development they are carefully regulated. Growth control, in developmental biology, has been linked to the establishment of spatially confined domains called organizers, defined by its capacity to instruct surrounding cells about patterning and growth. Clinical evidence implicating various organizer-forming genes in human carcinogenesis—for example, *Notch*—has revived the interest in the connections between growth control and organizers.

In this thesis I have used the *Drosophila melanogaster* compound eye as a model to study the function of *Notch* as an oncogene. It has an essential role in eye growth, and its overactivation alone causes mild overgrowth, but never tumour development. We envisioned that *in vivo* Notch needs the cooperation of additional co-factors. With this work I propose on one hand miR-7 as a new Notch cooperating microRNA and, on other hand, I add new insights to the mechanism behind the tumorigenic transformation of the Notch-mediated mild overgrowth by the BTB-transcription factor Pipsqueak.

The microRNA miR-7 is cooperating with the Notch signalling pathway in the *Drosophila* eye, being *ihog* a direct target of miR-7 in this context. At the same time, the functional co-receptor of iHog in the Hedgehog signalling pathway, Boi, is a direct or indirect target of Notch-mediated organizer function. The loss of Hedgehog signalling enhances Notch signalling activity, showing at the same time its unsuspected role as a tumour suppressor. The human counterpart of *ihog* (*CDON*) is also repressed by the human miR-7, as it has been demonstrated *in vitro* in tumour human cells.

It is the first time that Pipsqueak isoforms (with or without a BTB protein-protein interaction domain) can be studied independently. This gene has been described to be a Notch cooperating oncogene. Its capacity to induce tumour development in cooperation with Notch overexpression has been attributed to its BTB domain and to its effect over chromatin silencing, as occurs with other BTB-transcription factors in human cancer. However, and against all predictions, the long Pipsqueak isoforms containing the BTB domain (PipsqueakBTB) does not co-localize with the chromatin repressive machinery, and its function seems to be related to the BTB-mediated insulator function. On the other hand, the non-BTB isoforms (non-BTB Pipsqueak), has a higher percentage of overlapping binding sites with repressive proteins, predicting a possible role in Polycomb Group-mediated epigenetic function.

Desarrollo y cáncer son considerados dos caras de la misma moneda ya que ambos implican procesos similares con el fin de expandir la población celular. Para ello, ambos requieren genes comunes con la diferencia crucial de que durante el desarrollo normal estos genes están cuidadosamente regulados. El control de crecimiento, en biología del desarrollo, se ha relacionado con el establecimiento de dominios confinados llamados organizadores, caracterizados por su capacidad de instruir a las células colindantes sobre su trayectoria de diferenciación específica durante el desarrollo. Evidencias clínicas que implican a varios genes encargados del establecimiento de organizadores en carcinogénesis de humano -por ejemplo, *Notch*- ha revivido el interés hacia el estudio de la conexión entre control de crecimiento y organizadores.

En este trabajo de tesis se ha usado el ojo de *Drosophila* como modelo para estudiar la implicación de la vía de señalización mediada por Notch, en el proceso tumoral. La vía de Notch tiene un papel esencial en el crecimiento del ojo, pero el leve crecimiento causado por su sobrexpresión no se puede considerar de tipo tumoral. Por ello, podemos especular que Notch necesita de co-factores adicionales, como hemos demostrado *in vivo*. Con este trabajo propongo, por una parte, que miR-7 es un microRNA que coopera con Notch en su función oncogénica y por otra, añado nuevas perspectivas para explicar los mecanismos detrás del factor BTB llamado Pipsqueak en la transformación tumorigénica del crecimiento leve inducido por Notch.

El microRNA miR-7 está cooperando con la vía de señalización de Notch en la formación de tumores en *Drosophila,* siendo *ihog* su diana directa. El co-receptor funcional de iHog en la vía de señalización de Hedgehog (Boi) es, a su vez, una diana directa o indirecta de la función de Notch como organizador. La falta de función de la vía de Hedgehog incrementa la actividad de la vía de señalización de Notch, actuando como supresor de tumores en el desarrollo de cáncer. Se ha demostrado también en células tumorales de humano que el homólogo de *ihog* (*CDON*) también está reprimido por el microRNA miR-7 de humano, *in vitro*.

Es la primera vez que las isoformas de Pipsqueak (con o sin el dominio BTB de interacción proteína-proteína) pueden ser estudiadas de manera independiente. *pipsqueak* se ha descrito como un oncogén cooperante con Notch en la formación de tumores, gracias a su dominio BTB y a su efecto sobre silenciamiento de cromatina, al igual que otros factores de transcripción BTB en cáncer humano. Sin embargo, contra toda predicción, hemos visto que PipsqueakBTB está más relacionado con la función mediada por proteínas llamadas aislantes (“insulators” en inglés) y es la isoforma sin el dominio BTB la que tiene un porcentaje mayor de sitios de unión comunes con la maquinaria epigenética. Esto sugiere que este dominio no es necesario para la función represora mediada por el grupo Polycomb.

INTRODUCTION

Cancer is usually viewed as a result of the accumulation of somatic mutations in the progeny of a normal cell, leading to a selective growth advantage in the mutated cells and, ultimately, to uncontrolled proliferation (Janiszewska *et al.*, 2015; Merlo *et al.*, 2006). These somatic mutations include, for example, base substitutions, insertions and deletions of bases and chromosomal rearrangements by breakage and abnormal re-joining of DNA. They also often include epigenetic changes inherited during mitotic DNA replication (Laird, 2005; Stratton *et al.*, 2009). Thanks to the development of novel sequencing techniques, which have identified many genes that are mutated in different types of cancer, we have now a broad knowledge of the function of oncogenes and tumour suppressor genes. However, this enormous amount of data, showing the high complexity of the genetic network implicated in cancer, does not reveal which mutations are "drivers" in the process of tumorigenesis and which ones are just mere companions. Every cell within a tumour is the result of a combination of hundreds of molecular events and the failure of numerous biological mechanisms, so that each cell can behave slightly different respect to their neighbours. This intra-tumour heterogeneity of cancer cells hampers the design of effective therapies making it difficult to reproduce this genetic complexity in experimental models (Figure 1).

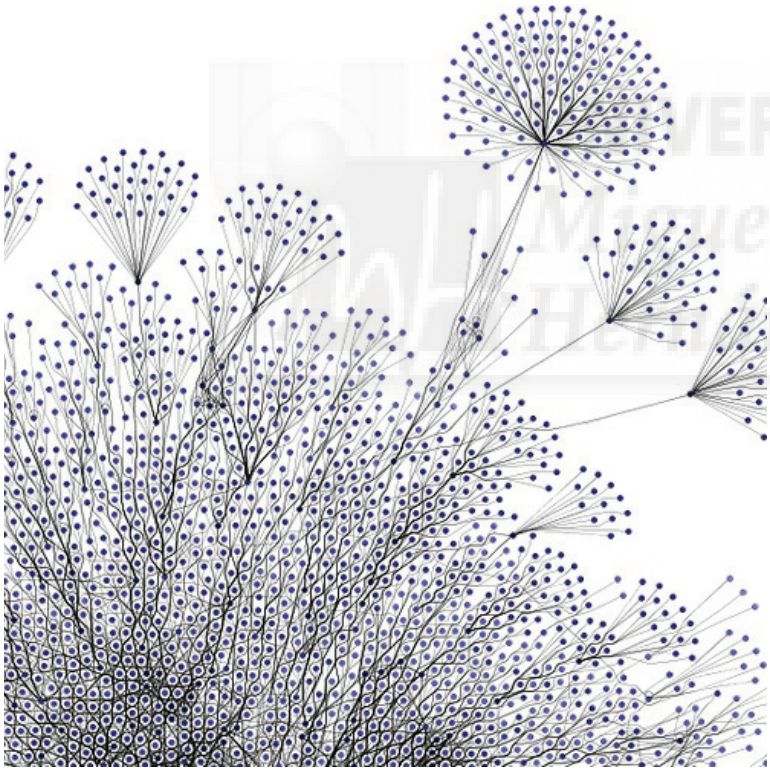

Figure 1. Picture made by Casey Hussein Bisson / Creative Commons BY-NC-SA, depicting the complexity of the genetic web of cancer cell within tumour formation.

In this context, the fruit fly *Drosophila melanogaster* emerged as an important model system for cancer studies. Its four-chromosome genome simplifies the genetic complexity behind tumour and secondary growths formation. This coupled with the powerful genetic toolkit available and the short life span of *Drosophila*, makes it a simple and effective animal model to molecularly characterize important signalling cascades, developmental and growth control programmes (Brumby *et al.*, 2005; Januschke *et al.*, 2008; Vidal *et al.*, 2006), as well as serve as an excellent platform for large-scale cancer gene discovery studies.

Studies in flies can provide valuable information that could guide us towards a better interpretation and understanding of how oncogenic mutations orchestrate cell proliferation and migratory behaviour.

1. Local, differential growth regulation by organizers and cancer.

Cancer and development are often considered as two sides of the same coin. Indeed, both processes involve extensive cell proliferation, resistance to cell death and mechanisms that prevent premature cell differentiation with the goal to expand cell populations. Cancer and development, hence, may involve common genes with the crucial difference that during normal development these genes are carefully regulated.

One strategy that organisms use to simplify the orchestration of development is the separation of cell populations into distinct functional units called compartments. Fields of cells are subdivided by the effect of morphogen gradients, and these subdivisions are then maintained and refined by local cell interactions. Once cell populations become distinct, specialized cells that occupy a restricted temporal-spatial niche, pattern the surrounding cells via secretion of signalling factors and cell-cell contacts. These spatially confined domains are called organizers (Diaz-Benjumea *et al.*, 1995; Irvine *et al.*, 2001).

Several studies in diverse vertebrate and invertebrate models have led to the identification of many organizer signals. The first organizer was described by Spemann and Mangold in the *Xenopus laevis* embryo, defined by its capacity, when transplanted, to instruct surrounding cells about growth and patterning. After that, many signalling pathways involved in organizer formation have been identified, for example EGF, Wnt (also known as Wingless in *Drosophila*), Hedgehog and Notch signalling pathways. But our understanding of how these organizers stop the growth of developing organs is still incomplete (reviewed in (Dominguez, 2014).

Recent clinical evidences have involved the aberrant activation of many of these organizing signals in the initiation and progression of numerous types of human cancers. These observations have revived the interest in understanding the association between the mechanisms that regulate the formation and function of these growth organizers and the processes that promote cancer (Steelman *et al.*, 2008; Vogelstein *et al.*, 2004).

2. The instructive role of Notch signalling pathway in growth.

Notch signalling is a critical cell communication form used throughout development. It is a highly evolutionarily conserved pathway (Artavanis-Tsakonas *et al.*, 1999; Mumm *et al.*, 2000) implicated in diverse functions during embryogenesis and in self-renewing tissues of the adult organism. Among its multiple and diverse functions, we can highlight its role in the maintenance of stem cells, cell fate specification, proliferation, and apoptosis (Artavanis-Tsakonas, 1988; Leong *et al.*, 2006). Not surprisingly, aberrant Notch signalling can result in a wide range of pathological consequences. In addition, Notch can also work in a dual way depending on the cellular context, for example, promoting stem cell maintenance or inducing terminal differentiation.

This signalling pathway was first identified in *Drosophila* and in *Caenorhabditis elegans* nearly a century ago, when the inactivation of just one copy of *Notch* (haploinsufficiency) was shown to produce notches at the wing margin in flies (Mohr, 1919) and defects in vulval development in worms (Ferguson *et al.*, 1985). The gene causing these particular phenotypes was cloned in the mid-1980s and encodes a single pass transmembrane receptor, harbouring a large extracellular domain (NECD) involved in ligand binding and an intracellular domain involved in signal transduction (NICD).

2.1. The Notch signalling cascade.

In mammals there are four genes that codify the NOTCH receptors (NOTCH1-4) while in *Drosophila* there is only one (Notch or dNotch). Five genes codify its mammalian ligands, three within the called Delta family (DELTA-LIKE1, 3 AND 4) and two of the called Serrate family (JAGGED1 and 2) being Delta and Serrate the *Drosophila* homologs of these ligands.

The Notch signalling pathway is conserved from *Drosophila* to humans and in all these organisms Notch receptor is activated in the secretory pathway (Hori *et al.*, 2013; Kopan *et al.*, 2009) (Figure 2). The signalling begins when a ligand of the DSL family (name coming from the names of the ligands found first is *Drosophila* and *C. elegans*: Delta/Serrate/LAG-2) binds to the NECD present at the cell surface (Fehon *et al.*, 1990) of an adjacent cell (Figure 2). NECD undergoes extracellular glycosylation by Fringe (an EGF-O-fucose 1,3 N-acetylglucosamyl transferase, called Lunatic Fringe, Radical-Fringe, and Maniac-Fringe in mammals), elongating the O-fucosylation induced by O-FucT-1 (Pofut1 in mice), crucial for all Notch-ligand interactions (Andersson *et al.*, 2011) (Figure 2). In *Drosophila*, Fringe inhibits the ability of Ser to activate Notch, whereas potentiates the ability of Dl to activate it (Fleming *et al.*, 1997; Panin *et al.*, 1997).

Activation of the Notch receptor upon ligand binding involves several proteolytic steps that trigger the shedding of the NECD. First the cleavage performed by members of the ADAM metalloprotease Kuzbanian (Kuz)/TACE family (S2 cleavage) (Brou *et al.*, 2000; Lieber *et al.*, 2002). Second, the presenilin (PS)-dependent secretase complex produces an intramembrane proteolysis (S3 cleavage) releasing a soluble NICD (De Strooper *et al.*, 1999; Struhl *et al.*, 1993) (Figure 2). The soluble, S3-cleaved NICD fragment translocates to the nucleus where it associates with a DNA-

binding protein called CSL (known as CBF in humans, suppressor of hairless in *Drosophila* and Lag-1 in *C. elegans)* and Master Mind (MAM) to regulate the expression of Notch target genes (Artavanis-Tsakonas *et al.*, 1999; Bray, 2006; Kovall, 2008; Le Borgne *et al.*, 2005) (Figure 2).

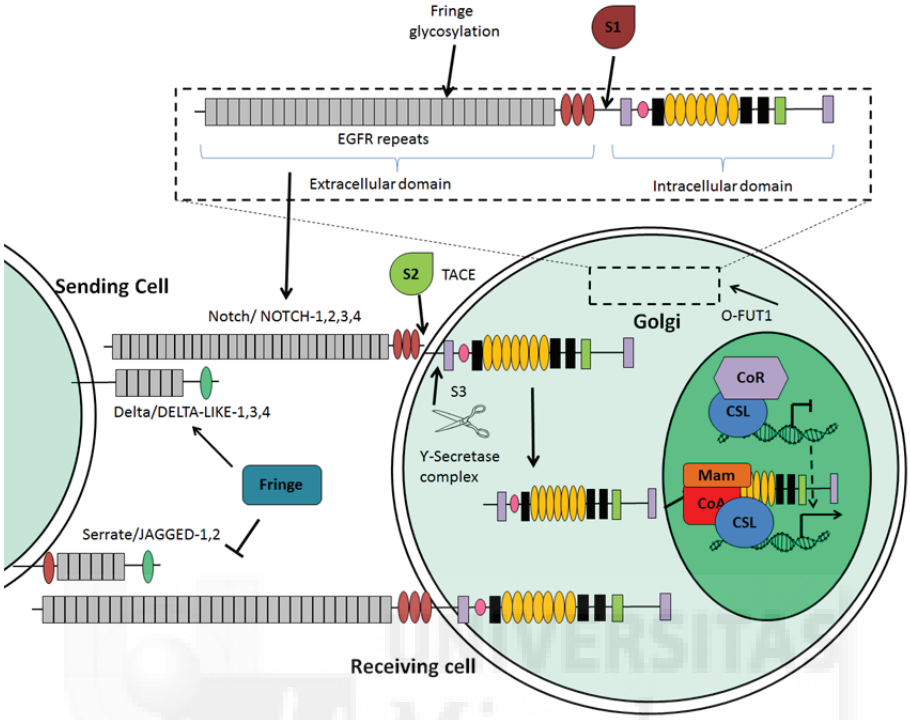

Figure 2. An overview of the Notch signalling pathway. Notch receptor is activated in the secretory pathway by a ligand independent cleavage called S1. A ligand of the DSL family binds to NECD at the cell surface between two adjacent cells. NECD undergoes extracellular glycosylation. In particular, O-fucosylation by O-FucT-1 is crucial for all Notch-ligand interactions, being elongated by Fringe. The release of a soluble intercellular Notch fragment (NICD) is trigged upon ligand binding and involves several proteolytic steps. It starts by members of the ADAM metalloprotease Kuzbanian (Kuz)/TACE family (cleavage S2) and it is followed by intramembrane proteolysis (S3 cleavage) by the presenilin (PS)-dependent secretase complex. The soluble, S3-cleaved NICD fragment translocates to the nucleus where it associates with a DNA-binding protein called CSL, Master Mind (MAM) and other co-activators (Co-A), to regulate the expression of Notch target genes. Picture modified from (Dominguez, 2014).

2.2. The dual role of Notch signalling in cancer.

The first evidence for the involvement of Notch signalling in cancer came from T-cell acute lymphoblastic leukaemia (T-ALL), where it was described as an oncogene (Ellisen *et al.*, 1991). This neoplastic disorder accounts for ~10–20% of all acute lymphoblastic leukaemia. In 1991, Ellisen and co-workers (Ellisen *et al.*, 1991) identified a translocation in T-ALL patients, overexpressing the active form of Notch1 (ICN1) and found in <1% of T-ALL cases. 14 years later, the group of Jon Aster found the recurrent truncated and active forms of the NOTCH1 receptor mutations in T-ALL (Aster, 2005). Subsequent studies have implicated Notch signalling working as an oncogene in various solid tumours, including breast and prostate cancer, medulloblastoma, colorectal cancer, non–small cell lung carcinoma (NSCLC), melanoma, and other (Karanu *et al.*, 2000; Leong *et al.*, 2007; Miele *et al.*, 2006; Ranganathan *et al.*, 2011; Santagata *et al.*, 2004), expanding our understanding of Notch

participation in cancer, and defining some of its partners in different cancer processes. We know that overexpressing mutations account for more than 50% of T-ALLs (Ferrando, 2009). However, in human cancers, Notch activation cooperates with other oncogenes or with the loss of tumour suppressors to initiate tumour progression (reviewed in (Dominguez, 2014)). Moreover, although Notch activation can be oncogenic, there is evidence that components of the same pathway may have tumour suppressive functions in other hematopoietic cells, skin, and pancreatic epithelium, as well as in hepatocytes (Lowell *et al.*, 2000; Rangarajan *et al.*, 2001; Viatour *et al.*, 2011). This is not surprising given that Notch is involved both during embryonic development and in adult tissues in a varied array of fundamental processes such as the maintenance of stem cells, cell fate specification, proliferation and apoptosis.

Studies in *Drosophila* have expanded our understanding of how Notch initiates and promotes the progression of tumorigenesis *in vivo*. Focusing our attention in the role of Notch as an oncogene, it is known that Notch induces tumour-like formation in cooperation with epigenetic regulators (Ferres-Marco *et al.*, 2006; Liefke *et al.*, 2010), microRNAs (Da Ros *et al.*, 2013) the Epithermal Growth factor receptor EGFR (Hurlbut *et al.*, 2007) or the Pten/PI3K/AKT pathway (Palomero *et al.*, 2007). Although all these studies report several outstanding advances, the knowledge about the mechanisms by which these oncogenic pathways contribute to the initiation and progression of invasion is still limited.

This project has been developed using *Drosophila melanogaster* as a model to study tumorigenesis driven by one of the highest evolutionarily conserved pathway, the Notch signalling pathway.

3. *Drosophila melanogaster* model for studies of Notch induced tumorigenesis.

3.1. *Drosophila* life cycle.

Starting with the American entomologist Charles W. Woodworth's proposal to use this species as a model organism, *Drosophila melanogaster* continues to be widely used for biological research in studies of genetics, physiology, microbial pathogenesis and life history evolution.

Generally known as the common fruit fly or vinegar fly, *Drosophila melanogaster* belongs to the family *Drosophilidae,* taxonomic order Diptera. It is a holometabolous insect, having three larval stages and undergoing metamorphosis to achieve the final adult form (Figure 3A). The adult *Drosophila* may live for more than 10 weeks, being during this time when mating takes place.

Most of the adult structures of the fly arise from a set of cells that have been carried as undifferentiated, mitotic cells within the larva throughout its instar stages: the imaginal discs (Figure 3B). Early in embryonic development, imaginal cells (i.e., cells that contribute to the adult animal,

the ‘‘imago’’) segregate from their neighbours by invagination from the ectoderm (Bate *et al.*, 1991). Later, these clusters of cells form sac-like structures originating the imaginal discs (Figure 3B) (Averof *et al.*, 1997; Cohen *et al.*, 1991; Wieschaus *et al.*, 1976).

The progression trough each larval stage is marked by an Ecdysone pulse (Figure 3C). These pulses coordinate postembryonic development in insects, including *Drosophila*. After the highest pulse, which occurs at the end of the third instar, the puparium is formed marking the onset of prepupal development (Delattre *et al.*, 2000; Kozlova *et al.*, 2002; Richards, 1981; Richards, 1981), which is why Ecdysone is called the molting or the metamorphosis hormone (Figure 3C). While in the majority of insects, Ecdysone is secreted by the prothoracic gland, in *Drosophila* is secreted specifically by the ring gland in the larvae. Ecdysone is then converted to 20-Hydrosyecdysone (20HE), the active form of the hormone (Reviewed in (Gilbert, 1996; Riddiford, 1993)). Released Ecdysone binds to its receptor (Ecdysone receptor, EcR) initiating a complex pathway of gene regulation that triggers a set of physiological and behavioural changes that characterize each life cycle stage.

EcR is a nuclear receptor which behaves as a transcriptional regulator upon ligand binding (Bender *et al.*, 1997; Koelle *et al.*, 1991; Riddiford *et al.*, 2000). The expression of this receptor is induced directly by Ecdysone, and provides an autoregulatory loop that increases the level of receptor protein in response to the hormone. EcR requires a partner called Ultraspiracle (Usp) that greatly stimulates the affinity in the EcR/20-HE binding. (Richards, 1981; Yao *et al.*, 1993). This interaction increases the EcR binding to Ecdysone response elements in the promoters of genes. Among the long list of Ecdysone-induced genes we can find, for example, the ones encoding for the Ecdysone-induced protein 75B *(Eip75B)* or Vrille (Vri) (Gauhar *et al.*, 2009). Moreover, products of the early responsive genes can repress their own transcription and induce the expression of late genes (Burtis *et al.*, 1990; Segraves *et al.*, 1990; Thummel *et al.*, 1990).

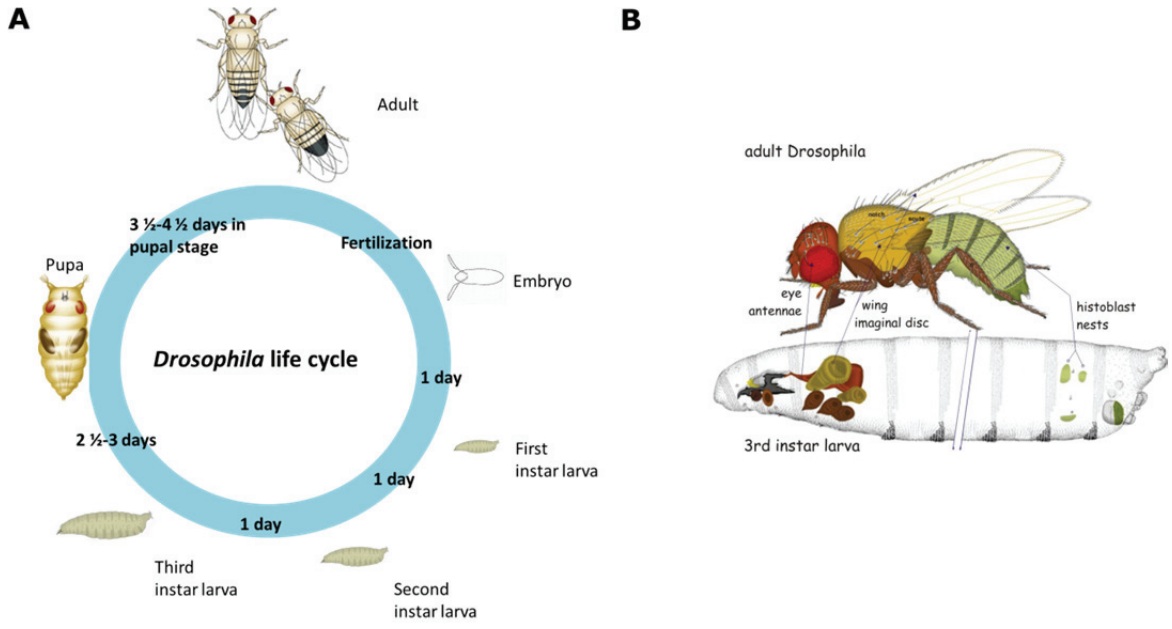

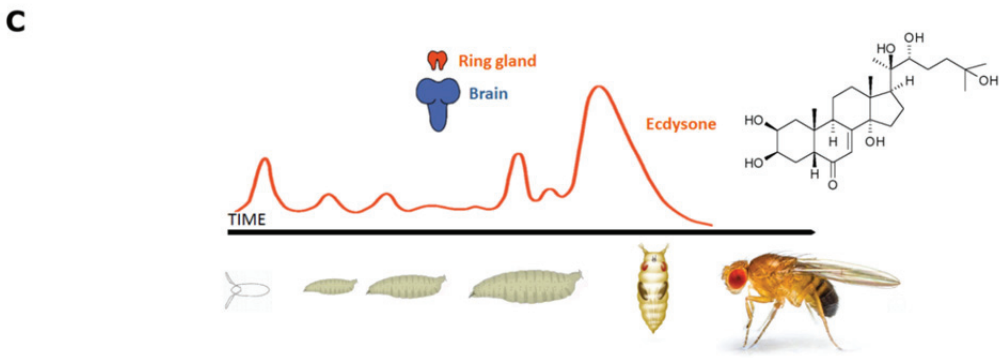

Figure 3. Life cycle and its hormonal control in *Drosophila melanogaster*. (**A**) After egg fertilization an embryo develops, hatching in 22–24 hr at 25°C. The larva that emerges is called the first instar larva. After another 25 hr it moults into a larger form, known as the second instar larva, which in turn gives rise to the third instar larva after another 24 hr. This larva starts to climb upward out of the food, so that it will be in a relatively clean and dry area to undergo metamorphosis, and afterwards the adult fly emerges. (**B**) Most of the adult structures arise from a set of cells that have been carried as undifferentiated, mitotic cells within the larva throughout its instar stages: the imaginal discs (From V. Hartenstein). (**C**) The ecdysteroid titer profile during *Drosophila* development. The composite ecdysteroid titer is depicted in 20-Hydroxyecdysone equivalents from whole-body homogenates.

3.2. *Drosophila* imaginal discs and growth organizers.

As it was mentioned before, the spatially confined domains called organizers are associated to growth control and patterning of tissues and organs (Diaz-Benjumea *et al.*, 1995; Irvine *et al.*, 2001). In *Drosophila*, Hedgehog and Notch signalling pathways are very well studied perpendicular organizing signals. They are both involved in the establishment of the anterior-posterior and dorsal-ventral organizers in the imaginal discs (Figure 4).

The appendages of *Drosophila* have proven to be ideal models for the study of limb development. The establishment of the two major limb axes considered here depends on the subdivision into distinct compartments. Compartments can be simply defined as separate, different, adjacent cell populations, which upon juxtaposition, create a lineage boundary. This boundary prevents cell movement from cells from different lineages across this barrier, restricting them to their compartment (Wolpert, 1969). These borders act as a reference to the establishment of different cellular populations that secrete morphogens controlling cell proliferation and differentiation (Turing, 1952).

In this thesis work we use the wing and eye-antenna imaginal discs as they are perfect models to study the crosstalk between Notch signalling with other organizer signals, in the correct formation of the organ establishing the anterior-posterior and dorsal-ventral organizers.

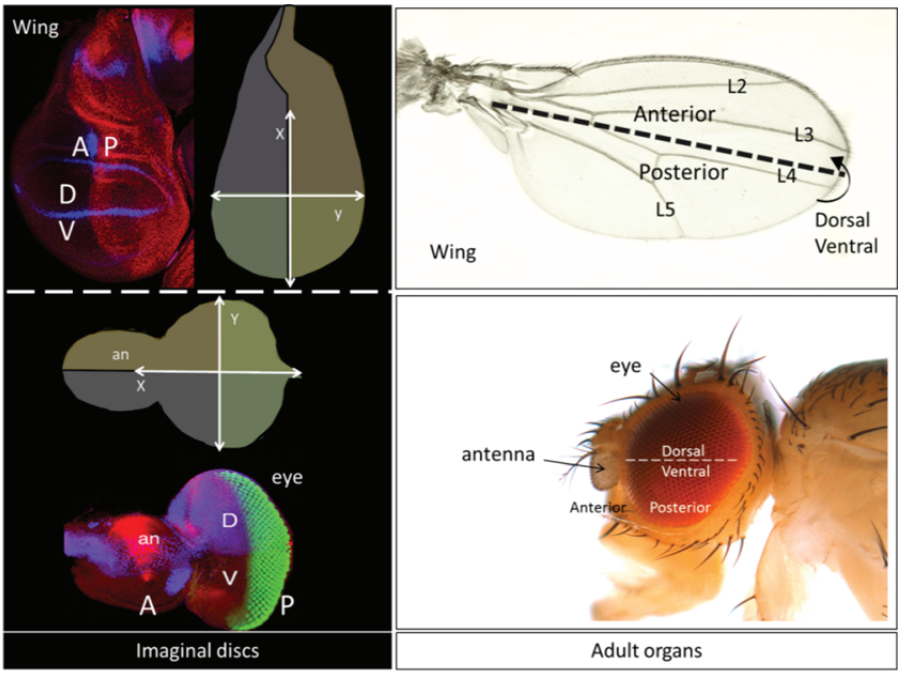

Figure 4. Establishment of the anterior-posterior and dorsal-ventral axes in imaginal discs. Patterning of the eye and wing imaginal discs need signals to generate an anterior–posterior and dorsal–ventral axes termed morphogens. This provides cells with the establishment of a heritable transcription factor expression conferring a specific identity on a field of cells. These subdivisions are then maintained by local cell-cell interactions giving rise to a correctly shaped adult organ. Wing disc is stained with a-Wg (marker of dorsal-ventral organizer in blue) and a-Ci (posterior marker in red), and eye discs with a-Elav (posterior marker in green), a-Wg (to correctly orientate the dorsal-ventral eye disc in red) and the dorsal marker mirr-LacZ with a-βGal (in blue).

- The wing imaginal disc:

The first subdivision between anterior and posterior compartments was first detected in the wing disc (Garcia-Bellido *et al.*, 1973; Garcia-Bellido *et al.*, 1976) (Figure 5B anterior–posterior organizer). This is a consequence of the function of the homeobox gene *engrailed* (*en* (in the wing-disc anterior–posterior organizer generates the area that includes wing veins 3 and 4 -Figure 4) (Morata *et al.*, 1975). In the imaginal discs, *en* behaves as what was originally called the classical selector gene (Morata *et al.*, 1975); it separates the anterior and posterior cell populations by selecting between anterior or posterior developmental programmes. (Lawrence *et al.*, 1996; Strigini *et al.*, 1999). In the wing, En activates the *hedgehog* (*hh*) gene, which encodes a secreted protein and initiates what is called the Hh signalling pathway (Nusslein-Volhard *et al.*, 1980).

The effect of the Hh protein in the posterior compartment cells is blocked by En, but the protein can move across the anterior–posterior border to the anterior compartment. Paracrine Hh signalling in these target cells involves the Patched (Ptc) receptor which activates the Smoothened (Smo) protein, which in turn initiates a series of post-translational modifications of components of the Hh signalling transduction pathway (reviewed by (Wilson *et al.*, 2010)). Although Ptc plays a critical role in sensing the Hh morphogenic gradient, the subsequently identified functionally redundant members of the immunoglobulin/fibronectin type III–like superfamily proteins, Ihog and

Boi (that bind to Hh ligand), are also required for Hh signalling in these tissues (Camp *et al.*, 2010; McLellan *et al.*, 2006; Yan *et al.*, 2010; Yao *et al.*, 2006; Zheng *et al.*, 2010) (Figure 5A and B; anterior-posterior organizer).

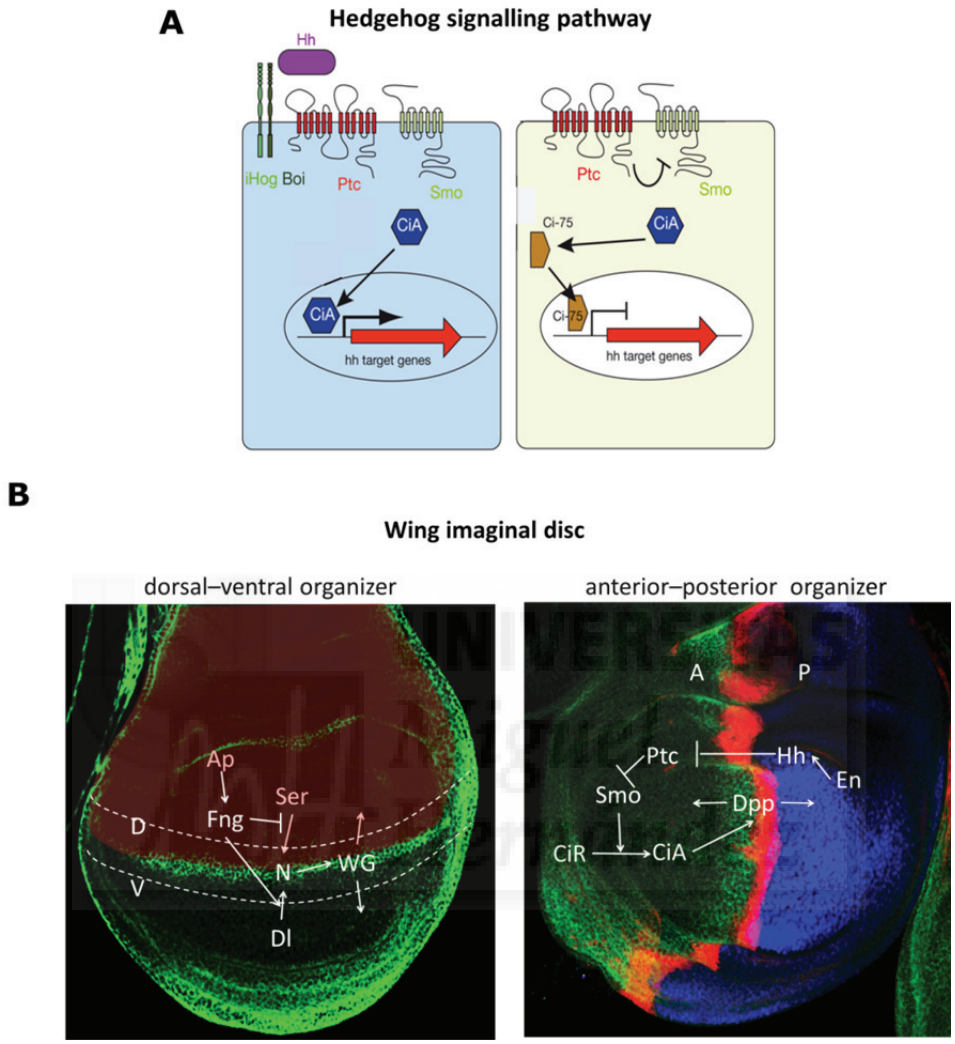

Figure 5. An overview of the Hedgehog signalling pathway in *Drosophila melanogaster* wing organizers. (A) In Hedgehog signalling Ihog and Boi (that bind to Hh ligand) and Ptc eceptor activate the Smo protein, which initiates the Hh signalling transduction pathway changing the form and intracellular distribution of the Ci protein, which in the absence of Hh signalling is a transcriptional repressor (Ci-75 or Ci-R) and with the Hh signal transduction the repressor form Ci-75 transforms Ci in an active transcription factor (CiA). Ci induces the expression of a number of target genes, including *ptc, dpp,* and *vein*. **(B)** Dorsal–ventral and anterior–posterior organizers in the wing imaginal disc are maintained by the Notch and the Hedgehog signalling pathway respectively. Discs are stained with a-Wg in green to mark the dorsal–ventral organizer, a-dpp in red to mark the anterior–posterior organizer and, in the same disc, the posterior marker a-En in blue and a-Ci to mark the anterior part of the disc in green are shown.

The output of this cascade changes the form and intracellular distribution of the Cubitus interruptus (Ci) protein (Aza-Blanc *et al.*, 1997), which in the absence of Hh signalling is an inactive proteolytically cleaved fragment that functions as a nuclear transcriptional repressor (Ci-75 or CiR). Hh signal transduction inhibits the repressor form Ci-75 and transforms Ci in an active transcription factor (CiA). Ci induces the expression of a number of target genes, including *ptc*, *dpp*, and *vein* (Amin *et al.*, 1999; Basler *et al.*, 1994; Biehs *et al.*, 1998; Schnepp *et al.*, 1996; Tabata *et al.*, 1994).

dpp (which encodes a transforming growth factor-β homologue) is expressed in the band of Hh-receiving cells adjacent to the anterior–posterior compartment border. From there it disseminates to target cells in both compartments (Lecuit *et al.*, 1996; Nellen *et al.*, 1996), regulates their proliferation and identity, embodying much of the functionality of the anterior–posterior organizer (Figure 5A and B; anterior–posterior organizer).

In the wing disc, a second compartmental subdivision appears during larval development (Garcia-Bellido *et al.*, 1973; Garcia-Bellido *et al.*, 1976) separating the dorsal from the ventral regions of the pre-existing anterior and posterior compartments (Figure 5B; dorsal–ventral organizer). LIM-homeobox gene *apterous* (*ap*) is expressed in the dorsal compartment as precisely defined by the dorsal-ventral border (Blair, 1993; Diaz-Benjumea *et al.*, 1993) (Figure 5B; dorsal-ventral organizer). *ap* activates the gene *fringe* (*fng*), which modulates the ability of two ligands, Delta (Dl) and Serrate (Ser), to activate their receptor Notch (Fleming *et al.*, 1997; Panin *et al.*, 1997). Notch is activated by Serrate in the Fringe-negative ventral cells along the boundary (region between dashed lines in Figure 5B dorsal-ventral organizer), and by Delta in the Fringe-positive dorsal cells along the other side of the boundary. In turn, Notch induces, among others, *wg* activity at the dorsal-ventral border. Wg acts as an organizer signal of wing development (Neumann *et al.*, 1996; Zecca *et al.*, 1996). Although the *Notch* gene was firstly identified for its effect on the wing margin (loss of one dose of *Notch* results in nicked wings), subsequent studies have revealed several roles for Notch in wing morphogenesis, where it is needed for cell growth and vein differentiation, as well as for wing margin formation (de Celis *et al.*, 1994; Shellenbarger *et al.*, 1978).

- The eye-antenna imaginal disc:

As occurs in the wing discs, eye-antennal discs also have anterior–posterior and dorsal-ventral organizers.

Drosophila has a compound eye comprising about 750 ommatidia that form a regular hexagonal array. Each ommatidium is formed by 8 photoreceptor cells and other type of pigmentary cells. Ommatidia are oriented in a specular symmetry along the eye midline (see Figure 4 and 6B). This dorsal–ventral distribution is determined at early developmental stages and is defined by the same organizer that controls its early development. The adult compound eye is originated from the posterior part of the eye-antenna imaginal disc. Below, I will summarize the development of the part of the disc that is regulated by organizers and originates the *Drosophila* compound eye.

During the second and third instar larval stages, cells start an active division to increment the size of the disc. However, at the beginning of the third larval stage, cells stop growing and start to differentiate in a coordinate manner, as a morphogenetic wave originated in the most posterior part of the disc begins to move anteriorly across the eye imaginal disc. This wave is associated with the formation of a transient furrow in the disc epithelium, known as the morphogenetic furrow (MF), and its apparition marks the start of neural differentiation (Ready *et al.*, 1976). The photoreceptors develop behind the furrow (Freeman, 1997; Tomlinson, 1985; Tomlinson *et al.*, 1987; Tomlinson *et al.*, 1987). Highly proliferative cells in the anterior part of the MF remain undifferentiated and proliferating. This spatial and temporal difference between proliferation and differentiation makes *Drosophila* eye an exceptional experimental model to dissect the mechanisms that control the

progression of the cell cycle, survival and apoptosis in tumorigenic and normal growth directed by an organizer. These events can be addressed without the interference of other mechanisms such as cell differentiation and specification.

The early growth of the eye imaginal disc depends on the activity of an organizer that controls, not only the global growth of the disc, but also its morphogenesis, the dorsal-ventral polarity and the initiation point of the MF. This organizer depends on the localized activation of Notch signalling pathway (Cavodeassi et al., 1999; Cho and Choi, 1998; Dominguez and de Celis, 1998; Papayannopoulos et al., 1998). The formation of this organizer first requires the establishment of the dorsal and ventral compartments, limited by different cell lineages (Dominguez *et al.*, 1998). The generation of this asymmetry relies on the expression of three related genes which form the *Iroquois* gene complex or *Iro-C* (Cavodeassi *et al.*, 1999). The expression of *Iro-C* complex is regulated early by the gene *wg*, which in turn acts synergistically with the Hh pathway to control the activation of the *Iro-C* complex in the dorsal compartment (Cavodeassi *et al.*, 1999; Heberlein *et al.*, 1998; Maurel-Zaffran *et al.*, 2000).

The *Iro-C* complex represses the expression of the gene *fng* in the dorsal region, restricting it to the ventral compartment. Such restriction originates the establishment of a border of *fng* expression in the medial dorsal–ventral line, essential for the formation of the Notch organizer (Cho *et al.*, 1998; Dominguez *et al.*, 1998; Papayannopoulos *et al.*, 1998), where it modulates the ability of Dl and Ser, to activate their receptor Notch (Figure 6A dorsal–ventral organizer) with the same mechanisms described for the dorsal–ventral organizer in the wing disc (Dominguez et al., 2004; Tsai et al., 2004). This differential modulation allows local activation of the Notch receptor along the border of the dorsal–ventral compartment of the eye (Figure 6A; dorsal–ventral organizer) (Cavodeassi *et al.*, 1999; Wu *et al.*, 1999), where it induces the expression of *eyegone* (*eyg*), a dorsal-ventral organizer-specific response gene and an obligatory Notch's effector in eye growth (Dominguez *et al.*, 2004; Tsai *et al.*, 2004). Generalized expression of *fng* impedes the activation of the gene *Ser*, blocking the feedback between the ligands and the high activation of Notch, resulting in flies with very small eyes or even absent eyes (Dominguez *et al.*, 1998; Dominguez *et al.*, 2004) (Figure 6B). On the contrary, Dl generalized expression expands Notch activated area to all the ventral region, producing an increase in cell proliferation leading to flies with overgrown eyes (Dominguez *et al.*, 1998) (Figure 6B).

Another important player in the proper development of the eye disc is Hh signalling pathway. As previously mentioned, Hh signalling is involved in controlling the activation of the *Iro-C* complex in the dorsal compartment. In addition to this, it directly controls initiation and propagation of retinal differentiation in the eye, by modulating the formation of the morphogenetic furrow (Dominguez *et al.*, 1997; Heberlein *et al.*, 1993). Hh is expressed in the differentiated photoreceptors behind the MF and diffuses anteriorly (Borod *et al.*, 1998; Dominguez, 1999; Dominguez *et al.*, 1997; Heberlein *et al.*, 1993) (Figure 6A; anterior–posterior organizer). The effects of Hh are partly mediated by Dpp, which is expressed within and ahead of the MF in response to Hh signalling (Blackman *et al.*, 1991; Heberlein *et al.*, 1993; Pignoni *et al.*, 1997). The primary function of Dpp in the establishment of the MF is the repression of Wg (another Hh secondary signal), which prevents ommatidial differentiation.

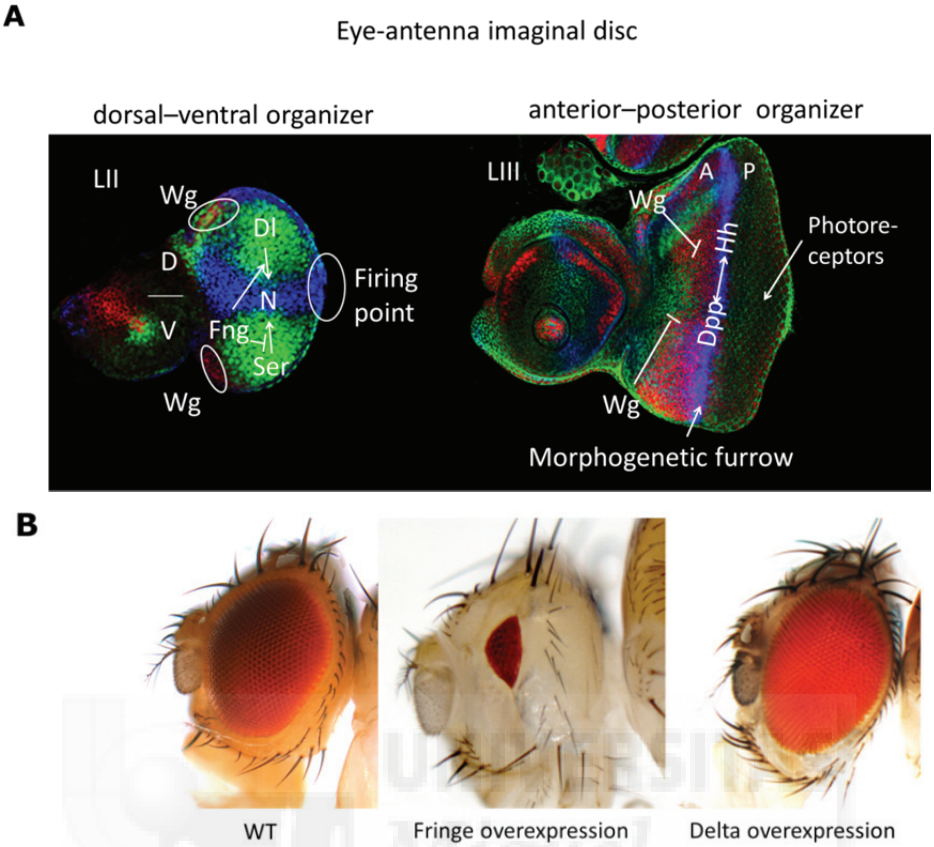

Figure 6. An overview of eye organizers. (A) Dorsal–ventral and anterior–posterior organizers in the eye imaginal disc are maintained by the Notch and the Hedgehog signalling pathway respectively. Eye discs stained to see the dorsal-ventral organizer with a-Eyg (blue), a-Wg (red) and Boi-LacZ (green) and the anterior-posterior organizer with a-Wg (green) and a-Ci (blue) **(B)** The alteration of Notch signalling during eye development produces viable flies with reproducible phenotypes of overgrown or reduced eyes. Notch loss-of-function, caused by the overexpression of the glycosyltransferase Fringe, produces an undergrown eye phenotype compared to a control eye. Notch gain of function due to overexpression of its ligand Delta promotes the expansion of the ventral compartment in the eye, originating an overgrown eye phenotype.

3.3. Drosophila compound eye, screen design, and concept of 'cooperative oncogenesis'.

Specific overexpression of Notch signalling pathway alone in the eye of *Drosophila* produces a mild overgrowth of the eye tissue that does not correspond to the tumour-like overgrowth produced by the oncogenic dysfunction of the Notch signalling pathway, as seen in Figure 6B. This observation suggests that Notch does not work alone. To find the endogenous genetic determinants that may limit Notch-driven tumorigenesis *in vivo*, Dolors Ferrés-Marcó and María Domínguez (Ferres-Marco *et al.*, 2006) carried out an unbiased (genome-wide) screen looking for loci that converted Dl-induced mild eye overgrowth into severe overgrowths or secondary eye growths throughout the body, using the UAS-Gal4 and the Gene Search system.

- *The GAL4–UAS system for directed gene expression*:

The yeast transcriptional activator Gal4 can be used to regulate gene expression in *Drosophila* in combination with its upstream activating sequence (UAS), situated next to a gene of interest (gene X) (Fischer *et al.*, 1988). The *GAL4* gene has been inserted at random positions in the *Drosophila* genome to generate 'enhancer-trap' lines that express *GAL4* under the control of nearby enhancers, and there is now a large collection of lines expressing *GAL4* in a huge variety of cell-type and tissue-specific patterns (Brand *et al.*, 1993). Therefore, the expression of gene X can be driven in any of these patterns by crossing the appropriate GAL4 enhancer-trap line to flies that carry the UAS–gene X transgene. This system has been adapted to carry out genetic screens for genes that give rise to phenotypes when misexpressed in a particular tissue (Rorth, 1996) (Figure 7).

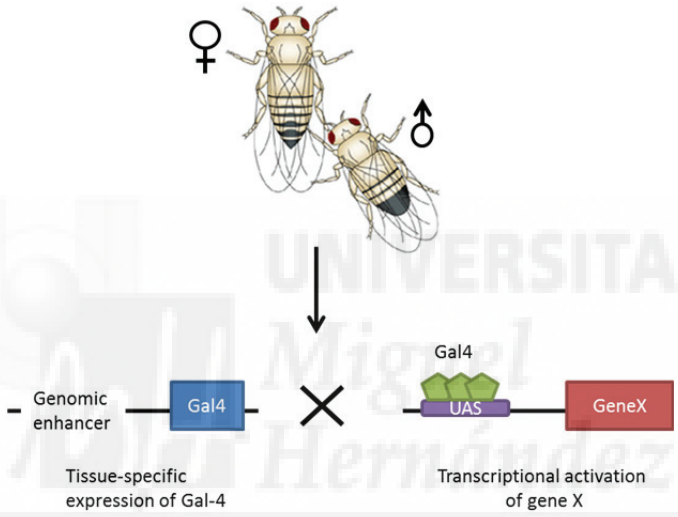

Figure 7. The Gal4-UAS system. 'Enhancer-trap' lines that express GAL4 under the control of nearby enhancers have been generated by the insertion of GAL4 at random positions in the *Drosophila* genome. Crossing the appropriate GAL4 enhancer-trap line to flies that carry the UAS–gene X transgene we can express the gene X. This system has been adapted to carry out genetic screens for genes that give rise to phenotypes when misexpressed in a particular tissue.

For the high throughput genetic screen previously done in the laboratory, the Notch ligand Dl was overexpressed in all eye cells during the proliferative phase of the disc using the regulatory sequences of the *eyeless* (*ey*) gene and a *UAS-Dl* transgene (*eyeless-Gal4>UAS-Dl*), used before in (Dominguez *et al.*, 1998). These flies were crossed with flies carrying individual insertions of the original transposable P-element GS (Toba *et al.*, 1999)(Figure 8) to screen for genes that provoked tumour-like growth when co-expressed with the Notch ligand Dl in the proliferating eye tissue.

- *The Gene Search (GS) System:*

The GS vector is similar to the EP element constructed by (Rorth, 1996). It contains sequences of the mini-white gene as a marker, five tandem Gal4 binding sites (UAS) capable of overexpressing or misexpressing gene(s) located on either side of the GS insertion, followed by the

gene hsp70 minimal promoter (Figure 8). The GS transposable P-elements allow Gal4-dependent inducible expression of sequences flanking the insertion site in both directions, so that the nearest gene in the opposite direction can also be expressed. It systematically generates gain-of-expression mutations (Toba *et al.*, 1999).

This method of combining misexpression via GS or EP lines in the Dl overexpression induced overgrown background is worldwide accepted to identify and validate genes for cancer induction and suppression.

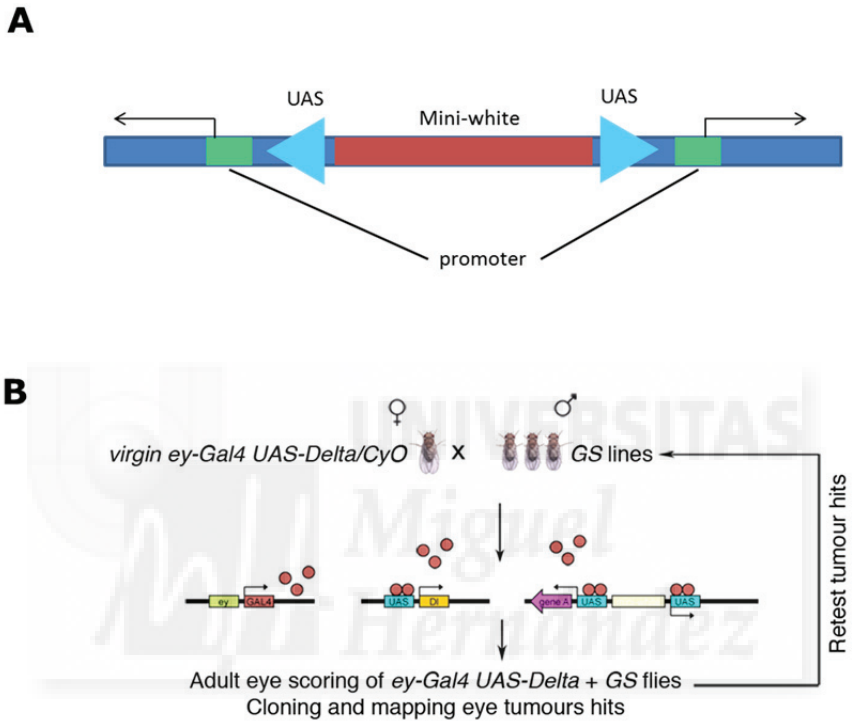

Figure 8. Scheme of a high throughput genetic screen. (**A**) Scheme of the Gene Search (GS) vector with the sequences of the mini-white gene in red, five tandem repetitions of the UAS binding sites in blue triangles and minimal promoter of the hsp70bB in green. (**B**) Notch ligand Dl was overexpressed in all eye cells during the proliferative phase of the disc using the regulatory sequences of the *ey* gene and a UAS-Dl transgene (*eyeless-Gal4>UAS-Dl*). These flies were crossed with flies carrying individual insertions of the original transposable P-element GS to screen for genes that provoked tumour-like growth when co-expressed with the Notch ligand Dl in the proliferating eye tissue. The GS vector contains five tandem Gal4 binding sites (upstream activating sequences, UAS) capable of overexpressing gene(s) lying on either side of the GS insertion.

The high throughput genetic screen started with a GS line inserted in the second chromosome. The GS element was mobilized and the individual new insertions generated were tested for their capacity to convert Dl-induced mild eye overgrowth into severe overgrowths or secondary eye growths throughout the body. In the original screen, 1514 GS lines were generated with independent insertions in the genome (Ferres-Marco *et al.*, 2006; Toba *et al.*, 1999). Among these lines approximately 0.2% induced secondary eye growth when combined with Dl overexpression.

I have divided this Thesis in two parts, in which I will describe in detail the molecular mechanisms underlying the interaction between two of these GS lines, *GS(2)518ND2* and *GS88A8*, and *Dl* in our tumour-like growth model.

4. microRNAs, and the conserved miR-7 microRNA in Delta-induced tumorigenesis.

GS(2)518ND2 can convert Dl-induced eye overgrowth (Figure 9B) into severely overgrown eyes (*ey>Dl>GS(2)518*, Figure 9C). As a control of the influence of Notch overexpression, in the absence of Dl, GS(2)518ND2 does not increase eye size (*ey>GS(2)518*; Figure 9D).

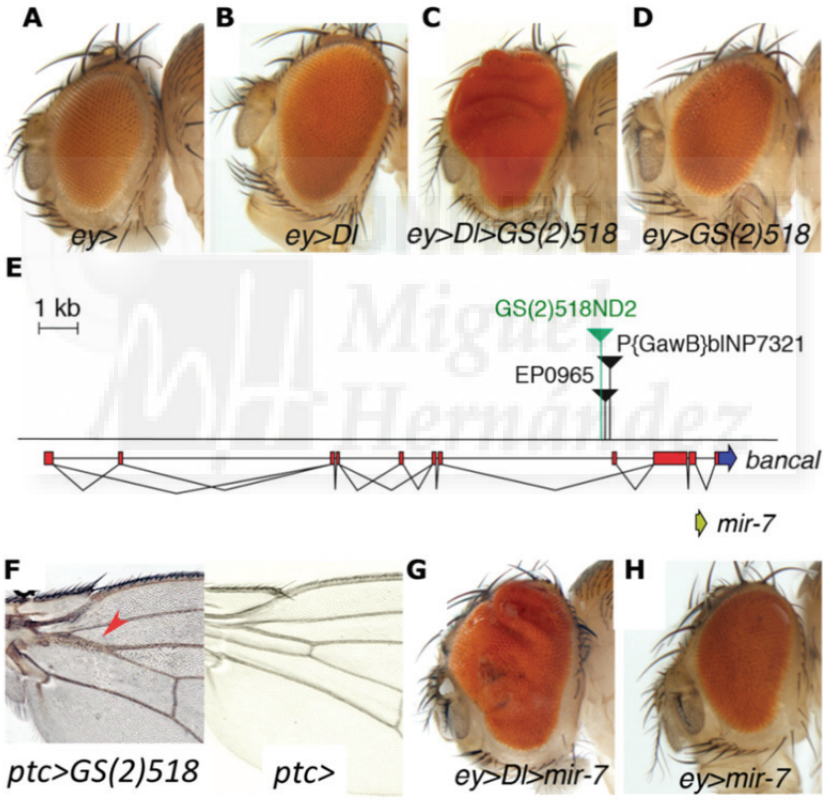

Figure 9. The microRNA miR-7 cooperates with Notch in *Drosophila melanogaster* oncogenesis. (**A-B**) *Dl* expression under the control of *ey-Gal4* results in a mild overgrowth in the eye (130% larger than wild type size). (**C**) Introducing the *GS(2)518ND2* line enhanced overgrowth by *Dl* (>320%). (**D**) The overexpression of the *GS(2)518ND2* line alone causes no eye overgrowth. (**E**) Scheme of the *GS(2)518ND2* insertion. (**F**) Overexpression of the *GS(2)518ND2* line driven by *ptc-Gal4* showed the typical wing vein L3–L4 fusion. Adult heads overexpressing *mir-7* driven by *ey-Gal4* in the presence (**G**) or the absence (**H**) of the *UAS-Dl* transgene.

The *GS(2)518ND2* line carries a 3.1 kb insertion upstream of the *mir-7* microRNA (miRNA) gene (Figure 9E), which is transcribed from an internal promoter within a 3' intron of the *bancal/heterogeneous nuclear ribonucleoprotein K* (*bl/hnRNP-K*) gene (Aboobaker *et al.*, 2005). A set

of EP elements in the vicinity of *GS(2)518ND2* has been previously described to induce proximal fusion of longitudinal (L) veins 3 and 4 (Aboobaker *et al.*, 2005; Charroux *et al.*, 2006; Li *et al.*, 2005) by overexpressing miR-7. In the same way, expressing *GS(2)518ND2* along the anterior-posterior compartment boundary in the wing imaginal disc using patched *(ptc)-Gal4*, caused similar L3–L4 fusion as that reported (*ptc>GS(2)518*; Figure 9F). In addition, direct overexpression of miR-7 together with Dl (*UAS-mir-7*) provoked overgrown *ey>Dl>mir-7* larval eye discs, resulting in adult overgrown eyes similar to that of the *GS(2)518ND2* flies (Figure 9G). As a control, there was no increase in eye size when *UAS-mir-7* alone was overexpressed by *ey-Gal4* (*ey>mir-7*; Figure 9H).

As a conclusion we can say that miR-7 cooperates with Delta to produce tumour formation in the *Drosophila* eye.

4.1 microRNAs processing and mechanisms of action.

miRNAs are small non-coding RNA molecules (containing about 22 nucleotides) found in plants, animals, and some viruses, which function regulating the levels of mRNA or protein of a specific target gene.

miRNAs are part of a genetic silencing mechanisms that was initially discovered in *Caenorhabditis elegans* by Victor Ambros' laboratory in 1993 (Lee *et al.*, 1993) while studying the gene *lin-14*. At the same time, Gary Ruvkun laboratory identified the first miRNA target gene (Wightman *et al.*, 1993). Those two ground-breaking discoveries identified a novel mechanism of post-transcriptional gene regulation. However, the recognition of the non-coding RNA molecule lin-14 as a microRNA and its importance was brought to light seven years later when Ruvkun and Horvitz laboratories identified a second miRNA, named *let-7*, in the same model nematode species (Pasquinelli *et al.*, 2000; Reinhart *et al.*, 2000) in addition to the discovery of another class of short RNA (siRNA) involved in the process of RNA interference. Both short RNA shares some members of their processing pathway.

Since its discovery, an increasing number of miRNAs have been recognized in mammals. In humans alone over 700 miRNAs have been identified and fully sequenced, and the estimated number of miRNA genes in a human genome is more than one thousand. Current estimations suggest that about one-third of human mRNAs appear to be miRNA targets (Lewis *et al.*, 2005). Each vertebrate miRNAs target about 200 transcripts and more than one miRNA might co-ordinately regulate a single target (Krek *et al.*, 2005).

The formation of a mature miRNA strand requires several steps, as seen in Figure 10. The majority of miRNA negatively regulate the expression of a gene by different processes such as translation inhibition by binding to the Untranslated Regions (UTRs) or in the Open Reading Frame (ORF) of target messenger RNAs or mRNA degradation. The last one is observed in yeast and plants (Wu *et al.*, 2008). However, it has been demonstrated that miRNAs are also able to positively regulate the genetic expression. Particularly, they have been shown to stimulate gene translation when cells are subjected to conditions that induce cell growth arrest, but the mechanisms regulating this phenomena still remain unknown (Vasudevan *et al.*, 2007).

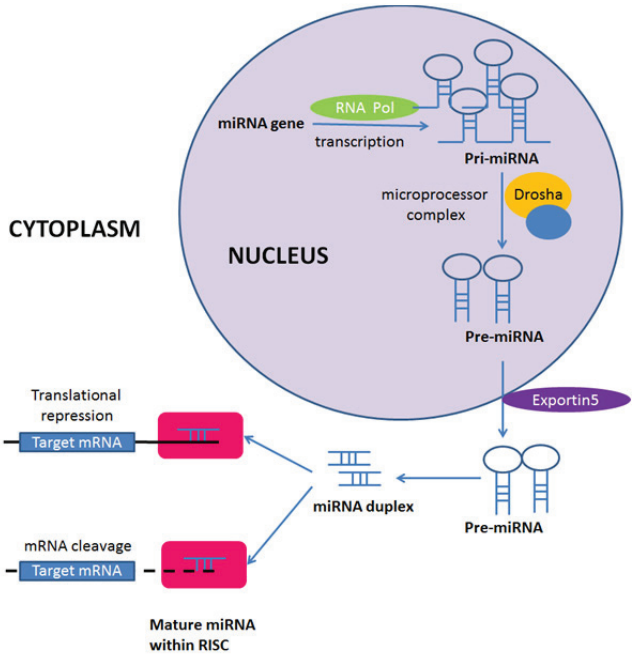

Figure 10. The microRNAs mechanisms of action. Pri-miRNAs are generated by the transcription of miRNA genes in the nucleus forming a hairpin containing the necessary instructions for its posterior processing. The microprocessor complex controls the next step in the nucleus where pri-miRNAs are digested to release hairpin structures called pre-miRNAs and it generates in the hairpin a 5' or 3' end that determines which of the arms of the pre-miRNA will be transformed into mature miRNA. Exportin-5 exports the pre-miRNAs to the cytoplasm, where Dicer cleaves the pre-miRNA to generate a double-stranded miRNA duplex. The miRNA duplex is rapidly divided. One strand is retained to become the mature miRNA and is loaded into RNA-induced silencing complexes (RISCs) to participate in the regulation of the expression of a specific mRNA, operating by either cleaving mRNA or inhibiting translation in concert with RISC. The strand is selected on the basis of its thermodynamic instability and weaker base-pairing relative to the other strand.

4.2 microRNAs in cancer

miRNAs have been described to have roles in developmental timing, neuronal cell fate, cell death, cell proliferation, regulation of insulin secretion, hematopoietic cell fate and stem cell division, etc.(Ambros, 2004; Bartel, 2004; He *et al.*, 2004). Among other roles, the influence of miRNA in stem cell division, cell proliferation and cell death is extremely interesting, due to the connection between these cellular processes and cancer development. For example, several works have demonstrated a relationship between miRNAs and other members of the processing pathway with stem cell self-renewal, from humans to *Drosophila* (Hatfield *et al.*, 2005; Houbaviy *et al.*, 2003; Suh *et al.*, 2004). As stem cells have the capacity to continuously divide, similar to what occurs in tumour cells, there is an increasing interest in the study of the mechanisms used by miRNA to control cell cycle progression.

The first human disease known to be associated with miRNA deregulation was chronic lymphocytic leukaemia (Calin *et al.*, 2002) and many miRNAs have subsequently been found to have links with various types of cancer (Esquela-Kerscher *et al.*, 2006; Hammond, 2006; Johnson *et al.*, 2005; Michael *et al.*, 2003; Mraz *et al.*, 2012; Mraz *et al.*, 2009). As they regulate the expression of protein-encoding genes it is not surprising that studies directly implicating miRNAs in cancer are emerging.

The miRNAs related with cancer development can have an anti-tumorigenic or pro-tumorigenic function. In humans, decreased levels of the anti-tumorigenic (tumour suppressor miRNAS) miR-15 and miR-16 provoke chronic lymphocytic leukaemia (Calin *et al.*, 2002; Cimmino *et al.*, 2005). They can also have a pro-tumorigenic function (oncomiRs) (Kent *et al.*, 2006) including a cluster formed by seven miRNAs (miR-17-92) amplified in different types of lymphoma (Hayashita *et al.*, 2005) (Figure 11).

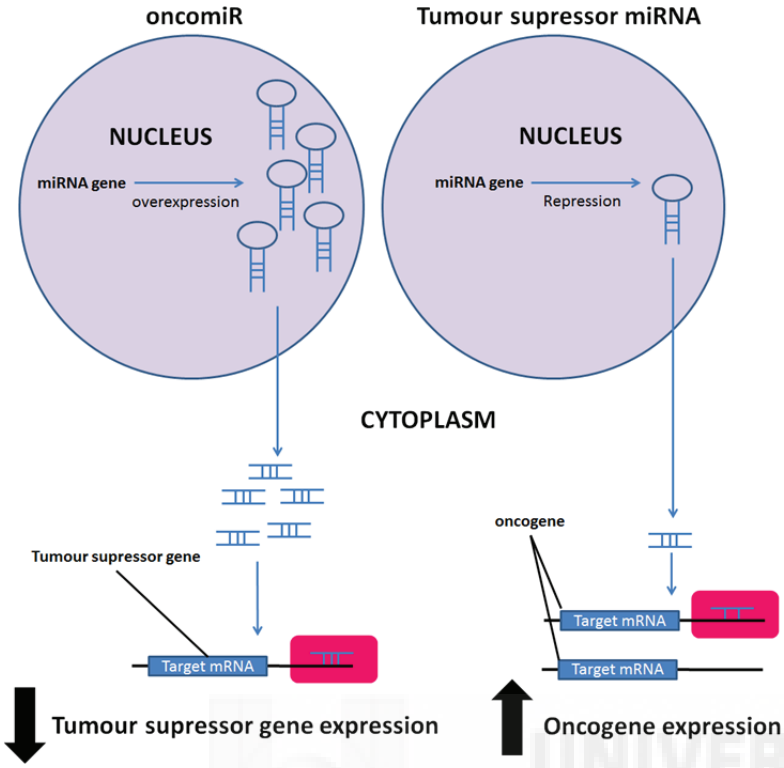

Figure 11. MicroRNAs can function as oncomiRs or as tumour suppressor microRNAs. Scheme showing that the overexpression of microRNA can repress the transcription of a tumour suppressor and its repression can release the transcription of an oncogene.

Regarding miR-7, it has a dual role, both as an oncogene (Chou *et al.*, 2010; Foekens *et al.*, 2008) and as a tumour suppressor, which may reflect the participation of the microRNA in distinct pathways. This can be due to the regulation of discrete target genes in different cell types, such as the gene Fos in mouse (Lee *et al.*, 2006), and Pak1 (Reddy *et al.*, 2008), IRS-2 (Kefas *et al.*, 2008), EGFR (Kefas *et al.*, 2008; Webster *et al.*, 2009), Raf-1 (Webster *et al.*, 2009), α-synuclein (Junn *et al.*, 2009), CD98 (Nguyen *et al.*, 2010), IGFR1 (Jiang *et al.*, 2010), bcl-2 (Xiong *et al.*, 2011), PI3K/AKT (Fang *et al.*, 2012; Xu *et al.*, 2013), and YY1 (Zhang *et al.*, 2013) in humans.

In this Thesis we aimed to reveal the mechanisms behind miR-7/Delta cooperation in tumour progression, as well as the target genes involved in this process.

5. Epigenetic repressors in cancer and BTB-containing Pipsqueak in epigenetic regulation and cancer.

The GS88A8 line has been very well characterized and studied in the laboratory (Ferres-Marco et al., 2006). The phenotype caused by its expression was called "*eyeful*" due to the formation of tumours and secondary eye growths when combined with Dl overexpression (Figure 12I). This vector is inserted in an intron of the gene *longitudinals lacking* (*lola*) (Figure 12A). The GS P-element induces a Gal4-dependent expression of *lola* and also the nearest gene in the opposite direction to transcription, *pipsqueak* (*psq*). Isolated point mutations that reverted the phenotype caused by

deregulated expression of l*ola* and *psq* showed an unequal contribution in tumour formation, being Psq the most important factor (Ferres-Marco *et al.*, 2006).

psq is a ubiquitously expressed gene that encodes eleven mRNA variants produced by alternative splicing and by the use of different promoters (Ferres-Marco *et al.*, 2006; Grillo *et al.*, 2011; Horowitz *et al.*, 1996; Lehmann *et al.*, 1998). These mRNA variants originate long and short protein isoforms that share a number of repetitive aminoacid sequences. These sequences include several OPA repeats (the sequence triplet CAX where X is either Glycine (G) or Alanine (A)) (Wharton *et al.*, 1985), regions enriched with serine/glycine (S/G), two regions containing poly- Glutamine (Q) stretches and a motif rich in histidine (H) residues, followed by four tandem copies of a conserved helix-turn-helix (HTH). This last motif is a sequence-specific DNA-binding domain called Psq DNA-binding motif (Horowitz *et al.*, 1996; Lehmann *et al.*, 1998), that binds to GAGA sequences and that, when discovered, defined a new family of DNA-binding proteins (Figure 12B). In addition to this, the long isoforms have a BTB/POZ domain (Broad-Complex, Tramtrack and Bric à brac/Poxvirus and Zinc finger (Bardwell *et al.*, 1994; Godt *et al.*, 1993; Zollman *et al.*, 1994)), which is a protein-protein interaction domain (Figure 12B). Both the BTB and the DNA-binding domain of Psq are essential for its oncogenic function, as mutations in either domain rescue the tumorigenic phenotype (Ferres-Marco *et al.*, 2006). In this Thesis we will use PsqBTB to refer to all long isoforms of Psq and non-BTB Psq for all the short isoforms.

The BTB domain was first found in some viral genes (Koonin *et al.*, 1992) and since then, it has been found in proteins of a variety of species from slime moulds (Escalante *et al.*, 1997) to humans (Albagli *et al.*, 1995). Lehman and colleagues (Lehmann *et al.*, 1998) demonstrated that a truncated form of Psq that lacks an essential part of the BTB domain showed strong binding to GAGA sequences, whereas binding of Psq with this domain could not be detected. This inhibition appears to be the result of oligomerization through protein-protein interactions mediated by the BTB domain. The tendency of BTB proteins to oligomerize in solution and their localization in distinct nuclear substructures (Bardwell *et al.*, 1994; Horowitz *et al.*, 1996; Koonin *et al.*, 1992; Raff *et al.*, 1994) suggests that they might act by modifying chromatin structure (Albagli *et al.*, 1995; Croston *et al.*, 1991; Dorn *et al.*, 1993; Kerrigan *et al.*, 1991).

Regarding the function of this gene, *psq* has pleiotropic functions during development of *Drosophila melanogaster*. It is required early during oogenesis, and it is also one of the posterior group genes responsible for pole cell formation, proper abdominal segmentation and establishment of the dorsal-ventral axis of the embryo (Horowitz *et al.*, 1996; Siegel *et al.*, 1993). During metamorphosis, *psq* is required for the formation of photoreceptors R3/R4 in the eye and for the proper differentiation of other adult structures, such as wings and legs (Weber *et al.*, 1995). Psq nuclear localization suggests that it acts, like many other BTB proteins, through binding to DNA (Horowitz *et al.*, 1996). In this line, Psq was described to encode a transcription factor essential for sequence-specific targeting of a Polycomb group protein complex (Huang *et al.*, 2004; Huang *et al.*, 2002) to its corresponding sequences called Polycomb/Trithorax Response Elements (PREs/TREs), being member of one of the three major protein complexes found in PcG (PCR1). PREs and TREs

respectively mediate epigenetic inheritance of silent and active chromatin states throughout development (reviewed in (Muller *et al.*, 2006; Schwartz *et al.*, 2007)).

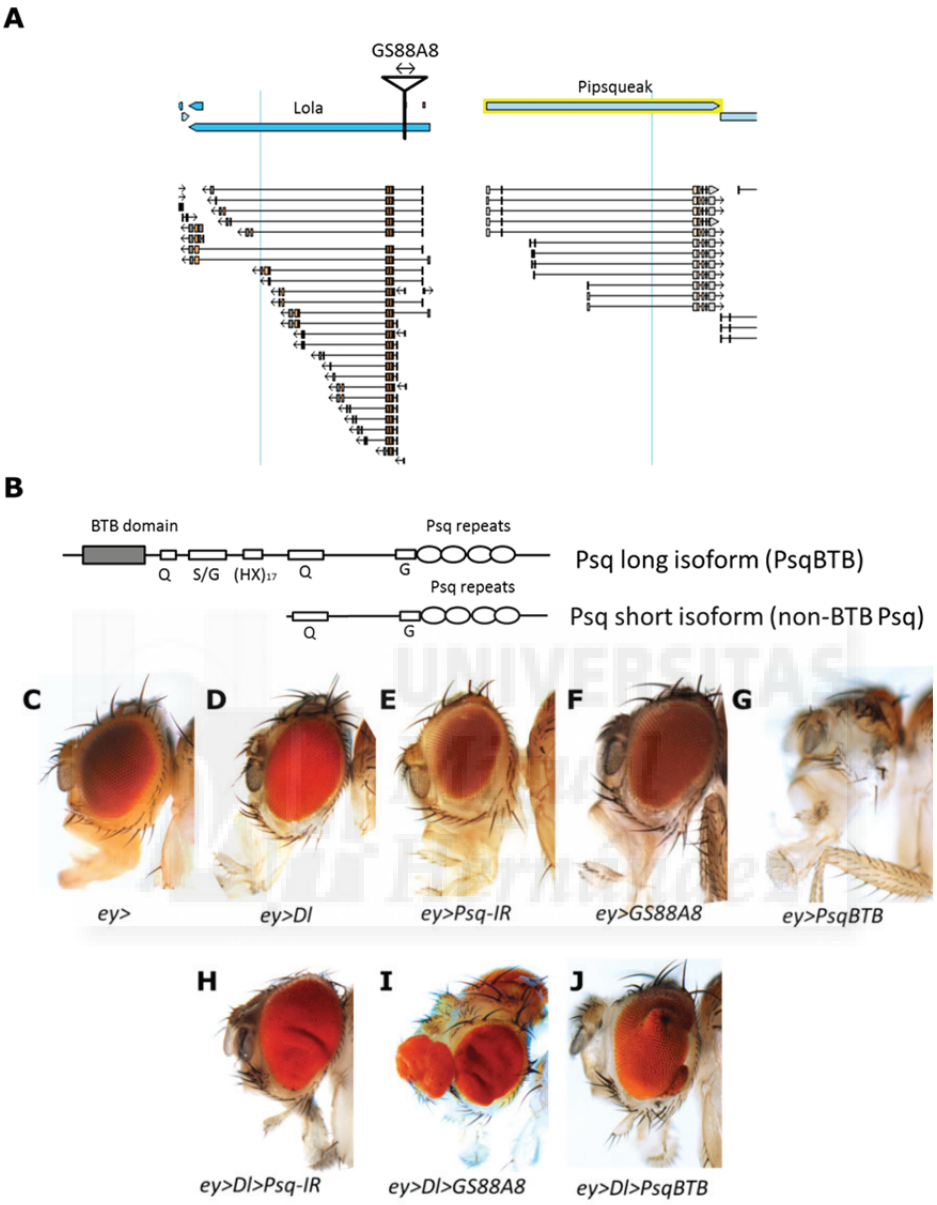

Figure 12. PipsqueakBTB induces tumour-formation in cooperation with Delta in the *GS88A8* line. (**A**) Scheme of the insertion of the *GS88A8*. The GS P-elements induces a Gal4-dependent expression of *lola* and also the nearest gene in the opposite direction to transcription, *psq*. See the different isoforms of *psq* and *lola* genes (**B**) Psq gives rise to long and short protein isoforms that share a number of repetitive aminoacidic sequences. These sequences include several OPA repeats (the sequence triplet CAX where X is either Glycine (G) or Alanine (A) and one Threonine (T)), regions enriched with serine/glycine (S/G), two regions containing poly- Glutamine (Q) stretches and a motif rich in histidine (H) residues, followed by four tandem copies of a conserved helix-turn-helix Psq repeats. Long isoforms have a BTB/POZ domain, which is a protein-protein interaction domain. (**C-J**) Control adult eyes (**C-G**, *ey>, ey>Dl, ey>UAS-Psq-IR, ey>GS88A and ey>UAS-PsqBTB*) and the effect of the loss (**H**) and gain of function of Psq using *GS88A8* (**I**) and *UAS-PsqBTB* (**J**) constructs. The loss of function of Psq in combination with Dl overexpression produces also overgrowth (**H**).

5.1 General role of Polycomb/Trithorax response elements in cellular memory.

All cells that form part of our bodies have the same genetic information but only a fraction of genes is expressed in a given cell type. It is the ability to select those genes and maintain the choice throughout multiple cell divisions which allows the existence of multiple morphologically distinct cell types in complex multicellular organisms. Epigenetics mechanisms are responsible for the maintenance of this cellular memory through cell generations without a change in DNA sequence and in the absence of their initiating signals.

Polycomb group (PcG) and Trithorax group (trxG) proteins mediate epigenetic changes conferring long-term, mitotically heritable memory by sustaining silent and active gene expression states respectively, playing a pivotal role in the dynamic regulation of many key developmental genes (called the Ying and Yang of gene regulation) (Klymenko *et al.*, 2004; Poux *et al.*, 2002). To silence or activate gene expression, PcG and trxG proteins bind to specific regions of DNA and direct the posttranslational modification of histones. These groups were discovered in *Drosophila melanogaster* as repressors and activators of *Hox* genes, a set of transcription factors that specify cell identity along the anterior-posterior axis of segmented animals (Maeda *et al.*, 2006; Ringrose *et al.*, 2004; Schumacher *et al.*, 1997; Soshnikova *et al.*, 2009).

The PcG and TrxG proteins act in several large multiprotein complexes, which have many variants (reviewed in (Lanzuolo *et al.*, 2012; O'Meara *et al.*, 2012; Schuettengruber *et al.*, 2011; Simon *et al.*, 2013) and Supplementary information, and reviewed in (Steffen *et al.*, 2014)). Regarding PcG, three major protein complexes have been described:

- PhoRC, which contains the *Drosophila* DNA-binding protein Pho (the homolog in mammals is YY1).
- Polycomb Repressive Complex 2 (PRC2), with histone methyltransferase activity and primarily trimethylates histone H3 on lysine, a mark of transcriptionally silent chromatin.
- Polycomb Repressive Complex 1 (PRC1), which recognizes these methylation marks.

In the TrxG group several proteins can be found:

- Proteins that bind to DNA in a sequence-specific manner and help to recruit chromatin-remodelling and histone-modifying complexes to regulate transcription.
- Large multimeric complexes that modify histones composed of SET domain factors like *Drosophila* Trx and Ash1 and vertebrate MLL, as well as their associated proteins.
- Large multimeric complexes that contain ATP-dependent nucleosome-remodelling activity like the SWI/SNF or the NURF complexes, and includes proteins specifically capable of reading the histone methylation marks laid down by the SET domain proteins.

For simplicity, in this Thesis we will only consider the PcG complexes PRC1, PRC2 and the TrxG Ash1 and Trx (Figure 13).

Given the antagonistic activities of PcG and TrxG, it is clear that histone modifications deposited by the two opposing groups of proteins can antagonize each other. For example, histone Lys methylation at Lys4 and Lys36 of histone H3 (H3K4 and H3K36), catalysed by Trx and Ash1, respectively, inhibits PRC2-mediated trimethylation at Lys27 of H3 (H3K27) (Schmitges *et al.*, 2011; Yuan *et al.*, 2011). These H3K27 methylation is also antagonized by H3K27 acetylation by CREB-binding protein (CBP) (Tie *et al.*, 2014; Tie *et al.*, 2009), being impossible for both modifications to coexist in the same residue (Jung *et al.*, 2010; Pasini *et al.*, 2010) (Figure 13).

A second antagonistic mechanism is found in the function of Polymerase II (Pol II). PRC1-mediated histone H2A Lys ubiquitylation adds a large molecule to the histone–DNA interface, which correlates with the presence of an unproductive Pol II state, which is phosphorylated at Ser5 and then pauses in a process referred to as promoter-proximal pausing (Brookes *et al.*, 2012; Stock *et al.*, 2007). Conversely, other proteins different from vertebrates to *Drosophila*, can phosphorylate Pol II at Ser2 promoting elongation (Devaiah *et al.*, 2012) (Figure 13).

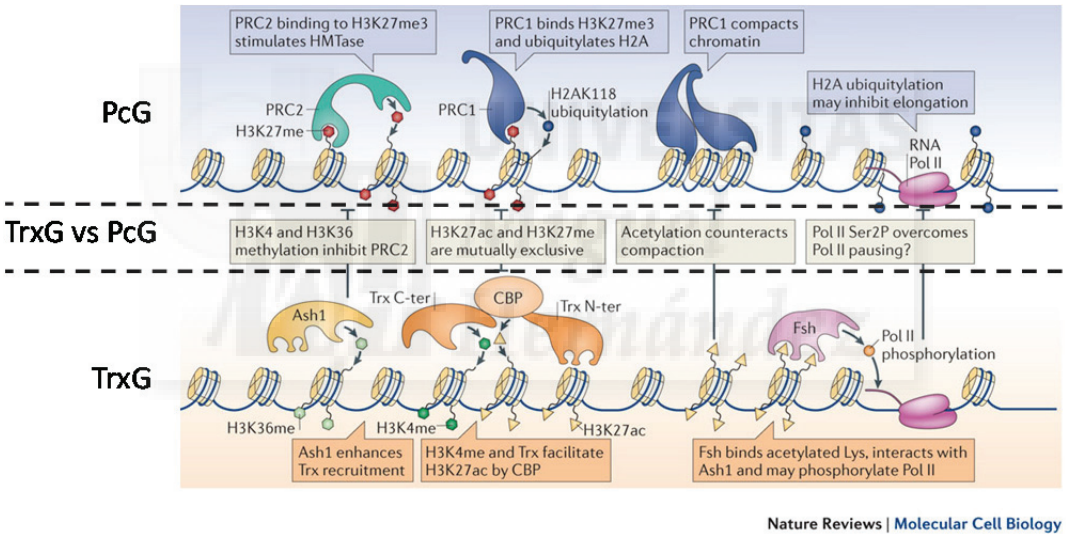

Figure 13. Overview of the Polycomb/Trithorax Group proteins. PcG and TrxG antagonize each other by histone modifications. PRC2-mediated H3K27me3 is inhibited by the methylation at Lys4 and Lys36 of histone H3 (H3K4 and H3K36), catalysed by Trx and Ash1, respectively. Moreover, the coexistence on the same residue of the antagonistic histone H3K27ac, and the methylation of H3K27 by PRC2, is impossible. A second antagonistic mechanism is found in the function of the Pol II.

Polycomb/Trithorax response elements in *Drosophila* (PREs/TREs, here called only as PREs for simplicity) are regulatory DNA elements that recruit both the PcG and TrxG proteins and their ability to switch between PcG and TrxG function may be essential for orchestrating a balance between proliferation and differentiation during normal development and also in cancer (Buszczak *et al.*, 2006; Pasini *et al.*, 2004; Ringrose, 2006; Valk-Lingbeek *et al.*, 2004). Although several fly PREs have been reasonably well characterized, their mammalian counterparts have been elusive. Recently, several vertebrate elements have been shown to share some properties of fly PREs (Kassis *et al.*, 2013).

Analysing the DNA sequences present within PREs, different binding proteins were identified: GAGA Factor (GAF, encoded by the *trl* gene), Pipsqueak (Psq), Zeste and Pho/Pho-like proteins ((Ringrose *et al.*, 2004) information review in (Steffen *et al.*, 2014) supplementary material). The GAF and Psq proteins bind to similar DNA sequences. *In vivo* imaging indicates that Psq co-localizes with GAF, both recognizing GAGA sequences, over hundreds of loci in polytene chromosomes (Schwendemann *et al.*, 2002). Both proteins operate in concert over many targets, including the homeotic genes (Decoville *et al.*, 2001; Hodgson *et al.*, 2001; Horard *et al.*, 2000; Huang *et al.*, 2002; Strutt *et al.*, 1997). They can be immunoprecipitated from nuclear extracts in a BTB mediated manner (Schwendemann *et al.*, 2002). Like Zeste, GAF, which was identified to have an important function within the TrxG proteins (Katokhin *et al.*, 2001), and Psq appear to function in both silencing and activation of genes adjacent to PRE/TREs (Bejarano *et al.*, 2004; Busturia *et al.*, 2001; Decoville *et al.*, 2001; Hagstrom *et al.*, 1997; Horard *et al.*, 2000; Huang *et al.*, 2002; Mishra *et al.*, 2001; Ringrose *et al.*, 2004).

Incorrect regulation of PcG and TrxG also plays a role in cancer initiation and progression (Richly *et al.*, 2011; Richly *et al.*, 2010). For example, in humans, the increased activity of PcG genes (EZH2, PC1, SU(Z)12 and BMI1, among others) is associated with invasive breast and prostate carcinomas, lymphomas and leukaemia (Bracken *et al.*, 2003; Chang *et al.*, 2012; Gil *et al.*, 2005; Kirmizis *et al.*, 2003; Kleer *et al.*, 2003; Raaphorst *et al.*, 2001; Varambally *et al.*, 2002). Overexpression of PcG genes (as in the case of Psq in the "*eyeful*" phenotype) possibly contributes to cancer formation by the aberrant silencing of tumour suppressor genes. Thus, it is paramount to understand the origin of the malignant epigenetic alterations in cancer precursor cells and the connection with other oncogenic pathways such as Notch.

5.2 Impact of altered BTB-containing Pipsqueak in epigenetic deregulation and tumours.

The study of the enhancement or suppression of the heterozygous Polycomb^3 ($Pc^3/+$) phenotypes that cause de-repression of *Hox* genes silencing (developing an extra sex comb on the second and third legs, as well as showing antenna-to-leg and halter-to-wing transformations at low penetrance) (Duncan *et al.*, 1975), permitted the identification of novel PcG or TrxG members, respectively. Lola and Psq mutations affect PcG-mediated epigenetic maintenance of gene silencing enhancing these phenotypes and suggesting that both Psq and Lola are members of the PcG family.

Furthermore, deregulation of *psq-lola* is sufficient to transmit epigenetic inheritance of a silenced state. Transposon silencing is a well-known phenomenon that is mediated by PcG. *Gal4*-induced overexpression of *psq-lola* with the *GS88A8* insertion caused transposon silencing in 20% of the flies tested, revealed by the inactivation of the *mini-white* gene within the transposon (Figure 14). Transposon gene silencing was reverted by both *psq* and/or *lola* mutations and the best revertants of the tumour phenotype (Psq revertants) were also the best revertants of the transposon gene silencing phenotype. *lola* encodes different transcription factors that share also a BTB domain and all but one of these contain zinc-finger motifs (Giniger *et al.*, 1994; Madden *et al.*,

1999; Ohsako *et al.*, 2003). This protein contributes also to the tumour phenotype and acts as an epigenetic silencer but only Psq contribution seems to play a predominant role in this process.

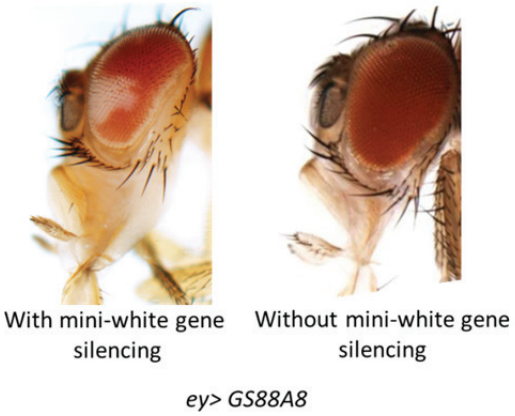

Figure 14. The *GS88A8* line inactivates the *mini-white* gene within the transposon. One of the effects that characterize the *GS88A8* line is the silencing of the *mini-white* gene (20% of the total flies in these crosses show silencing). Transposon gene silencing was reverted by both *psq* or/and *lola* mutations and the best revertants of the tumour phenotype (Psq revertants) were also the best revertants of the transposon gene silencing phenotype.

The epigenetic origin of the "*eyeful*" phenotype has been previously described (Ferres-Marco *et al.*, 2006). Like several human oncogenic proteins, such as PLZF (Promyelocityc Leukaemia Zinc Finger) or Bcl-6 (B cell lymphoma 6), which associates with PcG repressors through their BTB domain (Melnick *et al.*, 2002), Psq also interacts via its BTB domain with PcG repressors to recruit these complexes to particular genes (for example homeotic genes with GAGA sequences). Deregulation of *psq* induces tumorigenesis through aberrant epigenetic silencing of genes that contribute to the uncontrolled growth of tumour cells, shown by the loss or strong reduction of the active or open chromatin mark H3K4me3 in the developing eye tissue from which the tumour arises. This suggests that the chromatin in the mutant tissue has been condensed or silenced. Additionally, reducing the dosage of genes related to gene silencing and chromatin condensation, like *Rpd3/HDAC, E(z), Su(var)3-9, Pc,* and *Esc*, impeded tumour development. Finally, it was demonstrated that the increase in epigenetic silencing reduced the expression of the *Retinoblastoma family protein* (*Rbf*) gene, a well-known tumour suppressor gene, and this downregulation was shown to be necessary for tumour development. In summary, results from our laboratory confirmed that overexpression of Psq combined with Dl overexpression act as epigenetic regulators of PcG family in the formation of highly invasive tumours (Ferres-Marco *et al.*, 2006).

Based on this work, *psq* works as an oncogene, however there is evidence pointing also to a tumour suppressor function. First, the loss of function of all Psq isoforms in the same Dl overexpression background also produces hyperplasic eyes (Figure 12H). Second, in an epidermal growth factor receptor (EGFR) overexpression context, the knock-down of Psq also led to tumour formation (Herranz *et al.*, 2014). All together, these data suggests multi-faceted and apparently contradictory functions of Psq in tumorigenesis. To understand this riddle would represent a big step forward in the comprehension of cancer, as it could serve as a model to unveil how other BTB proteins with such dual roles exert their functions and contribute to tumour development. In the second part of this Thesis work we set out to address this paradox.

6. BTB-containing protein interactions.

The BTB domain is a protein–protein interaction motif that determines a unique tri-dimensional fold with a large interaction surface. The exposed residues are highly variable and allow dimerization and oligomerization, as well as interaction with a number of other proteins. BTB-containing proteins are numerous and control cellular processes that range from actin dynamics to cell-cycle regulation (Perez-Torrado *et al.*, 2006).

Already in 1994 (Zollman *et al.*, 1994) a set of BTB-domain families were described, where one particularly conserved subgroup is apparent, the ttk group (exclusively formed by *Drosophila* members). This group includes: the Broad-Complex, Bric à brac, GAF, Lola like, Fruitless, PsqBTB and Mod(mdg4), as well as Tramtrack, the first to be identified. This BTB-domain family is known to mediate the formation of multimers between different BTB proteins and it contains several highly conserved sequences not found in other BTB domains (Bonchuk *et al.*, 2011). As shown previously, the BTB domain of GAF can interact with the BTB domains of Lola like (Faucheux *et al.*, 2003; Mishra *et al.*, 2003), PsqBTB (Schwendemann *et al.*, 2002), Tramtrack (Pagans *et al.*, 2002) and Mod(mdg4) (Melnikova *et al.*, 2004), the last one implicating GAF in the insulator function (Schweinsberg *et al.*, 2004) among other multiple functions: transcription derepression/activation (Biggin *et al.*, 1988; Tsukiyama *et al.*, 1994), repression (Hagstrom *et al.*, 1997; Mishra *et al.*, 2001), barrier formation (O'Donnell *et al.*, 1994), enhancer blocking (Ohtsuki *et al.*, 1998), and insulator bypass (Melnikova *et al.*, 2004).

Insulators were defined as DNA-protein complexes that are experimentally classified by their ability to block enhancer-promoter interactions and/or serve as barriers against the spreading of the silencing effects of heterochromatin (Gaszner *et al.*, 2006). But they have been recently characterized as multi-protein DNA complexes capable of facilitating long-range inter-chromosomal and intra-chromosomal interactions, being crucial players in constructing appropriate three-dimensional nuclear architectures (reviewed in (Schoborg *et al.*, 2014; Van Bortle *et al.*, 2013)). There are different subclasses of *Drosophila* insulators and each subclass contains a different DNA binding protein that may define the specific function of the corresponding subclass (reviewed in (Gurudatta *et al.*, 2009)) and common BTB proteins that seem to mediate the contacts between individual insulators sites. We can find at least five insulators studied in detail. One of the most extensively studied insulators is located in the 5' UTR region of the *Drosophila gypsy* retrotransposon. Many of the spontaneous mutations caused by *gypsy* elements are due to the blocking of enhancer-promoter interactions attributable to this insulator sequence (Dorsett, 1993; Gdula *et al.*, 1996; Geyer *et al.*, 1992; Geyer *et al.*, 1986; Modolell *et al.*, 1983). A 430-bp fragment of *gypsy*, termed "the *gypsy* insulator," placed between an enhancer and its target promoter was sufficient to block enhancer stimulation (Parnell *et al.*, 2000; Smith *et al.*, 1992; Wei *et al.*, 2000). In *Drosophila*, several insulator binding proteins have been identified and characterized since then, including for example, the *Drosophila* homolog of CTCF (dCTCF), Boundary Element Associated Factor of 32 kDa (BEAF-32), and Suppressor of Hairy wing (Su(Hw)) (Gurudatta *et al.*, 2009). These

DNA-binding proteins require additional proteins for functional insulator activity, including Centrosomal protein 190 (CP190) and Modifier of mdg4 (Mod(mdg4)) (Gerasimova *et al.*, 2007; Ghosh *et al.*, 2001; Pai *et al.*, 2004). The *mod(mdg4)* gene encodes 29 different isoforms that arise by alternative cis- and trans-splicing (Buchner *et al.*, 2000). Mod(mdg4)2.2, one of the isoforms of the Mod(mdg4) group, interacts with the Su(Hw) protein and is involved in the enhancer-blocking activity of Su(Hw)-dependent insulators such as the *gypsy* insulator (Ghosh *et al.*, 2001; Golovnin *et al.*, 2012). Mod(mdg4)2.2 is essential for functional insulator activity (Pai *et al.*, 2004) and with its BTB domain in the N-terminal region mediates homo- and hetero-multimerization with other insulator components such as CP190. Although the BTB domain of *Drosophila* CP190 protein was not initially classified as a member of the ttk group (Bonchuk *et al.*, 2011) it was later described as essential for its association with the Su(Hw)-Mod(mdg4) insulator complex, and the interaction between Mod(mdg4)2.2 and CP190 BTBs, which mediates clustering of insulator complexes (Ghosh *et al.*, 2001; Oliver *et al.*, 2010) (Summary in table 1 of published interactions between BTB proteins).

	GAF	Lola Like	Mod(mdg4)	PsqBTB	CP190
GAF	+	+	+	+	
Lola Like	+	+	+	+	
Mod(mdg4)	+	+	+		+
PsqBTB	+	+		+	
CP190			+		+

Table 1. Known interactions between BTB-containing proteins. The BTB domains of GAF and Lola like formed a wide range of complexes and interact with other BTB domains tested, forming stable high-order multimeric complexes. The interaction between Mod(mdg4)2.2 and CP190 BTB domains mediates clustering of insulator complexes.

OBJECTIVES

UNIVERSITAS
Miguel
Hernández

The general objectives of this work are to expand our understanding of the fundamental mechanisms of tumorigenesis with a focus on the Notch pathway. Specifically, using an interdisciplinary approach, we have investigated the molecular mechanisms underlying the tumour initiation and progression by two factors that facilitate Notch-driven tumorigenesis, involving a conserved microRNA (miR-7) and a BTB-containing transcriptional regulator (Pipsqueak).

This work is presented in two sections (1 & 2):

- **Section 1**. Conserved microRNA miR-7 orchestrates the activities between two growth organizers and when deregulated it facilitates Notch-induced tumorigenesis.

- **Section 2**. Epigenetic regulator Pipsqueak is a multifaceted transcription factor that binds chromatin insulators and sites with potential wider roles in chromatin remodelling than anticipated.

UNIVERSITAS
Miguel
Hernández

RESULTS

UNIVERSITAS
Miguel
Hernández

Section 1. Conserved microRNA miR-7 facilitates Notch-induced tumorigenesis by orchestrating the activities between opposed organizers.

1. Interference Hedgehog is the functional relevant target of miR-7 in tumorigenesis.

As previously mentioned in the introduction, miRNAs are small noncoding RNAs that negatively regulate gene expression by binding to the UTRs or in the ORF of target messenger RNAs, inhibiting translation or driving mRNA degradation. Considering these mechanisms, we can assume that *mir-7* overexpression and its tumour phenotype induced in the context of Dl overexpression, would be mimicked by the endogenous downregulation of its functionally relevant target genes in the same context. We can select *a bona fide* miR-7 target gene considering only those that do not produce any effect when downregulated in the context of the endogenous or unaffected Notch signalling. For this purpose, we used RNA interference (RNAi) (Table S1 in Appendix I) to downregulate *in vivo* a set of *Drosophila* genes predicted to be miR-7 targets *in silico* by several algorithm, as was previously described (Maziere *et al.*, 2007). The UAS-IR or RNAi transgenes produce the degradation of specific mRNA transcripts with the generation of double-stranded RNA fragments complementary to the transcript driven by GAL4/UAS system (Dietzl *et al.*, 2007; Ni *et al.*, 2011).

A miRNA can potentially bind and regulate multiple mRNA molecules and, at the same time mRNA molecules can be regulated by different microRNAs, making the validation and the search of target genes a very difficult task. There are several algorithms to computationally identify target mRNA of miRNAs from different *Drosophila* species (Enright *et al.*, 2003; Stark *et al.*, 2003) to humans (miRanda http://www.microrna.org/microrna/home.do, PICTAR http://pictar.mdc-berlin.de/, TARGETSCAN http://www.targetscan.org/). The important parameters in the application of an algorithm are: complementarity between miRNA and mRNA in the first eight nucleotides, the conservation of the binding site among species and the number of binding sites in the 3'UTR sequence of the mRNA. Every algorithm generates a list of candidates suspected of being regulated by a miRNA which should be subsequently validated in a certain cellular context (Enright *et al.*, 2003).

In *Drosophila*, multiple cell-specific targets for miR-7 have been previously validated via luciferase or *in vivo* eGFP-reporter sensors or less extensively via functional studies (Aparicio *et al.*, 2015; Huang *et al.*, 2013; Lai *et al.*, 2005; Li *et al.*, 2005; Li *et al.*, 2009; Pek *et al.*, 2009; Stark *et al.*, 2005; Stark *et al.*, 2003; Tokusumi *et al.*, 2011; Yu *et al.*, 2009). Although microRNAs are thought to regulate multiple target genes, only a subset of the *in vivo* tested targets respond in a given cellular context.

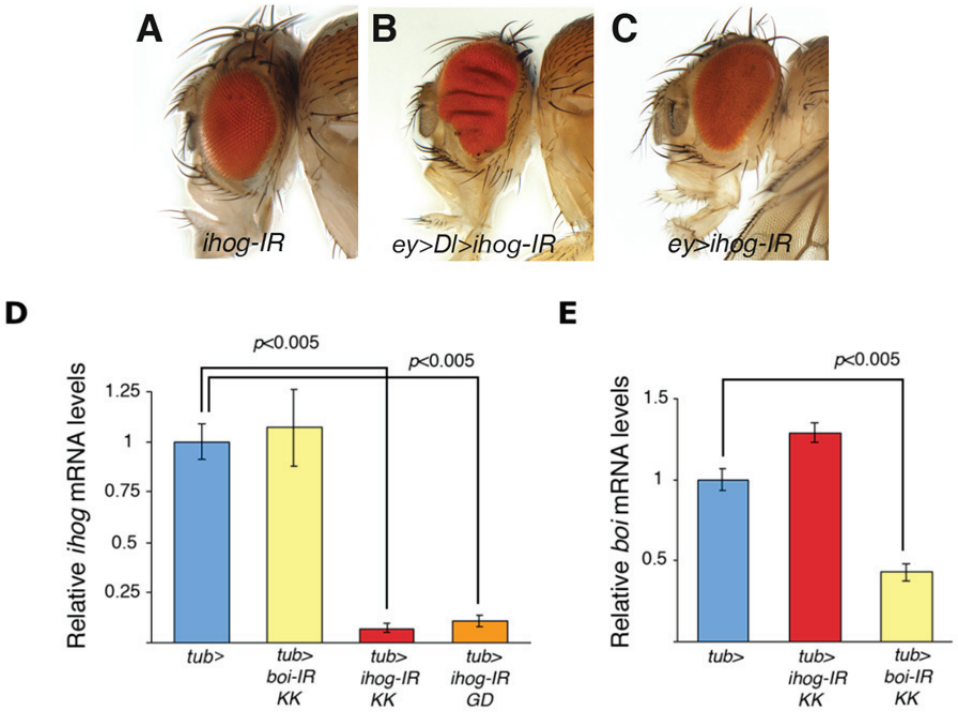

Figure 15. The Hedgehog co-receptor interference hedgehog (*ihog*) is a predicted target of microRNA miR-7 and its repression induces tumour formation with the Delta transgene. (**A–C**) Adult heads of female control *UAS-ihog-IR* (**A**) and combinations of *UAS-ihog-IR* and *ey-Gal4* in the presence (**B**) or the absence (**C**) of the Dl transgene. (**D-E**) Relative mRNA levels of *ihog* (**D**) and *boi* (**E**) in larvae expressing different *UAS-ihog-IR* and *UAS-boi-IR* under a *tubulin-Gal4* line, as a control of an effective knock-down of these genes.

Only two genes of the 39 candidate target genes tested robustly cooperated with Dl-Notch signalling to provoke severely overgrown and folded eyes. A previously validated target of miR-7, *hairy* (Stark *et al.*, 2003) was capable of converting Dl-induced mild overgrowth into tumour growth. The expression of the endogenous levels of *hairy* and its GFP-3'UTR sensor were described to be subtly reduced by miR-7 (Stark *et al.*, 2003). Thus, we focused our interest on other gene, *interference hedgehog* (*ihog*), whose downregulated in Dl-overexpressing cells provoked robust overgrowth and increased cell proliferation quantified by PH3 immuno-staining (Figure 15, Figure 16 and Table S1:80% of severe overgrown eyes, n=200) mimicking the miR-7 induced overproliferation (Figure 16C-D' and H). As was previously described in the introduction, iHog is one of the two functionally redundant co-receptors of the Hh signalling pathway in *Drosophila* (coded by the genes *ihog* and *boi*) which initiates the signalling cascade after the binding of the Hh secreted protein. We can mimic the boost in the levels of proliferating cells produce by the loss of function of iHog with the reduction in the amount of the downstream Hh signalling effector, Ci activator (Figure 16G). Moreover, the expression of ihog RNAi alone during eye development has no effect on the normal size of this organ (*ey>ihog-IR*; Figure 15C), confirming that the tumour phenotype is a consequence of the cooperation between miR-7 through Ihog and the overexpression of the Notch signalling pathway.

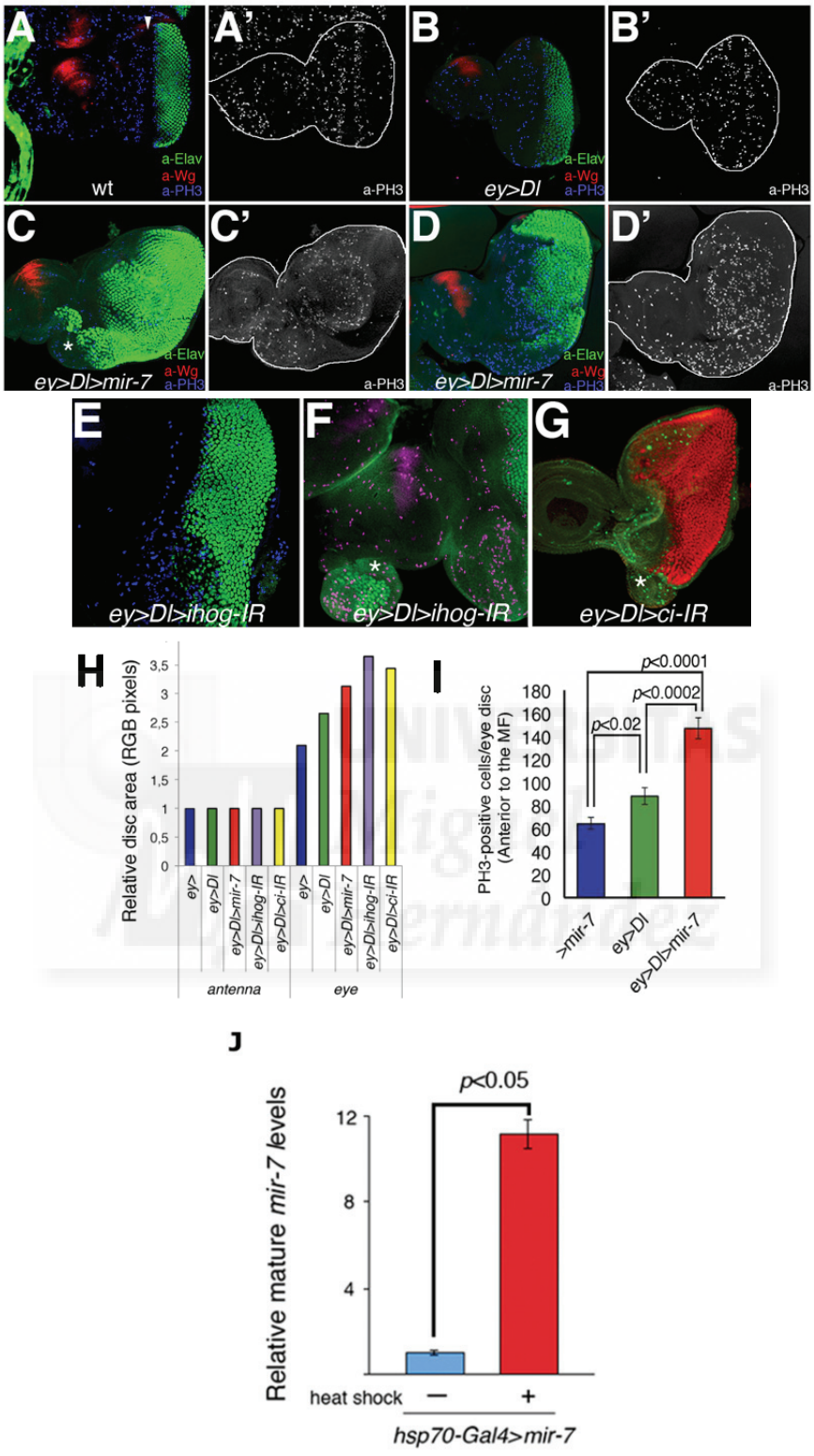

Figure 16. Overgrowth in eye discs co-expressing Dl and the knock-down of Hh signalling. Confocal images show the mitotic marker PH3 (blue in **A–E**; pink in F and green in **G**), neuronal marker Elav (green, **A–F** and red in **G**), and Wg (red, **A–D** and pink in **F**) staining of third instar eye-antennal imaginal discs of wild-type *ey-Gal4* (ey>, **A–A'**), *ey-Gal4 UAS-Dl (ey>Dl,* **B–B'***), ey-Gal4 UAS-Dl/+; UAS-mir-7/+ (ey>Dl>mir-7,* **C–D'***), ey-Gal4UAS-Dl/+; UAS-ihog-IR/+ (ey>Dl>ihog-IR,* **E–F***), and ey-Gal4 UAS-Dl/+; UAS-ci-IR/+ (ey>Dl>ci-IR,* **G**). The asterisks point to undifferentiated outgrowth of the eye discs (**C, F**, and **G**). Eye disc overgrowth is also accompanied by an aberrant retinal differentiation, seeing by the *ey-Gal4* transgene (driving

expression anterior to the MF (white arrowhead in **A**), where eye disc cells proliferate asynchronously). Posterior to the MF, subsets of cells start differentiating into photoreceptor neurons visualized Elav (green, **A**) and the remaining cells divide one last time synchronously (row of PH3 cells behind the MF). (**H**) Quantitation of the eye imaginal disc size of the indicated genotypes. The area for each disc was calculated in pixel using the software ImageJ and values were normalized with those of the corresponding to antennal disc or eye disc part. As expected, co-expressing Dl with the RNAi against *ihog* or *ci* with *ey-Gal4* provoked overgrowth similar to the one observed when miR-7 is overexpressed. (**I**) Quantitation of the number of PH3 positive cells in the anterior region to the morphogenetic furrow reveals a statistically significant enrich of these cells in the tumour phenotype compared to its controls. (**J**) Control of the expression of the mature *mir-7* levels with the *UAS-mir-7* construct expressed by *hsp70-Gal4* line with (red bar) or without a heat shock (blue bar).

Thus, specific down-regulation of endogenous ihog*, a predicted target of miR-7, facilitates overgrowth by Dl overexpression similar* to the phenotype observed *when* mir-7 *is overexpressed in this context*.

2. Direct silencing of Interference Hedgehog by miR-7 *in vitro* and *in vivo*.

To assess whether the genes corresponding to the co-receptors iHog and Boi are directly regulated by miR-7, we made a luciferase reporter-based cellular assays *in vitro* and *in vivo* (Figure 17).

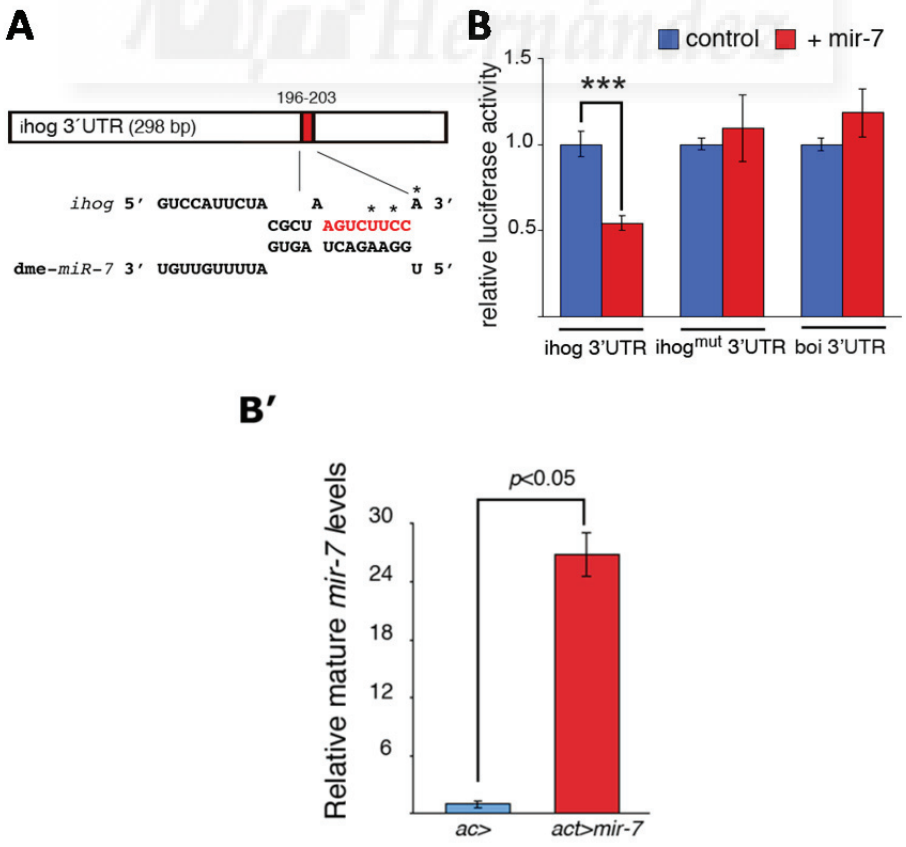

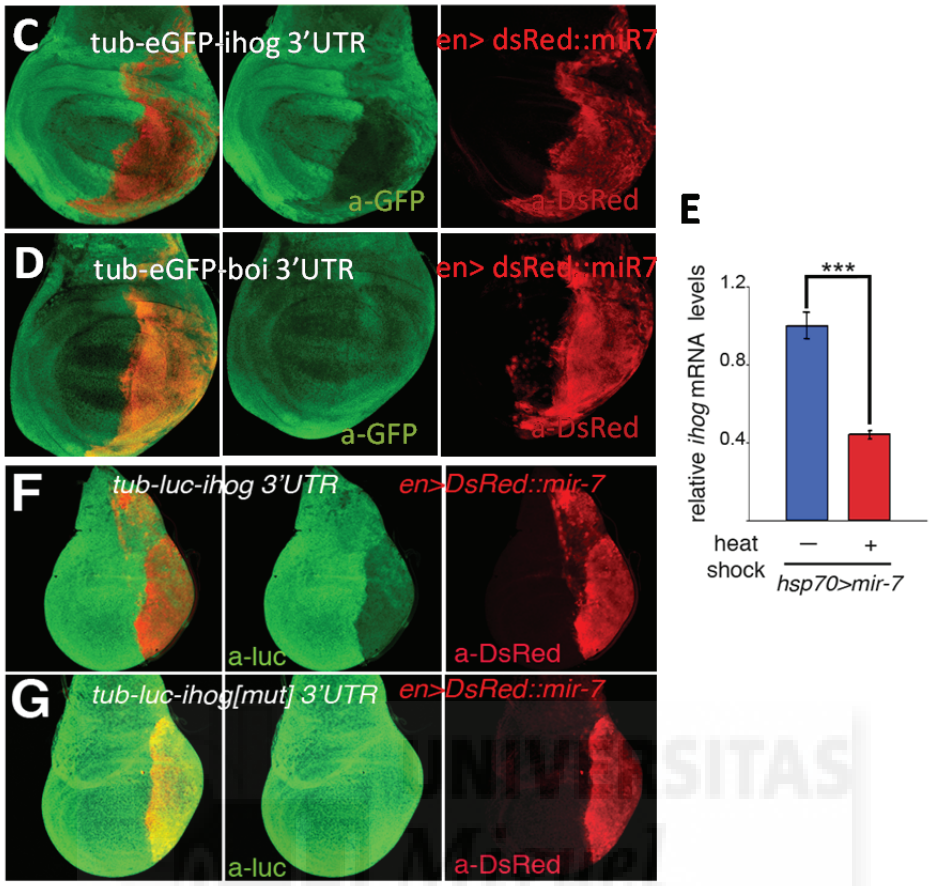

Figure 17. miR-7 directs repression of *interference hedgehog* (*ihog*). (**A**) Computer predicted consequential pairing of *ihog* target region (top) and miRNA (bottom). The conserved seed match in the 3'UTR of *ihog* is in red. (**B**) Luciferase assay in S2 cells co-transfected with *mir-7* (red bars) or the empty vector (blue bars), together with a firefly luciferase vector containing the ihog3'UTR (ihog3'UTR), or the luciferase vector with mutations in the seed sequence (asterisks in **A**, ihog^{mut}3'UTR) or control boi3'UTR (boi3'UTR). Firefly luciferase activity was measured 48 hr after transfection and normalized against Renilla luciferase. The values represent the mean ± s.e.m. of three independent experiments. Differences in ihog^{mut} and *boi* luciferase levels were not statistically significant between treatments. (**B'**) Quantitation of relative *mir-7* levels in S2 cells transfected with a plasmid *act-Gal4* in combination with (red bar) or without (blue bar) the plasmid *UAS-mir-7*. (**C–G**) Confocal images of mid third instar wing discs overexpressing *mir-7* by *en-Gal4* and *DsRed::mir-7* (*en>DsRed::mir-7*, red). This genetic combination causes reproducible *in vivo* downregulation of eGFP in a *tub-eGFP::ihog-3'UTR* (**C**) but not in a *tub-eGFP::boi-3'UTR* sensor (**D**). The same result was obtained using *tub-luc::ihog-3'UTR* (**F**) but not the *tub-luc::ihogmut3'UTR* sensor (**G**) with the overexpression of *mir-7* by *en-Gal4* (*en>DsRed::mir-7*, red) and stained with a-luciferase antibody (green). (**H**) Differences in *ihog* mRNA levels assessed by qRT-PCR between *hsp70>mir-7* larvae subjected to heat shock treatment (red bar) or not (blue bar). Values represent the mean ± s.e.m. of three independent experiments. P values were calculated by the unpaired Student's t test.

There is a single conserved miR-7 binding site in the 3'UTR of *ihog* (but not in *boi*) (Figure 17A). We observed that in S2 cells overexpressing *mir-7*, there was 45% less activity of a luciferase reporter containing the full-length ihog 3' UTR downstream of the firefly luciferase coding region driven by the tubulin promoter (*tub-luc::ihog-3'UTR*, Figure 17B) than the control *ihog* 3'UTR construct carrying point mutations in the miR-7 binding site (*tub-luc::ihog(mut)-3'UTR* Figure 17B).

Moreover, luciferase activity was unaffected by *mir-7* overexpression in S2 cells expressing a *tub-luc::boi-3'UTR* construct (Figure 17B).

After validating the direct regulation of *ihog* mRNA 3'UTR by miR-7 *in vitro*, we injected the *tub-luc::ihog(mut)-3'UTR* construct in flies to test if this regulation also occurred *in vivo*. To monitor *ihog* expression in this experiment we used a luciferase antibody or an eGFP construct (*tub-eGFP::ihog-3'UTR*) and a GFP antibody. In these conditions, we observed a specific *in vivo* repression of the *tub-luc::ihog(mut)-3'UTR* construct in the posterior compartment cells of third instar wing discs overexpressing *mir-7* driven by engrailed *(en)-Gal4* (Figure 17C and F). This repression was not visible when we used using the luciferase *ihog* 3'UTR construct that carried the mutations in the seed sequence (Figure 17G) or in the case of *boi* 3'UTR eGFP sensor (tub-eGFP::boi-3'UTR) (Figure 17D).

Finally, using heat shock induction of mature *mir-7* overexpression (*hsp70-Gal4 UAS-mir-7*) and performing qRT-PCR, we demonstrated that endogenous *ihog* mRNA was reduced 55% by miR-7 *in vivo* (Figure 17E).

These data provided the evidence that miR-7 is capable of directly repress ihog*, both in vitro and in vivo. Thus, the synergism between miR-7 and the Dl-Notch pathway activity in eye overgrowth appears to be owing to the silencing of* ihog.

3. RNAi-based silencing of other Hedgehog components and endogenous mutations mimics the effects produced by miR-7 overexpression in Notch induced tumorigenesis.

To further support the previously described results we replicated the tumour formation in the context of Dl overexpression by disrupting the expression of the different Hh signalling pathway components.

As a reminder, in *Drosophila*, the Hh signalling pathway begins with the binding of Hh molecule to its receptors iHog and Boi producing the release of the inhibition exerted by Ptc over Smo inducing the transcription of Hh target genes by the active form of Ci (Ci-155 or CiA). In the absence of Hh, Ptc inhibits Smo, leading to the proteolytical processing of Ci into a truncated form (Ci-75 or CiR) inhibiting Hh target genes transcription.

Combining the overexpression of the Notch ligand Dl with the loss of function of the Hh signalling pathway produced by the knock-down of *smo* (80% flies exhibited eye tumour-like growth, n >200), *ci* (100%, n>200) or *hh* secreted protein (30%–100%, n>200) or with the overexpression of the repressor form of *ci-75* or *CiR* (75% n = 100), mimics the tumour formation produced by the loss

of function of the initially found member of the Hh signalling pathway, iHog (Figure 18B-H). In the same way, the up-regulation of the Hh signalling pathway, through *hh* and *ci* activator form overexpression, in the context of Dl-miR7 expressing cells, causes a significant reduction in tumour eye size in flies *ey>Dl>mir-7>hh* (100% rescue, n>100 Figure 18K) and also in flies *ey>Dl>mir-7>ciA* (100% rescue, n>100 Figure 18L). In addition to the RNAi experiments, we also generated marked clones of cells homozygous for hh^{AC} (a null allele) in the *ey>Dl* background (hh^{AC}/hh^{AC} *ey>Dl*; Figure 18 I-J). Eye discs carrying small patches of hh^{AC} cells were larger than control wild-type eye discs (Figure 18J) or *ey>Dl* without hh^{AC} clones eye discs (see Figure 18I).

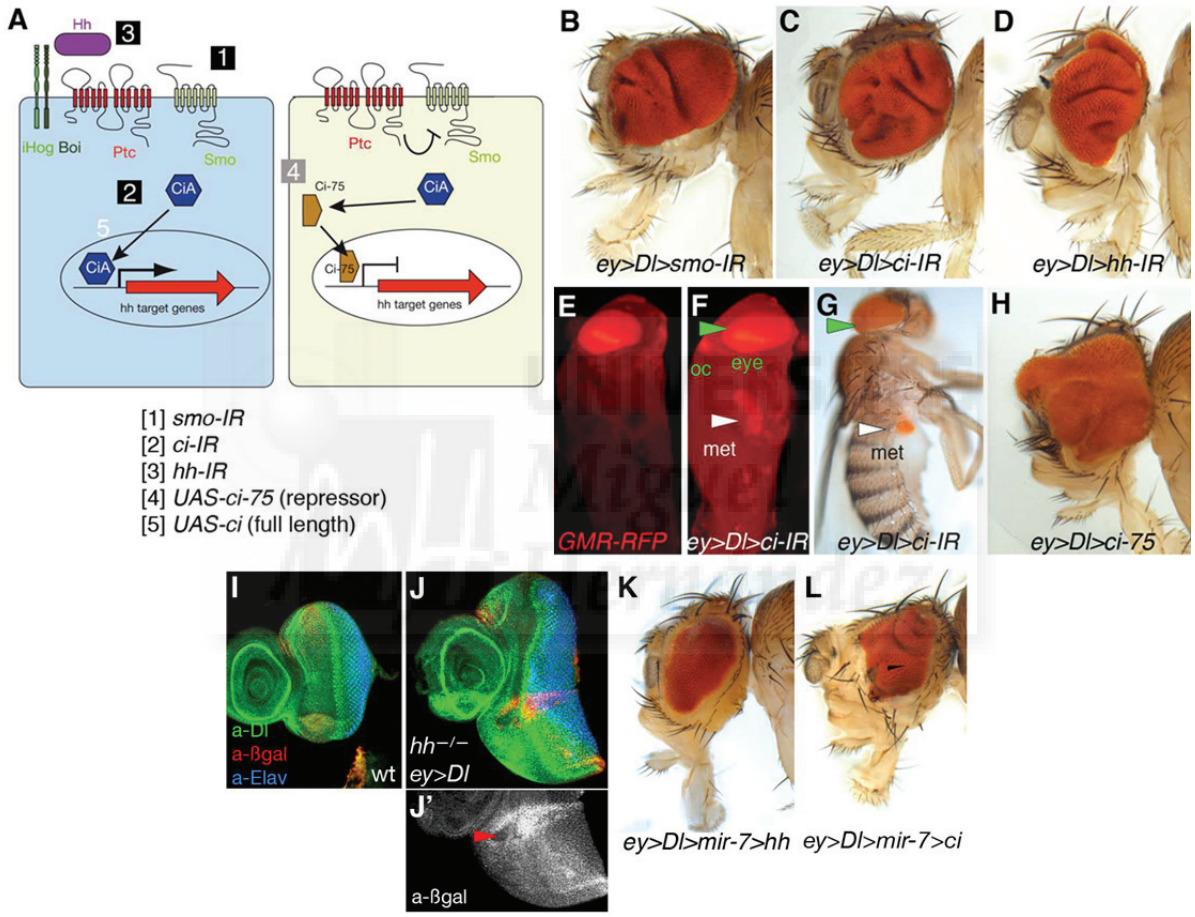

Figure 18. Deregulation of Delta with other elements in the Hedgehog pathway cooperates to tiger tumour growth in the *Drosophila* eye. (A) Schematic representation of Hh signalling showing the UAS transgenes used to downregulate by RNAi (IR) or activate Hh pathway components. (**B–D, H**, and **K–L**). Adult heads of female flies of combinations of the indicated UAS transgenes and *ey-Gal4*. (**E–F**) Fluorescent images of *Drosophila* pupae of sibling control (*ey>Dl*, **E**) or *ey>Dl>ci-IR* (**F**). (**G**) Adult fly of *ey>Dl>ci-IR* with a metastatic (met) growth in the abdomen. Eye tissue in the endogenous site (green arrowheads) and distant site (white arrowheads) is labelled by the retinal-specific *GMR-myrRFP* marker (**E, F**) or the retinal-specific red pigments (**G**). (**I–J'**) Third instar wild type of sized eye disc (**I**) and *ey>Dl* eye disc carrying clones of hh^{AC} labelled by the absence of *arm-lacZ* (ßgal, red in (**J**) and grey in (**J'**)). Arrowhead points to a clone and its associated twin spot (high red staining). Genotype in (**J**) is*: yw ey-Flp; ey-Gal4 UAS-Dl/+; FRT82B* hh^{AC}*/FRT82B arm-lacZ*.

Interestingly, downregulation of *ci* by RNAi (*ci-IR*) using *ey-Gal4* flies, caused a metastatic overproliferation of eye tissue in the context of Dl gain of function, resulting in flies with secondary eye growths within the thorax and abdomen (Figure 18E–G and Table S2 in Appendix I). This invasive overgrowth is also observed when Dl and the *ci* RNAi transgene are expressed in the wing imaginal discs using a *dpp-Gal4* enhancer trap (Figure 19).

Epithelial-to-mesenchymal transition (EMT) is a process in which cells lose their epithelial character and acquire a migratory mesenchymal phenotype (Thiery *et al.*, 2009). Although being crucial for normal development, EMT (and the reverse process mesenchymal-to-epithelial transition MET) is thought to be recapitulated in metastasizing cancer cells (Yilmaz *et al.*, 2009). Loss of the cell adhesion molecule E-Cadherin is considered a hallmark of EMT (Yang *et al.*, 2008). As it occurs in the case of cells overexpressing Dl in combination with a knock-down of *ci* and undergoing EMT, it has been reported that the RNAi-mediated knockdown of GLI1 (the mammal counterpart of Ci activator), abolished characteristics of epithelial differentiation and increased cell motility to induce EMT. This phenomenon occurs in pancreatic ductal adenocarcinoma and lung squamous cell carcinomas via direct regulation of E-cadherin transcription (Joost *et al.*, 2012; Tang *et al.*, 2015; Yue *et al.*, 2014). However, the conjunction of this phenomenon with the up-regulation of the Notch signalling pathway still remains unsolved.

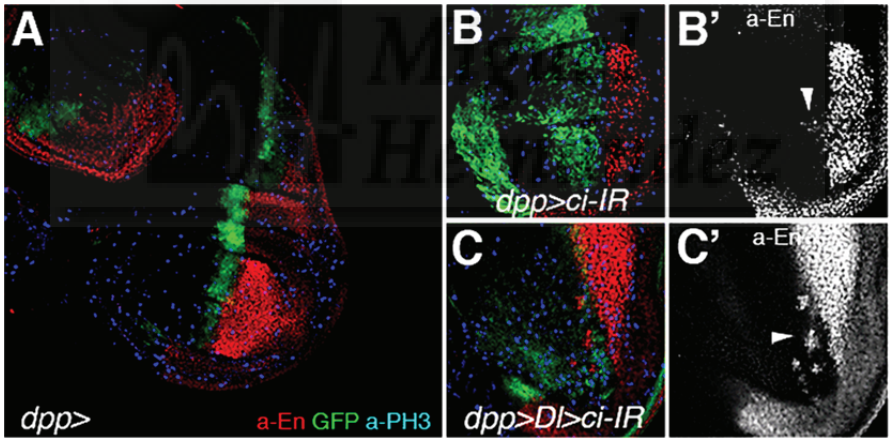

Figure 19. The loss of Cubitus active form and the co-expression of Delta produced invasive growth in the wing primordium. (**A**) Wild-type third instar wing imaginal discs. *dpp-GAL4 (dpp>)* drives expression of *UAS-GFP* (green) in a narrow band of anterior cells along the anterior-posterior compartment boundary. Expression of mitotic marker a-PH3 (blue) and a-En (red) are also shown. (**B**) Expression of the RNAi transgene against *ci* (*dpp>ci-IR*) led to anterior expansion of the *dpp* domain visualized by GFP (green) and ectopic posterior cells (grey in **B'**) in the anterior territory at the dorsal-ventral boundary, but the disc was not overgrown. (**C**) Co-expression of Dl along with *ci-IR* led to extensive overgrowths.

4. Notch pathway and miR-7 converge on Hedgehog inhibition.

Although *boi* mRNA expression was not affected in the *ihog-IR* lines and *boi* does not appear to be a target of miR-7, there is a well-documented functional overlap in the roles of Ihog and Boi, and a genetic inactivation of both genes is necessary to induce *hh* loss-of-function phenotypes (Camp *et al.*, 2010; Yao *et al.*, 2006; Zheng *et al.*, 2010). Indeed, the human homologs of these proteins, CDON (named after Cell adhesion Molecule-related/down-regulated by oncogenes) and BOC (Brother of CDON), also act as obligatory co-receptors for Hh signalling (Allen *et al.*, 2011; Camp *et al.*, 2010; Cohen, 2010; Izzi *et al.*, 2011; Kavran *et al.*, 2010; McLellan *et al.*, 2008; Okada *et al.*, 2006; Tenzen *et al.*, 2006; Zhang *et al.*, 2011; Zheng *et al.*, 2010).

Only the concomitant loss of both *ihog* and *boi* leads to a loss of eye tissue (Camp *et al.*, 2010) so we hypothesized that a similar situation might occur with respect to the *Dl-ihog-IR* overgrowth. The levels of both *boi* and *iHog* must be affected in the tumour phenotype by other mechanisms unrelated to miR-7, as we found that the expression of a *boi* RNAi transgene did not enhance Dl-induced eye overgrowth (*ey>Dl>boi-IR*; Figure 20A–B and Table S2; boi-IR effectively reduces *boi* but not *ihog* mRNA levels by 65%; p = 0.0005; data not shown)).

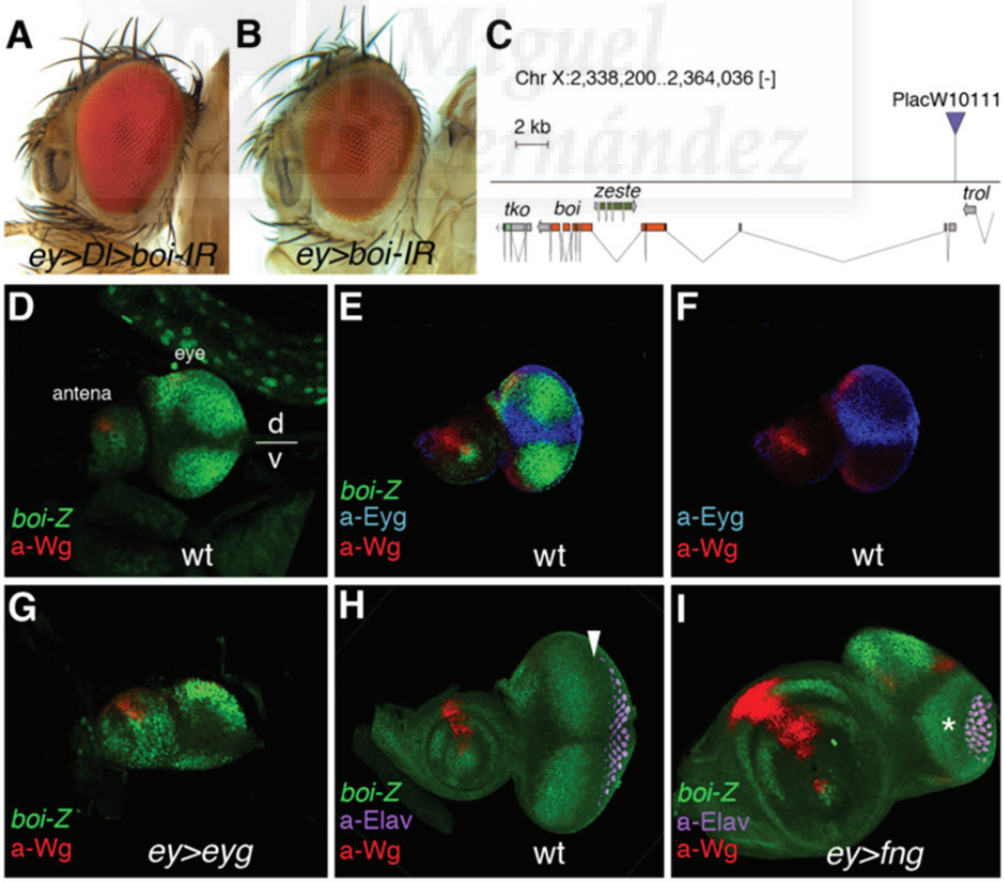

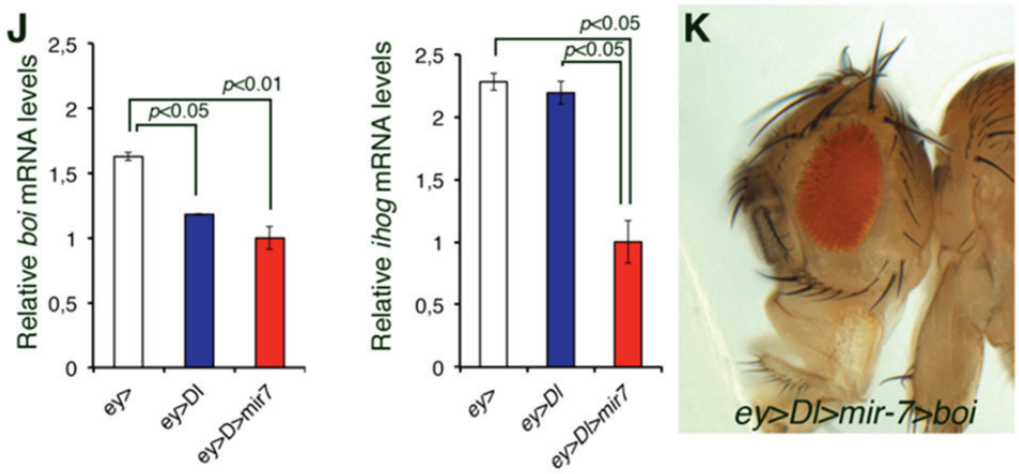

Figure 20. Notch signalling represses *brother of ihog* in the *Drosophila* eye. (**A–B**) Female flies overexpressing *UAS-Dl and/or UAS-boi-IR with ey-Gal4*. (**C**) Map of *PlacW10111* P-element insertion into the *boi* locus. (**D–I**) *boi* expression in wild-type (**D, E, F,** and **H**) and Notch pathway mutant (**G** and **I**) eye-antennal discs. The use of the gene wingless (a-Wg, in red) serves to orient the eye disc in the dorsal-ventral axis. Expression of Boi (green) in the eye disc is repressed along the dorsal-ventral organizer (**D** and **E**), marked by the expression of the gene *eyg* (blue, **E** and **F**). Retinal differentiation (neuronal marker a-Elav, magenta) is first detected at the posterior end of the eye disc and progresses in an anterior direction (**H**). The arrow points to the MF. (**G** and **I**) Expression of *boi-lacZ* (boi-Z, green) and wingless (a-Wg, red) in *ey>eyg* (**G**) and *ey>fng* (**I**) eye discs. The discs in (**H**) and (**I**) are from the same stage and magnification. The enlarged antennal disc in (**I**) and a reduced eye disc (white asterisk), is an effect of the undergrowth of the eye disc, caused in part by defective Notch activation in the dorsal-ventral organizer due to *fng* overexpression. (**J**) qRT-PCR analyses of *boi* (left) and *ihog* (right) in *ey-Gal4* (white bar), *ey>Dl* (blue bar), and *ey>Dl>mir-7* (red bar) late third instar eye discs. Two independent experiments of three replicates are shown in each case. Data were normalized to *rp49*. mRNA isolated from 50 pairs of eye-antennal discs per genotype. Data was analysed by a two-tailed unpaired t test. Error bars represent s.e.m. of three replicates. (**K**) Adult fly head showing no eye overgrown induced by Dl and *mir-7* when *boi* is overexpressed by a transgene (*UAS-boi*, 100% penetrance of rescue).

In our tumour phenotype there is a combination of two genetic alterations: Overexpression of the miRNA miR-7 and overexpression of the Notch signalling pathway. Our experiments show that miR-7 down-regulates the levels of *iHog* without affecting *boi*. It could be possible that Notch signalling pathway is involved in regulating the levels of the co-receptor *boi* in a miR-7 independent manner, thus explaining the previous result. To test this hypothesis we verified the status of *boi* transcription in relation to eye disc growth

We studied the spatial domain of *boi* in the developing eye disc *in vivo* using a ß-galactosidase enhancer trap inserted in *boi* (Figure 20D). Interestingly, we saw that in eye discs double labelled with a-Eyg [(a dorsal-ventral organizer-specific response gene and an obligatory Notch's effector in eye growth (Dominguez *et al.*, 2004; Tsai *et al.*, 2004)] and anti-ß-galactosidase (*boi-lacZ* in green), the expression of *eyg* is complementary to that corresponding to *boi* (Figure 20E–F). This led us to speculate that expression of *boi* is negatively regulated by Notch-Eyg at the growth-promoting organizer. To determine the veracity of this assumption we monitored the spatial domain of *boi-lacZ* in mutants of the dorsal-ventral organizer and measured *boi* mRNA levels by qRT-PCR analyses. For this purpose, we overexpressed the effector *eyg*, which expands the dorsal-ventral organizer domain (Dominguez *et al.*, 2004; Tsai *et al.*, 2004). Under these conditions, we observed an extended domain lacking *boi-lacZ* expression (Figure 20G). To explore the opposite situation, we

used the ubiquitous expression of the modulator *fng* which causes defective Notch receptor activation by its ligands and results in the thinning or loss of the dorsal-ventral organizer (Dominguez *et al.*, 1998; Gutierrez-Avino *et al.*, 2009; Tsai *et al.*, 2004). Under these conditions, the expression of *boi* was uniform throughout the eye disc due to the absence of the organizer in charge of repressing this gene in wild-type eye discs (Figure 20I). Furthermore, qRT-PCR analyses confirmed downregulated *boi* but not *ihog* transcripts in eye discs overexpressing Dl transgene alone by *ey-Gal4* (ey>Dl; left in Figure 20J). Importantly, both *boi* and *ihog* mRNA levels were downregulated in eye discs that co-expressed Dl with the microRNA miR-7 (*ey>Dl>miR-7*; Figure 20J).

Taken together, *these results demonstrate that* boi *is negatively regulated by Notch's organizer activity.*

Eyg has been already described as a transcriptional repressor (Salvany *et al.*, 2012; Yao *et al.*, 2005), so in this context it could be directly repressing *boi* gene transcription. This Hh co-receptor contains a consensus Eyg-binding site (TCACTGA (Yao *et al.*, 2005)) at position chrX: 2.359.784. Unfortunately, we could not validate the direct binding of Eyg to the *boi* promoter region by chromatin immunoprecipitation (ChIP) using embryos and already published procedures from Cavalli laboratory http://www.igh.cnrs.fr/equip/cavalli/link.labgoodies.html.

The phenotype observed in $ihog^{-}/boi^{-}$ flies was rescued using a *boi* transgene (*UAS-boi*) (Hartman *et al.*, 2010) fully suppressing the overgrowth induced by the combination of mir-7/Dl (Figure 20K, 100% penetrance, n = 100).

5. Dampening hedgehog signal transduction also enhances Delta-induced overgrowth in the wing.

As the overexpression of Notch signalling pathway alone in the eye produces a mild overgrowth that cannot be considered as a tumour phenotype, we can speculate that the loss of function of the Hh signalling pathway can be enhancing the Dl- Notch signalling activity. To test this hypothesis we carried out several tests using a very well established system in the wing disc.

As has been mentioned above, wing disc growth and patterning is also organized by Hh and Notch-mediated organizers (Irvine *et al.*, 2001), with Hh secreted by cells in the posterior compartment inducing short-range targets in anterior cells near the anterior-posterior boundary (e.g., ptc, blue staining in Figure 21A) (Chen *et al.*, 1996; Tabata *et al.*, 1994). Notch signalling is activated locally along the dorsal-ventral boundary by its ligands Dl and Ser, and it induces symmetric expression of targets in boundary cells (e.g., wg, red staining in Figure 21A; reviewed in (Irvine *et al.*, 2001).

To investigate the effects of the antagonistic interaction between loss of Hh and gain of Notch we used the wing imaginal discs to generate clones. As can be seen in Figure 5B in the introduction, Dl-expressing clones in the wing induce ectopic *wg* expression in dorsal cells, where *fgn* is expressed (which induces this Dl-Notch receptor interaction), whereas ventrally situated clones did not activate *wg* due to the lack of the expression of this gene (e.g., (Baonza *et al.*, 2005; de Celis *et al.*, 1997; de Celis *et al.*, 1996; Doherty *et al.*, 1996; Pitsouli *et al.*, 2005). We ectopically induce *wg* in different regions of the wing disc to examine Dl activity in homozygous MARCM clones for a *smo* allele (smo^3/smo^3), allowing us to test the effects of the loss of function of Hedgehog over Notch signalling pathways in the wing disc.

As shown in Figure 21, we found that ventrally situated anterior cells homozygous for smo^3 and expressing Dl expressed high levels of Wg, similar to the levels of Wg induced by dorsally situated clones, in contrast with most smo^3 Dl-expressing clones situated ventrally in posterior cells away from the boundary (Figure 21B and C) or clones of smo^3 cells that did not overexpress Dl (Figure 21A).

Clones of smo^3 cells abutting the anterior-posterior boundary often sort to the posterior compartment territory (Blair *et al.*, 1997; Rodriguez *et al.*, 1997). As seen in Figure 5B in anterior-posterior organizers, the loss of *smo* activity in anterior cells at the boundary fail to up-regulate Ci expression and did not induce *ptc* transcription non cell- autonomously (Chen *et al.*, 1996). The clones at the anterior-posterior boundary overexpressing *wg* (asterisks in Figure 21A''–B'') are of anterior origin as they retain the anterior features (low levels of Ci protein) characteristic of the loss of *smo* activity in anterior cells.

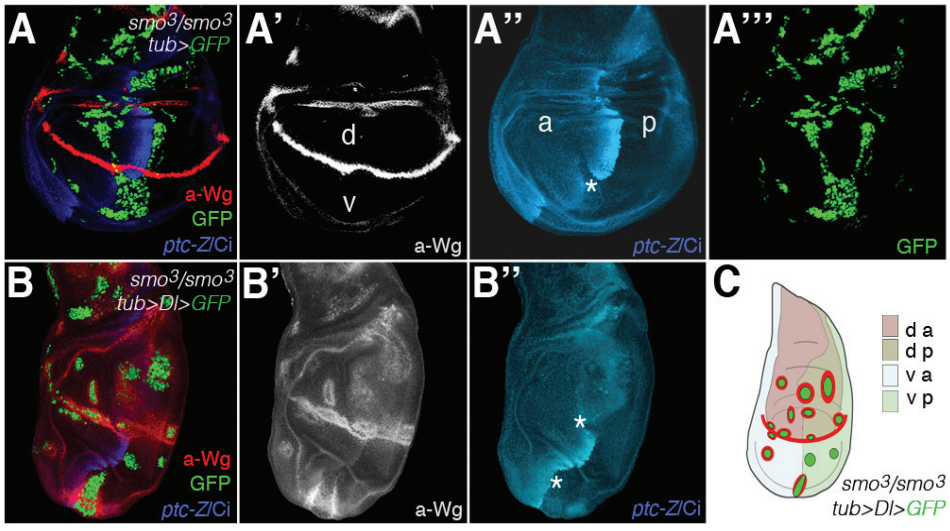

Figure 21. Loss of Hedgehog signalling by *smoothened* enhances Delta-Notch signalling activity in the wing. (**A–B''**) Confocal images of wing discs bearing MARCM GFP (green)-labelled clones homozygous for smo^3 without (**A**) or with (**B**) Dl overexpression. Mosaic discs were stained for Wg (red in **A** and **B**, and grey in **A'** and **B'**), and Ci (blue) and *Ptc-lacZ* (Ptc-Z, blue). (**C**) A schematic summary of clones in (**B**). Asterisks in (**A''**) and (**B''**) point to "posteriorly" situated clones that were of

anterior origin as denoted by the failure to induce Ptc and the low levels of Ci protein (white line delineates the anterior-posterior boundary in the discs in **B**). Clones were generated at 24–42 hr after egg laying by a 1 h heat shock at 37°C (n = 60 clones analysed). Genotypes: (**A**) *yw hsp70-Flp tub-G4 UAS-GFP; tub-Gal80 FRT40A/smo^{3} FRT40A ptc-lacZ and (**B**) yw hsp70-Flp Tub-G4 UAS-GFP; Tub-Gal80 FRT40A/smo^{3} FRT40A ptc-lacZ; UAS-Dl/+.*

Taken together, these findings show that Dl-expressing cells unable to transduce the Hh signal behave as if they expressed hyperactivated Dl. Coupled with the analysis of RNAi transgene, these results confirm that the loss of Hh signalling enhances Dl-Notch signalling activity.

6. miR-7 overexpression and Hedgehog Signalling regulation is context-dependent.

microRNAs are thought to regulate multiple target genes; however, when tested *in vivo* in a determined cellular context, it often occurs that only a subset or even only one of the targets act as the main effector of the activity of the microRNA. For this reason we tested whether *ihog* also acts as the main target of miR-7 in Dl-induced tumorigenesis in other tissues.

mir-7 misexpression driven by *ptc-Gal4 (ptc>mir-7*) has been reported to produce wing margin notches and a reduction of the space between vein L3 and L4 (Bejarano *et al.*, 2012; Stark *et al.*, 2003). Both phenotypes were attributed to defects in Notch signalling (Lai *et al.*, 2005; Stark *et al.*, 2003), but we noted that L3–L4 fusion is very reminiscent to the phenotype produced by *hh* loss-of-function mutations. Since we have previously shown that iHog is a direct target of miR-7, we depleted *ihog* using RNAi driven by *ptc-Gal4, but* did not produce a defect as it occurs with *mir-7* overexpression (Figure 22E). The lack of effect of *ihog* RNAi is almost certainly due to the activity of the other Hh co-receptor, *boi*, which is expressed at high levels in the wing margin and in the presumptive L3 vein territory (*boi-lacZ* in green; Figure 22F). Hh loss-of-function can be also produced by *ci* cell mutation, producing a truncated form of Ci which behaves as a constitutive repressor (Methot *et al.*, 1999). Indeed, we observed a clear downregulation of Ci protein levels in *ptc>mir-7* cells (Figure 22A and B), which are precisely the cells receiving endogenous Hh signals, stabilizing Ci protein levels and preventing the conversion of Ci-155 or CiA into truncated Ci repressor (Ci-75 or CiR). Plots of fluorescence intensity profiles from the wild-type and *ptc>mir-7* discs are shown in Figure 22A' and 22B''. The weak downregulation of Ci by mild RNAi expression using *ptc-Gal4* mimicked the L3–L4 fusion defect of *ptc>mir7* (Figure 22C -D and Figure 9F).

These results raised the possibility that like ihog, ci is also a direct target of miR-7. Indeed, ci *mRNA does contain a presumptive miR-7 binding site in the ci 3'UTR, although this site is not conserved across* Drosophila *species. Thus, the Ci low protein levels in* ptc>mir-7 *wing discs could*

reflect the direct repression of ci *by the microRNA or the dampening of Hh signalling response by an indirect miR-7-mediated effect.*

In agreement with this indirect regulation of Ci by miR-7, ectopic expression of miR-7 away from the normal Hh secreting cells (the posterior compartment cells marked by the absence of Ci green in Figure 22G), using the *Beadex* (*Bx*)-*Gal4* driver produced no change in Ci protein levels (Figure 22G). Therefore, it can be that either Ci is not a target of miR-7 or that this regulation is context dependent. It is generally considered that when an individual miRNA affects the expression of various proteins in the same pathway, it does so in a rather mild manner (Uhlmann *et al.*, 2012).

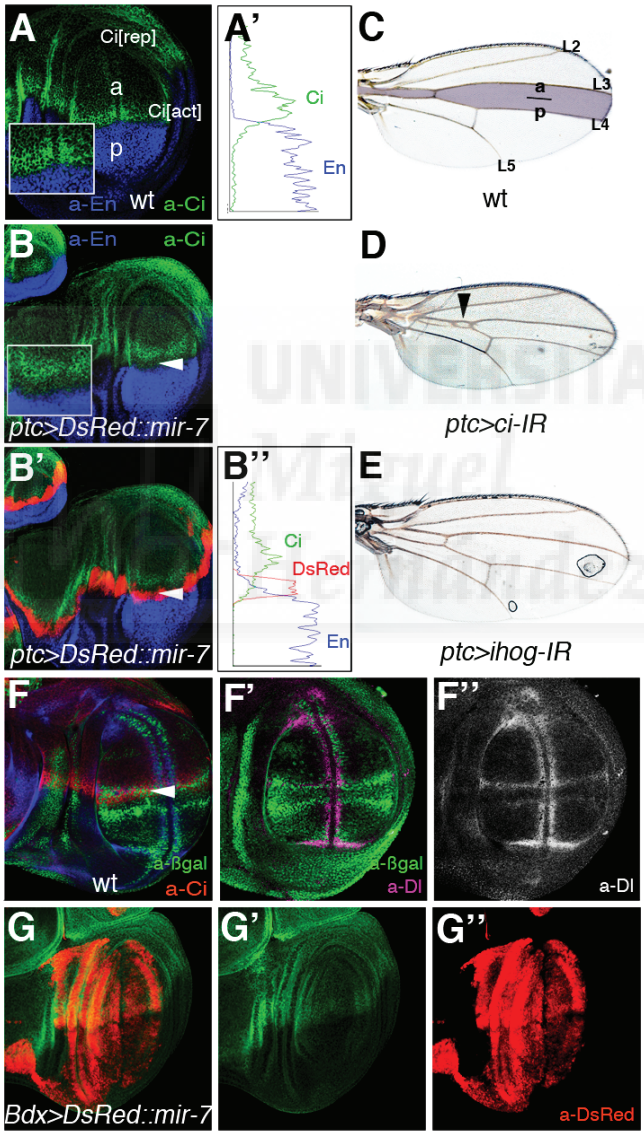

Figure 22. miR-7 silencing of Hedgehog signalling explains veins L3–L4 fusion in the wing. (A) Ci protein (green) is distributed across the entire anterior compartment of the discs. Hh signals from posterior cells induce high levels of Ci in cells along the anterior-posterior border blocking Ci proteolysis into the repressor form thereby allowing the Ci activator to accumulate. (**B–B'**) Overexpression of *mir-7* denoted by red labelling (*UAS-DsRed::mir-7*) driven by patched (*ptc)-Gal4* downregulates Hh signalling as visualized by low Ci levels (green; white arrowhead). Insets show magnifications. Engrailed (En) staining in blue serves to mark the posterior compartment in (**A–B''**). Plots of fluorescence intensity profiles of the

anterior-posterior compartments from the WT (**A**) and *ptc>DsRed::mir-7* (**B'**) discs are shown in (**A'**) and (**B"**), respectively. Green trace, Ci; blue trace, En; red trace, DsRed. (**C**) Adult wild-type wing. The shaded area denotes the domain of expression of the *ptc-Gal4* reporter. (**D**) *ci-IR* expression by *ptc-Gal4* mimicking the L3–L4 fusion defect seen in adult wings that is caused by *mir-7* overexpression. (**E**) Adult wing expressing *ihog-IR* driven by *ptc-Gal4*. (**F–F"**) The expression of *boi-lacZ* (green) defines all longitudinal veins (L2–L5). Note the high *boi-lacZ* expression (green in F) along L3, marked by high Ci (red in **F**) and Dl (magenta in **F"**). (**G–G"**) Overexpression of *mir-7* (in red) by *Bx-Gal4* did not alter Ci protein levels (green).

To sum up we can say that we have identified cooperation between the microRNA miR-7 and Notch in the Drosophila *eye. miR-7 acts over its direct* target ihog *in this context, being its co-receptor in the Hh signalling pathway,* boi*, a target of Notch-mediated activity at the dorsal-ventral eye organizer, although whether this regulation is direct or indirect remains unknown. We have discovered an unanticipated tumour suppressor activity of the endogenous Hh signalling pathway in the context of gain of Dl-Notch signalling that is also apparent during wing development.* See next Figure 23 for a schematic summary of these results.

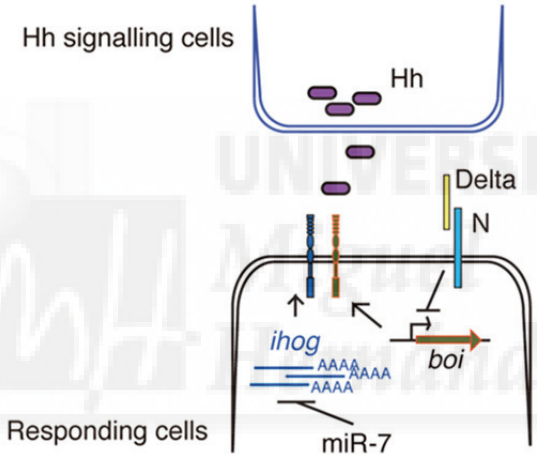

Figure 23. Model of regulatory interactions among the microRNA, Notch pathway, and the Hh receptors iHog and Boi. There is cooperation between the microRNA miR-7 and Notch: miR-7 acts over its direct target *ihog*, and its co-receptor in the Hh signalling pathway, *boi*, is a target of Notch-mediated activity.

7. Human miR-7 also targets Hedgehog signalling pathway.

In both flies and humans, Hh signalling relieves the inhibition exerted by Patched (Ptc/PTCH1) on the intermediate pathway component Smoothened (Smo/SMO), allowing Smo to stabilize full-length Ci, which acts as a transcriptional activator (CiA or Ci-155 in flies; Gli2,3 in mammals) and inhibiting the processing of CiA to the truncated transcriptional repressor (CiR or Ci-75, in flies; Gli1 in mammals) (Ingham, 2012). In addition to these core components, as has been said before, the two Hh co-receptors iHog and Boi have the human counterparts CDON and BOC that also act as obligatory co-

receptors for Hh signalling (Allen *et al.*, 2011; Beachy *et al.*, 2010; Cohen, 2010; Izzi *et al.*, 2011; Kavran *et al.*, 2010; McLellan *et al.*, 2008; Okada *et al.*, 2006; Tenzen *et al.*, 2006; Yao *et al.*, 2006; Zhang *et al.*, 2011; Zheng *et al.*, 2010). As their counterparts in *Drosophila*, these co-receptors were also shown to act as tumour suppressors *in vitro* (Kang *et al.*, 1997). Moreover, recurrent somatic mutations in the Hh pathway were identified in human pancreatic cancers through global genomic studies, affecting *GLI1*, *GLI3*, and *BOC* (Jones *et al.*, 2008).

To test if, as in *Drosophila*, the human miR-7 is controlling the expression of some of the two Hh receptors, we performed a luciferase assay testing the effects of human *mir-7* overexpression, over the activity of luciferase reporters containing the full-length 3'UTRs of *CDON* and *BOC*. We also introduced point mutations in miR-7 binding sites (two in *CDON* 3'UTR and one in *BOC* 3'UTR, $CDON^{mut}$ and BOC^{mut}) to use these constructs as controls (Figure 24A). This luciferase assay was done in human cells available in the laboratory such as pancreatic cancer cells (PC3) and non-tumorigenic human pancreatic cells (PNT1A) to discard the possibility of variations between different cell lines. The overexpression of human *mir-7* produced a significant reduction in the luciferase activity of CDON 3'UTR, while the $CDON^{mut}$ 3'UTR showed no change. In the case of BOC constructs, *mir-7* overexpression did not affect luciferase activity, both in the wild type and mutated versions of the construct (Figure 24B).

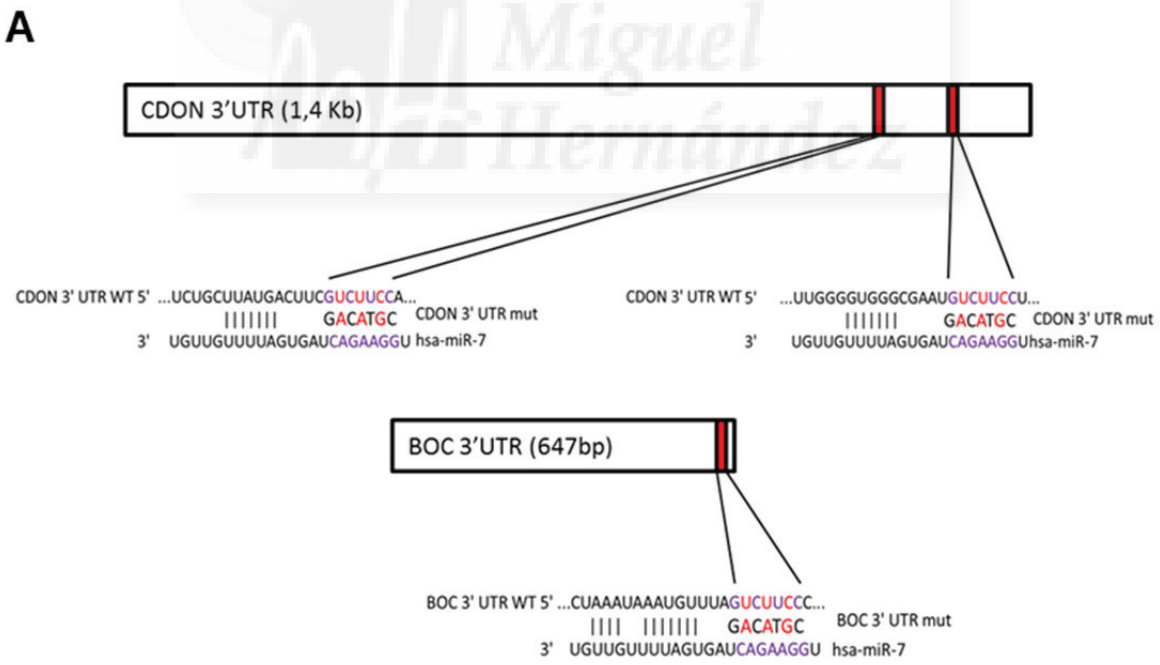

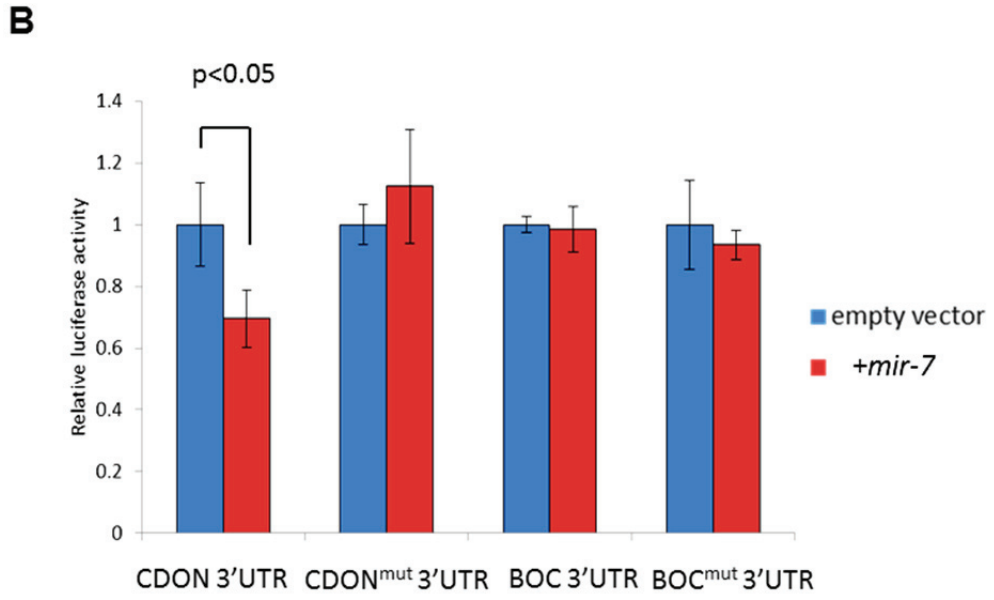

Figure 24. MicroRNA *mir-7* inhibits *in vitro* the transcription of the human homolog of iHog, CDON. (A) Computer predicted consequential pairing of *CDON* and *BOC* target regions and miRNA miR-7. The conserved seed match in the 3'UTR of *CDON* and *BOC* is in red. **(B)** Luciferase assay in PC3 cells co-transfected with *mir-7* (red bars) or the empty vector (blue bars), together with a firefly luciferase vector containing the *CDON* 3'UTR or *BOC* 3'UTR, or the luciferase vector with mutations in the seed sequence (red nucleotides in **A**, *CDON*mut 3'UTR and *BOC*mut 3'UTR). Renilla luciferase activity was measured 48 hr after transfection and normalized against Firefly luciferase. The values represent the mean ± s.e.m. of three or four independent experiments. Differences in $CDON^{mut}$, BOC^{mut} and *BOC* luciferase levels were not statistically significant between treatments. P values were calculated by the unpaired Student's t test.

To test the effects of miR-7 over its target *CDON* we used PC3 cells to overexpress *mir-7*. The mRNA levels of *CDON* are mild but consistently reduced, as reported by qRT-PCR (Figure 26 A-B). This result confirms the luciferase results and *CDON* is a direct target of human miR-7. Nevertheless, *BOC* mRNA levels were slightly higher but not significantly different after the overexpression of *mir-7.* These two receptors can be redundantly acting in order to maintain constant levels of the Hedgehog signalling pathway.

As in Drosophila*, the human counterpart of* iHog*,* CDON*, is a direct target of human* miR-7*, demonstrated by measuring the relative luciferase levels of a* CDON 3'UTR *construct and the mRNA levels of CDON by qRT-PCR. The expression of its Hh co-receptor* BOC *is not affected.*

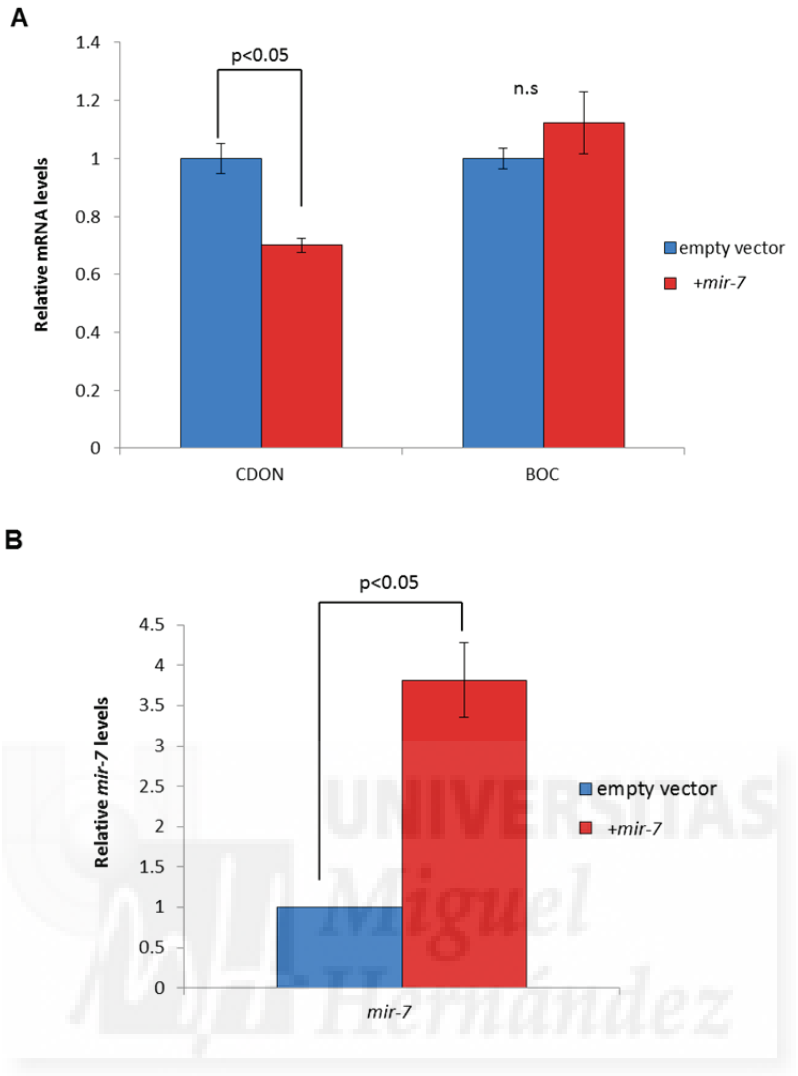

Figure 26. Levels of CDON are consistently reduced by miR-7. (**A**) Relative mRNA levels of CDON and BOC measured in PC3 cells transfected with a control vector (blue bars) or overexpressing the microRNA miR-7 (red bars). (**B**) Effects over the microRNA levels of miR-7 after its overexpression. P values were calculated by the unpaired Student's t test. The values represent the mean ± s.e.m. of three independent experiments.

Subsequently, we search for human tumorigenic cell lines with high levels of Notch signalling. PC3 cells overexpress the Notch signalling pathway due to an upregulation of Jagged (the human ligand of Notch signalling pathway and homolog of Serrate in *Drosophila*) compared the non-tumorigenic prostate cell line PNT1A (Vallejo *et al.*, 2011). To further characterize these cell lines, we measured the levels of *BOC* and *CDON* by qRT-PCR. We observed that the mRNA levels of *CDON*, are consistently increased in PC3 compared to PNT1A, but *mir-7* levels are not significantly different. Regarding *BOC*, there is a mild but consistent reduction of its mRNA levels compared to the levels observed in PNT1A. This result is consistent with the negative regulation of *boi* induced by the overexpression of Notch signalling pathway seen in *Drosophila* (Da Ros *et al.*, 2013) (Figure 25A and B). To confirm this regulation, we studied the presence of Notch-effector binding sites within the *BOC* genomic region.

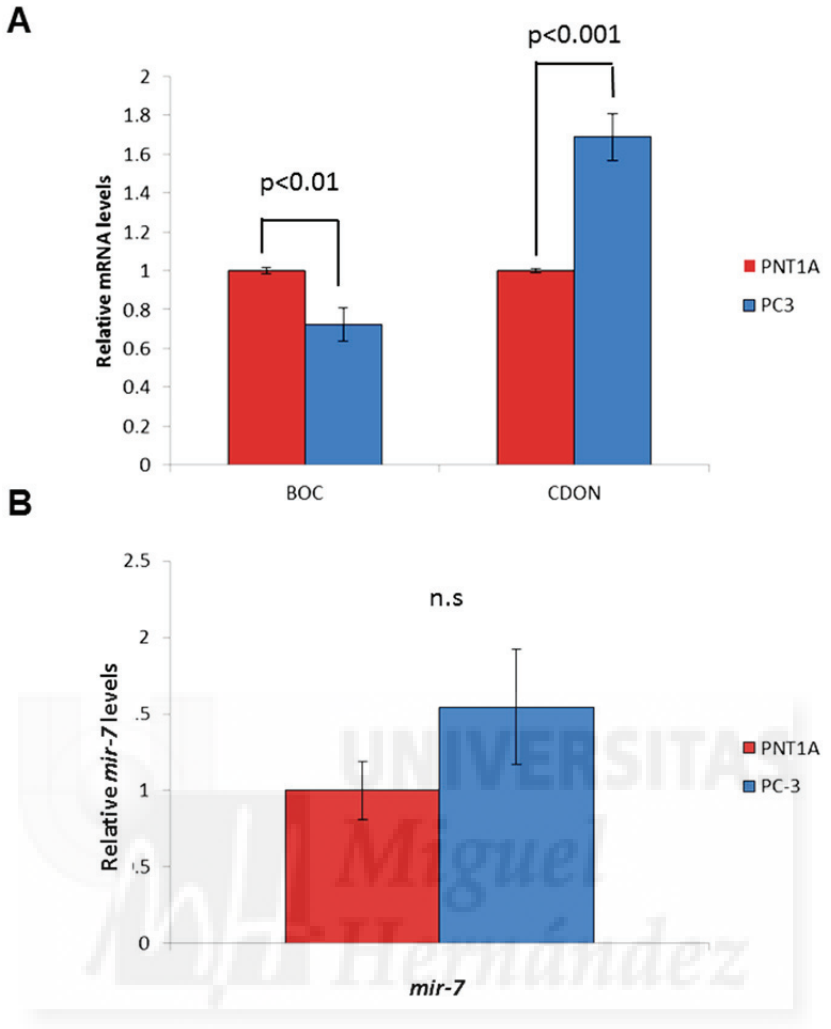

Figure 25. Characterization of the prostatic cancer cell line (PC3) compared to its non-tumorigenic prostatic cell line (PNT1A). The levels of Serrate in the PC3 cells had been previously reported to be higher in comparison with the levels found in non-cancerous prostatic cell line PNT1A. (**A**) Correlating with the results obtained in *Drosophila* where the Notch pathway is negatively regulating the levels of *BOC*. *BOC* levels are decreased in PC3 (blue bars) compared to PNT1A (red bars). The levels of *CDON* are increased although the amount of miR-7 observed in these cells is not significantly different (**B**). P values were calculated by the unpaired Student's t test. The values represent the mean ± s.e.m. of three independent experiments

The obligatory effector of Notch in *Drosophila* eye growth, *eyg* is one of the four *Drosophila Pax6* orthologous, which shares functional homology with the vertebrate Pax6(5a) isoform. Pax proteins are defined by a conserved DNA-binding domain called the paired domain. An alternative splicing event in the sole *PAX6* gene in humans and rodents creates the isoform PAX6(5a) (Epstein *et al.*, 1994; van Heyningen *et al.*, 2002). Like the human PAX6(5a) isoform, the fly Eyg protein has similar DNA sequence-recognition characteristics (Czerny *et al.*, 1993; Epstein *et al.*, 1994; Jun *et al.*, 1998). The TCA C TGA consensus sequence forms a palindromic sequence that is very similar to either half of the Pax-6 5a binding site. This binding site is made of two direct repeats of an 11-bp sequence (Epstein *et al.*, 1994). We analysed the genomic region of *BOC*, looking for Pax-

6(5a) binding sites. To do a fast analysis of binding motives in the promoter of human *BOC* we used the webpage Pscan http://159.149.160.51/pscan/. Among the sites identified, we found Pax6 sites with lower score (hence, lower probability to be a bona fide functional binding site), than in the case of other proteins as Pax5 or Pax2 sites. A detailed analysis using bioconductor http://www.bioconductor.org/help/workflows/generegulation/ and a complementary ChIP-seq can be formed. It must be considered the possibility that the different mRNA levels of *BOC* between these two cell lines might be also produced by other mechanisms not related with the Notch signalling pathway.

8. Drawing parallels in human cancer cells.

To answer the question if in humans, like in our *Drosophila* model, the loss of Hh signalling pathway is able to enhance Notch signalling, we made use of the luciferase tools to report the state of these pathways.

As has been previously described, the human counterparts of Ci in *Drosophila* are Gli1, 2 and 3. Gli1 has only an activator domain, so that, it can only act as an activator. Gli2 and 3 have an activator and a repressive domain having a dual function in the absence or presence of CDON/BOC ligands (Buttitta *et al.*, 2003; Ding *et al.*, 1998; Hui *et al.*, 1993; Matise *et al.*, 1998; McDermott *et al.*, 2005; Pan *et al.*, 2007; Pan *et al.*, 2009; Wang *et al.*, 2010; Wang *et al.*, 2007).

To modulate the levels of the Hh and the Notch signalling pathway, we used a Gli3 repressor construct without its activator domain (Gli3Rep) and a dominant active form of the murine Notch-1 (here called NotchDE) (Oswald *et al.*, 2002), in combination with two luciferase reporters, GLI and RBP. Mammalian GLI proteins are known to encode a nuclear protein, containing five zinc finger motifs, which binds to DNA in a sequence-specific manner (Kinzler *et al.*, 1990). The human GLI reporter form (Sasaki *et al.*, 1997) is a construct containing 8 repetitions of this sequence-specific binding sites before a firefly luciferase coding region (Kamachi et al., 1993). The luciferase reporter plasmid RBP-J (Jung *et al.*, 2013; Minoguchi *et al.*, 1997; Oswald *et al.*, 2002) contains a 50-bp oligonucleotide harbouring RBP-J binding sites, the fly homolog of Su(H) and the main transcriptional mediator of Notch signalling. The transfections performed are described in detail in materials and methods chapter.

In PC-3 cells the expression of NotchDE produced, as expected, an increased luciferase signal of the RBP luciferase reporter compared to an empty vector (Figure 27A). Conversely, this increase was not significantly changed by the co-expression of the repressive form of Gli3. This result does not correlate with what we saw with smo^{3}/smo^{3} MARCM clones in the wing disc (Figure 27A), where the loss of function of Hh signalling pathway in combination with Dl overexpression, induced the ectopic expression of *wg* (Notch signalling pathway) in clones located in the ventral part of the

wing disc, where *wg* endogenously cannot be activated as the *fng* gene is not expressed. Gli3 repressor alone caused a mild increase of the basal levels of RBP^{mut} luciferase reporter activity and could not be used as a control.

Gli3 repressor is correctly working, as it causes a decrease in the level of luciferase activity of the Gli reporter compared to the empty vector control (Figure 27B) and no changes were found when the expression of the repressive form of Gli3 was combined with the constitutive active form of Notch intracellular domain (Figure 27B). To discard a false result due to the effect of the luciferase reporters, I measured the mRNA levels of different *NOTCH1* target genes and no changes were reported before and after the expression Gli3 repressive form alone or in combination with NotchDE (Figure 27C).

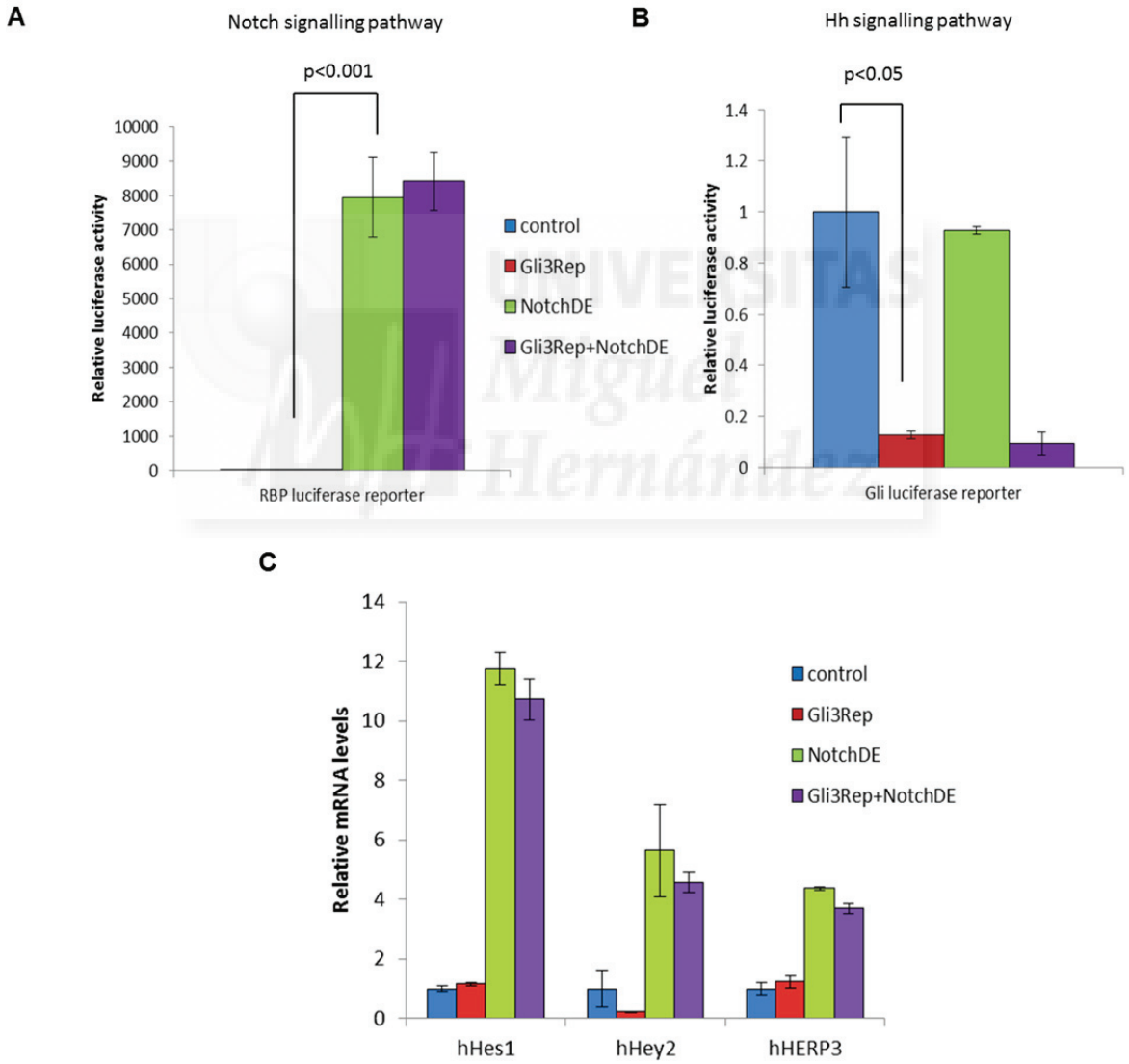

Figure 27. No changes of the Notch signalling pathway can be reported with the loss of the Hedgehog signalling in human cells. (**A** - **B**) The loss of Hh signalling pathway (red bars) is unable to enhance the Notch signalling compared to the control condition (blue bars), as what happens previously shown model using *Drosophila* imaginal discs, due to the fact that luciferase assays using PC3 cells showed no changes in the Notch signalling pathway (here reported by the RBP

luciferase reporter) with the inhibition of the Hh signalling pathway expressing the repressive form of Gli3 (Gli3rep). The combination of the Gli3rep and NotchDE (violet bars) does not significantly change the luciferase signal of Notch signalling pathway or the Hh signalling pathway. (**C**) No changes were reported in the levels of expression of different Notch-induced genes with the combination Gli3rep+NotchDE compared to the conditions of both constructs alone (green and red bars). The values represent the mean ± s.e.m. of three or four independent experiments. P values were calculated by the unpaired Student's t test.

Section 2. Pipsqueak acts as an unexpected multifaceted transcription factor with wider than anticipated roles in chromatin remodelling.

1. Discovery of new Pipsqueak partners using Yeast-two-Hybrid and Chromatin Immunoprecipitation coupled with massively parallel DNA sequencing.

The gene *psq* has a dual role, acting as an oncogene in the context of Dl overexpression in the "*eyeful*" phenotype (Figure 12I), and as a tumour suppressor, since the loss of function of all its isoforms causes a phenotype of hyperplastic eyes with 100% penetrance (Figure 12H). This tumour suppressor role has also been reported in a context of EGFR overexpression, where *psq* knockdown induces tumour formation (Herranz *et al.*, 2014). To understand this riddle, which suggests a multi-faceted function of Psq, we performed several assays: Yeast Two-Hybrid (Y2H) and Chromatin immunoprecipitation coupled with massively parallel DNA sequencing (ChIP-Seq) to find new functional partners of Psq.

1.1 A Yeast-two-Hybrid assay identifies interactions between the BTB-containing Pipsqueak isoform and new Pipsqueak partners.

The Y2H technique allows detection of the interaction between two proteins through the activation of a reporter gene (Figure 28). Classically, a eukaryotic transcriptional activator contains a domain that specifically binds to DNA (binding domain) and a domain that recruits the transcription machinery (activating domain). In the Y2H system, these domains are separated in two different polypeptides, each of them fused to different proteins that will act as bait or prey. The basis of this assay is that the transcription of the reporter gene only occurs if bait and prey interact, bringing together both parts of the transcriptional activator (further reviewed in (Bruckner *et al.*, 2009)). We used as prey a *Drosophila* embryo library from Hybrigenics Services, which consist of a pool of two cDNA libraries prepared from 0-12 hr and 12-24 hr embryo mRNA. Each cDNA was cloned in frame with the *Gal4* transcription factor activation domain (Figure 28).

The BTB domain of Psq is essential for its oncogenic function (Ferres-Marco *et al.*, 2006) and it mediates oligomerization with other BTB proteins. Thus, in order to find new Psq partners, we used as bait for the Y2H the coding sequence of PsqBTB isoform B, spanning aa 1-720 (which contains the BTB and the central region of this protein, between the BTB and the DNA binding domain) (Figure 28 and table S3 in Appendix I). See materials and methods for a detailed description of the Y2H.

The sequence between the BTB and Psq DNA-binding domain contains several regions that are particularly rich in certain amino acid residues, including two glutamine rich (Q) regions and a region of 17 histidine (H) residues alternating with other residues. These regions were chosen in addition to the BTB binding domain because they are believed to serve as interfaces for protein-protein interactions (Janknecht *et al.*, 1991; Stott *et al.*, 1995) and are frequently found in transcription factors (Frigerio *et al.*, 1986; Karlin *et al.*, 1996). Poly-glutamine tracts, in particular, have the potential to interact with components of the basal transcriptional machinery and can thus act as transcriptional activation domains (Triezenberg, 1995).

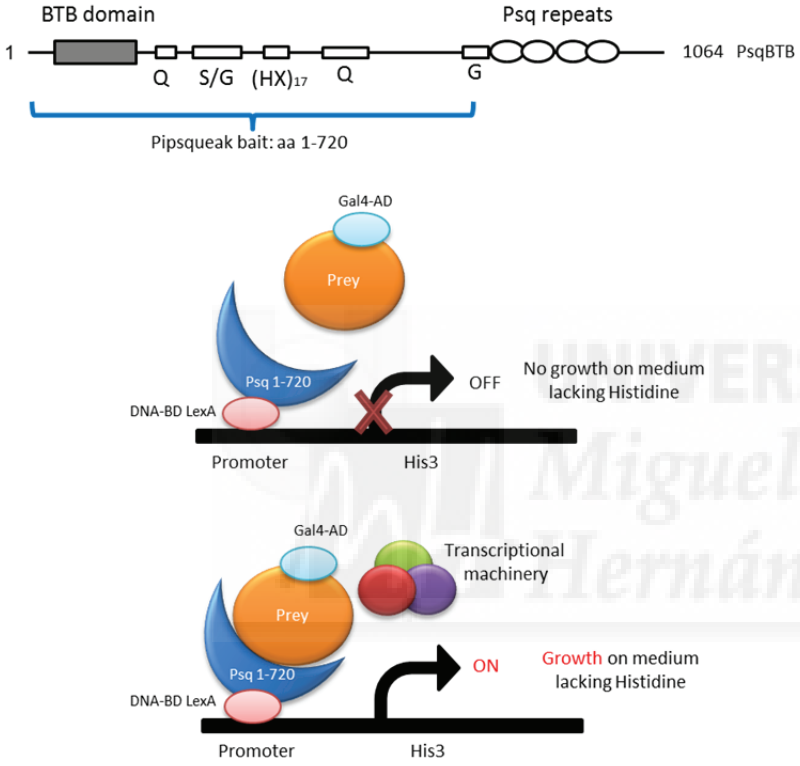

Figure 28. Yeast-two-Hybrid performed using as bait aa 1-720 of PipsqueakBTB isoform B. Scheme of the aminoacidic region of PsqBTB used as bait in the Y2H assay and the domains present within. Several OPA repeats can be found between these domains (the sequence triplet CAX where X is either Glycine (G) or Alanine (A) and one Threonine (T), regions enriched with Serine/Glycine (S/G), two regions containing poly-Glutamine (Q) stretches and a motif rich in Histidine (H) residues. The diagram illustrates the Y2H system using the *HIS3* reporter gene (growth assay without histidine).

Comparison of the cDNA sequence of all the fragments corresponding to a given protein that interact with Psq in the Y2H, allowed us to identify a common sequence called Smallest Interaction Domain (SID), which very likely contains all the structural determinants required for the interaction with Psq.

1.1.1 The spindle matrix and chromatin insulator protein, Chromator, interacts with the BTB domain of Pipsqueak.

From all the BTB-containing proteins interactions described in the Introduction and associated with Psq, only Lola-like appears in our Y2H screen as well as Psq, as a positive control (see Table S4 in Appendix I). Additionally, we found the insulator protein Chromator (Chro) in the list of interactors with nine positive clones and a Predicted Biological Score (PBS) of A (very high confidence of

interaction). Only two of the nine clones were fully sequenced reducing the accuracy in the establishment of the SID of this protein with Psq, which is situated in the C-terminal domain of Chro (Figure 29A).

Chro was originally identified as an interaction partner of putative spindle matrix components, and localizes to the spindle and the centrosomes during mitosis (Rath *et al.*, 2004; Yao *et al.*, 2014), directly affecting spindle function and chromosome segregation as is a novel tubulin binding protein. Full co-localization of Chro with the interband-specific zinc-finger protein Z4 and Jil-1 kinase have implicated this protein in mantaining chromatin structure (Eggert *et al.*, 2004; Gan *et al.*, 2011; Rath *et al.*, 2006). Moreover, Chro was first identified as an insulator (Gan *et al.*, 2011; Sexton *et al.*, 2012) and its insulator function was subsequently confirmed being required to form higher-order DNA interactions (Golovnin *et al.*, 2014; Vogelmann *et al.*, 2014). Chro can be divided into two main domains, a C-terminal domain containing a nuclear localization signal and a N-terminal domain containing a chromo-domain (ChD) required for proper localization to chromatin during interphase (Yao *et al.*, 2012). This C-terminal domain has been described to interact with the BTB domain of other BTB insulator proteins, such as CP190 (Vogelmann *et al.*, 2014) and Mod(mdg4) (Golovnin *et al.*, 2014). Figure 29A shows a diagram of the SID of Chro with the PsqBTB isoform B in the C-terminal domain of Chro.

To determine which region of Psq mediates the interaction with Chro, we performed a 1-by-1 Y2H assay using different fragments of Psq protein as baits: aa 1-720 (BTB and the central region between the BTB and the DNA binding domain), aa 1-131 (BTB region) and aa 132-720 (central region) (Figure 29B). As prey for the assay we used the full protein Chro, which contains the SID with Psq.

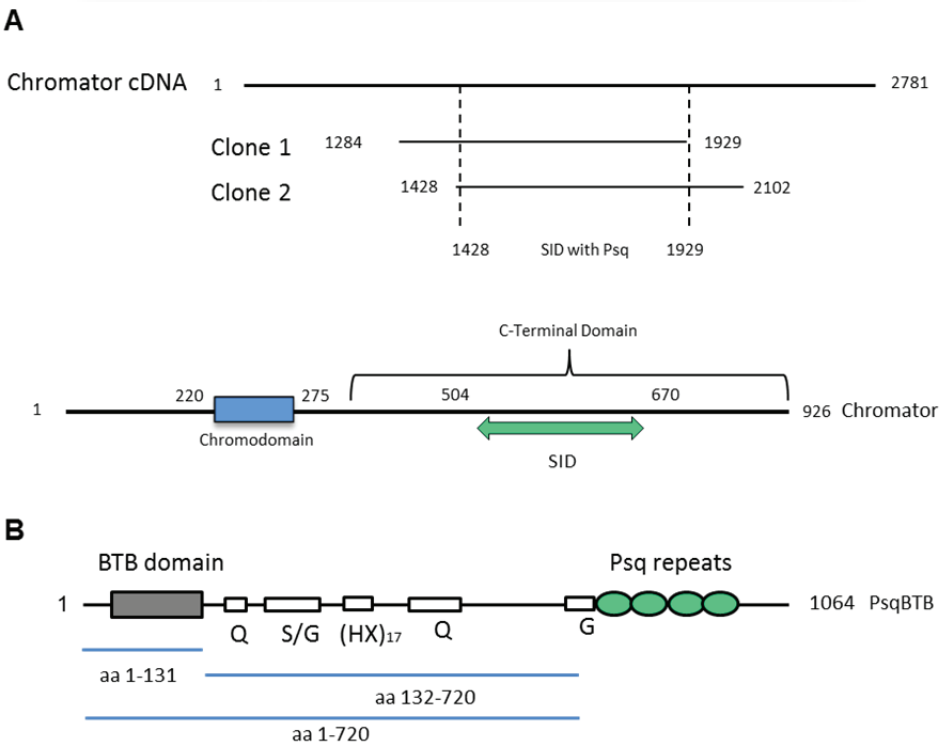

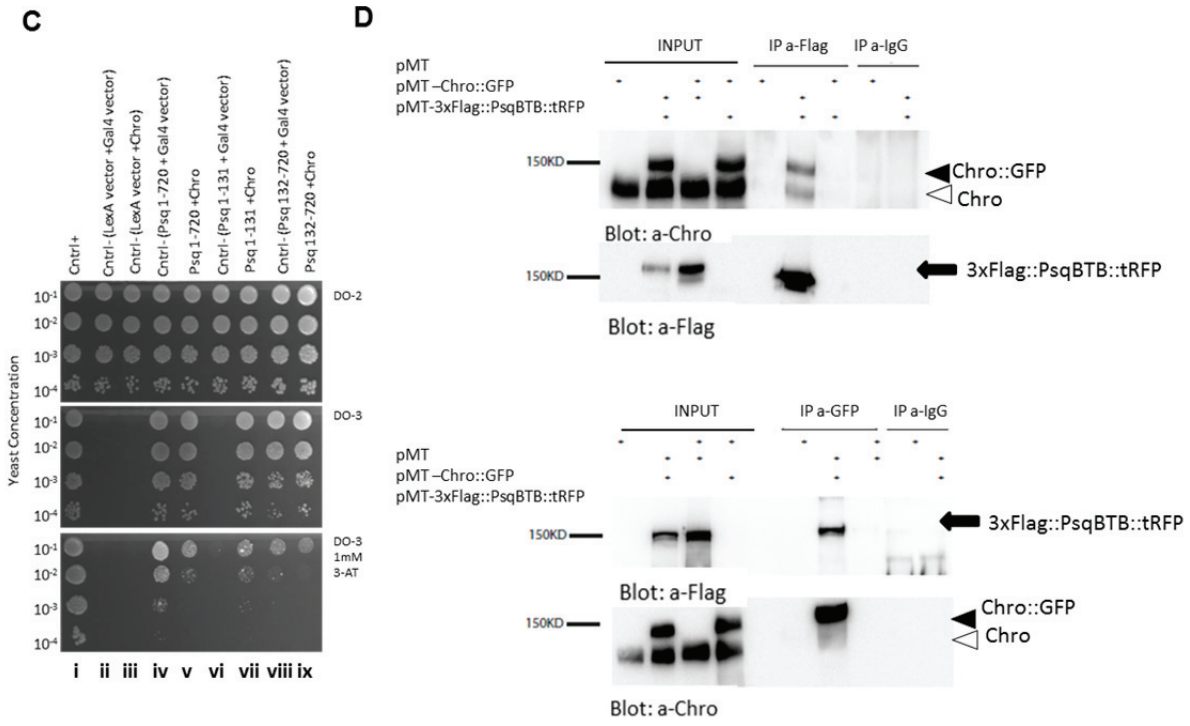

Figure 29. Chromator interacts with the BTB domain of Pipsqueak. (**A**) Results from the Y2H assay show an interaction between Chro and aminoacid residues 1-720 of Psq. The SID region of interaction between both proteins (in green) has been obtained using two fully sequenced clones and localized to the C-terminal domain of the protein Chro, a region of known interaction with other BTB proteins and out of the chromodomain region (in blue). (**B**) A 1-by-1 Y2H assay has been performed using two different fragments of the 1-720 aminoacid region of Psq: aa1-131, aa132-720 (lines in blue). The 1-720 aminoacid region of Psq contains the BTB domain (in grey) and several Glutamine and Histidine rich regions (white boxes), and not the DNA binding domain (green). (**C**) The following interaction pairs were tested: i) positive control (Colland et al., 2004). ii) empty LexA bait vector / empty prey vector (negative control). iii) empty LexA bait vector / AD-Chro (negative control). iv) LexA-Psq (Psq 1-720)/ empty prey vector (negative control). v) LexA-Psq (Psq 1-720)/ AD-Chro. vi) LexA-Psq (Psq 1-131)/ empty prey vector (negative control). vii) LexA-Psq (Psq 1-131)/ AD-Chro. viii) LexA-Psq (Psq 132-720)/ empty prey vector (negative control). ix) LexA-Psq (Psq 132-720)/ AD-Chro. The DO-2 selective medium lacking Tryptophan and Leucine was used as a growth control and to verify the presence of both the bait and prey plasmids. Different dilutions of yeast were also spotted on a selective medium without Tryptophan, Leucine and Histidine (DO-3). Different concentrations of 3-aminotriazole (3-AT), an inhibitor of the *HIS3* gene product, were added to the DO-3 plates to increase stringency. (**D**) Psq-Chro co-immunoprecipitations in S2 *Drosophila* cells. As indicated, the constructs pMT, pMT-Chro::GFP and/or pMT-3xFlag::BTBPsq::tRFP were transiently transfected and their expression has been induced with 1.4 mM $CuSO_4$ to the culture medium, 24hr after transfection. Cells were collected and lysed 48hr after transfection. The IP was performed using the protocol described in materials and methods. The protein lysates were immunoprecipitated with a-Flag or a-GFP antibodies, and the immunoprecipitates were analysed in WB probed with antibodies against anti-Flag or a-Chro, for Psq and Chro detection respectively.

This 1by1 Y2H is based on the *HIS3* reporter gene (growth assay without Histidine), and it was performed as described in Material and Methods (Yeast Two-Hybrid). The assay shows that the N-terminus of Psq (Psq 1-131) interacts with Chro in the presence of 1mM 3-AT (Figure 29C 1-by-1 Y2H, columns vi and vii). The other two Psq fragments tested Psq 1-720 and Psq 132-720, autoactivate the Y2H system on DO-3 medium (Figure 29C 1-by-1 Y2H, columns iv and viii), since we observe growth of yeast clones in the absence of prey. However, on DO-3 medium supplemented

with 1mM 3-AT, we observed a decreased growth for the negative control (Figure 29C 1-by-1 Y2H columns vi and viii) and a similar decrease for the interaction assay with Chro (Figure 29C 1-by-1 Y2H columns v and ix). Therefore, we cannot trust the interaction detected between these two Psq fragments and Chro. This autoactivation domain is located in the region between the BTB and the DNA binding domain and it was also reported in previous 1-by-1 Y2H done in the laboratory with Psq but the origin of this autoactivation remains unknown.

The interaction between Psq and Chro was confirmed also by co-immunoprecipitation (Figure 29D). S2 cells were transfected with $CuSO_4$ inducible constructs, pMT control vector; pMT-Chro::GFP and/or pMT-3xFlag::BTBPsq::tRFP. On figure 29D, in lane 6 of the upper gels we can observe that by immunoprecipitating PsqBTB with the a-FLAG antibody, we are able to detect both the endogenous and the GFP tagged Chro. The same occurs when we immunoprecipitate Chro with a-GFP and we detect PsqBTB (Figure 29D lower gels, lane 6). These results demonstrate that Chro interacts with Psq, specifically with a BTB containing isoform, further supporting the results obtained in the 1-by-1 Y2H.

To sum up, our biochemistry experiments demonstrate that Chro interacts with the BTB domain of Psq through a region located in its C-terminal part, spanning aa 504-670*. This Chro region has been previously involved in mediating the interaction with other BTB insulator proteins, such as CP190 and Mod((mdg4) (see Table 2 with a summary of BTB-protein interactions).*

	GAF	Lola Like	Mod(mdg4)	PsqBTB	CP190	Chromator
GAF	+	+	+	+		
Lola Like	+	+	+	+		
Mod(mdg4)	+	+	+		+	+
PsqBTB	+	+		+		+
CP190			+		+	+

Table 2. Summary of interactions between different BTB proteins. In previous works, different experiments showed that the BTB proteins GAF, Lola like, Mod(mdg)4 and CP190 are able to interact with each other. Our results add evidences for PsqBTB and Chro to also join this group of proteins, pointing to a possible new role of Psq in chromatin insulation.

1.2 Pipsqueak out of the spindle matrix during mitosis.

To study the functional significance of the interaction between Chro and PsqBTB, we tested their co-localization in polytene chromosomes, to see if they co-localize in different bands or interbands, and throughout the cell cycle, due to the roles of Chro during mitosis.

Immunohistochemistry of polytene chromosomes was performed using an antibody that recognizes both isoforms of Psq (with and without the BTB domain). This a-Psq total polyclonal antibody was generated against a fragment located between aa 453-552 of Psq protein, which is common to all Psq isoforms. Inmunohistochemistry shows a partial co-localization of Psq and Chro in

interbands (Figure 30A, marked by the absence of DAPI in figure 30A'), regions with low concentrations of condensed chromatin and characterized by active transcription.

However, Psq seems to not interact with Chro during mitosis. In mitotic cells, as has been described in (Schwendemann *et al.*, 2002), Psq and GAF co-localize and are associated with the centromeric regions of chromosomes (Figure 30D-D' marked with CID: CENP-A centromere marker) throughout the cell cycle of S2 cells, derived from a primary culture of late stage (20–24 hr old) *Drosophila* embryos (Figure 30B-C, endogenous Psq fully co-localizing with chromosomes, DAPI in B-B' Phosphohistone3 in 30C-C' and CID in 30D and its single stack in D'). In *Drosophila*, these centromeric regions are characterized by the presence of GAGA-rich regions (Brutlag, 1980; Lohe *et al.*, 1993). Since GAF and Psq have been shown to bind directly to GAGA -rich DNA sequences (Lehmann *et al.*, 1998; Soeller *et al.*, 1993), it is not rare to find GAF and Psq in these centromeric regions.

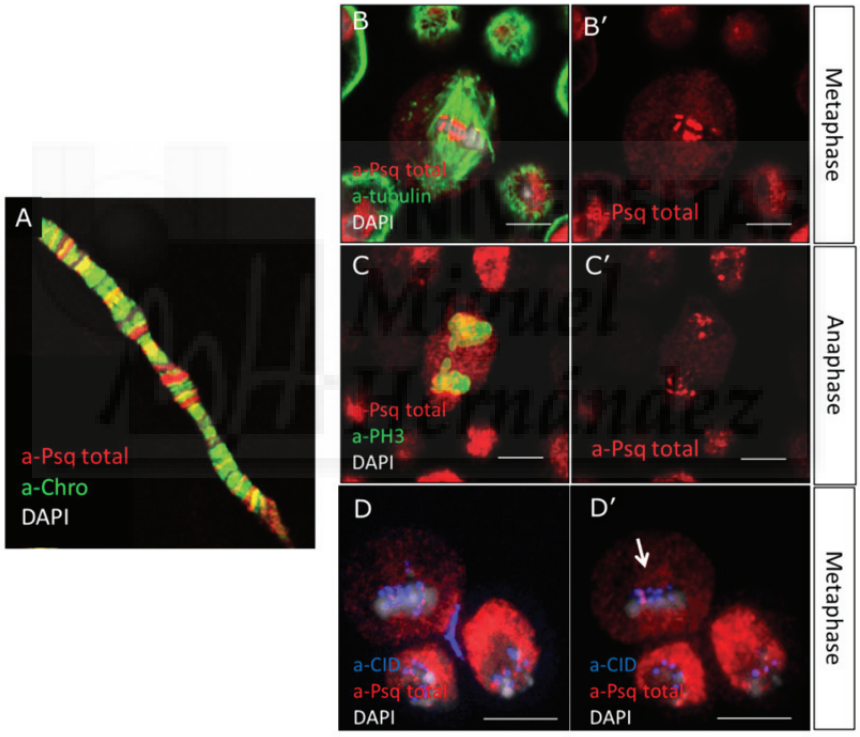

Figure 30. Pipsqueak binds to different bands in polytene chromosomes and it is present in centromeric regions of chromosomes. (**A**) Polytene chromosomes show a co-localization of Psq and Chro in certain bands. Polytene chromosomes have been squashed using the technique described in materials and methods and stained with Psq total and Chro antibodies and the DNA marker DAPI. (**B-D'**) Psq total isoforms have been localized in centromeric regions of chromosomes during mitosis using different mitotic markers, such as tubulin, to see the mitotic spindle (green) (**B-B'**), Phosphohistone 3 showing mitotic chromosomes (green) (**C-C'**) and the centromere-specific histone variant CENP-A (CID in *Drosophila,* in blue), (**D-D'**) used to unveil the co-localization of Psq in centromeric regions.

Although Psq is present throughout the cell cycle, it does not co-localize with Chro, which is known to be a member of the mitotic spindle matrix (Rath *et al.*, 2004; Yao *et al.*, 2014) away from chromosomes, since it is a tubulin binding protein (shown in Figure 31A-B'' in different phases of mitosis).

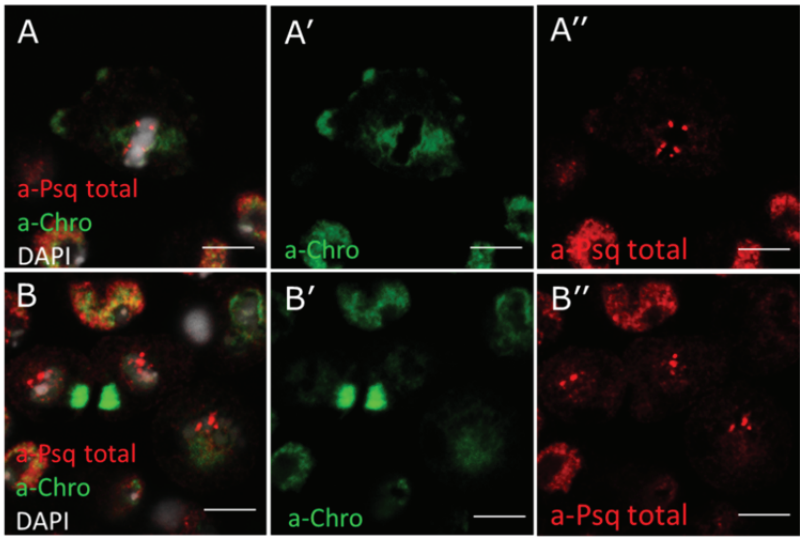

Figure 31. Chromator and Pipsqueak have different locations within the cell during mitosis. (**A-B''**) Chro (green) is a member of the mitotic matrix in charge of the correct establishment of the mitotic spindle, whereas Psq (in red) localizes at centromeric regions of chromosomes, as seen in *Drosophila* S2 cells with antibodies against Chro and all isoforms of Psq. (**A-A''**) S2 cells in metaphase and (**B-B''**) S2 cells in telophase.

Psq and Chro co-localize in a subset of interbands of polytene chromosomes, where actively transcribed genes are present, suggesting that these two proteins may interact in order to regulate gene expression rather than mitotic events. In this way, we focused our efforts on unveiling the possible relation between both proteins at the transcriptional level. For that, we performed several Chromatin Immunoprecipitations coupled with massively parallel DNA sequencing (ChIP-seq) in other to study their chromatin distributions.

1.3 Mapping BTB- and non-BTB Pipsqueak binding sites in the genome.

1.3.1 Bioinformatic analysis of Pipsqueak ChIP-seq data reveal potential and specific roles of the BTB-containing Pipsqueak as a chromatin insulator.

Due to the evidences we have regarding Psq relationship with PcG, where it acts as a recruiter to PREs (Huang *et al.*, 2002), and its relationship with insulator members like Chro, we wanted to determine its genome-wide distribution to unravel the roles of the different Psq isoforms in transcriptional regulation. For that we performed several ChIP-seqs taking advantage of the homogeneous population of Kc167 cultured cells, as recently carried out for several DNA-binding factors (Heger *et al.*, 2013; Sanyal *et al.*, 2012; Soshnev *et al.*, 2013; Van Bortle *et al.*, 2012; Van Bortle *et al.*, 2012; Xu *et al.*, 2011). In this way, we count with a long list of ChIP-seqs from different histone modifications and transcription factors, performed in these *Drosophila* cells, to characterize the genomic distribution of the different Psq isoforms.

We designed an antibody that recognizes the BTB isoforms of Psq alone, since all the previously described work has been performed with an antibody against Psq that recognizes both short and long isoforms, with and without the BTB domain. It is not possible to obtain antibodies

specific to short isoforms because the entire sequence of non-BTB Psq is contained in PsqBTB. These BTB-isoforms have never been studied alone before. All the data published from Psq usually includes both types of isoforms, attributing a functional role without distinctions or only speculating about the origin of this role mediated by the BTB domain. To further explore whether non-BTB Psq and PsqBTB have the same or different functions, we looked for differences in their genomic distribution by ChIP-seq. The specificity of Psq antibodies was first tested in the wing disc using the *Gal4-UAS* system by knocking-down all isoforms of Psq under *MS1096-Gal4* and overexpressing PsqBTB under *dpp-Gal4* (Figure 32).

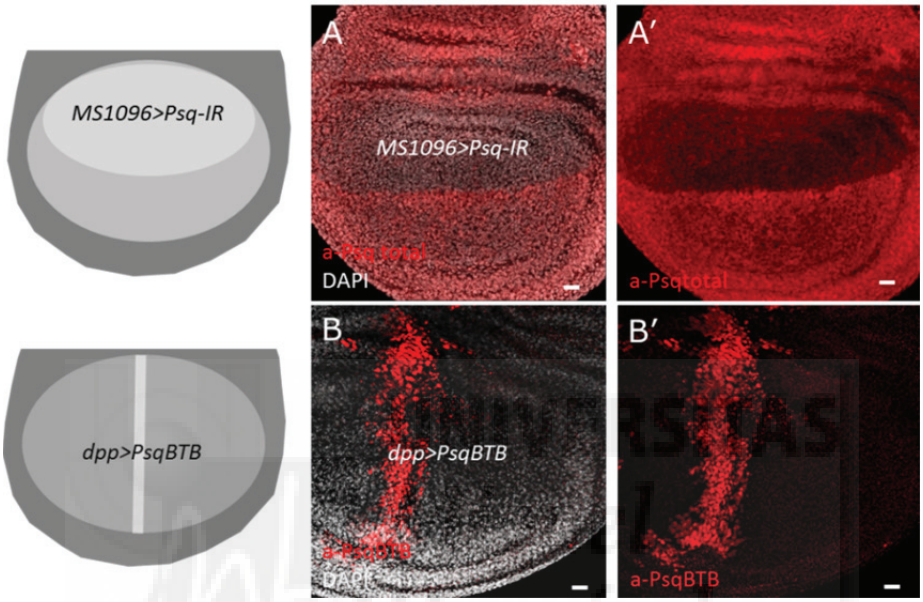

Figure 32. Antibodies for all isoforms of Pipsqueak and PipsqueakBTB show their specificity for Pipsqueak isoforms. (**A**) a-Psq antibody recognizing both forms of Psq has been tested by using the *UAS-Gal4* system knocking-down by RNAi both forms under the *MS1096-Gal4* line expressed at higher levels in the dorsal compartment of the mature third-instar disc than in the ventral compartment. No signal can be detected for Psq in the dorsal compartment after the knock-down induction. (**B**) The a-PsqBTB antibody cannot detect levels of PsqBTB in the WT wing. These isoforms can only be detected with the overexpression under the *dpp-Gal4* line. The schemes show the expression region of the RNAi and the UAS-line under *MS1096* and *dpp* in the wing imaginal disc.

Chromatin immunoprecipitation followed by sequencing, first described in 2007 (Barski *et al.*, 2007; Johnson *et al.*, 2007; Mikkelsen *et al.*, 2007; Robertson *et al.*, 2007), allows *in vivo* determination of where a protein binds the genome, which can be transcription factors, DNA-binding enzymes, histones, chaperones, or nucleosomes. ChIP-seq first cross-links bound proteins to chromatin, fragments the chromatin, captures the DNA fragments bound to one protein using an antibody specific to it, and sequences the ends of the captured fragments using next-generation sequencing. Once we validated the specificity of both Psq antibodies, we used them to perform ChIP-seq experiments using Kc167 *Drosophila* cells (See Materials and Methods). Peaks reflecting DNA binding points and levels of occupancy of each protein, were identified using MACSv1.4.2 with P-value cut-off of 10^{-5}, and those found in two biological replicates were analysed further (final number n= 2191 conserved peaks for PsqBTB and n= 4136 for Psq total ChIP-seqs). The sites in the genome where Psq is present in the Psq total data set (containing both BTB and non-BTB isoforms),

but absent in the PsqBTB data should be specific for the non-BTB Psq isoform (n= 3219). That is to say, the non-BTB Psq data will contain sites where these isoforms are present without PsqBTB. This number had to be close to, but higher than, the expected non-BTB Psq 1945 peaks, if both antibodies were completely efficient and specific. The discrepancy between expected and observed results suggests that the a-PsqBTB antibody recognizes some sites that are not recognized by the Psq total antibody. Only 917 peaks of 2191 from PsqBTB overlap with Psq total binding sites. This can be due to the fact that the amount of PsqBTB in Kc167 cells is lower than that of the non-BTB Psq isoform and PsqBTB peaks, recognized by the Psq total antibody, are not identified by MACS. Additionally, since the peak height reflects the levels of occupancy of each protein bound to a specific site, small peaks identified by PsqBTB antibody that are recognized by the Psq total antibody as high and very well defined peaks were considered as sites with PsqBTB and non-BTB Psq at the same time. In the thesis, to simplify the information presented, sites with both types of isoforms will be considered only if they add relevant information.

- **The binding motif of both isoforms of Pipsqueak reveals different locations throughout the chromatin.**

To study the general binding of the BTB and non-BTB Psq isoforms, we determined the enriched consensus sequence motifs by MEME-ChIP using default settings (Machanick *et al.*, 2011) considering Psq total and PsqBTB summits of the binding peaks ±200 bp.

We observed that there is an enrichment of the GAGA sequence for Psq total binding sites (77% of total binding sites) (Figure 33A). This motif was already described for GAF binding sites (Lehmann *et al.*, 1998) and also attributed to Psq, since they both are found complete overlapping on polytene and mitotic chromosomes (Schwendemann *et al.*, 2002).

Regarding PsqBTB alone, we can see an enrichment of the Su(Hw) motif (53% of total binding sites) and not enrichment in GAGA sequences (Figure 33B). This Su(Hw) motif was also found in the Psq total data but not really enriched in the peak summit and only detected with lower probability (Figure 33A Psq total 400 bp window). The Su(Hw) motifs predict a co-localization of PsqBTB with other insulator proteins in addition to the Chro protein found by Y2H, as it has been described in the introduction of BTB-containing protein interactions (See Table 1 and Table 2).

Peaks present in the Psq total data set that are not present in the PsqBTB ChIP-seq should be specific for the non-BTB Psq isoforms. Thus, these peaks were identified using the public available intersect tool in Galaxy software (Blankenberg *et al.*, 2010; Giardine *et al.*, 2005; Goecks *et al.*, 2010) after detecting the overlap between Psq total and PsqBTB binding sites. Using MEME-ChIP we then obtained the motif enriched in the binding sequences of this isoform (81% of total binding sites). Analysing the distribution of both proteins using the Interactive Genomic Viewer (IGV) software from the Broad Institute (http://www.broadinstitute.org/software/igv) we can see in Figure 33C (for example in Chromosome 3L form site 17,812,349 to site 19,288,134) that non-BTB Psq (in the absence of PsqBTB) shows almost the same finger print over the chromatin as the protein GAF. However, there is not a full overlap between their summits, as can be seen also in the data obtained

by MEME-ChIP (Figure 33C). This finding can correlate with the new DNA binding domain proposed for Psq total binding sites, which is similar but not identical to the GAGA sequence (Kasinathan *et al.*, 2014). Detailed and complementary bioinformatics analysis can be performed to obtain the non-BTB Psq binding motif in the centre of the summit using, for example, the strategy developed by Kasinathan and colleagues (Kasinathan *et al.*, 2014) searching non- previously described motives. Other software programs, such as Regulatory Sequence Analysis Tools (RSAT), give similar binding motives for the different isoforms of Psq.

These results are consistent with the finding of Lehman and colleagues (Lehmann *et al.*, 1998), who show that a truncated form of Psq lacking an essential part of the BTB domain has stronger binding affinity for GAGA sequences than the full-length isoforms, raising the possibility that both types of isoforms encoded by *psq* have two different roles in chromatin biology.

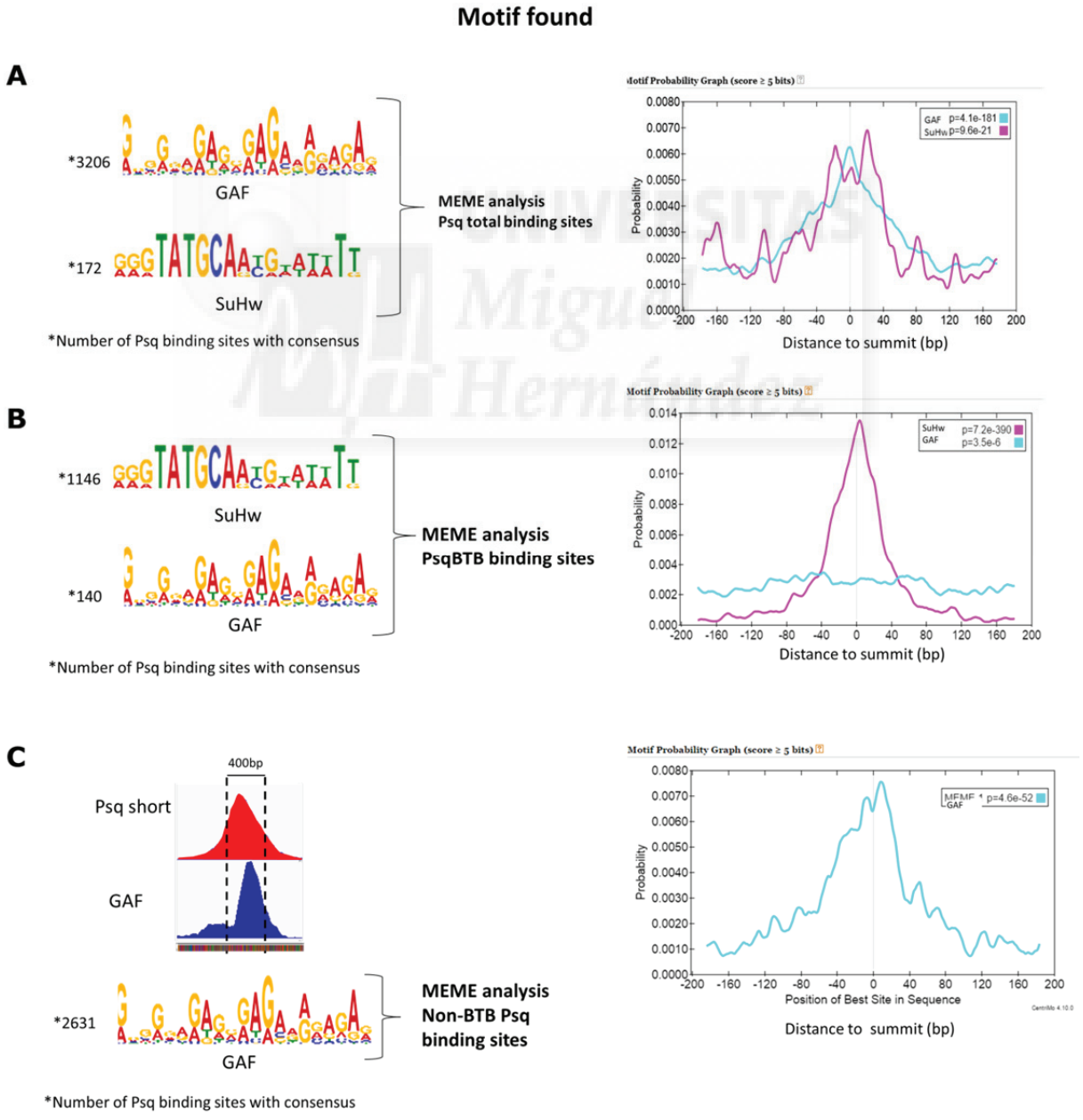

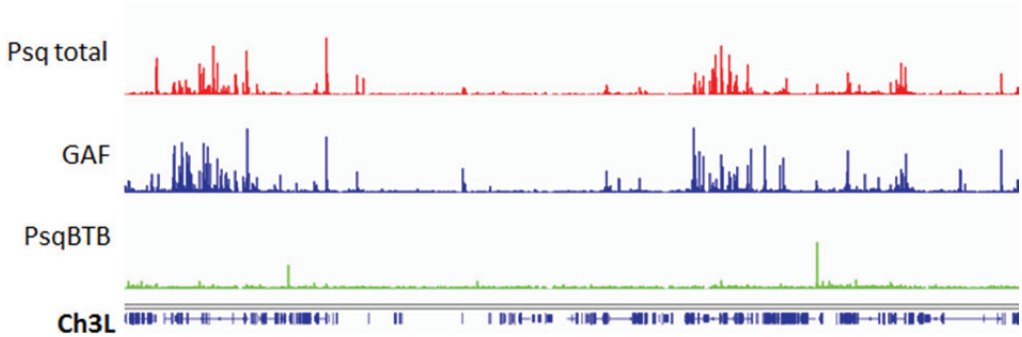

Figure 33. Both types of isoforms of Pipsqueak differentially locate throughout the chromatin. (**A**) For total binding sites of Psq (here referred to as Psq total) there is an enrichment of the GAGA sequence (77% of total binding sites) almost at the centre of the summit, as can be seen in the probability vs. distance to the summit observed for this motif. (**B**) For PsqBTB alone there is an enrichment of Su(Hw) motifs (53% of total binding sites) and not for GAGA sequences. This motif was also found in the Psq total data (**A**) but not really enriched in the peak summit and with lower probability. (**C**) Peaks present in the Psq total data set that are not present in the PsqBTB ChIP-seq should be specific for the non-BTB Psq isoform. The GAGA motif is enriched in the binding sequences for this short isoform (81% of total binding sites). Analysis of the distribution of both proteins using the Interactive Genomic Viewer (IGV) from Broad Institute in (**C**) (Chromosome 3L form site 17,812,349 to 19,288,134) shows that non-BTB Psq (red, not overlapping with PsqBTB in green) binds to the same regions as GAF (blue). However, there is not full overlap between their summits. This information has been obtained by using MEME-ChIP and confirmed with other predictor programs such as Regulatory Sequence Analysis Tools (RSAT).

- **ChIP-seq data show different clusters of proteins co-localizing with Pipsqueak isoforms.**

To study the binding regions and co-localizing proteins characterizing Psq, the binding peaks of Psq total and PsqBTB identified by MACS in two biological replicates (n = 5115 and n= 2355 respectively), were used as anchors to generate heatmaps. The heatmaps were then K-means clustered using Cluster 3.0 in 3 clusters and viewed in Java Treeview. Each column in Figure 34 corresponds to one heatmap and represents the distribution of ChIP-seq signal for an individual protein or histone modification in relation to the location of the Psq total binding sites used as anchors in a +/- 2 kb region. In the case of Psq total in the first column, this distribution is manifested as a red line in the centre of the column. The different shades of red inside each column represent different amounts of protein present in the +/- 2 kb region of the genome around the peak summits of Psq total used as anchors. Other columns in Figure 34 represent the distribution of other proteins or histone modifications in the same regions of the genome with respect to the location of Psq total.

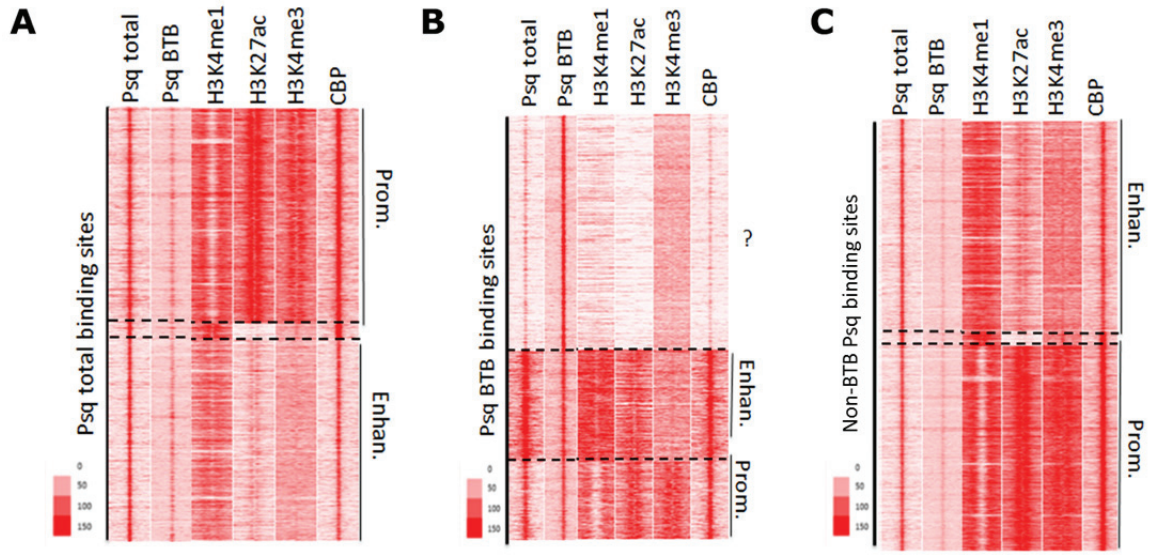

Figure 34. Pipsqueak isoforms are differentially located along the chromatin. (**A-C**). Heatmaps show the localization of the different proteins or histone modifications around the genomic locations corresponding to Psq total (data from both isoforms) in (**A**), to PsqBTB in (**B**) or to non-BTB Psq in (**C**)). Heatmaps were generated using the peaks obtained in Kc167 cells of Psq total, PsqBTB and non-BTB Psq identified by MACS as anchors. The heatmaps were then K-means clustered using Cluster 3.0 in 3 clusters and viewed in Java Treeview using key features of active enhancer elements (H3K4me1 and H3K27ac produced by CBP and no H3K4me3) and promoters (H3K4me3 and no H3K4me1). All these Psq isoforms are located at enhancers and promoters but PsqBTB is present in an extensive region of the genome (marked by ? in panel B) that cannot be classified as enhancers or promoters based on this analysis.

Hereafter, we study the presence of Psq at enhancers and promoters, or co-localizing with Pc, GAF and insulators, including Chro.

Enhancers and promoters:

PsqBTB and non-BTB Psq (and consequently Psq total) are present at enhancers and promoters (Figure 34A, 34B and 34C), suggesting that this transcription factor has a wide variety of roles in transcriptional regulation. As seen in Figure 34B, in the heatmap done with PsqBTB as an anchor there is an enrichment of Psq total binding sites at enhancers, showing that non-BTB Psq and PsqBTB co-localize at enhancers.

Precise regulation of gene expression in time and space is required for development, differentiation and homeostasis (Bulger *et al.*, 2010). Sequence elements within or near promoter regions contribute to regulation, but promoter distal regulatory regions like enhancers are essential in the control of cell-type specificity (Bulger *et al.*, 2010). Enhancers were originally defined as remote elements that increase transcription independently of their orientation, position and distance to a promoter (Banerji *et al.*, 1981). They were only recently found to initiate Pol II transcription, producing the so-called eRNAs (Kim *et al.*, 2010). Genomic locations of enhancers can be detected by mapping their chromatin marks and transcription factor binding sites using chromatin immunoprecipitation.

Genomic studies have identified several key features of enhancer elements. Specifically, they correlate with the location of mono-methylated lysine 4 of histone H3 [H3K4me1 (Heintzman *et al.*, 2009; Lupien *et al.*, 2008; Schnetz *et al.*, 2010) (Barski *et al.*, 2007; Heintzman *et al.*, 2007) (Xi *et al.*, 2007)]. Although a large number of regions in the genome display these characteristics, only a fraction of the H3K4me1-marked elements are actively engaged in modulating transcription in a given cell type (Creyghton *et al.*, 2010; Heintzman *et al.*, 2009; Rada-Iglesias *et al.*, 2011). These elements are referred to as active enhancers, characterized additionally by the presence of H3K27ac. Other H3K4me1-marked enhancers modulate transcription in response to differentiation cues or other cellular stimuli and are thus considered poised (Creyghton *et al.*, 2010; Rada-Iglesias *et al.*, 2011). The initial clustering presented in Figure 34 suggests that there are significant numbers of Psq peaks at regions enriched for H3K4me1 and lacking H3K4me3 (promoter histone modifications characteristic of enhancers). To further explore the presence of Psq at these sequences, a previously published set of enhancers from STARR-Seq project (also known as self-transcribing active regulatory region sequencing (Arnold *et al.*, 2013)) was used to generate enrichment heatmaps of Psq total, PsqBTB and H3K27ac, a histone modification found at active enhancers (Figure 35A). Although all regions with H3K4me1 enrichment may be enhancers, the correlation of Psq binding with the H3K27ac modification, carried out by the histone acetyltransferase CBP, supports a role in active transcription (Tie *et al.*, 2009).

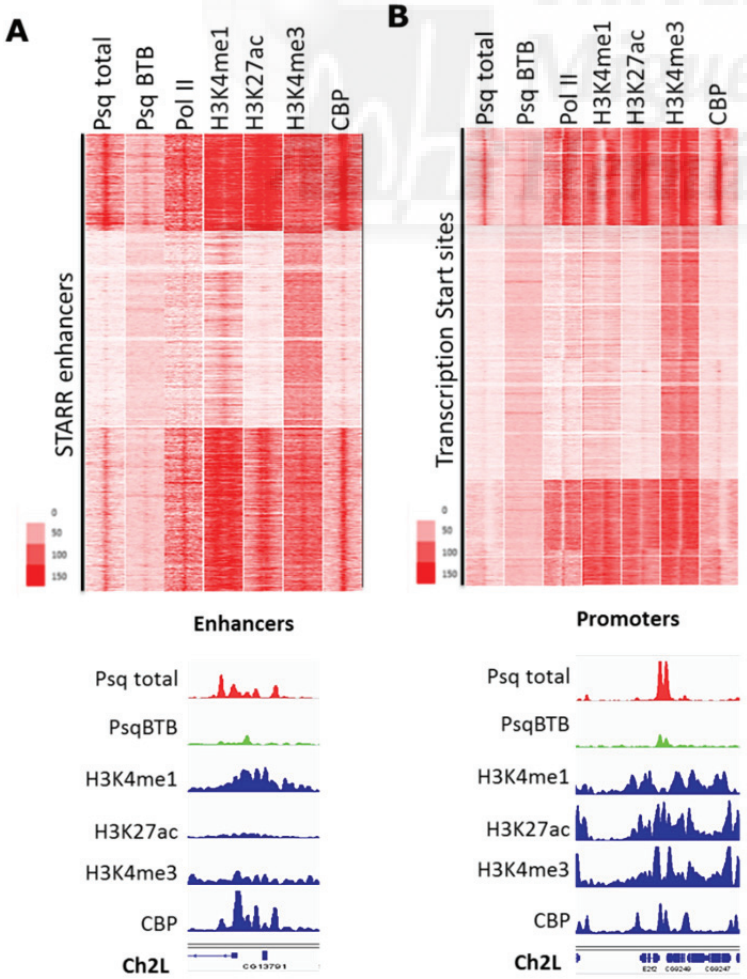

Figure 35. Pipsqueak is located at active enhancers and promoters. (**A**) Heatmaps were generated using enhancers obtained by STARR-Seq as anchors and features of active enhancer elements (H3K4me1, Pol II, H3K27ac produced by CBP, and no H3K4me3). Using the Interactive Genomic Viewer (IGV) from Broad Institute, we can confirm the presence of Psq total and PsqBTB at enhancers (Chromosome 2L from site 7,497,805 to 7,578,980). (**B**) TSSs were used as anchors to perform clustering analyses. Using IGV the presence Psq total (both isoforms of Psq) and PsqBTB at promoters can be confirmed (Chromosome 2L from site 21,153,122 to 21,159,578).

To further investigate the role of Psq present in regions enriched in H3K4me3 presumed to be promoters, TSSs from the genome annotation data at UCSC Genome Bioinformatics (https://genome.ucsc.edu/) were used as anchors to obtain a heatmap. Both forms of Psq are present at transcription start sites (Figure 35B). The presence of Psq at promoters suggests an involvement of this protein in transcription activation. This conclusion is supported by the Y2H (see table S3 in Appendix I) and experiments performed by Dr. Verónica Miguela showing that Psq interacts with Bip2 (Bric-à-brac interacting protein 2, the fly homolog of TAF3). Bip2 is a histone fold and a homeodomain containing subunit of Transcription factor II D (TFIID). TFIID is one of several general transcription factors that make up the Pol II pre-initiation complex (PIC) at promoters.

Insulator proteins:

PsqBTB is present in regions of the genome that cannot be classified as enhancers or promoters, based on the clustering analysis described above, and that do not overlap with Psq total (Figure 34B region classified as "?"). Since we found the Su(Hw) binding motif to be present in PsqBTB binding sites by MEME-ChIP, we used ChIP-seq data from Su(Hw) and its interacting partners CP190 and Mod(mdg4)2.2 to perform a clustering analysis. Results from this analysis show that PsqBTB sites that do not correspond to enhancers or promoters co-localize instead with the specific Su(Hw) binding sites along the genome (Figure 36).

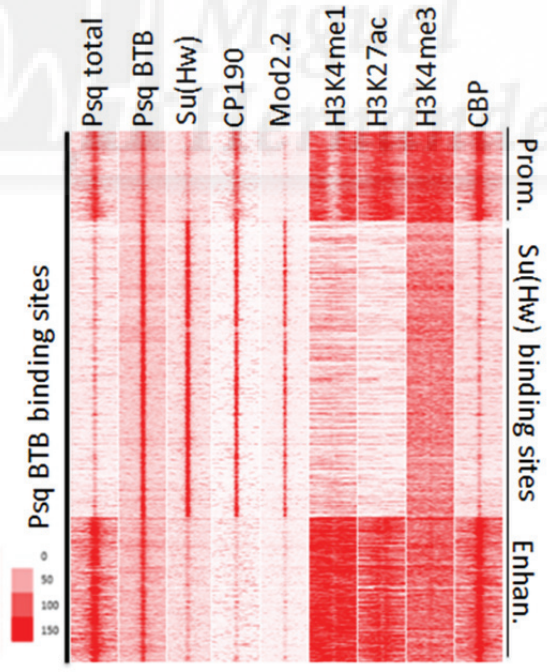

Figure 36. PipsqueakBTB co-localizes with insulator proteins at Su(Hw) binding sites. PsqBTB, Su(Hw), CP190 and Mod(mdg4)2.2 (insulator protein found in the *gypsy* insulator) co-occur at what we call here Su(Hw) binding sites. Information obtained using PsqBTB binding sites as anchors and adding new information to the enhancer and promoter features*:* active enhancer elements and promoters.

This finding may involve PsqBTB in the BTB- induced 3D structure of the chromatin or in insulator-mediated enhancer-blocking activity, supported also by the interaction with Chro.

Chromator binding sites:

We also analysed the protein interaction between PsqBTB and Chro predicted by Y2H. Insulators are sometimes present at promoter regions (Raab *et al.*, 2010). As an insulator protein interacting with other BTB insulators, we can find Chro and its partner Z4 (Eggert *et al.*, 2004; Gan *et al.*, 2011) co-localizing with all isoforms of Psq (PsqBTB and non-BTB Psq Figure 41B and 41C), further confirming the interaction observed between these two proteins in the Y2H assay performed in the laboratory (Table S3).

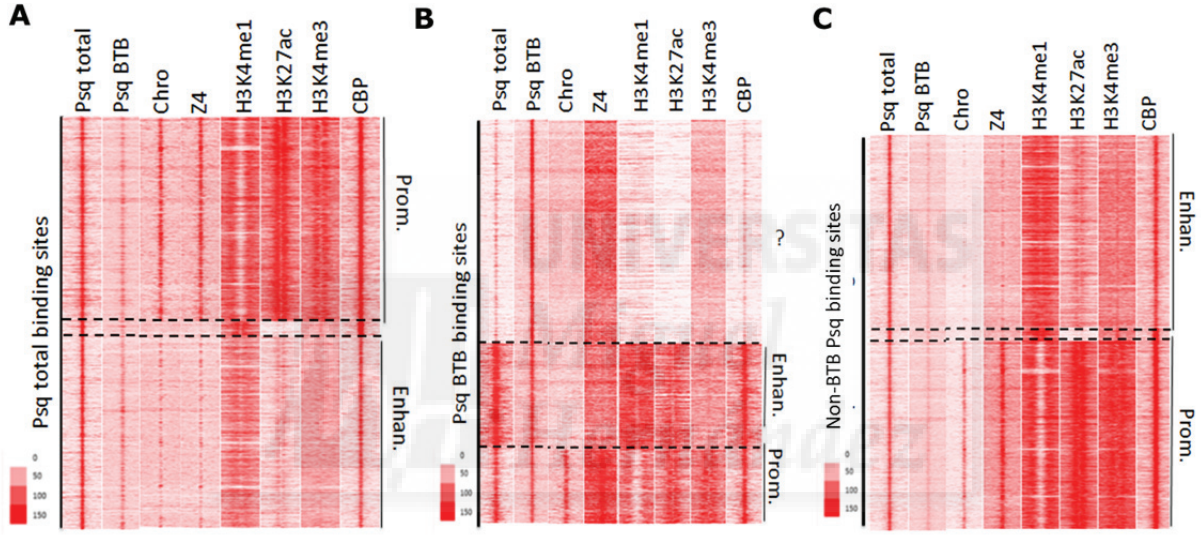

Figure 41. Pipsqueak isoforms co-localize with Chromator and its partner Z4 at promoters. Using Psq total (for both isoforms) (**A**)**,** PsqBTB (**B**) and Psq non-BTB isoforms (**C**) as anchors for the heatmaps, it is shown that Chro and the protein described to interact with Chro (Z4) are found with Psq isoforms at promoters, not enhancers or Su(Hw) binding sites. Features for active enhancer elements and promoters were used. Dotted lines only delimit the different regions present in the heatmaps and the "?" is probably the Su(Hw) insulator protein region, here not identify since we did not include this protein in this analysis.

Using Chro as an anchor to generate a heatmap, we can see that all Chro binding sites, which are situated at promoters, have Psq total and PsqBTB (Figure 42), so that Chro fully co-localizes with Psq along promoters.

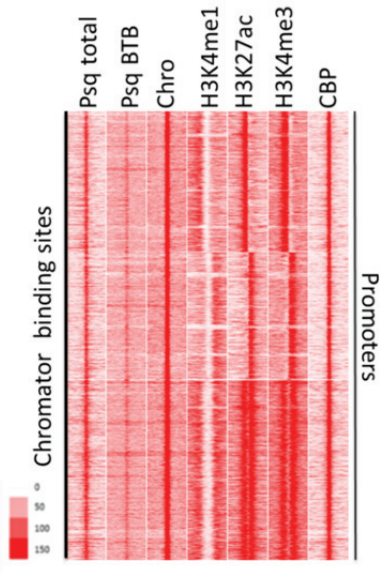

Figure 42. All Chromator binding sites at promoters also contain Pipsqueak isoforms. The usage of Chro binding sites as an anchor for the performance of heatmaps shows the presence of Psq total and PsqBTB in all binding sites of Chro at promoters. Features for active enhancer elements promoters were used.

To gain a deeper understanding of how Psq and Chro interact with insulator proteins, we analysed a specific region in chromosome 3L using the IGV software (Figure 43) as an example of a region showing the previously described Chro-interacting proteins (Z4, Jil-1, GAF and CP190 (Eggert *et al.*, 2004; Gan *et al.*, 2011; Rath *et al.*, 2006)) and both isoforms of Psq. Again, our data from the 1-by-1 Y2H and Co-IP experiments suggest that PsqBTB interacts with Chro through its BTB. This interaction can be attributed to the BTB mediated insulator protein interaction (red asterisk in Figure 43). Likewise, non-BTB Psq can be co-localizing with Chro at promoters acting through other unrelated proteins and functions (Red square in Figure 43).

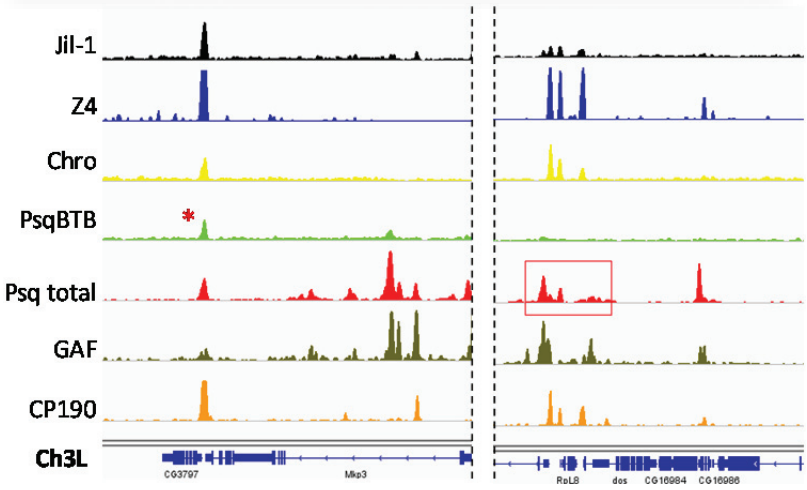

Figure 43. The co-localization between Chromator and Pipsqueak isoforms can be demonstrated analysing their binding sites. Using IGV we can see that both PsqBTB and non-BTB Psq (red not overlapping with PsqBTB in green) are found with Chro (yellow) and its interacting proteins (Jil-1 black and Z4 blue, red square) along the genome. PsqBTB (green) aligns with insulator proteins such as CP190 (orange, red asterisk) or GAF (brown). At these sites non-BTB Psq is absent (isoform seen with a-Psq total antibody for both isoforms of Psq in the absence of PsqBTB). Two examples are shown in chromosome 3L from site 19,047,540 to 19,093,657 (right) and from site 2,579,424 to 2,602,482.

Polycomb response element- related proteins:

Heatmaps with Psq total binding sites show its presence in a region where there is a high enrichment of PcG proteins (two data sets of Pc protein ChIP-seq using two different antibodies obtained from V. Pirrota, and R. Jones VP and RJ in Figure 37), and their direct repressive H3K27me3 marks are in the surrounding chromatin environment, which are then bound by Polycomb proteins to promote silencing. These types of regions have been previously described as classic PREs, where we can also find GAF, described as a Psq recruiter partner (Figure 37A and in 37C, the region between dashed lines).

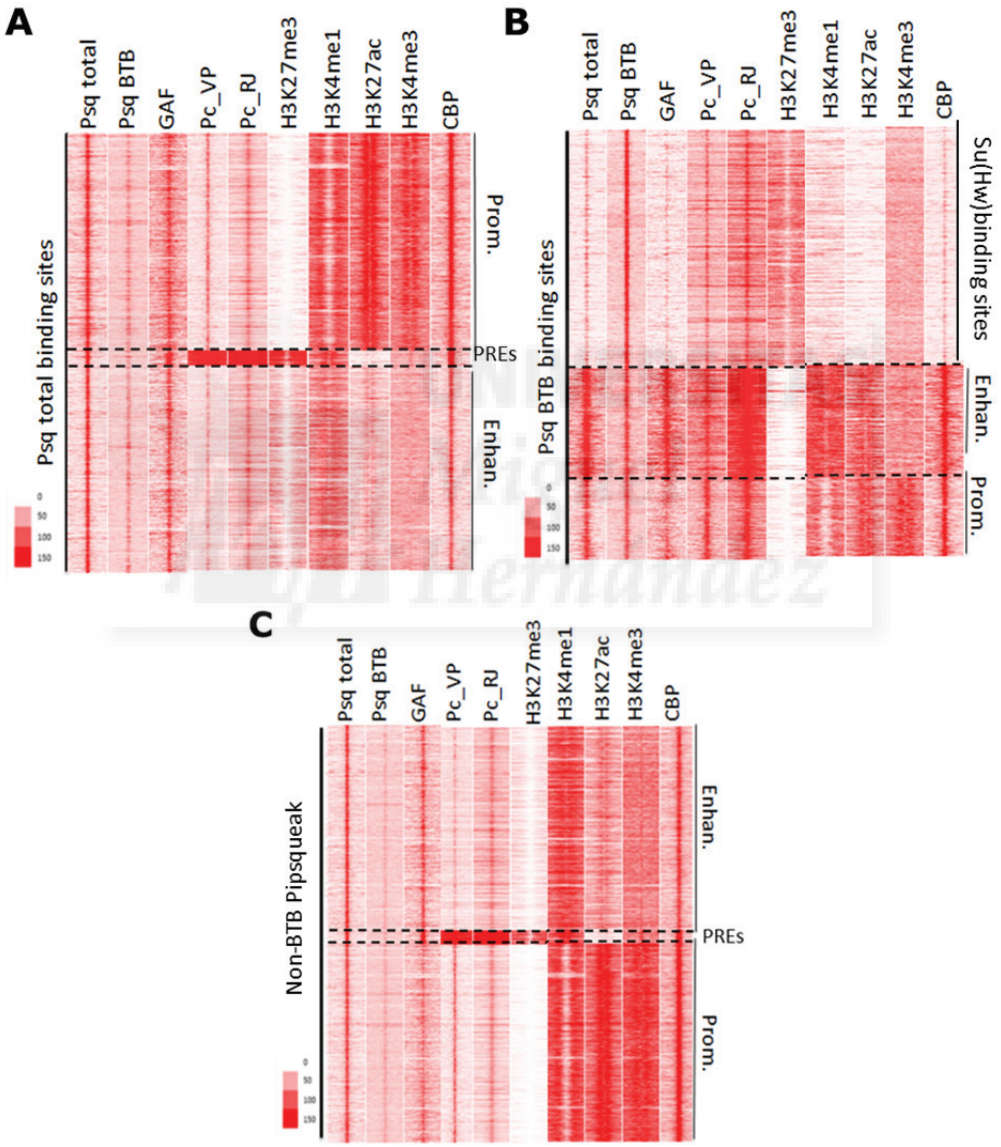

Figure 37. Pipsqueak isoforms co-localize with GAGA Factor and Polycomb along the chromatin. (**A-B**) Heatmaps for Psq total (both isoforms of Psq) (**A**), PsqBTB (**B**) and non-BTB Psq (**C**) show their co-occurrence with GAF and Pc (a polycomb-group member) along the genome, but only non-BTB Psq shows its presence at Polycomb Response Elements (PREs, regions characterized by the enrichment in Pc and the repressive histone modification H3K27me3) shown between dashed lines in (**B** and **C**). Features for active enhancer elements and promoters were used.

The Psq isoforms present at PREs seems to be mainly the non-BTB Psq isoform as we can find a region with the same characteristics between dashed lines in Figure 37C, not found for PsqBTB in Figure 37B. Supporting this finding, the MEME-ChIP analysis shows that the presence of the GAF motif (GAGA sequences) in PsqBTB binding sites is very low (Figure 33B). The presence of the non-containing BTB forms of Psq in GAGA binding sequences, adds new insights to the predicted BTB-mediated functional relation of Psq with PcG (Huang *et al.*, 2002; Schwendemann *et al.*, 2002).

Using the Pc protein as an anchor for the heatmap, we can see that this protein co-localizes with Psq at all sites in the genome (Figure 38). Apart from the reduced set of Pc sites classified as PREs (Figure 38 dashed lines), Psq and Pc are also present at promoters and enhancers showing a high correlation with active transcription. Although the best known functions of Polycomb proteins are those in which it functions as part of the PRC1 complex, activities as individual subunits are also reported, for instance in gene activation events: In prostate cancer cells, EZH2 HMTase from PRC2 and homolog 2 of the *Drosophila* Enhancer of zeste [E(z)], is needed for gene expression (Xu *et al.*, 2012). Likewise, EZH1 (enhancer of zeste homolog 1) inactivation in a tissue cultured model of skeletal differentiation interacts with Pol II and acts as a positive regulator of transcriptional elongation (Mousavi *et al.*, 2012).

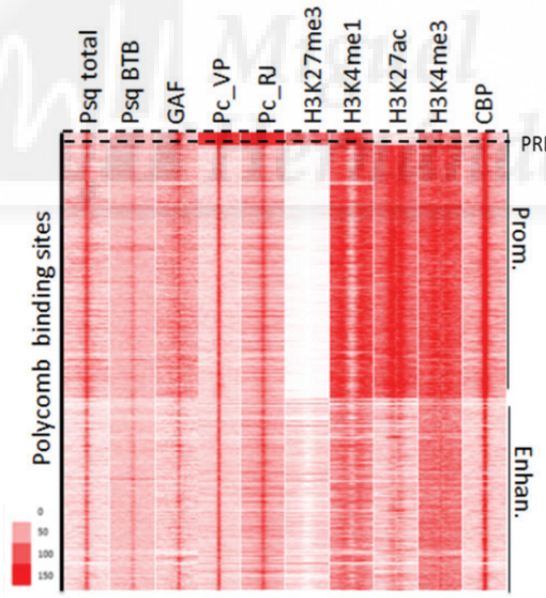

Figure 38. The co-localization between Pipsqueak and Polycomb is not only restricted to its repressive function. Using Pc binding sites as anchor for this heatmap is evident that this protein highly co-localizes with non-BTB Psq and less with PsqBTB all over the genome. This co-occurrence is not restricted to PREs, Psq can also be found with Pc at promoters and enhancers showing a high correlation with active transcription. Features for active enhancer elements and promoters were used.

All the isoforms of Psq co-localize also with GAF binding sites at enhancers and promoters showing multiple roles of Psq and GAF outside of the PRE recruitment function (Figure 37). They regulate many genes independently of the PcG/TrxG system, and thus functional sites occur in many

regulatory regions that are not PREs. Using GAF as an anchor (Figure 39), we can see that Psq total co-localizes widely with GAF and only a fraction of PsqBTB sites share GAF sequences (as also seen in Figure 38B using PsqBTB as an anchor). We can find GAF also at PREs (dashed lines Figure 39).

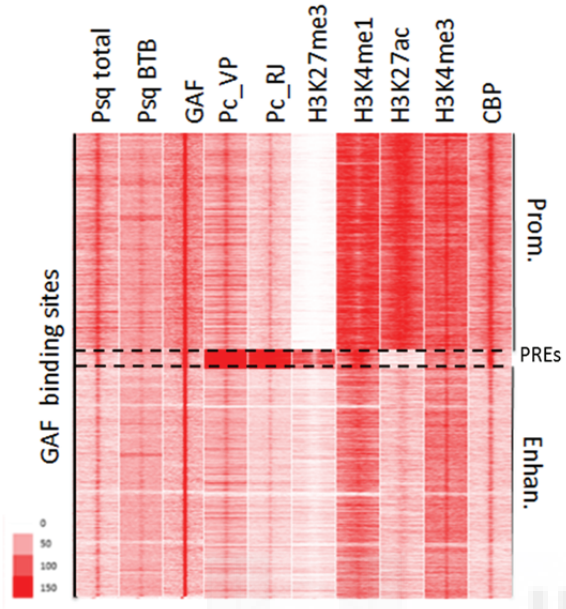

Figure 39. The non-BTB isoforms of Pipsqueak extensively co-localizes with GAGA Factor along the *Drosophila* genome. Using GAF as anchor for the heatmap is evident that this protein is present along the genome with Pc (including at enhancers, promoters and PREs) and the repressive histone modification H3K27me3. PsqBTB information shows a very weak presence at GAF binding sites. Features for active enhancer elements and promoters were used.

In summary, and taking into account the MEME-ChIP results for Psq isoforms, we can conclude that non-BTB Psq has a higher percentage of overlapping binding sites with GAF than the BTB isoforms and probably part of the data published until now for repressive GAGA binding sites and the confluence of Psq and GAF corresponds to the non-BTB isoforms. This result adds new *perspectives* to what was predicted for the "*eyeful*" phenotype and the human oncogenic BTB-proteins, PLZF and BCL-6. In these contexts, their oncogenic function was associated to their BTB, interacting with histone-deacetylases (HDACs), co-repressors and PcG proteins ((Melnick *et al.*, 2002) and citations therein), not correlating with the insulator relation, found for the BTB-oncogenic form of Psq.

As GAF has been previously described in the literature to interact with Psq through its BTB domain (Bonchuk *et al.*, 2011; Schwendemann *et al.*, 2002), we wanted to study in detail their possible co-localization, apart from the interaction found for non-BTB Psq. We can observe co-localization of GAF and PsqBTB in the heatmap, and coordinates extracted from the overlapping sites of both proteins show an enrichment of GAGA sequences using MEME-ChIP. Moreover, having a closer look of both proteins using the IGV software we can see that there are some regions where PsqBTB is present at GAF-Mod(mdg4)2.2-Su(Hw)-CP190 proteins binding sites (red asterisks in Figure 40), showing the previously described relation of GAF with insulators (Table 1 and Table 2). PsqBTB found co-localizing with GAF without the above mention insulators in the genome (red square in Figure 40) is part of the sites containing both types of isoforms of Psq. This means that although it has been published that the BTB-interaction of both proteins mediates their repressive function (Bonchuk et al., 2011; Schwendemann et al., 2002), PsqBTB and GAF are interacting mainly in an insulator related manner. Additionally, the presence of both types of isoforms of Psq in sites that co-

localize with GAF may reflect the processing of PsqBTB, previously described in our laboratory (Thesis of Dr. Verónica Miguela), in a non-BTB containing form, very similar to the non-BTB isoforms of Psq.

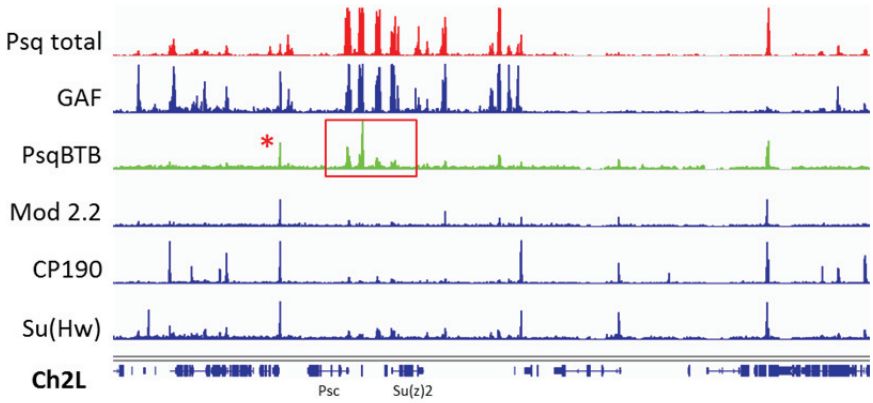

Figure 40. PipsqueakBTB also co-localizes with GAGA Factor but to a lesser extent than the non-BTB isoform. Using the IGV to see the binding sites of Psq total (for both isoforms, in red), PsqBTB (green) and GAF (blue) there are some PsqBTB that overlap with GAF. Some of them are there because its co-occurrence with other insulator proteins (Mod 2.2, CP190 and Su(Hw) red asterisk) and some of them not. An example of chromosome 2L from site 12,890,524 to 13,056,468 is above depicted.

GAF is one of the DNA-binding BTB-proteins used by the Fab 7 insulator located in the Bithorax complex (Schweinsberg *et al.*, 2004) and is present and required for the function of the SF1 insulator found in the Antennapedia complex (Belozerov *et al.*, 2003). The interaction between PsqBTB and GAF can be due to their possible insulator function (Hagstrom *et al.*, 1997; Melfi *et al.*, 2000; Mishra *et al.*, 2001; O'Donnell *et al.*, 1994) as will be subsequently described in the following sections.

1.3.2 PipsqueakBTB forms a complex with Suppressor of Hairy-wing.

Results from the genome-wide analysis of the distribution of PsqBTB with Su(Hw) insulator proteins (CP190 and Mod(mdg4)2.2), suggest the following:

1. PsqBTB Sites are enriched in Su(Hw) binding motifs (Figure 34B).

2. PsqBTB co-localizes genome-wide with Su(Hw) and its partners Mod(mdg4)2.2 and CP190 (Figure 36).

3. Using the location of Mod(mdg4)2.2 or CP190 as anchors, the overlapping sites between PsqBTB and Su(Hw) correspond to those in which Su(Hw) is most abundant (Figure 44A, 44B, 44C).

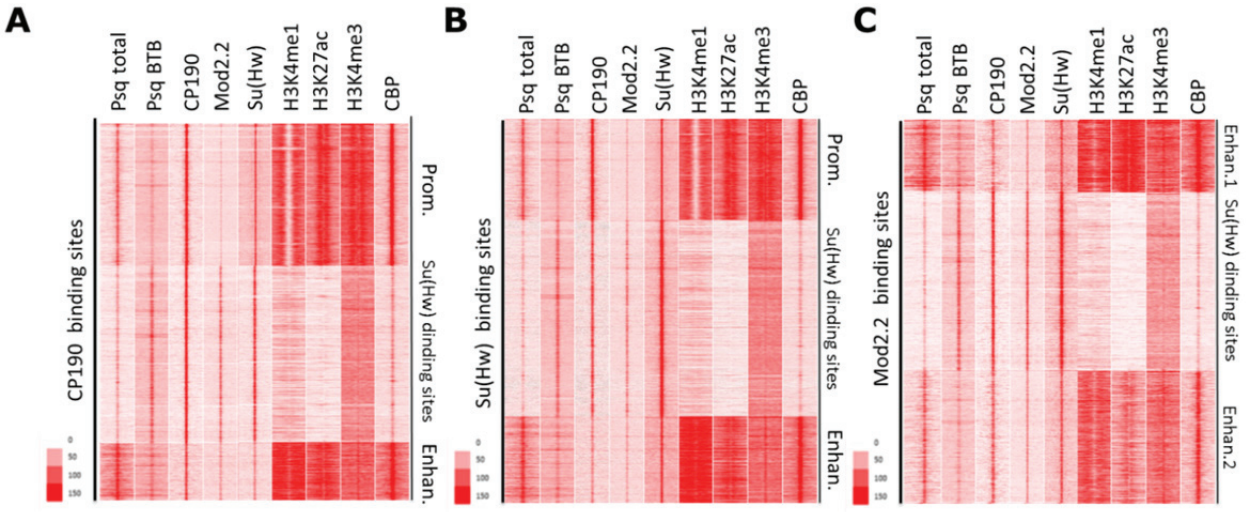

Figure 44. CP190, Mod(mdg4)2.2 isoform and Su(Hw) are found with PipsqueakBTB at specific Su(Hw) binding sites. The co-localization between Su(Hw) and other insulator proteins (CP190 (**A**), Su(Hw) (**B**) and Mod(mdg4)2.2 isoform ,here called Mod2.2 for simplicity (**C**)) can be demonstrated using them as anchors to generate heatmaps. Features for active enhancer elements and promoters were also used. Heatmaps were generated by K-means clustered using Cluster 3.0 and viewed in Java Treeview.

To further characterize the relationship between Psq and these insulator proteins, Co-IPs were performed using antibodies against PsqBTB, Su(Hw), CP190 and Mod(mdg4)2.2. In Figure 45A-B, we observed that we can detect PsqBTB when Mod(mdg4)2.2 and CP190 were immunoprecipitated with specific antibodies. Conversely, we can get all the elements of the complex inmunoprecipitated with PsqBTB. Moreover, this interaction is specific as we cannot significantly immunoprecipitate a control protein such as the EcR (the inmunoprecipitated EcR band is much lower that the input control). Further evidences supporting the co-localization between these proteins and PsqBTB can be seen in preparations of polytene chromosomes immunostained with antibodies against Mod(mdg4)2.2 isoform and PsqBTB (Figure 45C).

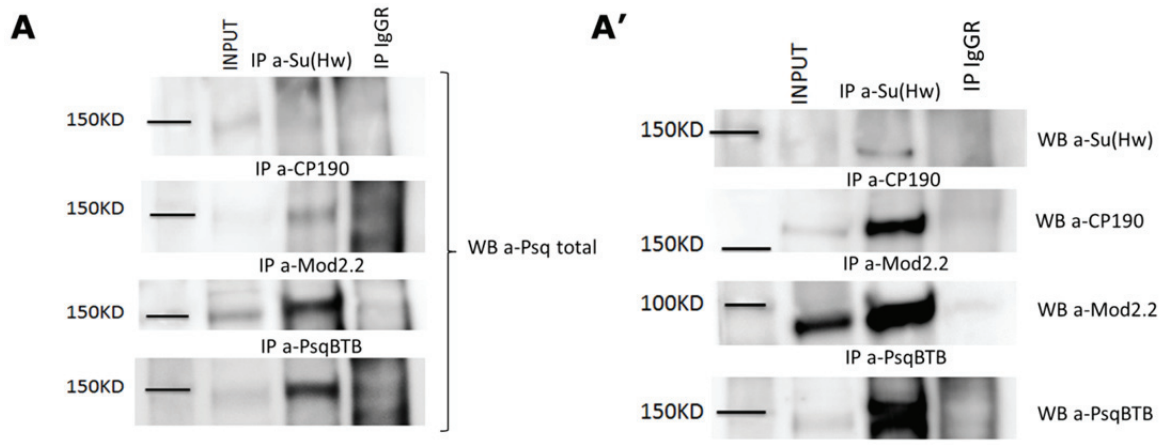

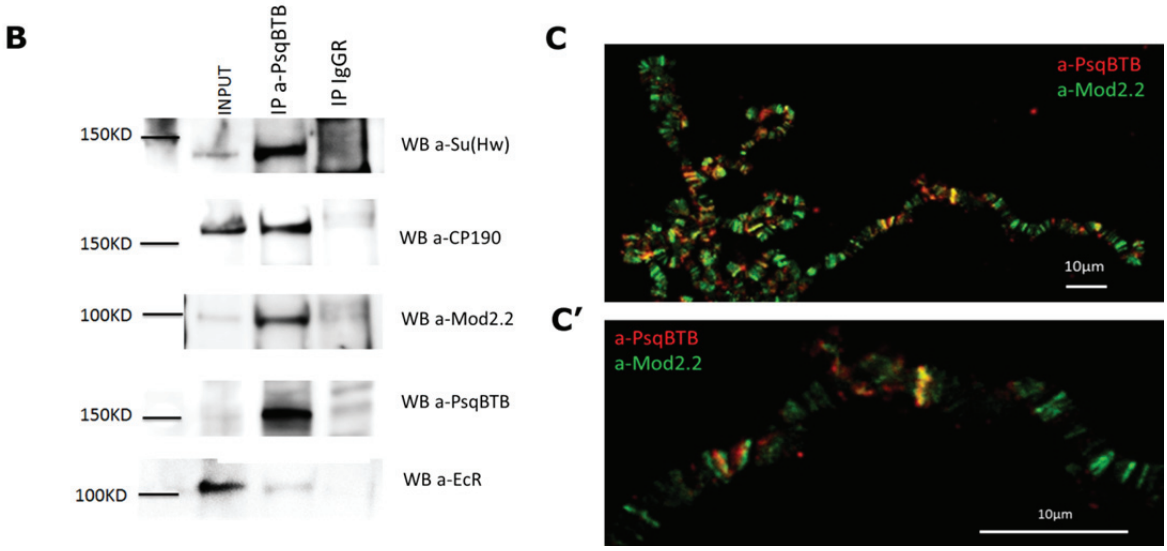

Figure 45. PipsqueakBTB co-immuprecipitates with all the members of the Su(Hw) insulator complex. (**A**) Psq can be Co-IPed with antibodies against CP190, and Mod(mdg4) 2.2 isoform but not with Su(Hw). In (**A'**) we can see the control of the immunoprecipitation of each antibody. (**B**) All these proteins can co-immunoprecipitate with the endogenous PsqBTB using the Ecdysone Receptor (EcR) as a negative control. (**C-C'**) Inmunohistochemistry of Polytene chromosomes using PsqBTB (red) and Mod(mdg4)2.2 isoform (green) show the confluence of both proteins in certain bands.

The results presented up to this point add new elements in the interrelation between different BTB proteins. Psq specific function as insulator will be tested and discussed in subsequent sections of this Thesis.

1.3.3 PipsqueakBTB insulator function tested with the *gypsy* insertion.

The role of Psq as an insulator was evaluated using a *gypsy* insertion mutation that causes adult phenotypes: the *cut* wing phenotype on the ct^6 mutation (Figure 46A). ct^6 wing margins lack bristle cells (Figure 46A). This method permits the evaluation of a protein as strong or weak insulator, depending of the level of suppression of the ct^6 phenotype. For example, the ct^6 margin phenotype is almost completely suppressed in a *mod(mdg4)2.2*-deficient background ($mod(mdg4)^{T6}$ nonsense mutation), which specifically disrupts functioning of the Mod(mdg4)2.2 protein, leading to loss of insulator function (Gerasimova *et al.*, 1995).

For *psq* we used a loss-of-function allele called psq^{0115}, which is a *P[lacZ; ry+]* insertion into the largest *psqBTB* intron that creates an aberrant fusion BTB protein (Horowitz *et al.*, 1995) and a deficiency called *Df(2R)psq-lola Δ18* (here shown as *dfΔ18*), which is an excision that deletes a site in the largest intron of *psqBTB*, deleting all DNA between *psq* and *lola* (Horowitz et al., 1996). The combination of this *mod(mdg4)2.2* deficient background with these two lines has not an evident visual effect in the ct^6 phenotypes when looking at the pictures of adult wings (Figure 46B). Additionally, we used the combination of ct^6 in a background of psq^{0115} allele over *dfD18* to completely remove PsqBTB isoforms (Huang *et al.*, 2002), but we could not significantly supress the

ct^{6} phenotype observed in the wing (Figure 46B). Altogether, with these results we cannot confirm the insulator function of PsqBTB.

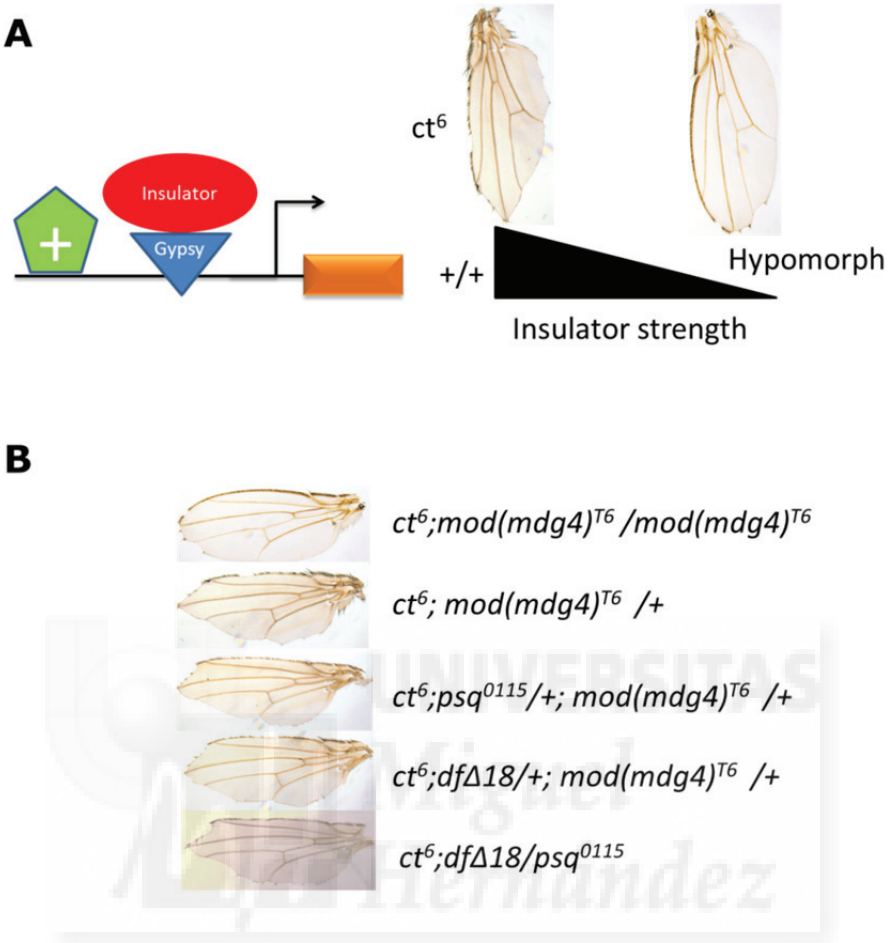

Figure 46. The role of PsqBTB as an insulator can be demonstrated using the repression of the expression of the *cut* gene assayed in the wing. (**A**) Scheme of the *gypsy* insulator inserted between the enhancer and the promoter of the *ct* gene. The loss of function of this gene causes the cut wing phenotype with wing margins lacking bristle cells (*ct*^{6} phenotype). This method permits the evaluation of a protein as strong or weak insulator depending of the level of suppression of the *ct*^{6} phenotype. For example, the *ct*^{6} margin phenotype is almost completely suppressed in a *mod(mdg4)2.2*-deficient background, *mod(mdg4)*^{T6}. (**B**) Pictures of adult wings of *ct*^{6} with homozygous *mod(mdg4)*^{T6}, heterozygous *psq*^{0115} or *dfΔ18* and *psq*^{0115}*/dfΔ18*. No evident visual changes can be reported.

1.3.4 PipsqueakBTB co-localizes with other insulator proteins at architectural protein binding sites and at the borders of H3K27me3 domains.

Multiple studies suggest that many insulator elements are not capable of enhancer-blocking or chromatin barrier activity (Schuettengruber *et al.*, 2013; Schwartz *et al.*, 2012; Van Bortle *et al.*, 2012), and may instead be reserved for other activities such as gene repression, activation, or enhancer-promoter interactions (Sanyal *et al.*, 2012; Soshnev *et al.*, 2013; Xu *et al.*, 2011). Architectural proteins are associated with insulator function, and are referred to insulators only when they are in a genomic location at which they are capable of enhancer-blocking activity (Van Bortle *et al.*, 2014).

The use of 3C-derived approaches to detect intra- and inter-chromosome interactions reveals that chromosomes are divided into distinct regions of highly interacting chromatin called topologically associating domains (TADs), and architectural proteins are actively involved in the three-dimensional organization of the genome, probably due to their ability to mediate interactions between distant loci by forming chromatin loops (Nora *et al.*, 2012). They contribute to the formation of TAD borders and mediate the chromatin interactions between enhancers, promoters and PREs within TADs (Bonora *et al.*, 2014; Li *et al.*, 2013; Li *et al.*, 2015). To date, several architectural proteins have been identified in *Drosophila* and these proteins co-localize in different combinations at architectural protein binding sites (APBSs) (Van Bortle *et al.*, 2014). These proteins include Rad21 (cohesin), CAP-H2 (condensin II), *Drosophila* homolog of CTCF (dCTCF), Boundary element associated factor of 32 kDa (BEAF-32), Su(Hw), GAF, CP190, Zeste white 5 (Zw5), Mod(mdg4), the chromo-domain protein Chro and Z4, previously shown to co-localize and co-immunoprecipitate with BEAF-32 (Gan *et al.*, 2011), and the tumour suppressor L(3)mbt protein, recently shown to co-localize with CP190 (Richter *et al.*, 2011) (Figure 47). We performed two new heatmaps to see if PsqBTB belongs to the group of architectural proteins and if it is therefore present at APBSs.

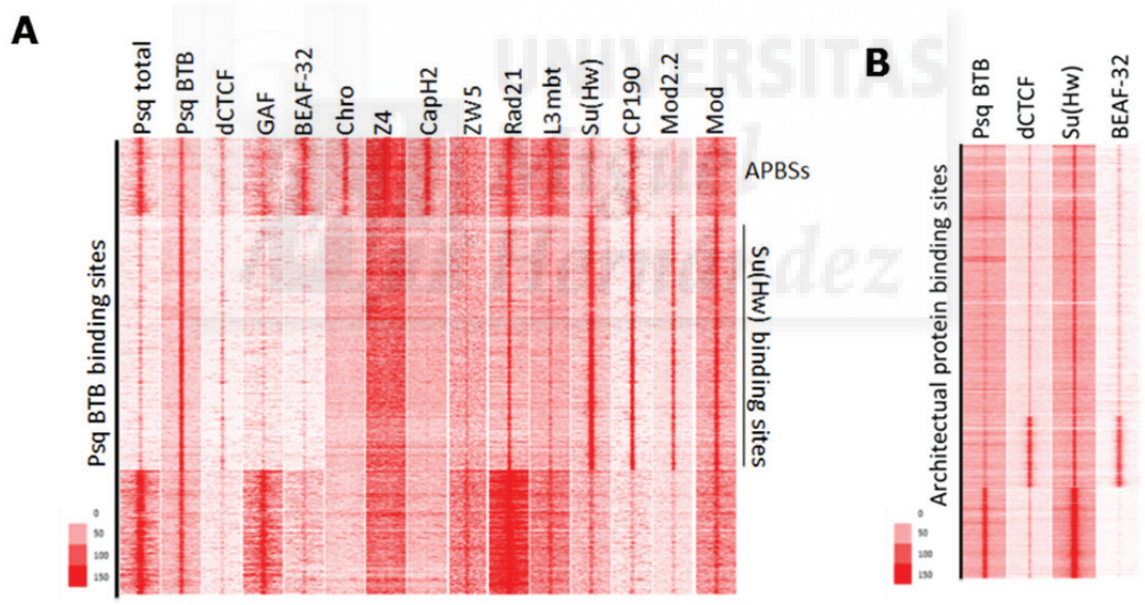

Figure 47. PipsqueakBTB is found with architectural proteins at architectural protein binding sites. (**A**) Heatmap obtained with PsqBTB as an anchor and ChIP-seq data for the architectural proteins Rad21, CAP-H2, dCTCF, BEAF-32, Su(Hw), GAF, CP190, Zw5, Mod(mdg4), Mod(mdg4)2.2, Chromator, Z4 and L(3)mbt. PsqBTB is located at a subclass of APBSs containing Su(Hw) and also at APBSs containing other architectural proteins. (**B**) Using a list of APBSs as anchors for the heatmap we can see the presence of PsqBTB in the same regions as Su(Hw) and co-localizing less with other architectural proteins such as dCTCF or BEAF-32. Heatmaps were generated by K-means clustered using Cluster 3.0 in 3 clusters and viewed in Java Treeview.

The heatmap in Figure 47 shows that PsqBTB is present at three classes of sites:

1. Sites containing GAF, cohesin (Rad21) and a Mod(mdg4) isoform, different from 2.2 isoform (not characterized).
2. A subclass of APBSs containing Su(Hw), Mod(mdg4)2.2 and CP190. These are the APBSs present in gypsy insulator, in Figure 47 shown as Su(Hw) binding sites.
3. A subclass of APBSs containing BEAF-32, Chro, Z4, CAPH2, Rad21, L3mbt, CP190 and Mod(mdg4).

Drosophila APBSs also border domains of H3K27me3 mediating long-range intrachromosomal contacts, observed between PcG domains throughout the *Drosophila* genome (Sexton *et al.*, 2012). In mammals, broad domains of repressive H3K27me3 characterized by Polycomb, have been shown to silence clusters of developmentally important genes (Bracken *et al.*, 2006; Pauler *et al.*, 2009) and a similar repression of developmental genes has been shown in H3K27me3 domains in *Drosophila* (Negre *et al.*, 2011). Genes within H3K27me3 domains are highly enriched for developmental genes in Kc167 cells, including the *even-skipped* (*eve*) gene, which encodes a homeodomain-containing transcription factor involved in segmentation (Macdonald *et al.*, 1986), and other early-stage developmental genes such as *eyes absent* (*eya*) and hybrid sterility gene *Odysseus- site homeob*ox (*OdsH*) (Figure 48). In Figure 48, PsqBTB is present at APBSs located at the borders of H3K27me3 domains with other architectural proteins.

Although the insulator protein function of PipsqueakBTB cannot be demonstrated in vivo*, we reveal the co-localization of these BTB-containing isoforms with other insulator proteins at architectural protein binding sites and at the borders of H3K27me3 domains.*

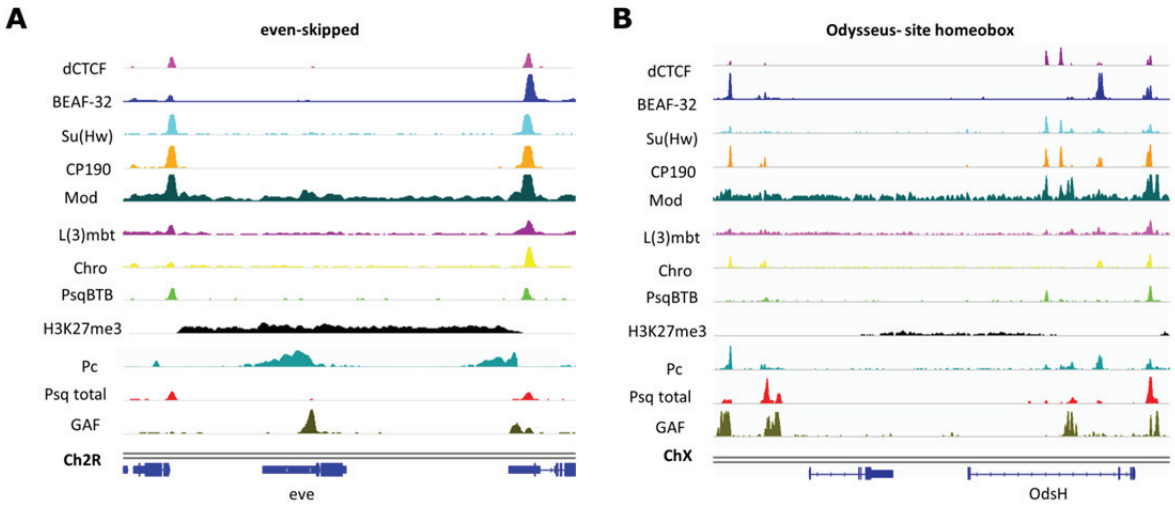

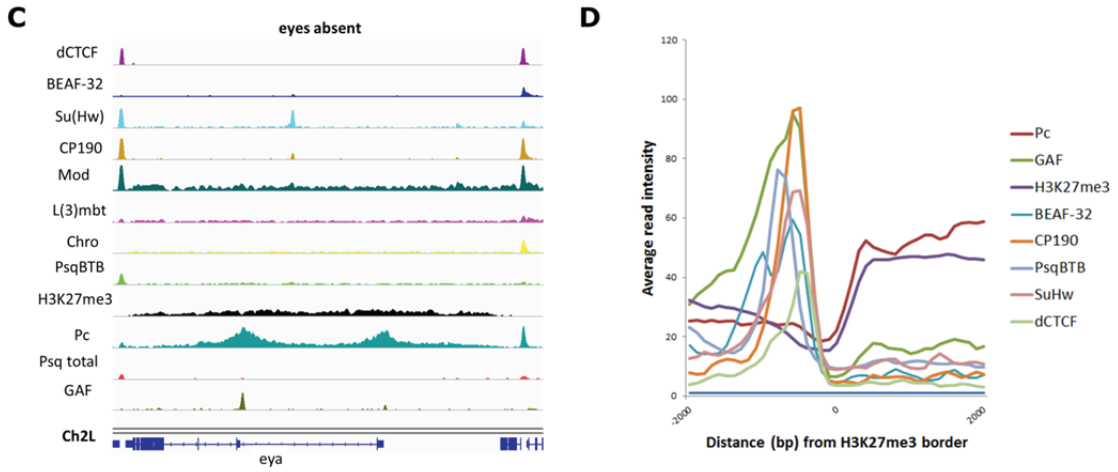

Figure 48. PipsqueakBTB is present with architectural proteins at the borders of H3K27me3 domains. (**A-C**) Domains of repressive H3K27me3 characterized by Polycomb have been shown to silence clusters of developmentally important genes in *Drosophila*. Genes within H3K27me3 domains are highly enriched for developmental genes in Kc167 cells, including the even-skipped (eve) gene (**A**). This model for insulator alignment at H3K27me3 domain borders is consistent throughout the genome, including hybrid sterility gene Odysseus- site homeobox (OdsH) (**B**) and early-stage developmental gene eyes absent (eya) (**C**). (**D**) Average read intensity for H3K27me3 and insulator proteins at H3K27me3 domain borders, ±2 kb. Comparison of insulator profiles normalized by total read numbers.

1.4 'Repressor' Pipsqueak is involved in active gene transcription.

The implication of Pc and GAF proteins in transcriptional repression and activation (Farkas *et al.*, 1994; Mousavi *et al.*, 2012; Ringrose *et al.*, 2004; Strutt *et al.*, 1997; Xu *et al.*, 2012) made us consider the effect of Psq isoforms on transcription. Pol II transcription is regulated primarily at two steps early in the production of mRNA (Nechaev *et al.*, 2011). First is the recruitment of Pol II to promoters where, with the aid of the general transcription factors (TFs), Pol II rapidly initiates transcription (Core *et al.*, 2012). The second is promoter-proximal Pol II pausing and the subsequent escape into productive elongation. As has been already described in the introduction, the C-terminal domain (CTD) of Pol II is firstly recruited to the promoter and its CTD becomes phosphorylated at Ser5 (Pol II ser5) (Feaver *et al.*, 1991; Lu *et al.*, 1992; Serizawa *et al.*, 1995). It then pauses in a process referred to as promoter-proximal pausing. Pol II is released when phosphorylated in the CTD at Ser2 (Pol II ser2), marking the onset of productive elongation (Marshall *et al.*, 1996). Moreover, studies in *Drosophila* suggest that histone H3S10 phosphorylation may be required for the transcription of most genes in this organism, as it is a modification that occurs at the promoter-proximal pause and is required for the release of polymerase into transcription elongation during interphase (Ivaldi *et al.*, 2007). In *Drosophila* this modification is attributed to Jil-1 (Jin *et al.*, 1999) and its release of the polymerase has been demonstrated measuring its levels of phosphorylation at Ser2 and H3S10ph establishing new transcriptional programs: Heat-shock and the Ecdysone inducible gene expression system (Ivaldi *et al.*, 2007; Kellner *et al.*, 2012; Nowak *et al.*, 2000) in the presence or absence of Jil-1, using homozygous mutant flies (*Jil-1*^{z2}). Furthermore, Jil-1 and H3S10ph are also present at enhancers defined by the presence of H3K4me1 and H3K27ac, suggesting that the Jil-1 kinase is a regulator of histone dynamics at enhancers and promoters genome-wide (Figure

49), including Ecdysone-induced genes (Kellner *et al.*, 2012). It is required for transcription of most *Drosophila* genes, since flies homozygous for *Jil-1*^{z2} show a reduction in the levels of Pol II Ser2 and in the transcriptional levels of Ecdysone response genes (Ivaldi *et al.*, 2007).

As can be seen in Figure 49 there is full co-localization between Jil-1 and all isoforms of Psq. We subsequently tested if, in general, Psq was involved in transcription acting upstream (pausing transcription) or downstream (activating transcription) of Jil-1.

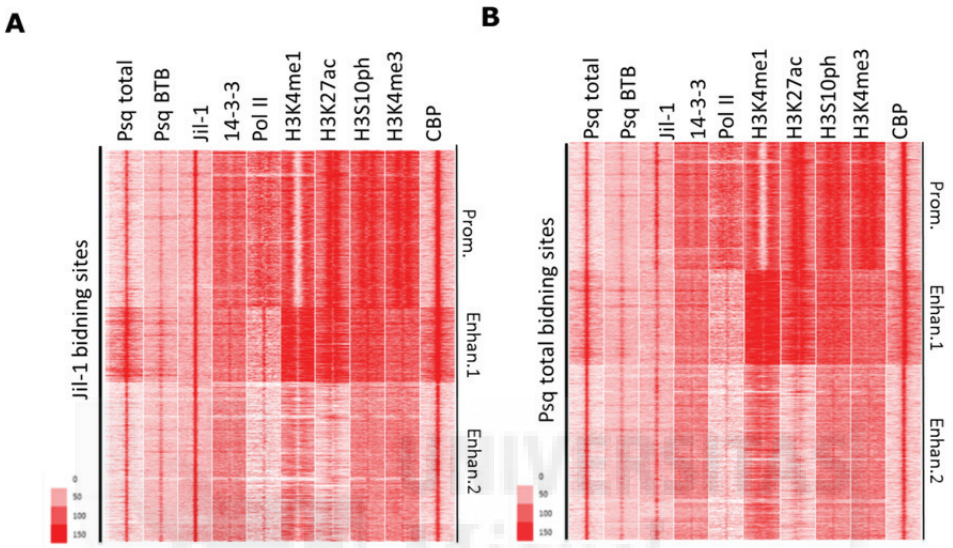

Figure 49. Pipsqueak co-localizes with Jil-1 at enhancers and promoters. (**A-B**) Heatmaps were obtained using Jil-1 and Psq total binding sites as anchors. Psq total highly co-localizes with Jil-1 at enhancers and promoters. Here two types of enhancers are shown, characterized by the presence or absence of Pol II (Enhancers 1 or 2 respectively). 14-3-3 has been added to the heatmap as it has been shown to act downstream of Jil-1 in transcriptional activation. Features for active enhancer elements and promoters were used. Heatmaps were generated by K-means clustered using Cluster 3.0 in 3 clusters and viewed in Java Treeview.

To test the possible general role of Psq in transcriptional activation we studied as a reference 14-3-3. This protein is a well characterized phospho-binding protein, which binds H3S10ph upon transcriptional activation, recruited to active genes in a JiL-1-dependent manner and is required for phosphorylation of Pol II Ser2 (Macdonald *et al.*, 2005). The genome-wide loss of Jil-1 in the *JiL-1*^{z2} mutant produces a genome-wide loss of 14-3-3 binding to the chromosomes (Macdonald *et al.*, 2005). To test whether Psq acts, as 14-3-3, downstream of Jil-1 in the release of the promoter-proximal pausing, we performed several ChIP-seq of Psq total in the presence and in the absence of Jil-1, but no differences were detected between these two data sets (Figure 50).

This result suggests that Psq acts before the binding of Jil-1 at the promoter, thus we subsequently tested its possible role in the promoter-proximal pausing process upstream of Jil-1, pausing Pol II with GAF or helping in the recruitment of Jil-1.

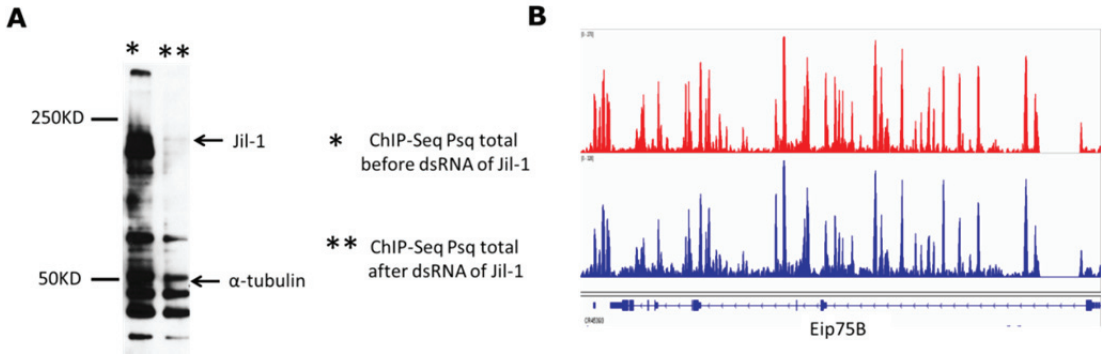

Figure 50. Pipsqueak is not affected by eliminating Jil-1 from *Drosophila* Kc167 cells. (**A**) The knock-down of Jil-1 has been correctly done with dsRNA but the ChIP-seq performed with these Kc167 cells does not report changes in the binding patterns of Psq total to the chromatin. Here we show an example of Psq total binding sites around the Ecdysone response gene *Eip75B*. The transcriptional level of this gene is reduced in the absence of Jil-1. (**B**). Asterisk (*) denotes control Kc167 cells and two asterisks (**) indicate Kc167 cells with the knock-down of *Jil-1*.

Sequence-specific transcription factors such as GAF have been implicated in pausing. GAF and its binding motif, the GAGA sequence, are enriched on paused genes in *Drosophila*, but only about 20% of paused genes are GAF-bound (Hendrix *et al.*, 2008; Lee *et al.*, 2008) and enriched for developmental genes (Fuda *et al.*, 2013). Since non-BTB Psq has been functionally related with GAF, we expect the same function for these non-BTB isoforms of Psq. We therefore calculated the pausing index of genes associated with Psq total and GAF-associated Psq (Core *et al.*, 2008). The pausing index is defined as the difference between Pol II levels at TSSs and Pol II levels in the gene body. The pausing index of paused genes is higher than that of non-paused genes, since Pol II levels in the gene body are lower than Pol II levels at TSS.

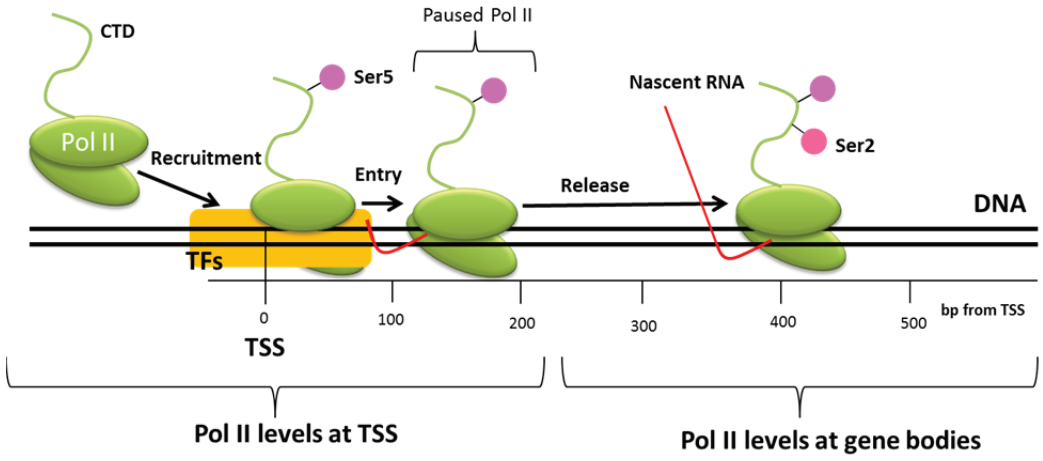

Figure 51. Schematic of RNA Polymerase II during transcription initiation. Pol II transcription is regulated primarily at two steps early in the production of mRNA. First is the recruitment of Pol II to promoters where, with the aid of the general transcription factors (TFs), Pol II rapidly initiates transcription. The second, is promoter-proximal Pol II pausing and the subsequent escape into productive elongation. The C-terminal domain (CTD) of Pol II is first phosphorylated at Ser5 (Pol II ser5). Pol II then pauses in a process referred to as promoter-proximal pausing. Pol II is released when phosphorylated in the CTD at Ser2 (Pol II ser2), marking the onset of productive elongation.

Pausing index = Pol II levels at TSS– Pol II levels at gene bodies

Gene Pausing: Pol II levels at gene bodies < Pol II levels at TSS

Gene transcription: Pol II levels at gene bodies > Pol II levels at TSS

The Pausing index of Psq total and GAF-associated genes was calculated using ChIP-seq datasets of Pol II in Kc167 cells obtained from modENCODE. Pol II levels at TSS was considered as the mean enrichment of Pol II in the ±200 bp region around each TSS of Psq and GAF binding sites. Pol II levels at gene bodies was considered as the mean enrichment of Pol II from +200 bp to the end of the corresponding gene (Figure 51).

Using the global distribution of Pol II binding sites all over the genome as a control (downloaded from modENCONDE), we can compare the pausing index of other protein-associated genes. Genes associated with GAF show a higher pausing index than the control, indicating that GAF is preferentially associated with paused genes (pale blue in Figure 52 A-B). When examined, genes associated with Psq total have a higher pausing index than Pol II in the control of all genes, but lower than the pausing index levels calculated for GAF (green in Figure 52 A-B). When we separate the genes that share the presence of Psq and GAF at the same time (mainly the non-BTB Psq), we can see that their pausing index levels are the same as for GAF alone (purple in Figure 52 A-B).

Non-BTB Psq associated with GAF may be involved in transcription pausing. Additionally, PsqBTB or the non-associated Psq with GAF might have an additional role in the release of pausing, contributing negatively to the total pausing index levels of Psq total containing genes.

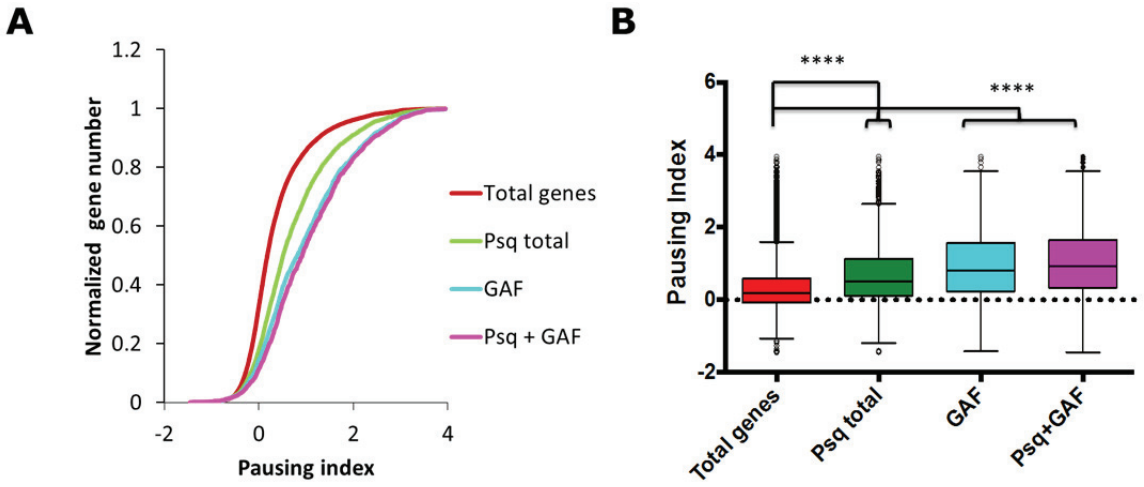

Figure 52. GAGA Factor-associated Pipsqueak is preferentially associated with paused genes. (A) Chart showing the general pausing index distribution of different protein-associated genes. In red we can see the total distribution of Pol II all over the genome (all genes). In green, the pausing index of genes associated with all the isoforms of Psq (Psq total). In pale blue, the pausing index of genes associated with GAF (GAF) and in purple, the pausing index of genes associated with Psq

and GAF at the same time (Psq+GAF). Psq and GAF are preferentially associated with paused genes. The pausing index of genes containing Psq and GAF was calculated using ChIP-seq datasets of Pol II in Kc167 cells obtained from modENCODE, considering Pol II levels at TSS as the mean enrichment of Pol II in the ±200 bp region around each TSS of Psq and GAF binding sites. Pol II levels at gene bodies was considered as the mean enrichment of Pol II from +200 bp to the end of the corresponding gene. (**B**) We found significant differences between the levels of Pol II along the genome and in Psq total-containing genes ($p< 0.0001$), and between general Pol II binding and GAF or GAF+Psq containing genes ($p<0.0001$), as has been calculated for each condition with Prism6 software (t-unpaired test).

To test the general effect of all the isoforms of Psq in gene pausing we depleted all these isoforms in Kc167 cells by using dsRNA against *psq* mRNA. Then we tested its effects on the levels of Ser5 and Ser2 phosphorylation in the CTD repeat YSPTSPS of Pol II (Figure 53A-B) and the levels of H3S10ph (Figure 53C) by WB. We tried to test the consequences of depleting PsqBTB isoforms alone, however the different dsRNA designed for this assay did not work properly. As can be seen in Figure 53A and C, the knock-down of Psq total in Kc167 cells (see Figure 53B for efficiency of dsRNA transfection) reduces the levels of Pol II Ser2 and H3S10ph, while the phosphorylation of Pol II Ser5 remain unchanged (Figure 53A).

From figure 53A-C we can conclude that transcription initiation can take place independently of Psq as shown by the normal levels of Pol II Ser5 phosphorylation. Regarding gene pausing, if Psq is causing the pause, then in the absence of Psq, Pol II should not pause and we would see an increase in Pol II Ser2 phosphorylation. If it is involved in the release, then in the absence of Psq, Pol II would not go into elongation and we would see less phosphorylation of Pol II Ser2. Thus, although non-BTB Psq is found associated with GAF in paused genes, it is not necessary to pause Pol II, since we see decreased levels of Pol II Ser2 phosphorylation after the knock-down of Psq total, instead of an increase (Figure 53 A). Therefore, PsqBTB may be implicated in the release of pausing, up-stream of Jil-1, as the levels of H3S10ph are also reduced (Figure 53C).

We calculate the pausing index of genes associated with Jil-1 and PsqBTB, and both at the same time. Since Jil-1-associated genes show a lower pausing index than the control (orange in Figure 53D-E), Jil-1 is associated with non-paused genes (it is required for phosphorylation of H3S10, releasing Pol II from its paused state). Although all the PsqBTB associated genes have a higher pausing index than the control (green in Figure 53D-E), when we isolate the Jil-1 + PsqBTB-associated genes, we see that they are associated with non-paused genes (blue in Figure 53D-E). As PsqBTB binding sites have a very high percentage of regions at Su(Hw) binding sites, that cannot be classify as enhancers or promoters, this sites may contribute to the deviation of the pausing index of PsqBTB-associated genes.

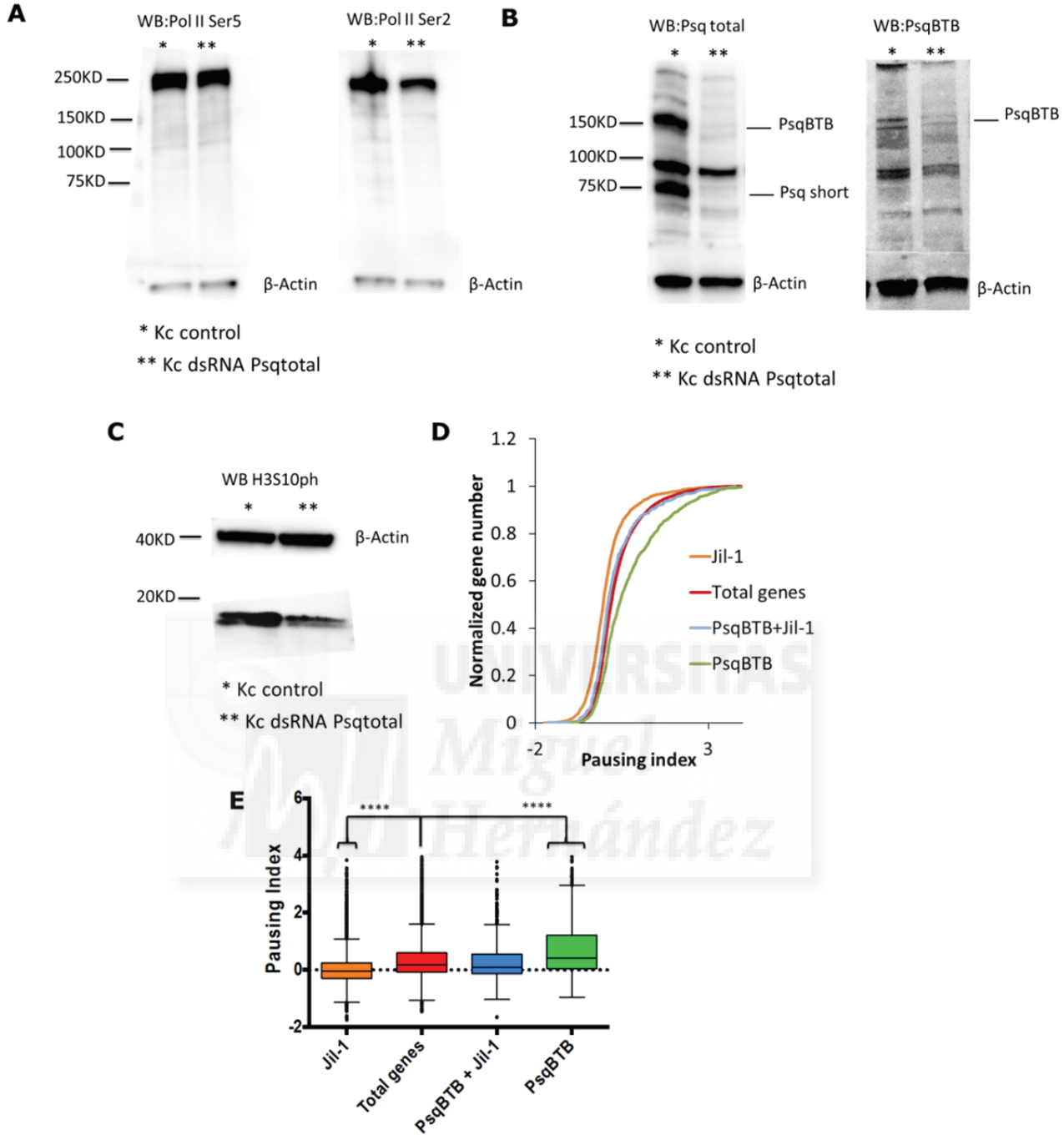

Figure 53. Pipsqueak is required for promoter-proximal release of pausing. (**A**) WB images of the effect of knocking-down *psq* on Pol II phosphorylation found in the Ser5 and Ser2 of the CTD. Its knock-down reduces the levels of Pol II Ser2 phosphorylation while the Pol II Ser5 phosphorylation remains unchanged (n=3). (**B**) WB showing that the dsRNA decreases Psq protein levels as expected, as can be seen by using the Psq total and PsqBTB antibodies. (**C**) WB image of the effect of the knock-down of both forms of *psq* on the levels of H3S10ph (n=3). An asterisk (*) has been used to denote control Kc167 cells and two asterisks (**) have been used to indicate Kc167 cells with reduced levels of *psq*. β-actin has been used as a loading control in the WB assay. (**D**) Pausing index of genes containing Jil-1 (orange), PsqBTB (green) and Jil-1+PsqBTB at the same time (blue). In red we can see the total distribution of Pol II all over the genome (all genes). (**E**) We found significant differences between the levels of Pol II along the genome and in Jil-1-containing genes ($p< 0.0001$), and between general Pol II binding and PsqBTB containing genes ($p<0.0001$), as has been calculated for each condition with Prism6 software (t-unpaired test). The different intensities of WB bands has been quantified using ImageJ.

To gain further insights into the role of Psq in transcriptional regulation, we established a new transcriptional program in Kc167 cells inducing Ecdysone response genes expression as a model to test if Psq also regulates the expression of Ecdysone-induced genes. Ecdysone-induced genes are paused in Kc167 cells and in the presence of Ecdysone, Jil-1 is recruited for transcriptional activation of Ecdysone-responsive genes (Kellner *et al.*, 2012). During this assay cells are treated with the active form of the steroid hormone Ecdysone, 20-HE, which binds to the Ecdysone receptor complex (EcR-C), a classic nuclear receptor complex (Riddiford *et al.*, 2000). The EcR-C contains two nuclear receptors: the EcR (Koelle *et al.*, 1991) that binds directly to 20-HE and its heterodimer partner Ultraspiracle (USP) (Yao *et al.*, 1993). These receptors can function as repressors in the absence of a ligand molecule and maintain target gene repression by using co-repressor complexes. In the presence of hormones, co-activator proteins are recruited and co-repressors are displaced, resulting in the activation of the target genes (Chawla *et al.*, 2001; King-Jones *et al.*, 2005; Mangelsdorf *et al.*, 1995). This treatment results in G2-arrest within 12–24 hr and morphological changes. Kc167 cells are plasmatocytes and they differentiate into macrophages after Ecdysone treatment (Cherbas *et al.*, 2011). Treatment of cultured cells with 20-HE allows analysis of changes of individual genes.

We performed several ChIP-seq using Kc167 cells before and after the treatment with 20-HE adding it directly to the medium (20-HE 41 µM for 24 hr (Gauhar *et al.*, 2009) or 20-HE 0,5 µM for 3 hr (Wood *et al.*, 2011)) with Psq total, PsqBTB and EcR antibodies. See figure 54 for an example of the Psq and EcR binding sites at the early Ecdysone-induced gene *Eip75B*. After the addition of 20-HE to the medium there is an increase in the initial amount of Psq total and EcR in two regions marked by a red asterisk in the *Eip75B* gene (Figure 54A). Both proteins are present around these genes before the 20-HE treatment, however after the treatment we can detect an increase in the amount of both proteins at these sites. PsqBTB binding sites are not affected by the treatment with 20-HE (Figure 54B).

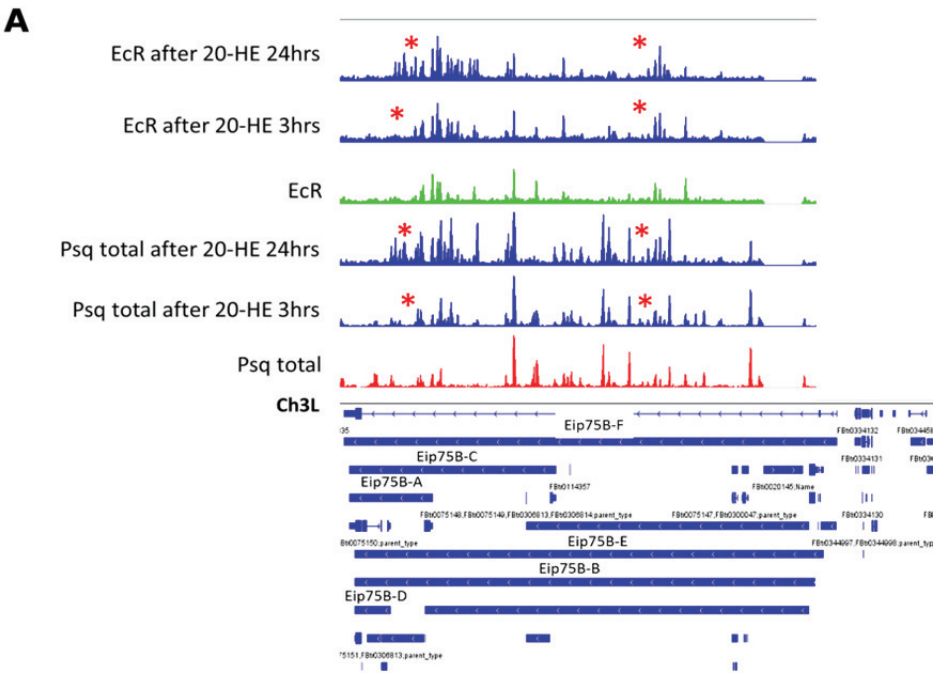

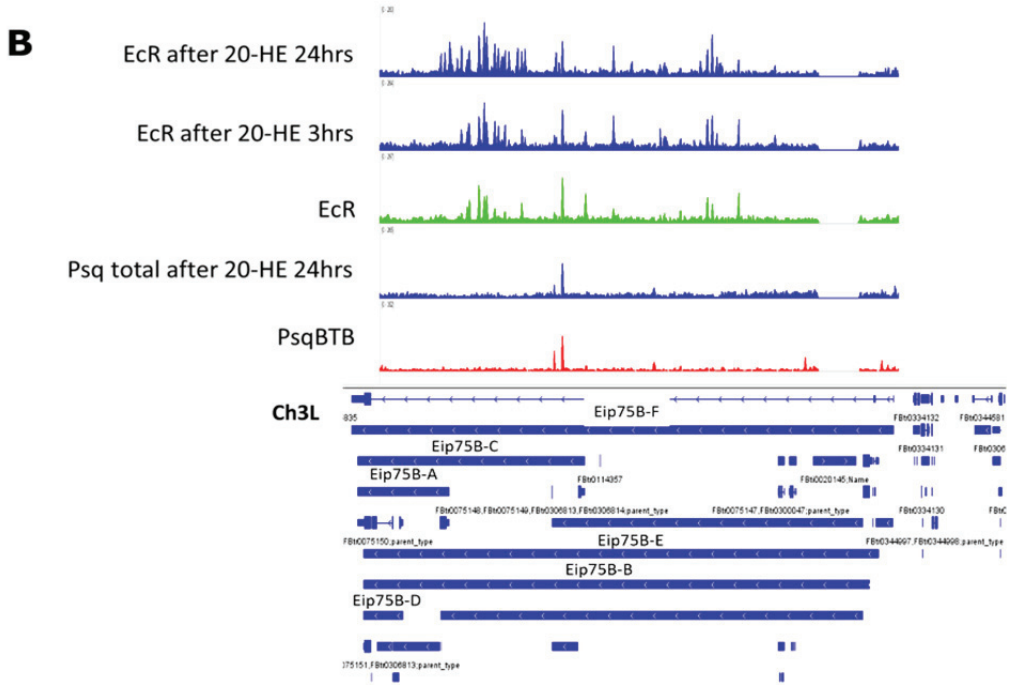

Figure 54. The treatment of Kc167 cells with 20-HE produces changes in the binding patterns of Pipsqueak to the chromatin around the Ecdysone response genes. (**A**) Binding site of the EcR and Psq total (for both isoforms of Psq) around the early Ecdysone response gene *Eip75B* at chromosome 3L. Several treatments have been performed: 3hr 20-HE 0,5 µM and 20-HE 41 µM for 24 hr, with a-Psq total (red) and a-EcR (green) antibodies. Red asterisks mark the differences of Psq total binding sites at the Eip75B gene. (**B**) PsqBTB (red) shows no changes after Ecdysone treatment.

It has been shown that there is an increase in the number of binding sites of CP190 at the *Eip75B* gene after 20-HE exposure (48 hr 0,5 µM and not after 24 hr) (Wood *et al.*, 2011) accompanied by a parallel increase of its mRNA levels reported by qRT-PCR. CP190 seems to be necessary for the stabilization of specific chromatin loops and for proper activation of transcription of genes regulated by this steroid hormone (Wood *et al.*, 2011). In the same way, we performed several qRT-PCRs of samples treated with 41 µM of 20-HE during 24 hr (our ChIP-seq conditions) and 0,5 µM during 48 hr (Wood *et al.*, 2011), or with ethanol used as a solvent. mRNA levels of Psq total do not change in the cells treated with 20-HE compared with the total levels of Psq in the control samples (See figure 55A). The mRNA levels of *Eip75B* were measured as a control. In addition, we tested the levels of *Eip75B* before and after the knock-down of all isoforms of *psq* in Kc167 cells with or without adding 20-HE to the Kc167 growth medium (Figure 55B and 55C). This result shows an up-regulation of the mRNA levels of these early induced genes (*Eip-75B* isoform RA, *EcR* and *Vri*) in the absence of Psq compared to the control conditions. The control of the knock-down of *psq* with dsRNA in these cells can be seen in Figure 55B'.

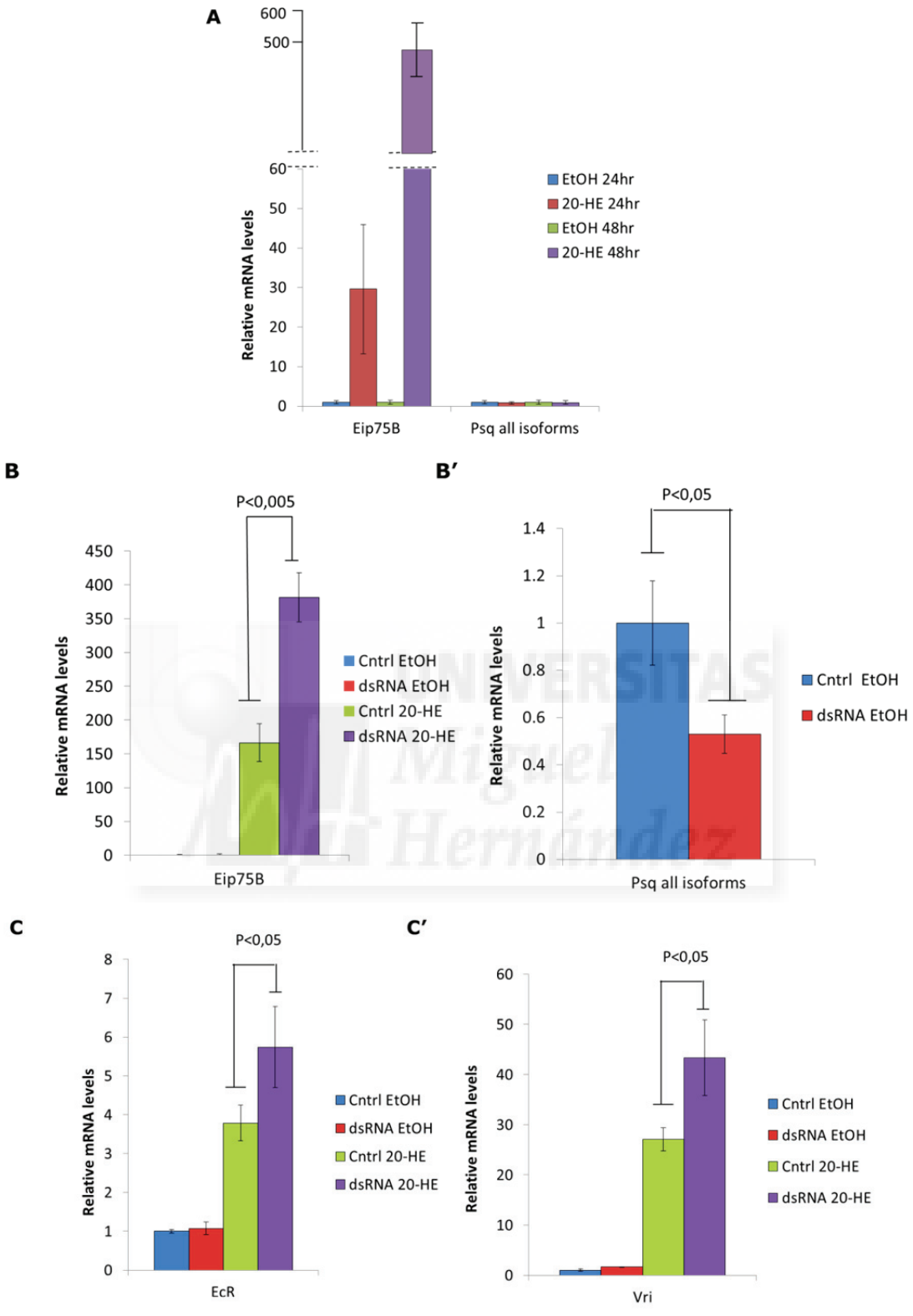

Figure 55. Pipsqueak relocates to the vicinity of Ecdysone-induced genes after 20-HE treatment. (**A**) Kc167 cells treated with 20-HE 0,5 µM for 24hr (red bar) and 48hr (purple bar), and no change in the levels of mRNA of all the *psq* isoforms was detected. The treatment with 20-HE works properly, as the *Eip75B* mRNA levels increase after 24hr and 48hr treatment compared to the control (24hr (blue bar) and 48hr (green bar) of ethanol treatment). (**B-B'**) The knock-down of all *psq* isoform, done with dsRNA, produces an increase of the *Eip75B* mRNA levels after a treatment of 3hr with 0,5 mM 20-HE (purple bar), compared to the same treatment with 20-HE in the presence of Psq (green bar). (**B**) The depletion of

psq by dsRNA transfection was correctly done (significant difference between the control (blue bar) and the dsRNA transfection (red bar) (**B'**). (**C-C'**) The depletion of all *psq* isoforms in Kc167 cells increases the mRNA levels of *EcR* and *Vri,* Ecdysone-induced genes (purple bars compared with green bars). The values represent the mean ± s.e.m. of six independent experiments. P values were calculated by the unpaired Student's t test.

The previous experiments show that non-BTB Psq (Psq total in the absence of PsqBTB) increases its levels around the Ecdysone-induced genes after the treatment with Ecdysone. mRNA and protein levels of Psq remain unchanged, suggesting a relocation of Psq protein to the vicinity on Ecdysone-induced genes. Control of the Ecdysone response in flies is vital since this steroid hormone coordinates postembryonic development. Here we show the effects of Psq in Kc167 cells acting in the tight control of the levels of Ecdysone response genes during the 20-HE treatment. Eliminating Psq we note an increase in cell response to Ecdysone exposure, suggesting that Ecdysone limits its own response by recruiting non-BTB Pipsqueak repressor to Ecdysone responsive genes.

Larval development progresses through three instars, each marked by an Ecdysone pulse (see in the introduction). Ecdysone is a steroid hormone which coordinates postembryonic development in insects (Review in (Gilbert, 1996; Riddiford, 1993)). To test the role of Psq in the regulation of Ecdysone-induced genes and its possible implication in the control of *Drosophila* development, we tried to reproduce the experiment done for *Jil-1*^{z2} homozygous mutants and measure the levels of *Eip75B* mRNA before and after the larval exposure to 20-HE. Unfortunately, larvae homozygous for *psq* mutations are not viable at this stage of development. Other strategies such as heat-sock or *Gal80* promoters to induce the loss of function of Psq during a certain time of development will be needed to address this issue in the future.

2. Antibodies specific to PipsqueakBTB unveil the low presence of these isoforms in proliferative tissues.

We studied PsqBTB expression for the first time within the larval tissue, thanks to the PsqBTB specific antibody obtained in our laboratory.

Immunohistochemistry of larval tissue with this PsqBTB antibody reveals its presence in the polytene chromosomes of salivary glands, fat body, ovaries and in differentiated post-mitotic cells called enterocytes in the gut, characterized by their bigger size compared to other cell types in the gut (Figure 56A-D). PsqBTB protein levels are under the detection limit of this antibody in proliferative tissues, such as imaginal discs (wing or eye discs), and cannot be detected unless we overexpress it (Figure 56E-F). PsqBTB is present in these tissues but at very low levels, since use of a-Psq total and a-PsqBTB antibodies in WB of concentrated protein samples obtained from ~20-30 wing discs, allows the detection of the 150KD band of the PsqBTB protein (Figure 57C).

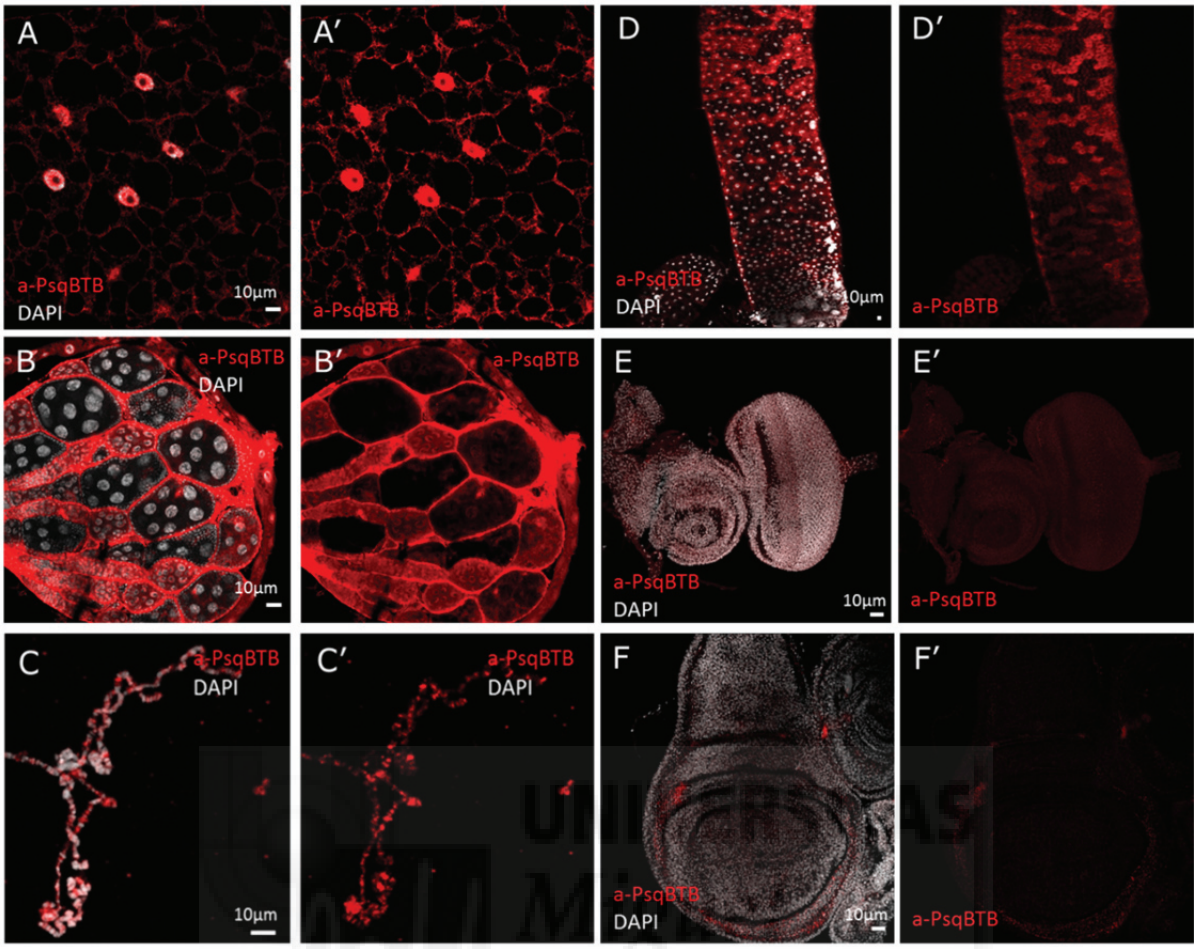

Figure 56. PipsqueakBTB levels are tightly regulated in proliferative tissues.(**A-C'**) Immunohistochemistry with the a-PsqBTB antibody (red) in non-proliferating tissues such as fat body (**A**), ovaries (**B**) and polytene chromosomes from salivary glands (**C**). (**D**) PsqBTB is expressed in differentiated post-mitotic cells called enterocytes in the gut, distinguished by the size of these cells compared to the other cell types within this organ. (**E-F'**) PsqBTB levels in imaginal discs cannot be distinguished from the background.

In proliferative tissues such as the wing imaginal disc, the RNAi against both types of isoforms of *psq* (*UAS-psq-IR*) under the *MS1096-Gal4* line, reducing the levels of the transcribed protein in the wing pouch, produces growth defects (Figure 57A). As previously shown, the *MS1096-Gal4* line produces the knock-down of *psq* in the dorsal compartment in the wing disc (see Figure 32A). The loss of function of Psq in this region produces a reduction in the proliferation of these dorsal cells, giving rise to an adult wing with a smaller dorsal surface, compared to the ventral (curved wings in Figure 57A). This phenotype produced by the RNAi line in the wing disc (where PsqBTB cannot be detected) can be hypothesized to be mainly caused by the loss of non-BTB Psq isoforms. It has been described that PcG complexes are involved in cell cycle control in *Drosophila*, where a repressive PRE regulates CycA expression (Martinez *et al.*, 2006). We found Pc at the promoter of CycA with GAF and non-BTB Psq proteins in Kc167 cells (Figure 57B). Since Psq has been described as a recruiter of PcG and TrxG at PREs, we analysed by WB the effect of the loss of function of both Psq isoforms in the wing discs with *MS1096>Psq-IR* and in Kc167 cells with a down-regulation performed by dsRNA. In these assays we report a downregulation of the CycA protein

levels (Figure 57C) showing an activator function of Psq in the context of the regulation of *cycA* expression. We cannot discard in this case the fact that Psq may be acting through other mechanisms different from its PRE-related function.

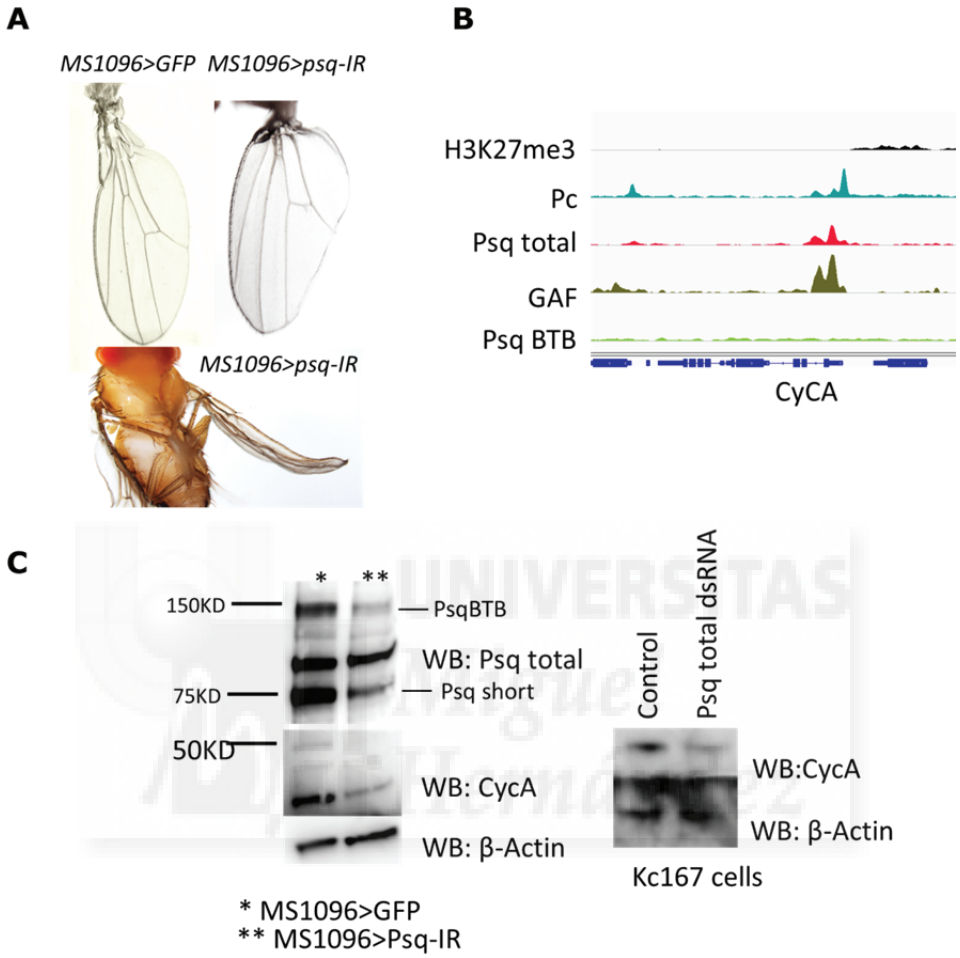

Figure 57. The non-BTB isoforms of Pipsqueak regulate CycA. (**A**) Picture of a wild type wing and a wing with reduced levels of both isoforms of Psq under the *MS1096-Gal4* line using the *UAS-Gal4* system. (**B**) A picture taken with the IGV from the Broad Institute of CycA and the binding peaks of Psq total binding sites (red), GAF (brown) and Pc (blue) to its promoter in Kc167 cells. (**C**) The reduction of the protein levels of Psq in the wing and in Kc167 cells produces a reduction in the protein levels of CycA, shown by WB. An asterisk * has been used for wild type conditions and two asterisks ** have been used for the loss of function of Psq. β-Actin has been used as a loading control in the WB assay.

In summary, non-BTB Psq expression has a positive effect in expansion of cell population in proliferating tissues (here shown in the wing imaginal disc), since its absence blocks this process, for example, by reducing directly or indirectly the levels of CycA. The reason why the levels of PsqBTB in proliferating cells are tightly controlled remains unknown, but its overexpression alone or in combination with Dl has big and opposite effects over cell proliferation (See Figure 12G,I and J).

3. Linking the knowledge gained by ChIP-seq data to tumorigenesis: PipsqueakBTB and architectural proteins align in the gene *fruitless*, a BTB transcription factor that induces sex determination and courtship behaviour.

To further explore the transcriptional deregulation model mediating tumour formation, an oligonucleotide microarray has been performed in the laboratory and published in the Gene Expression Omnibus (GEO) repository (accession GSE35471). My colleagues carried out an analysis comparing data from *ey>Dl>GS88A8* versus *Dl>GS88A8* (Garelli *et al.*, 2012). See materials and methods for the raw data analysis and Table S5 in Appendix I for genes up-regulated and down-regulated with respect to the control.

Analysis of the results indicate that *dilp8* (CG14059) is among the genes up-regulated in cells displaying the original tumour phenotype induced by the *GS88A8* line. This gene has been described to be autonomously activated in tumour imaginal discs causing abnormal growth and postponing maturation (Garelli *et al.*, 2012).

A second gene up-regulated in tumour cells is *CG9925*. It is expressed exclusively in the germline of both female and male flies early during gametogenesis (Ying *et al.*, 2012). This protein acts as a read-out of the overexpression of PsqBTB isoforms (but not non-BTB Psq) and in the laboratory we have observed that its overexpression with *ey>Dl* does not produce tumour formation. This gene can be directly or indirectly up-regulated by different PsqBTB overexpressing constructs in Kc167 and S2 cells, but we cannot find a peak of PsqBTB at the promoter of this gene in Kc167 cells by ChIP-seq (See Figure 58A). Therefore, it is possible that its regulation by Psq is indirect. We have also tried to perform several ChIP-seq experiments in the context of the overexpression of PsqBTB with a *pUASt-PsqBTB-tRFP-3xFlag* construct and using a-Flag and a-RFP or a-PsqBTB antibodies, but the efficiency of transfection has not been sufficient to observe differences in the ChIP-seq signal of PsqBTB in transfected cells, compared to the control. As observed in Figure 58B-C, qRT-PCR of the different samples from eye disc shows an evident up-regulation in the transcription of *CG9925* by *PsqBTB* and *GS88A8* under the *ey* promoter, but not with the overexpression of non-BTB Psq, being the BTB domain essential for the derepression of this gene (Figure 58B-C).

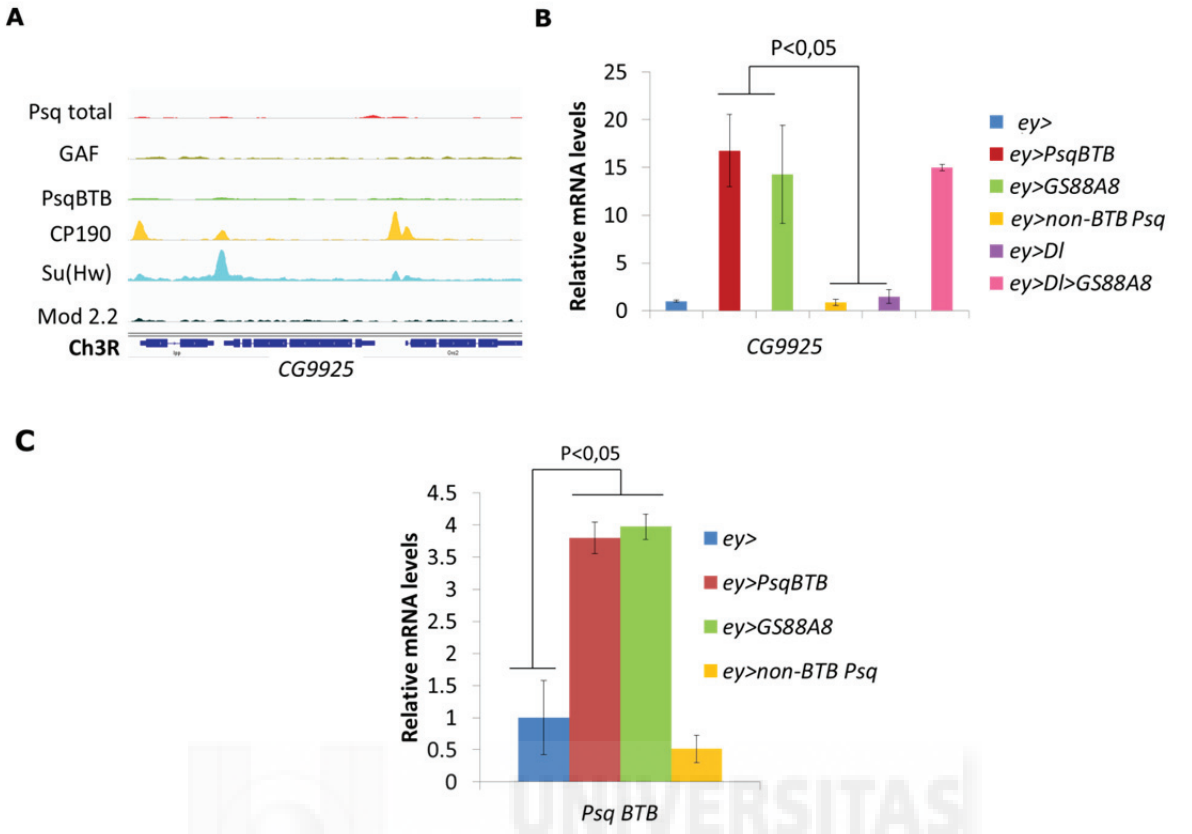

Figure 58. CG9925 acts as a specific read-out for the BTB isoforms of Pipsqueak. (**A**) Presence of Psq total (red), PsqBTB (green), GAF (brown) and Su(Hw) insulator proteins (Su(Hw) blue, CP190 orange and Mod(mdg4)2.2 isoform in black) at the promoter of the *CG9925* gene. Although PsqBTB induces its transcription it does not directly bind to its promoter in Kc167 cells. (**B**) Measurement by qRT-PCR of the *CG9925* mRNA levels in different conditions in eye imaginal discs. The overexpression of PsqBTB has been done with the *UAS-PsqBTB* (red bar) or with *GS88A8* (green bar) lines. Overexpression of Dl does not produce the up-regulation of this gene (purple bar), so the increased levels observed in the "*eyeful*" phenotype (pink bar) are induced by PsqBTB. Non-BTB Psq (yellow bar) cannot induce the transcription of *CG9925*. (**C**) Relative mRNA levels of PsqBTB are shown in *ey>UAS-PsqBTB* (red bar), *ey>UAS-non-BTB Psq* (yellow bar) and *ey>GS88A8* (green bar) conditions. The values represent the mean ± s.e.m. of three - four independent experiments. P values were calculated by the unpaired Student's t test.

It has been described in the introduction that epigenetic silencing may be the cause of the *GS88A8/Dl*-induced tumour growth (Ferres-Marco *et al.*, 2006). In this paper my colleagues showed that *Rbf* was aberrantly silenced in the *"eyeful"* phenotype. As they show, this gene is subtly repressed by Dl overexpression alone and this repression is significantly increased in the tumour combination, overexpressing both Dl and Psq. Overexpression of *Rbf* rescued the tumour phenotype, probably due to its function in cell cycle control (Weinberg, 1995). However, we cannot discard an influence over this phenotype by PsqBTB-mediated overexpression of some other genes, more so if we consider the multiple and unpredicted effects that the overexpression of PsqBTB can have over chromatin remodelling and transcription regulation. That is why we continue the search of new genes selectively affected in the tumour phenotype compared to the non-tumour condition, and inducing this *"eyeful"* phenotype.

Combining the data from the analysis of up-regulated or down-regulated genes in the microarray and the Notch/GS screen looking for oncogenes or tumour suppressors enhancing the Dl overgrowth, we found by chance another BTB-containing transcription factor called *fruitless (fru)*. Interestingly, this gene shows, additionally in Kc167 cells, multiple binding sites for both forms of Psq, suggesting a transcriptional regulation mediated by either of the two protein groups (insulators or polycomb proteins) (Figure 59L). *fru* has been characterized by the laboratory of Sarah Bray (Djiane *et al.*, 2013) as a Notch-induced gene. It is required for proper development of several anatomical structures necessary for courtship, including motor neurons that innervate muscles needed for fly sexual behaviours (Demir *et al.*, 2005). It does not have an obvious mammalian homolog, but appears to function in sex determination in species as distant as the mosquito *Anopheles gambiae* (Gailey *et al.*, 2006). By qRT-PCR we reported a significant increase in its total mRNA levels (not distinguishing males or females, as both present tumour phenotypes) measured in the tumour condition compared to *ey>Dl* or *ey>GS88A8* samples (Figure 59A), characteristics of the perfect oncogene candidate to be influencing the induction of the tumour phenotype.

The *fru* gene has been cloned and examined at the nucleotide level by two research groups (Ito *et al.*, 1996; Ryner *et al.*, 1996), who have each found it to encode a predicted BTB-family transcription factor. The organization and functions of the about 140 kb *fru* locus are complex: It has at least four promoters, it codes for male-specific, female-specific, and sex-nonspecific transcripts, which are selectively translated; and the 3'region of *fru* encoding the DNA-binding zinc fingers is alternatively spliced (Anand *et al.*, 2001; Ito *et al.*, 1996; Ryner *et al.*, 1996; Usui-Aoki *et al.*, 2000).

Preliminary results show that the general overexpression of this gene in combination with Dl produces tumour overgrowth (Figure 59F and 59H 53% tumour eyes; n>200 results average for different *UAS-fru* lines overexpressing different *fru* isoforms) with secondary eye growth (~3% of total flies; n>200). The knock-down of all isoforms of *fru* in the "*eyeful*" phenotype reduces the incidence of the tumour (Figure 59H from 70% to 44%; n>200), taking into account that a RNAi line does not completely eliminate the expression of a gene and complementary mechanisms may be involved in the tumour phenotype, considering the multiple and unpredicted effects that the overexpression of PsqBTB can have over gene expression. Moreover, the overexpression of the male or female specific isoform of *fru* induces tumour formation in a sex-dependent manner (Figure 59I FruB female specific isoform and FruBM male specific isoform). Although these are very preliminary results and we do not know which isoform of *fru* is responsible for the *"eyeful"* phenotype, Fru can explain the higher probability of development of tumour eyes in females, observed in the case of the *"eyeful"* phenotype. A more extensive study should be carried out to validate the role of PsqBTB on the expression of *fru* (see the binding of Psq isoforms to the gene region in Figure 59L). Moreover, the epigenetic origin of the "*eyeful*" phenotype should be revised and linked to the insulator function of PsqBTB here proposed.

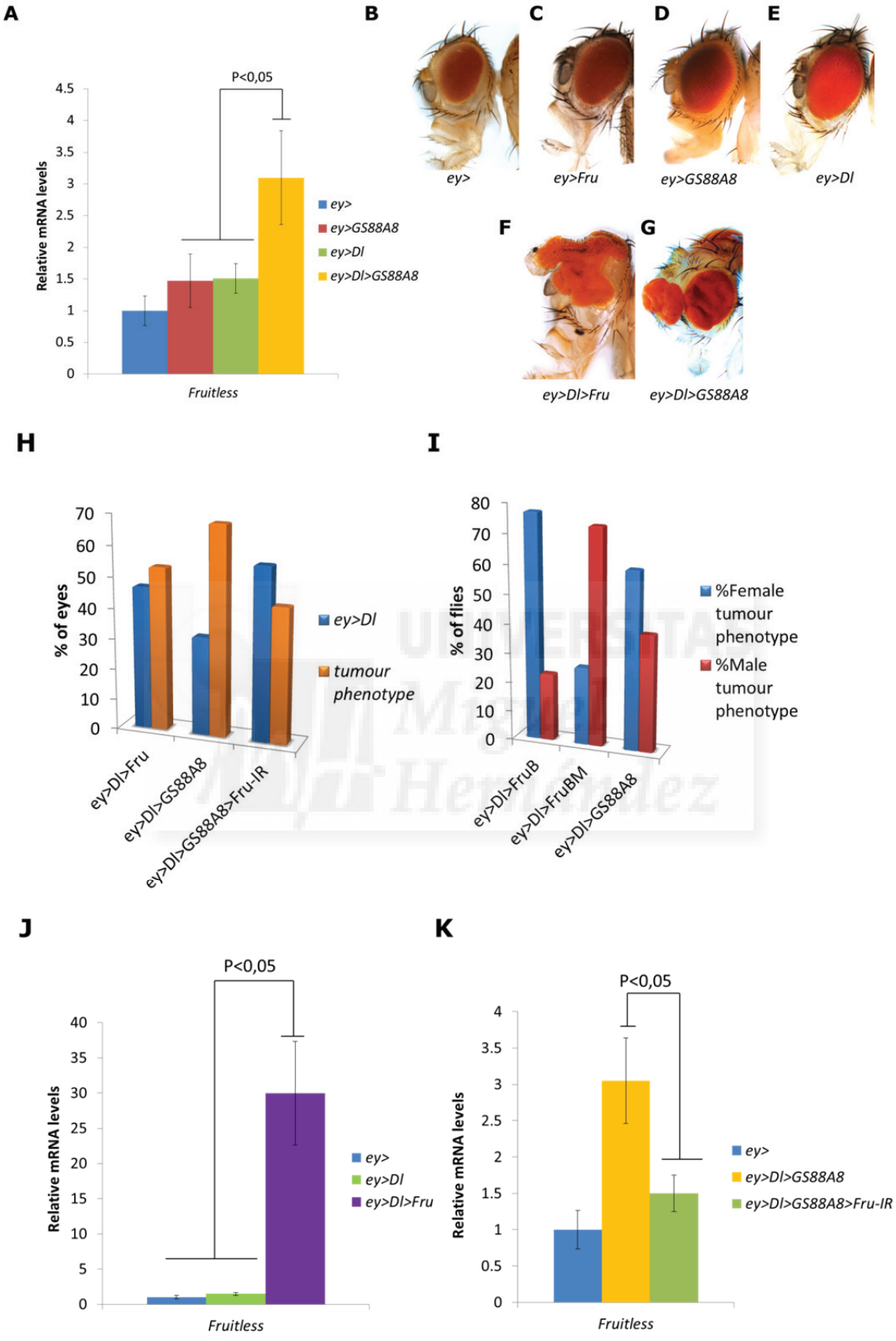
A
B
C
D
E
P<0,05
Relative mRNA levels
4.5
4
3.5
3
2.5
2
1.5
1
0.5
0
Fruitless
ey>
ey>GS88A8
ey>Dl
ey>Dl>GS88A8
ey>
ey>Fru
ey>GS88A8
ey>Dl
F
G
ey>Dl>Fru
ey>Dl>GS88A8
H
I
% of eyes
70
60
50
40
30
20
10
0
ey>Dl
tumour phenotype
ey>Dl>Fru
ey>Dl>GS88A8
ey>Dl>GS88A8>Fru-IR
% of flies
80
70
60
50
40
30
20
10
0
%Female tumour phenotype
%Male tumour phenotype
ey>Dl>FruB
ey>Dl>FruBM
ey>Dl>GS88A8
J
K
P<0,05
Relative mRNA levels
40
35
30
25
20
15
10
5
0
Fruitless
ey>
ey>Dl
ey>Dl>Fru
P<0,05
Relative mRNA levels
4
3.5
3
2.5
2
1.5
1
0.5
0
Fruitless
ey>
ey>Dl>GS88A8
ey>Dl>GS88A8>Fru-IR

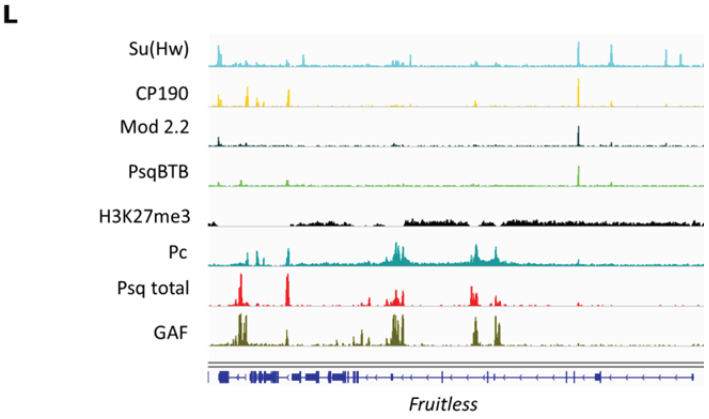

Figure 59. The expression of the BTB-protein Fruitless is specifically induced in the "*eyeful*" phenotype. (**A**) mRNA levels of all the *fru* isoforms were measured by qRT-PCR in eye discs overexpressing *G88A8* (red bar), *UAS-Dl* (green bar), or both (yellow bar). The graph shows an up-regulation of this gene in the "*eyeful*" condition. (**B-G**) Adult heads of ey>, *ey>UAS-Fru*, *ey>GS88A8* and *ey>Dl* flies as controls of ey*>UAS-Fru>UAS-Dl* tumour phenotype and the *"eyeful"* phenotype. (**H-K**) The loss of function of Fru at the "*eyeful*" phenotype produces a reduction of the incidence of tumour eyes from the 70% to 44% (**H**). The male specific *fru* isoform (*UAS-FruBM*) induces tumour formation specifically in males and the same occurs with the female specific isoforms (*UAS-FruB*) (**I**). Levels of total *fru* mRNA have been measured in order to verify the overexpression induced by the *UAS-Fru* line (male or female specific) (**J**) and its depletion by the *UAS-Fru-IR* line (**K**). A further analysis of the isoform involved in the *"eyeful"* phenotype can explain the higher percentage of females suffering from overgrown eyes. (L) IGV image of the binding sites of Psq total (red) and PsqBTB (green) around the *fru* gene, also showing their two main groups of interacting proteins (Su(Hw) and PRE recruiters, in Kc167 cells.

DISCUSSION

1. microRNA miR-7: A new Notch cooperating oncomiR.

To understand the oncogenic function mediated by signalling pathways, such as Notch and Hh, it is necessary to unveil the complex cross-talk, cooperation, and antagonism between these signalling pathways in the appropriate contexts.

Studies performed in different models such as flies, mice, and human cell lines, have revealed critical insights into the contribution of Notch to tumorigenesis. These studies highlight that oncogene Notch does not work alone, needing additional mutations or genes in the process of tumour initiation and progression (e.g., (Bossuyt *et al.*, 2009; Ferres-Marco *et al.*, 2006; Fre *et al.*, 2009; Herz *et al.*, 2010; Liefke *et al.*, 2010; Ntziachristos *et al.*, 2012; Pallavi *et al.*, 2012; Vallejo *et al.*, 2011; Vidal *et al.*, 2006; Weng *et al.*, 2004)). In this sense, we propose here that miR-7 cooperates with Notch-induced tumour-like overgrowth in the *Drosophila* eye and wing.

Several microRNAs have been implicated in the initiation or progression of human cancers (e.g., (Calin *et al.*, 2006; Cho, 2007; Iorio *et al.*, 2007; Lee *et al.*, 2015; Ma *et al.*, 2008)) and in the case of miR-7 it has been postulated to have oncogenic (Chou *et al.*, 2010; Foekens *et al.*, 2008) or tumour suppressor functions, participating in distinct pathways (Erkan *et al.*, 2011; Jiang *et al.*, 2010; Kefas *et al.*, 2008; Reddy *et al.*, 2008; Skalsky *et al.*, 2011; Webster *et al.*, 2009).

In *Drosophila*, multiple cell-specific targets for miR-7 have been previously validated via luciferase, *in vivo* eGFP-reporter sensors or via functional studies (Lai *et al.*, 2005; Li *et al.*, 2005; Li *et al.*, 2009; Pek *et al.*, 2009; Stark *et al.*, 2005; Tokusumi *et al.*, 2011; Yu *et al.*, 2009). In general, although different target genes can be described for the different microRNAs, when tested *in vivo* not all the expected targets respond to the microRNA in a given cellular context. The same occurs with miR-7 target genes, as from 49 predicted targets only *ihog* fully mimicked the effect of miR-7 overexpression in the transformation of Dl-induced mild overgrowth into tumour-like growth. In this way, we confirmed that endogenous *ihog* is directly silenced by miR-7 through its binding to sequences in the 3'UTR of *ihog* both *in vivo* and *in vitro*. Nevertheless, we cannot discard that other miR-7 target genes may contribute to the cooperation of Dl-Notch pathway with *ihog*. In the Table S1 in Appendix I section of this Thesis, we can see genes such as *hairy* and *Tom* among others, which show subtle effects that should be considered in the context of Dl- induced overgrowth.

While miR-7 can directly silence *hairy* in the wing and it is capable of converting Dl-induced mild overgrowth into tumour-like growth, these effects have been shown to be very modest (Stark *et al.*, 2003). *hairy* is involved in eye development (Brown *et al.*, 1995) retinal differentiation (Brown *et al.*, 1995) and is a target of Hh that negatively sets the pace of MF progression (Heberlein *et al.*, 1995; Pappu *et al.*, 2003), and although it might contribute to Dl-induced tumorigenesis, it is unlikely to be essential in this tumour model. Regarding the gene *Tom*, two of the RNAi lines tested, one did not modify Dl-induced overgrowth and the other caused tumours in less than 40% of the progeny (Table S1 in Appendix I). *Tom* is required to counteract the activity of the ubiquitin ligase Neuralized in regulating the Notch extracellular domain, and Dl in the signal emitting cells. (De Renzis *et al.*, 2006). However, the moderate enhancement of Dl that is induced when *Tom* is downregulated by RNAi, suggests that miR-7-mediated repression of *Tom* may contribute to the oncogenic effects of miR-7 in the context of Dl gain of function cooperating with *ihog*.

In conclusion, we have discovered cooperation between the microRNA miR-7 and the Notch signalling pathway in the *Drosophila melanogaster* eye, and we have identified and validated *ihog* as a direct target of the miR-7 in this context. The functional co-receptor of iHog in the Hh signalling pathway, *boi*, is a target of Notch-mediated activity at the dorsal-ventral eye organizer being this regulation either direct or indirect, as we could not demonstrate the direct binding of Eyg to the *boi* promoter by ChIP-seq.

Although these are very preliminary results, we have demonstrated *in vitro*, that in human PC3 and in its non-tumour control PNT1A, the human counterpart of iHog, CDON, is downregulated in the context of human *mir-7* overexpression. Further supporting this result, miR-7 is unable to downregulate *CDON* when we mutate its putative binding sites at *CDON* 3'UTR. Also, its functional co-receptor *BOC* is not affected by the microRNA. The consistent reduction of *CDON* expression by miR-7 might add new information to explain the mechanisms behind tumour induction mediated by *CDON* loss of function. *CDON* expression is a constraint for tumour progression in the human pathology (Delloye-Bourgeois *et al.*, 2013). The high-throughput sequencing consortia have reported the presence of a large number of sprayed missense mutations in the coding sequence of *CDON* in human cancers (see http://cancer.sanger.ac.uk/cosmic/gene/overview?ln=CDONN). All these data support that *CDON* is a *bona fide* tumour suppressor that does not seem to have a causal implication in tumour progression (Delloye-Bourgeois *et al.*, 2013).

To answer the question if in humans, like in our *Drosophila* model, the loss of Hh signalling pathway is able to enhance Notch signalling, we made use of the luciferase tools to report the state of these pathways, but we could not reproduce the *Drosophila* results. All these discrepancies can be explained due to a difference in the crosstalk between both organizers when comparing *Drosophila* organizer function in the context of imaginal discs development, to human cell lines. Another explanation can be that the antagonistic crosstalk seen in the *Drosophila* discs is the result of a direct effect in their effort to maintain, during development, the correct size and morphology of a future adult organ.

In a further step, we will work with a circular RNA also called sponge RNA. Animal microRNAs directly bind to target mRNAs by complementary base pairs and can trigger cleavage of mRNAs depending on the degree of complementarity. Both artificial and natural sponges RNAs contain complementary binding sites to a miRNA of interest. Due to a sponge's binding sites are specific to the miRNA seed region, these RNAs can "sponge up" miRNAs of a particular family, thereby serving as competitive inhibitors that suppress the ability of the miRNA to bind its mRNA targets (Ebert *et al.*, 2010; Ebert *et al.*, 2010). Mammals have thousands of circular RNAs with predicted microRNA binding sites. For instance, CDR1as/ciRS-7 is encoded in the genome antisense to the human CDR1 gene locus (namely CDR1as), and targets miR-7 (namely ciRS-7: circular RNA sponge for miR-7) (Hansen *et al.*, 2013; Memczak *et al.*, 2013). We can use this ciRS-7 to reduce the levels of free miR-7 in miR-7-induced cancer cells and quantify its effect over the endogenous *CDON* mRNA levels present in human cells.

2. miR-7 exposed an unanticipated tumour suppressor role for the Hedgehog signalling pathway.

We have shown that the Hh tumour suppressor role is revealed when components of the Hh pathway are lost in conjunction with a gain of Dl expression in both the eye and wing discs.

To date, Hh has not yet been perceived as a tumour suppressor, although it is noteworthy that human homologs of *ihog*, *CDON*, and *BOC* were initially identified as tumour suppressors (Kang *et al.*, 1997). Importantly, both *CDON* and *BOC* are downregulated by *RAS* oncogenes in transformed cells (Kang *et al.*, 1997) and their overexpression can inhibit tumour cell growth *in vitro* (Kang *et al.*, 2003; Kang *et al.*, 1997; Kang *et al.*, 2002). Since human *RAS* regulates tumorigenesis in the lung by overexpressing *mir-7* in an ERK-dependent manner (Chou *et al.*, 2010), it is possible that RAS represses *CDON* and/or *BOC* via this microRNA. Indeed, as occurs with *Drosophila iHog,* the 3'UTR of both *CDON* and *BOC* contain predicted binding sites for miR-7 (www.targetscan.org), and in this Thesis we show that *CDON* is negatively regulated by this microRNA in PC3 human cells.

There are additional clinical and experimental evidences relating elements of the Hh pathway with tumour-suppression. The function of *Growth Arrest Specific gene 1*, a Hh ligand-binding factor, overlaps that of *CDON* and *BOC* (Allen *et al.*, 2011; Izzi *et al.*, 2011) and its downregulation is positively associated with cancer cells (Jiang *et al.*, 2010) and melanoma metastasis (Gobeil *et al.*, 2008), while its overexpression inhibits tumour growth (Lopez-Ornelas *et al.*, 2011). More speculative is the association of some cancer cells with the absence of cilium, a structure absolutely required for Hh signal transduction in vertebrate cells (Ingham, 2012).

In *Drosophila*, Hh and Notch respectively establish signalling centres along the anterior-posterior and dorsal-ventral axes of the disc to organize global growth and patterning, as has been extensively described in the introduction of this Thesis. At the point where the organizer domains meet, there is a specification of the position of the MF in the eye disc and the proximodistal patterning in the wing disc (Cavodeassi *et al.*, 1999; Li *et al.*, 2005; Stark *et al.*, 2003). Our results suggest that the antagonistic interaction between Hh and Notch signalling pathways might help to ensure correct disc growth. Thus, we show that Hh signalling limits the organizing activity of Dl-Notch signalling, as the loss of Hh signalling enhances a non-cell autonomous oncogenic role of Dl-Notch pathway. Competitive interplay as the one described here between Notch and Hh may not be more common than expected among core growth control and cancer pathways that act within the same cells at the same or different time to exert multiple outputs (such as growth and cell differentiation). Moreover, context-dependent tumour suppressor roles could explain the recurrent, unexplained, identification of somatic mutations in Hh pathway in human cancer samples (e.g., (Jones *et al.*, 2008)). Indeed, our findings stimulate a re-evaluation of the signalling pathways previously considered to be exclusively oncogenic, such as the Hh pathway.

3. Conserved miR-7 tumour model as a potential pre-clinical paradigm.

Cancer is increasing as a cause of death worldwide. The uncontrolled malignant growth of cells can combined with secondary metastatic tumours, being these last ones the more difficult to detect and control. Secondary tumours can spread via the blood or lymphatic system and are highly invasive

and aggressive. The metastatic process involves several biological steps: loss of cellular adhesion, increased motility and invasiveness, entry and survival of tumour cells in the circulation, exit into new tissue, and colonization of a distant site (Chambers *et al.*, 2002; Gupta *et al.*, 2006). All these steps require an Epithelial-to-Mesenchymal Transition (EMT). This is a process in which cells lose their epithelial character and acquire a migratory mesenchymal phenotype (Thiery *et al.*, 2009). EMT and the reverse process (Mesenchymal-to-Epithelial Transition (MET)) are essential also for normal development of multiple tissues and organs. They also contribute to tissue repair and are thought to be recapitulated in metastasizing cancer cells (Yilmaz *et al.*, 2009). Loss of the cell adhesion molecule E-Cadherin is considered a hallmark of EMT (Yang *et al.*, 2008). A challenge to understand the genetic processes behind metastasis formation and the role of the microenvironment is to develop therapeutic strategies to treat metastatic cancers and develop model systems that permit fast drug screens and the easy monitoring of metastatic invasion (Hanahan *et al.*, 2011; Nguyen *et al.*, 2009; Yang *et al.*, 2008).

Over the last decade, the fruit fly *Drosophila melanogaster* has become an important model system for cancer studies determining the molecular characterization of important signalling cascades, developmental and growth control processes. Several characteristics make this animal suitable model for cancer research. Among others, we can highlight a reduced redundancy in its genome compared with that of humans, the facility to conduct large-scale genetic screens in this organism and long-time of usage and development of a wide variety of genomic tools. Moreover, epithelial cells within imaginal discs have many similarities with mammalian stem cells and, as they do, they can produce tumour masses (neoplasm) (Gateff, 1978; Plaglianiri *et al.*, 2003). Tumours within imaginal discs present cancer cells properties: (1) uncontrolled proliferation; (2) evasion of programmed cell death; (3) invasion and metastasis associated with the breakage of the basal membrane; loss of *E- cadherin* expression and metaloprotease production. Regarding the processes of invasion, dissemination and metastasis, should be mentioned that there are important physiological differences between *Drosophila* and mammals, so that *Drosophila* is not the perfect model to study certain aspects of cancer dissemination. The open circulatory system of the fly will permit, in theory, the passive dissemination of tumour cells. This type of dissemination only occurs in certain types of tumours present in highly irrigated tissues as lung or pancreas. Dissemination of cancer cells occurs in an active way and implicates processes such as the intra- and extra-vasation, blood and linfatic vessel circulation, processes that do not occur in the epithelial tumour in *Drosophila*. However, the initial steps (local invasion) and the final steps (distant metastatic organ growth) of metastasis can be modelled in *Drosophila*. Results from different laboratories, including ours, clearly show the molecular and cellular conservation of these processes between *Drosophila* and mammals, being the *Drosophila* studies relevant for human cancer.

Models of tumour formation and cell invasion have been created in *Drosophila* using a wide variety of gene targeting strategies used through this Thesis, such as loss-of-function mutations and tissue-specific RNAi knockdown, as well as transgenic overexpression of activated oncogenes found in human cancers. We use the pseudostratified epithelia of the *Drosophila* larval wing and eye imaginal discs, since they are 'two-hit' models of tumour overgrowth and invasion, caused by miR-7 in combination with *Dl* overexpression. Alterations in microRNAs have been implicated in the initiation or progression of human cancers (e.g., (Calin *et al.*, 2006; Cho, 2007; Iorio *et al.*, 2007)),

although such roles of microRNAs have rarely been demonstrated *in vivo* (e.g., (Foekens *et al.*, 2008; He *et al.*, 2004; Voorhoeve *et al.*, 2007)). Here we work with models that are susceptible to be used for pharmacological screening.

In the case of the PsqBTB-induced tumour-metastatic model in combination with Dl driven overexpression by the GS88A8 line (Ferres-Marco *et al.*, 2006), pigmented or fluorescent cells coming from the compound adult eye (under the *ey-Gal4* promoter) suffering an EMT transformation can be easily seen throughout the body of the animal. Additionally in this Thesis, we propose tumour-metastatic combination of Dl with the loss of function of the active form of Ci (the fly counterpart of the human Gli1) under the *dpp-Gal4* promoter as a potential pre-clinical paradigm. Crossing *dpp-Gal4>UAS-Fluorescent protein* flies with different UAS-lines we can easily monitored metastasis following the fluorescent cells that migrate out of the *dpp* region. Human *Gli* loss-of-function has also been previously described as a metastatic inducer in different contexts such as pancreatic ductal adenocarcinoma and lung squamous cell carcinomas (Joost *et al.*, 2012; Tang *et al.*, 2015; Yue *et al.*, 2014)). Complementary screens and mammal extrapolations should be performed in the constant fight to find new hallmarks of cancer progression.

4. BTB- and non-PipsqueakBTB link up Polycomb, and Chromatin Insulators in unsuspected ways:

4.1. PipsqueakBTB as a possible chromatin insulator protein.

The origin of the "*eyeful*" phenotype has been attributed to the epigenetic silencing mediated by the protein-protein interaction domain of Psq (Ferres-Marco *et al.*, 2006), as occurs with the oncogenic BTB-proteins in humans, PLZF (promyelocytic leukaemia zinc finger) and BCL-6 (B cell lymphoma 6), that associate with histone deacetylases (HDACs), co-repressors, and PcG repressors through their BTB domain (Melnick *et al.*, 2002). Extrapolating this results to the "*eyeful*" phenotype it has been proposed that it is possible that Psq and/or Lola (which also possesses a BTB domain), interact through their BTB with histone deacetylases (HDACs) and PcG repressors to recruit this complexes to particular genes, for example to homeotic genes with GAGA sequences (Ringrose *et al.*, 2004). In the case of Psq, it has been previously described to be bound to these sequences co-localizing with GAF (Lehmann *et al.*, 1998; Schwendemann *et al.*, 2002). Psq is found in a complex with Polycomb proteins, where Psq may be responsible for the sequence-specific targeting of a Polycomb-group (PcG) complex that contains HDAC activity (Ringrose *et al.*, 2004). So deregulation of *psq* might induce tumorigenesis through aberrant epigenetic silencing of genes that contribute to the uncontrolled growth of tumour cells. Supporting this proposal, there is a loss or strong reduction of the open chromatin mark H3K4 trimethylation (H3K4me3) in the developing eye tissue from which the tumour arises in the *"eyeful"* flies, suggesting that the chromatin in the mutant tissue has been condensed or silenced (Ferres-Marco *et al.*, 2006). Additionally, reducing the dosage of genes related to gene silencing and chromatin condensation, like *Rpd3/HDAC*, *E(z)*, *Su(var)3-9*, *Pc*, and *Esc*, impeded tumour development. Finally, it was demonstrated that the increase in epigenetic silencing reduced the expression of the retinoblastoma family protein (*rbf*) gene, a well-known tumour suppressor gene, necessary for preventing tumour development.

Our results add new perspectives to what was predicted for the *"eyeful"* phenotype. In these contexts, the oncogenic function of Psq was associated to their BTB, interacting with histone-deacetylases (HDACs), co-repressors and PcG proteins (Ferres-Marco *et al*., 2006), not found in our Y2H with Psq aa1-720 and not correlating with the insulator relation found for the BTB-containing forms of Psq. We have demonstrated that PsqBTB can directly interact with Su(Hw) insulator protein members and with Chro, adding new insights into the composition of insulator-mediated structures present in the genome. See Table 3 with a summary of the known and the new BTB interactions presented in this Thesis work.

	GAF	Lola Like	Mod(mdg4)	PsqBTB	CP190	Chromator
GAF	+	+	+	+		
Lola Like	+	+	+	+		
Mod(mdg4)	+	+	+	+	+	+
PsqBTB	+	+	+	+	+	+
CP190			+	+	+	+

Table 3. Table with the summary of the known BTB interactions and the new interactions obtained from this work in red boxes.

We cannot forget to take into account the limitations of extrapolating the results found in *Drosophila* Kc167 cells to animal tissue. It is the first time that we can study PsqBTB and non-BTB Psq isoforms individually, as we designed antibodies that specifically recognise each of them, allowing us to study them individually. Through Y2H and co-immunoprecipitations we first revealed the possible relation of PsqBTB with insulator proteins through it interaction with Chro. Afterwards, ChIP-seq data analyses unveil differences between both types of Psq isoforms (with or without the BTB), regarding the sequence of their respective binding sites in the genome.

All the previously described data known for Psq about its binding to GAGA sequences present in the chromatin, its co-localization with GAF and the recruitment of PcG, seems to belong to the non-BTB Psq isoforms. This assumption is endorsed by the information obtained with different heatmaps and a motif enrichment analysis within the non-BTB Psq binding sequences. Although this data locates this short isoform co-localizing with GAF, a new binding motif should be searched through additional methods (different to the programs available in internet as MEME-ChIP or RSAT), as the only motif attributed to these binding sites is GAGA and is not directly enriched at the peak summit. A new motif for Psq total was published in 2014 and obtained by ChIP-seq without the traditional PFA crosslink (Kasinathan *et al.*, 2014), and it might be the same as the corresponding to our non-BTB data.

We can find co-immunoprecipitated PsqBTB with other members of the insulator family apart from Chro. This family is known as Su(Hw) insulator proteins and they were first described as the *gypsy* insulator binding proteins. They include two BTB proteins (Mod(mdg4)2.2 and CP190) and Su(Hw) (Ghosh *et al.*, 2001; Golovnin *et al.*, 2012). CP190 and Mod(mdg4) isoforms are also common proteins of other chromatin insulator complexes (Gerasimova *et al.*, 2007; Ghosh *et al.*, 2001; Pai *et*

al., 2004). Regarding the tendency of BTB proteins to oligomerize (Bardwell *et al.*, 1994; Horowitz *et al.*, 1996; Koonin *et al.*, 1992; Raff *et al.*, 1994) different authors suggested that they might act by modifying chromatin structure (Albagli *et al.*, 1995; Croston *et al.*, 1991; Dorn *et al.*, 1993; Kerrigan *et al.*, 1991), and this is the basis of insulator proteins behaviour. The insulator function of PsqBTB has been tested using the *gypsy* insulator situated between the promoter of the *cut* gene and its enhancer (ct^6). Unfortunately, measuring the total area of adult wings, we cannot detect a significant suppression of the ct^6 phenotype. With these results we cannot confirm the insulator function of PsqBTB, not surprisingly since, as it will be described in Figure 56F-F', we could not detect the presence of this protein in the larval wing imaginal disc. These BTB isoforms must be present at wing discs but in a very low level, since it can be detected by WB in concentrated wing disc protein extracts (Figure 57C). Other possibility could be that this protein is present and helps insulator function in maintaining the differentiated state of adult wing cells, but it is not essential in the insulator function, as its depletion does not show a direct effect over enhancer-blocking activity. The possible insulator function of PsqBTB seems to depend on larval tissue or developmental stage. Further analysis will be performed using other insulator constructs affecting the expression of genes showing phenotypes in tissues characterized by the presence of PsqBTB. As we can find these BTB isoforms at, for example, in the fat body, we can use a previously described strategy (Wei *et al*., 2001) to address the effects of the insulator on basal transcription. This strategy consists of using constructed reporter genes with spacing between the insulator and a minimal alcohol dehydrogenase gene (*adh*) promoter, and to analyse alcohol dehydrogenase activity after transient transformation of larval fat body (McKenzie *et al*., 1994; Wei *et al*., 2000).

PsqBTB is part of the called architectural proteins (known to be regulators of 3D genome organization in cell fate (Gómez-Díaz *et al.*, 2014)), possibly mediating the interaction between different TADs along the chromatin and at the borders of the repressive H3K27me3 domains. The correct establishment of repressive chromatin states within a cell are so crucial that they need to be strictly controlled. It seems that both isoforms of Psq converge in the control of the formation of this chromatin states through different mechanisms depending on the presence or the absence of the BTB-interaction domain.

In Figure 60, we propose a model for the location and function of the BTB and non-BTB Psq isoforms. PsqBTB isoforms are probably co-localizing with architectural proteins at APBSs and with Su(Hw) insulator proteins, while non-BTB Psq co-localizes with GAF recruiting PcG and TrG proteins to PRE/TREs. We have seen that non-BTB Psq isoforms seems to co-localize with GAF all over the genome, being possibly regulated with other functions of GAF.

A full understanding of the origin of a tumour-like growth caused by the overexpression of different transcription factors will be a very challenging task due to the unpredicted effect of this context far from an endogenous situation. However, all the data proposed in this thesis work, lead us consider the possible relation between the epigenetic changes observed in the "*eyeful*" phenotype and its insulator function. Since long ago, it has been shown that insulators control the behaviour of PcG proteins (Cai *et al.*, 2001; Comet *et al.*, 2006; Mallin *et al.*, 1998; Muravyova *et al.*, 2001; Sigrist *et al.*, 1997) supporting recent models wherein chromatin insulators are involved in mediating long-range interactions important for Polycomb-mediated repression (Pirrotta *et al.*, 2012). We will perform complementary studies testing the effects of insulator proteins over the

epigenetic origin of the "*eyeful*" phenotype, as for example, testing the impact of the depletion of different insulator proteins by RNAi or loss-of-function alleles over the "*eyeful*" context.

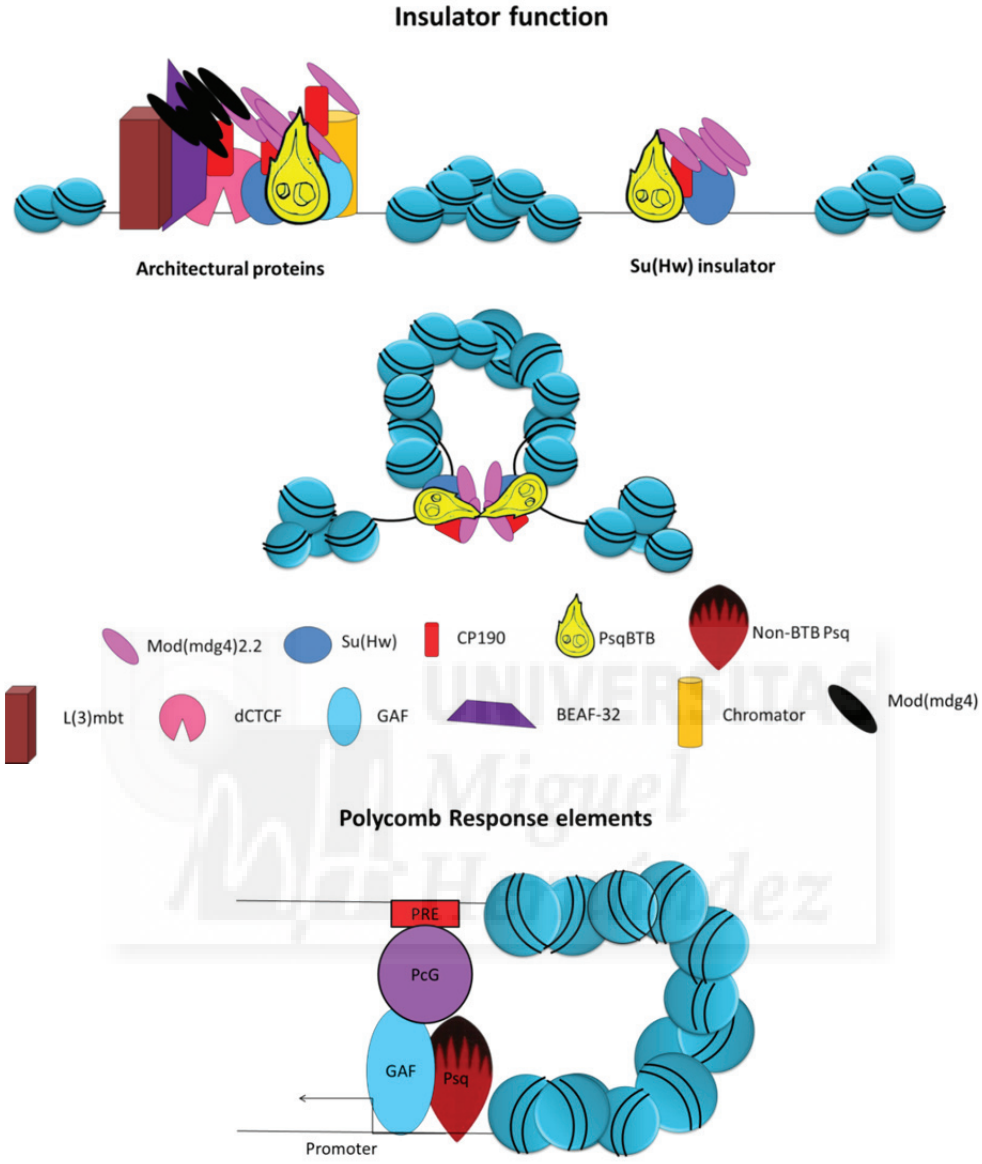

Figure 60. Model for the function of the different protein isoforms of Pipsqueak. See the here represented insulator function of PsqBTB (yellow), accompanied by architectural proteins, localized in APBSs, or with Su(Hw) insulator proteins, possibly mediating the interaction between distant sequences of the chromatin, through the formation of topological associated domains. Non-BTB Psq is associated with GAF in the recruitment of PcG and TrG proteins to PRE/TREs, and also, but not represented here, it is associated with GAF along the genome probably involved in its additional functions. In the figure legend is represented the identity of each form in the scheme.

4.2. Pipsqueak and its effect in transcription.

The simultaneous implication of Pc and GAF in transcription repression and activation, within and/or out PREs (Farkas *et al.*, 1994; Mousavi *et al.*, 2012; Ringrose *et al.*, 2004; Strutt *et al.*, 1997; Xu *et al.*, 2012), forces the revision of the functional relevance of Psq isoforms in transcription. Both forms of

Psq are located at active enhancers and at transcription starting sites, suggesting a function in active transcription. However, PsqBTB and its relation with insulators, suggests an enhancer-blocking insulator function, so an implication in transcriptional repression cannot be discarded. The same occurs with non-BTB Psq with its co-localization with GAF and the epigenetic machinery all over the genome.

Eliminating the non-BTB isoform in a context where PsqBTB cannot be detected (proliferative tissues such as imaginal discs) slows cell proliferation directly or indirectly reducing the levels of CycA. This Cyclin has been reported to count with a classical PRE at its promoter, showing non-BTB Psq co-localizing with GAF and Pc at this site. However, in this case we have a scenario where Psq is acting as an activator collaborating preferably with the TrxG instead of the PcG, similar to the bifaceted function of GAF at these sites. The additional information we can extract from these findings is that non-BTB Psq is selectively expressed in proliferative tissues as its expression seems to be paramount for the expansion of cell population. PsqBTB expression is tightly controlled in these tissues due to unknown reasons, and its overexpression (like in the case of the "*eyeful*" phenotype) unbalances its effect over these cells, making them more susceptible to respond to the overexpression of Dl resulting in hyper-proliferation.

Psq total biding sites are not affected by the absence of Jil-1 in Kc167 cells. This protein is involved in the release of Pol II from its paused state, and so activating transcription. This result leads us to study the effect of Psq up-stream in the transcriptional regulation cascade, specifically in the relation of Psq with the process of Pol II pausing where GAF has been implicated.

Calculating the pausing index of genes characterized by the presence of GAF and Psq (mainly the non-BTB isoforms), reveals a possible relation of Psq in gene pausing. However, the negative deviation of pausing indexes for genes containing total Psq (non-associated with GAF or PsqBTB) involves PsqBTB in the opposite process. In relation to this result, the knock-down of Psq total in Kc167 cells shows a reduction in the released form of Pol II (reduced levels of Pol II Ser2 and H3S10 phosphorylation). This result combined with the pausing index calculated for PsqBTB and Jil-1 containing genes, suggests that PsqBTB is helping in the release of Pol II from its paused state up-stream of Jil-1. PsqBTB through its interaction with Chro (demonstrated by Co-IP and 1-by-1 Y2H) can be implicated in the release of Pol II, since the complex formed by Chro and Z4 has been involved in the recruitment of Jil-1 (required for phosphorylation of H3S10) (Gan *et al.*, 2011; Rath *et al.*, 2006). In this regard, we will study the distribution of Jil-1 along the genome, in the absence of PsqBTB.

Additionally, we used another two strategies to test the effect of transcription factors, such as Psq, in transcription induction: Heat-sock experiments and 20-HE treatment.

Heat-shock of Kc167 cells did not show a modification of Psq total binding sites, but the treatment of these cells with 20-HE in different conditions highlights an effect over the levels of non-BTB Psq bound around Ecdysone-induced genes (no changes were reported for PsqBTB). Indeed, the absence of Psq in these cells during the treatment with 20-HE, shows an up-regulation of early Ecdysone-induced genes, such as *Eip57B*, *EcR* and *vri*. This result suggests that Ecdysone limits its own response by recruiting non-BTB Psq repressor to Ecdysone-responsive genes. This finding takes

on far greater significance when extrapolated to the coordination of *Drosophila* development, but the lethality of the Psq loss-of-function alleles, makes it difficult to work with them. Further analysis will be done with Gal80 or heat-sock-GAL4 strategies. Additional repressive proteins, such as GAF or Pc, could be studied in this context in order to discover additional the proteins involved in this process.

Like all other holometabolous insects, the size of *Drosophila* adult flies is set by the size of the larvae prior to metamorphosis, at the time of pupariation. The major developmental hormone in *Drosophila,* 20-HE is required for all the developmental transitions needed for metamorphosis (Thummel, 1995; Thummel, 1996; Thummel, 2001). Ecdysone is produced in and released by the prothoracic gland (PG), a component of the ring gland, endocrine glands located in the prothorax (McBrayer *et al.*, 2007; Zitnan *et al.*, 2007). Ecdysone release is controlled by a complex combination of upstream factors, including peptide hormones and neuropeptide signals. For example, Prothoracicotropic hormone (PTTH) from the central nervous system is required to regulate the synthesis and release of Ecdysone from the endocrine gland PG (McBrayer *et al.*, 2007). Ecdysone pulses from the PG are required for all aspects of morphogenesis, starting with the formation of the body plan during embryogenesis, hatching and development of the first larval instar, and for cuticle moulting at the end of the first and second instars larvae. It has been demonstrated that Torso acts as the receptor of PTTH (Rewitz *et al.*, 2009). In this work, they show that *torso* is expressed specifically in the PG, and its loss phenocopies the removal of PTTH. The activation of Torso by PTTH stimulates extracellular signal–regulated kinase (ERK) phosphorylation, and the loss of ERK in the PG phenocopies, the loss of PTTH and Torso, concluding that PTTH initiates metamorphosis by activation of the Torso/ERK pathway. At the same time, it has been shown that the control of germline *torso* expression by Psq is required for embryonic terminal patterning in *Drosophila* (Grillo *et al.*, 2011). In our laboratory we have observed an up-regulation of the transcription of this gene in response to the overexpression of both forms of Psq in cell culture and imaginal discs (data not shown). Considering all these data, it is reasonable to connect Psq, Torso and PTTH in the *Drosophila* development. To explore the possible implication of Psq in this paramount process we measured the developmental acceleration or delay of *Drosophila* pupariation time when we overexpress or decrease *psq* levels in the PG. Preliminary results show that the loss of function of Psq total in the PG has no effect over the pupariation time. On the other hand, overexpression of PsqBTB isoforms, which has been reported to also activate the transcription of *torso,* was lethal and caused the death of L2 instar larvae. We are planning to overexpress non-BTB Psq at the PG, which is not so larval lethal.

In summary, the results described in this Thesis show Psq as a multifaceted transcription factor with isoforms implicated in different processes. This, in addition to its assumed repressive function, may explain the riddle of Psq ability to act in the same context as an oncogene or as a tumour suppressor.

5. Unexpected partnership between PipsqueakBTB, and chromatin insulators may be relevant to tumorigenesis: The case of *Fruitless.*

In this work, we have reported the up-regulation of another BTB protein Fru by the synergistic effect of the overexpression of Dl and Psq, the last one driven by the expression of the *GS88A8* line (overexpressing two other BTB-family genes proteins, *psq* and *lola*) in the *Drosophila* eye. The up-regulation of *fru* has been shown in other tumour contexts, combined with the up-regulation of other genes belonging to the BTB family such as *broad*, *tramtrack*, *chinmo, abrupt* or *lola* (Doggett *et al.*, 2015). The tumour growth we have shown, produce by the overexpression of the gene *fru* in combination with a Notch gain of function has also been recently confirmed (Doggett *et al.*, 2015). BTB proteins are increasingly implicated in the aetiology of human cancers, as both tumour suppressors and oncogenes, and are also highly oncogenic in *Drosophila* when ectopically over-expressed. Taking into account our results regarding Psq function as an insulator, missregulated expression of these BTB-containing proteins may produce an insulator-related rearrangement of 3D chromatin organization and the subsequent changes in general transcriptional regulation.

With all this data and inspired by a paper from Dr. Victor Corces group (Li *et al.*, 2015), I venture to say, just as pure speculation, what can be happening in a BTB-mediated tumour condition. In this paper, they study the origin of the dramatic changes in the general transcription profile produced by temperature stress. Expression of most active genes is quickly repressed, whereas a few previously silenced genes, the heat shock genes, are upregulated (Gonsalves et al., 2011; Guertin et al., 2012). They show that this stress induces relocalization of architectural proteins from TAD borders to inside TADs, reducing TAD border strength and allowing for an increase in long-distance inter-TAD interactions. This produces a dramatic rearrangement in the 3D organization of the nucleus that increases contacts among enhancers and promoters of silenced genes, which recruit Pc and form Pc bodies in the nucleolus, increasing subsequently the general chromatin silencing. These results suggest that the TAD organization of metazoan genomes is plastic and can be reconfigured quickly. I venture to extrapolate these results to our tumour context in *"eyeful"*, characterize by the overexpression of BTB-proteins and an increase in transcriptional repression. The ability of these BTB-proteins to oligomerize may rearrange architectural protein contacts, changing TAD interactions that can increase contacts among enhancers and promoters of silenced genes. This may produce an increase in transcriptional repression in response to the new far-from-endogenous situation.

On other hand, alternative splicing of *fru* transcripts produces sex-specific proteins. The sex-biased tumorigenesis observed in this work and produced by *fru* is interesting given that gender differences in tumorigenesis have not yet been reporter for any tumour type in *Drosophila*. This opens the possibility that gender differences in Fru function can also impact on the different response of female and male imaginal disc cells to tumours. Importantly, our preliminary data suggest that loss of endogenous *fru* via RNAi transgenic expression can partially rescue the PsqBTB ("*eyeful*") phenotype, further implicating *fru* in this tumour model.

In summary, the work presented in this Thesis broadens our knowledge on Psq activity respect to the work of (Ferres-Marco *et al*., 2006), unveiling new mechanisms underlying Psq-

mediated tumorigenic function and adds a new microRNA acting as an oncomir in the context of Notch induced tumorigenesis. The miR-7 project has been already published (see Appendix II). However, to prove some of the hypothesis suggested in this manuscript and to verify if PsqBTB could serve as a model to understand how other BTB-oncogenes carry out their functions during oncogenesis, we will have to perform further experiments.

CONCLUSIONS

The conclusions drawn from this Thesis work are the following:

Related to Section 1:

1. Luciferase reported-based cellular assays *in vitro* and *in vivo* show that the conserved microRNA miR-7 directly silences the Hedgehog receptor *ihog* by binding to a single conserved miR-7 binding sites in its 3' UTR region.

2. Delta-Notch signalling represses expression of Boi, the second functionally redundant Hedgehog receptor, either directly or indirectly via the Pax6-related transcription factor Eyegone.

3. The synergy between miR-7 and the Delta-Notch pathway activity converged on the dampening of Hedgehog signalling activity.

4. Tumour formation in the eye and wing imaginal discs can be provoked by cooperative activation of Notch signalling and reduced activity of Hedgehog signalling.

5. Increasing Hedgehog signalling or the loss of Cubitus interruptus repressor form can suppress tumorigenesis by miR-7/Delta cooperation.

6. Loss of Hh signalling enhances Dl-Notch signalling activity.

7. The human counterparts of the receptor iHog (CDON), is similarly repressed by the human miR-7 by binding to the seed sequences in its 3' UTR as shown by our assays *in vitro* in human prostate cancer cells PC3 cells.

Related to Section 2:

8. Y2H experiments reveal that Chromator insulator protein is a binding partner of PipsqueakBTB.

9. PipsqueakBTB isoforms interact through the BTB domain with the C-terminal domain of Chromator, as revealed in 1-by-1 Y2H experiments.

10. PipsqueakBTB and Chromator fully co-localize in the genome at promoter regions as revealed by ChIP-seq.

11. Pipsqueak bound to Polycomb Response Elements seems to be the non-BTB Pipsqueak isoforms.

12. Resolution of ChIP-seq assay unveils that GAGA factor binding sites align closely to non-BTB Pipsqueak binding sites.

13. PipsqueakBTB may be implicated in the release of RNA polymerase II pausing.

14. PipsqueakBTB may act as a chromatin insulator protein.

15. PipsqueakBTB directly binds to Suppressor of Hairy Wing insulator members.

16. PipsqueakBTB binds at architectural protein binding sites at the borders of H3K27me3 domains.

17. Non-BTB Pipsqueak binding sites co-localize with Ecdysone receptor sites.

18. Ecdysone limits its own response by recruiting non-Pipsqueak repressor to Ecdysone-responsive genes.

Las conclusiones derivadas de este trabajo de tesis, se detallan a continuación:

Relacionadas con la Sección 1:

1. El microRNA miR-7, conservado desde *Drosophila* hasta humanos, silencia directamente el receptor de la vía de Hedgehog *ihog,* a través de la unión de este microRNA a un único sitio en la región 3'UTR de este gen. Como se ha demostrado en ensayos con reportero de luciferasa *in vivo* e *in vitro*.

2. La vía de señalización Delta-Notch reprime la expresión de Boi, el segundo receptor funcionalmente redundante de la vía de Hedgehog, de manera directa o indirecta, a través del factor de transcripción relacionado con Pax6, Eyegone.

3. miR-7 y la vía de Notch convergen y sinergizan reduciendo la actividad de la vía de Hedgehog.

4. La formación de tumores en los discos imaginales de ojo y ala están producidos por la cooperación entre la activación de la vía de señalización de Notch y la reducción de la vía de Hedgehog.

5. El aumento de la señalización de la vía de Hedgehog o la pérdida de la forma represora de Cubitus interruptus suprimen la formación del tumor producida por la cooperación miR-7/Delta.

6. La pérdida de la vía de señalización de Hedgehog aumenta la actividad de la vía se señalización Dl-Notch.

7. El homólogo en humano del receptor iHog (CDON), es reprimido por el microRNA miR-7 de humano uniéndose a sus regiones *seed* en el 3'UTR *in vitro* en células de cáncer de próstata PC3.

Relacionadas con la Sección 2:

8. La proteína aislante (*insulator* en inglés) Chromator se une a PipsqueakBTB, como revela un ensayo de Y2H.

9. La isoforma PipsqueakBTB interacciona a través de su dominio BTB con la región C-termina de Chromator, como se ha visto a través de experimentos de 1-by-1 Y2H.

10. PipsqueakBTB y Chromator co-localizan en el genoma en regiones promotoras como se ha visto a través de ChIP-seq.

11. La forma de Pipsqueak unida a Elementos de respuesta a Polycomb (*PREs* en inglés) no contiene el dominio BTB.

12. Los sitios de unión de la forma corta de Pipsqueak (sin el dominio BTB) solapan con los sitios de unión de GAGA Factor.

13. PipsqueakBTB parece estar implicado en la liberación de la polimerasa II de su estado pausado.

14. PipsqueakBTB probablemente actúe como una proteína *insulator*.

15. PipsqueakBTB se une directamente a *Suppressor of Hairy Wing insulators*.

16. PipsqueakBTB se une a los sitios correspondientes a proteínas arquitectónicas en los bordes de los dominios de H3K27me3.

17. Las isoformas de Pipsqueak sin el dominio BTB co-localizan con los sitios de unión del receptor de la hormona Ecdisona.

18. La Ecdisona limita su propia respuesta reclutando la forma sin el BTB de Pipsqueak hasta sus genes de respuesta.

MATERIALS AND METHODS

1. Fly genetics.

1.1 Drosophila Husbandry.

miR7 project: The *GS(2)518ND2* line was isolated in a genetic screen for enhancers or suppressors of a mild overgrown eye phenotype induced by Dl overexpression when driven by the eye specific *ey-Gal4* driver (*ey-Gal4 UAS-Dl*). The *PlacWP1O111* stock was a gift from Dr C. Klambt (Munster University, Munster, Germany). The other *Drosophila* stocks used in this project were: *UAS-mir-7* and *UAS-DsRed::mir-7* (Li *et al.*, 2005), *UAS-boi* (Hartman *et al.*, 2010), *UAS-ci* (Dominguez *et al.*, 1996) and *UAS-ci-75* (Aza-Blanc *et al.*, 1997; Methot *et al.*, 1999). A detailed description of the stocks and transgenic flies used in this study can be found at *http://flybase.org/* for *ey-Gal4, ptc-Gal4, en-Gal4, hsp70-Gal4, Bx-Gal4, UAS-Dl, UAS-fng, UAS-hh, UAS-eyg, EP(X)1447 (boi),* hh^{AC} and smo^{3} or at *http://flystocks.bio.indiana.edu/ and http://stockcenter.vdrc.at/control/main* for the BDSC and VDRC RNAi stocks, respectively. Clones of hh^{AC} surrounded by Dl-expressing tissue were generated by the *ey-Flp* in eye-antennal imaginal discs of the genotype: *yw ey- Flp; ey-Gal4 UAS-Dl/+; FRT82B* hh^{AC}*/FRT82B arm-lacZ.* The MARCM GFP-labelled clones of smo^{3}/smo^{3} only or smo^{3}/smo^{3} *tub-Gal4 UAS-Dl* cells were induced in larvae 48-72 hr after egg laying by 1 hr heat shock at 37°C at 48-72 hr after egg laying in larvae: *yw tub-Gal4 UAS-GFP hsp70-FLP122;* smo^{3} *FRT40A ptc-lacZ/ tub-Gal80 FRT40A and y w tub-Gal4 UAS-GFP hsp70-FLP122;* smo^{3} *FRT40A ptc-lacZ/ tub-Gal80 FRT40A; UAS-Dl/+*, respectively.

All the combinations of Gal4, GS and the different UAS transgenic lines and mutants were raised at 26.5°C.

GS-element and PlacW Mapping Genomic DNA flanking the P-element insertion in the *GS(2)518ND2* and the *PlacWP1O111* stock were recovered by inverse PCR using the $Pwht^{1}/Plac^{1}$ and $Plw^{3\text{-}1}/Pry$ 4 primers, respectively (http://www.fruitfly.org/about/methods/inverse.pcr.html), and they were subsequently sequenced. A BLAST search with the sequence produced perfect matches to the genomic region on chr2R:16491078 for *GS(2)518ND2* and on chrX: 2364036 for *PlacWP1O111*.

Pipsqueak project: A detailed description of the stocks and transgenic flies used in this study can be found at *http://flybase.org/,* the *Bx-Gal4, ey-Gal4, UAS-Dl,* psq^{0115} and *Df(2R)psq-lola Δ18* (Grillo *et al.*, 2011; Horowitz *et al.*, 1996; Huang *et al.*, 2002; Schwendemann *et al.*, 2002; Siegel *et al.*, 1993) and *Df(2R)psq-lola Δ18* (Horowitz *et al.*, 1996; Huang *et al.*, 2002) or at *http://flystocks.bio.indiana.edu/ and http://stockcenter.vdrc.at/control/main* for the BDSC and VDRC RNAi stocks, respectively.

Other stocks used here were: *UAS-*psq^{11} (PsqBTB) from laboratory of Dr. María Dominguez, *UAS-*psq^{2} (Psq non BTB) from (Grillo *et al.*, 2011), *UAS-88A8* from (Ferres-Marco *et al.*, 2006), $y^{2}ct^{6}$*;Mod(mdg4)*^{T6}*/Mod(mdg4)*^{T6}, $y^{2}ct^{6}$*;CP190*$^{4\text{-}1}$*/TM6* and $y^{2}ct^{6}$*;Su(Hw)*^{V}*/TM6* a gift from laboratory of Dr. Victor Corces (Emory University in Atlanta) (Capelson *et al.*, 2005) and *UAS-fruitless* a gift from the laboratory of Dr. Daisuke Yamamoto.

1.2 Image acquisition.

Drosophila images (eyes and wings of adult flies) were captured on an optical microscope ZEISS Axiophot, using a MicroPublisher 5.0 camera (QImaging) and the QCapture software (QImaging). All pictures were taken using a 5X objective with 1.5X zoom. Each image is a composite of 15 to 25 images of the same sample focused at different heights of the specimen. The in-focus composites were generated using the software AutoMontage Essentials 5.0.

2. Yeast two-hybrid experiments.

2.1 Yeast two-hybrid screen.

The coding sequence for aa Met1-Gln720, which contains the BTB and the central region of the *Drosophila* Psq protein (GenBank accession number gi: 24652499, FlyBase ID FBgn0004399), specifically the isoform B, was used as bait for the assay.

The sequence was PCR-amplified and cloned in frame with the LexA DNA-binding domain (DBD) into plasmid pB29 (orientation N-bait-LexA-C). pB29 bait plasmid derives from the original pBTM116 (Vojtek *et al.*, 1995). The DBD constructs were checked by sequencing the entire inserts. The bait plasmid was transformed in the yeast strain L40ΔGal4 (mata) (Fromont-Racine *et al.*, 1997).

As prey we used a *Drosophila* embryo library from Hybrigenics Services, which is an equimolar pool of two cDNA libraries prepared from 0-12 hr (zygotic + maternal mRNA) and 12-24 hr embryo mRNA. The different cDNA were cloned in frame with the Gal4 activation domain (AD) into plasmid pP6, derived from the original pGADGH (Bartel et al., 1993). The AD constructs were checked by sequencing the insert at its 5' and 3' ends.

Interaction assays are based on the reporter gene HIS3 (growth assay without histidine). The general logic of the assay is as follows: upon physical binding of protein X with protein Y, the DNA Binding Domain (DBD) of a transcriptional activator is brought in close proximity to its Activation Domain (AD) counterpart. Reconstitution of a functional transcription factor activates the production of an auxotrophy marker (HIS3 in this assay), which in turn allows His- yeast cells to grow on a selective medium lacking histidine. The DBD constructs were transformed in L40ΔGal4 (mata) yeast cells and the AD constructs in Y187 (matα) yeast strain. The interactions were then tested using a mating approach to generate diploid yeast that will express both fusion proteins, as previously described (Fromont-Racine *et al.*, 1997). The screen was first performed on a small scale to test the autoactivation of the bait, its toxicity and to select the most appropriate selective medium for the assay. The selective medium DO- 2, which lacks tryptophan and leucine, was used as a growth control. DO-3 medium, which lacks tryptophan, leucine and histidine, was used to test protein interaction. The full-size screen was performed using 50mM of 3-aminotriazol (3-AT), an inhibitor of imidazole glycerol phosphate dehydrates the product of the HIS3 reporter gene. This increases stringency and reduces possible autoactivation by the bait proteins.

Following the procedure described in (Formstecher *et al.*, 2005), 78.2 million interactions were tested, from which 154 positive clones were selected on DO-3 selective medium plus 3-AT. The corresponding prey fragments were amplified by PCR and sequenced at their 5' and 3' ends. They

were identified by sequence comparison with the release 3.1 of Berkeley *Drosophila* Genome Project (BDGP) using BLASTN (Altschul *et al.*, 1997). For the complete list of positive clones see Table S3 Appendix I.

For each interaction, a Predicted Biological Score (PBS) was computed to assess interaction reliability. This score represents the probability of an interaction being non-specific. The scores are divided into four categories, from A (lowest probability) to D (highest probability). A fifth category, E, specifically tags interactions involving highly connected prey domains. This category represents highly likely two hybrid artefacts. The PBS has been shown to positively correlate with the biological significance of protein interactions (Colland *et al.*, 2004; Formstecher *et al.*, 2005; Terradot *et al.*, 2004).

2.2 One-by-one yeast two-hybrid experiments.

The coding sequence for aa Met1-Gln720, Met1-Asp131 and Ala132-Gln720 of the *Drosophila* Psq protein (FlyBase ID FBgn0004399), specifically isoform B (containing the BTB domain), were PCR-amplified and cloned in frame with the LexA DBD into plasmid pB29 (orientation N-bait-LexA-C). The DBD constructs were checked by sequencing the entire inserts, and then transformed in L40ΔGal4 (mata) yeast cells, as in the case of the yeast two-hybrid screen.

A prey fragment, corresponding to the full *Drosophila* Chromator protein (FlyBase ID FBgn0044324), was extracted from the yeast two-hybrid screening of Psq (aa Met1-Gln720) against Hybrigenics Services *Drosophila* embryo cDNA library. The Chromator sequence was cloned in frame with the Gal4 AD into plasmid pP6. The AD construct was checked by sequencing the insert at its 5' and 3' ends, and then transformed in Y187 (matα) yeast strain. The interaction pairs were tested using a mating approach as previously described (Fromont-Racine *et al.*, 1997). Interaction pairs were tested in duplicate, as two independent clones from each mating reaction were picked for the growth assay.

For each interaction, several dilutions (10^{-1}, 10^{-2}, 10^{-3} and 10^{-4}) of the diploid yeast cell culture normalized at $5x10^4$ cells and expressing both bait (DBD fusion) and prey (AD fusion) constructs were spotted on several selective media (DO-2 and DO-3). Six different concentrations of the inhibitor 3-AT were added to the DO-3 plates to reduce the background generated by baits that activate transcription alone (so-called autoactivating baits). The following 3-AT concentrations were tested: 1, 5, 10 and 50mM.

3. Cell culture and transfections.

Schneider 2 (S2) cells (Invitrogen, ref. #10831-014), were maintained in Express Five serum free cell culture medium (Invitrogen, ref. #10486-025), and supplemented with L-Glutamine (LabClinics, ref. #M11-004) and penicillin/streptomycin stock of antibiotics (Sigma, ref. #P4333-100ML). Kc167 cells (DGRC cat. no. 1) were maintained in Schneider's *Drosophila* Medium (Gibco, ref. #21720-024), supplemented with 10% inactivated fetal bovine serum (Invitrogen, ref. #10108-165) and penicillin/streptomycin stock of antibiotics (Sigma, ref. #P4333-100ML).

S2 and Kc167 generated from spontaneously immortalized cells in cultures of mechanically dissociated embryos, were grown in an incubator at 25ºC without CO_2. For transient transfection experiments, 6 well plates were used in which 8 x 10^5 cells were placed per well in 2 ml of Express Five serum free medium or Schneider's *Drosophila* Medium, depending on the cell line used, supplemented with L-Glutamine and no antibiotics or serum. 1µg of total DNA was added per well. The amount of each plasmid was adjusted to obtain equimolar concentrations. Cells were transfected using Cellfectin II Reagent (Invitrogen, ref. #10362-100). In transfections including plasmids with the metallothionein promoter (pMT), activation of the promoter was induced by adding 1.4 mM $CuSO_4$ to the medium 24 hr after transfection. Cells were lysed 24 hr after $CuSO_4$ addition (48 hr after transfection).

Human prostate cancer cells (PC-3) and human prostate non-transformed epithelial cells (PNT1A: obtained from ATCC) were cultured in RPMI-1640 + Glutamax medium (Gibco) supplemented with 10% FBS incubated at 37ºC in 5% CO_2. They were transfected with Lipofectamine2000 reagent (Invitrogen) following manufacturer instructions into PC-3 cells at a density of 5x10^5 cells per well in 24-well plates with 500ng of total DNA. Cells were incubated 48 hr and then collected for experiments.

dsRNA transfections were performed with Cellfectin II Reagent. (Invitrogen, ref. #10362-100), following the manufacturer's instructions. dsRNA was generated using the Megascript T7 High Yield Transcription Kit (Ambion NC. Ref# 1404051) and the primers used for the RNAi KK recognizing all isoforms of Psq were obtained from *Drosophila* Vienna Stock Centre (For 5'-TAATACGACTCACGCTGCCCTGCTTA-3'; Rev 5'- TAATACGACTCACAAGGCTCACAATG-3').

4. Construction of Sensor Transgenes.

The tub-luc::ihog3'UTR or tub-luc::boi3'UTR constructs were generated by cloning the full length 3' UTR of the *Drosophila ihog* or *boi* genes into the 3´ end of the tub-firefly luciferase plasmid.

To construct the tub-luc::ihogmut3'UTR reporter, 3 nucleotides of the predicted binding-site for miR-7 in the ihog 3´UTR were mutated using the QuickChange Site-Directed Mutagenesis kit (Agilent Technologies Inc.). The tub-eGFP::ihog3'UTR or tubeGFP:: boi3'UTR constructs were generated by cloning the full length 3'UTR of *ihog* or *boi* genes into the 3´ end of the tub-eGFP reporter vector (a gift from Dr Cohen). The final constructs were verified by sequencing. Transgenic eGFP and luciferase sensor flies were generated on a w1118 background by standard transformation into Drosophila embryos (BestGene Inc.).

The *BOC* and *CDON* 3'UTR constructs were generated by cloning the full length 3'UTR of *BOC* and *CDON* into the pRL-TK plasmid after the T7 promoter (Promega). Target sites were mutated using the QuickChange Site-Directed Mutagenesis kit (Stratagene). All primer lists are in the Table S4 in Appendix I.

5. Luciferase Reporter Assays.

Luciferase is a generic term for the class of oxidative enzymes responsible for bioluminescence. The luciferase assays performed for this project were done with the objective to report a direct regulation of a protein over a target gene or sequence. For that we prepare constructs with the DNA region of interest controlling a firefly luciferase or the sea pansy Renilla luciferase coding region under a specific promoter, using one of them as a control (firefly luciferase pRL-TK from Promega as experimental reporter and the Renilla luciferase plasmid pGL3 from Promega as a control). The luciferase or Renilla activity was measured with a commercial kit (*in vitro*) or with a luciferase antibody (*in vivo*) anti-luciferase (luci27) (Mouse 1:200, Thermo Scientific Ref# 12556).

The following reaction happens in *in vitro* assays (Figure 61):

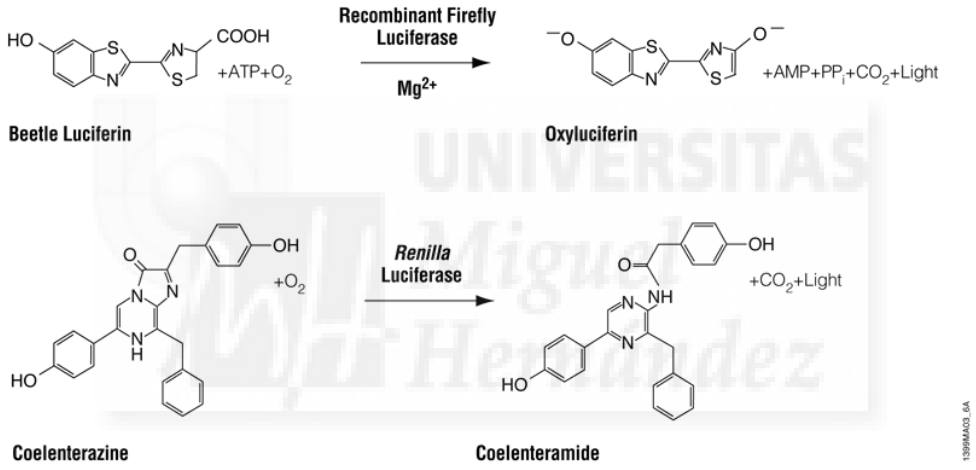

Figure 61. Firefly luciferase is a 61kDa monomeric reporter protein that catalyses the oxidation of beetle luciferin in a reaction that requires ATP, Mg^{2+} and O_2 and produces light. Renilla luciferase is a 36kDa monomeric protein and catalyses a bioluminescent reaction that uses O_2 and coelenterazine.

For *Drosophila* S2 cell luciferase assays, cells were plated in 24-well plates and co-transfected as described previously in materials and method-transfections with the Renilla luciferase plasmid (75 ng) for normalization, and different combinations of the following plasmids: actin-Gal4 (400 ng), pUAS-mir-7 or empty pUAST (400 ng; (Stark *et al.*, 2003), tub-luc::ihog3'UTR, tub-luc::boi3'UTR or tub-luc::ihogmut3'UTR (25 ng). The relative luciferase activity was measured 48 hr after transfection using the Dual-Glo Luciferase Reporter Assay system (Promega) according to the manufacturer's instructions.

In the case of the luciferase experiments with human cells we used two different human prostatic cell lines, immortalized non-malignant prostatic cell line PNT1A (Mitchell et al, 2000) and

metastatic PC-3 cells. Cells were co-transfected in 24-well plates with the pRL-TK-BOC-UTR, pRL-TK-CDON-UTR or pRL-TK-BOC-UTR-mut, pRL-TK-CDON-UTR-mut construct (200 ng) and the pGL3-control plasmid (20 ng; Promega) for normalization, using mirVec with or without the human *mir-7* expression (from Dr. Brabletz laboratory). The relative luciferase activities were determined 48 hr after transfection and in all cases, luciferase activity was measured using Dual-Glo Luciferase Assay system (Promega).

PC-3 cells were transfected as previously described with the plasmids kindly gifted by Dr. Tilman Borggrefe and Dr. Mathias Lauth. Mammalian GLI proteins are known to encode a nuclear protein, containing five zinc finger motifs, which binds to DNA in a sequence-specific manner (Kinzler *et al.*, 1990). The human GLI reporter form (Sasaki *et al.*, 1997) is a construct containing 8 repetitions of this sequence-specific binding sites cloned upstream of a firefly luciferase coding region controlled by a minimal promoter in a pdδ1LucII from (Kamachi et al., 1993) (200ng transfected). The luciferase reporter plasmid RBP-J (Jung *et al.*, 2013; Minoguchi *et al.*, 1997; Oswald *et al.*, 2002) contains a 50-bp oligonucleotide harbouring RBP-J binding sites in a TP1 promoter in pGa981–6 (200ng), and the mutant version was cloned by Francesca Ferrante in the laboratory of Dr. Tilman Borggrefe. Gli3 repressor construct without its activator domain (Gli3Rep)(140ng transfected) was a gift from Dr. Mathias Lauth and a dominant active form of the murine Notch-1 pcDNA3 mN1 deltaE IC+OP (here called NotchDE)(140ng transfected) was obtained from (Oswald *et al.*, 2002); all using 20ng of renilla luciferase control plasmid pRL-CMV (Promega).

The results of the luciferase assays are shown as the mean ± standard error of the mean of three independent experiments that were analysed by a two-tailed unpaired t-test.

6. Co-immunoprecipitation assays.

To detect the interaction between Pipsqueak and Chromator, CP190, Mod2.2 and Su(Hw), Kc167 cells were grown in 10 cm plates with Express Five serum free medium (gibco) supplemented with L-Glutamine and no antibiotics. For each condition, one plate with $5x10^6$ cells in 10 ml medium was used.

In the case of the Psq and Chro Co-IP, the cells were transiently transfected with pMT-3xFlag::Psq::tRFP (María Domínguez) and pMT-Chromator::GFP (Gift Kristen Johansen) according to the protocol described above. Cells were collected from the plate using a cell scrapper and centrifuged for 5 minutes at 1100 r.p.m. in a centrifuge cooled to 4ºC to separate them from the medium. Then, 1500 µl RIPA buffer was added to each sample (20 mM Tris-HCl [pH 7.4], 150 mM NaCl, 1% Triton and 5mM EDTA) supplemented with protease and phosphatase inhibitors (2 mM Pefabloc (Sigma-Aldrich), 1X cOmplete Mini EDTAfree protease inhibitor cocktail (Sigma-Aldrich), 1mM Na_3VO_4 and 1mM NaF).

After addition of the cell lysis buffer, the samples were sonicated using a Biorruptor sonicator (Diagenode). In order to completely break the cells, especially the nuclear membrane, the samples underwent 7 cycles of 30 seconds ON/OFF at maximum power. After sonication, the lysates were incubated in ice for 30 minutes and then cleared adding magnetic beads conjugated with Protein A (rabbit antibodies) or G (mouse antibodies) (Millipore, ref. #16-661). After this, the

samples were incubated overnight at 4ºC in a rotating shaker (slow rotation). The cleared lysates were incubated with 1µg of the primary antibodies a-FLAG (Sigma, ref. #F3165), a-GFP (Abcam, ref#ab290) for 2 hr at 4ºC in a rotating shaker (slow rotation). After the incubation, 30 µl of magnetic beads conjugated with Protein A or G were added to each sample and incubated for 2 hr at 4ºC in a rotating shaker (slow rotation). The samples were then washed three times with native buffer without inhibitors (20 mM Tris-HCl [pH 7.4], 150 mM NaCl, 1% Triton and 5mM EDTA). The samples were finally resuspended in 30 µl of 6X SDS loading buffer (300 mM Tris-HCl [pH 8.8], 12% SDS, 0.6% bromophenol blue and 30% glycerol) with β-mercaptoethanol (1 µl for each 50 µl of 6X SDS buffer) and boiled for 10 minutes at 95ºC. Using a magnet, the magnetic beads were separated from the sample to be analysed by WB as it will be described below.

The Co-IPs between PsqBTB and all the other insulator proteins were done using endogenous protein levels and the following antibodies: 5ug of the rabbit anti-Mod(mdg4)2.2, rabbit anti-CP190 and rabbit anti-Su(Hw) (all three a gift from the laboratory of Dr. Victor Corces), rabbit PsqBTB and rabbit Psq total (both designed in the laboratory of Dr. María Domínguez and synthetized by SDIX company using SDIX Genomic Antibody Technology® and Eurogentec).

7. Western blot.

To prepare the cell lysates, cells were collected from the plate using a cell scrapper and mechanically lysed in RIPA buffer (20 mM Tris-HCl [pH 7.4], 150 mM NaCl, 1% Triton and 5mM EDTA), supplemented with protease and phosphatase inhibitors (2 mM Pefabloc, 1X cOmplete Mini EDTAfree, 1mM Na_3VO_4 and 1mM NaF). The lysates were incubated for 30 minutes at 4ºC. Total cell lysates were stored at -80ºC after the incubation.

Supernatant and pellet were separated and 150µl of RIPA buffer were added to the pellet samples. Protein concentration of the samples was determined using BCA Protein Assay Kit (Pierce, ref. #23227). 25 µg of protein sample were resuspended in 6X SDS loading buffer (300 mM Tris-HCl [pH 8.8], 12% SDS, 0.6% bromophenol blue and 30% glycerol) with β-mercaptoethanol (1 µl for each 50 µl of 6X SDS buffer), and boiled for 10 minutes at 95ºC.

Protein samples were separated in 8% SDS-PAGE gels and transferred to a PVDF membrane (Inmovilon-P Transfer membranes, Millipore, ref. #IPVH00010). Membranes were blocked in PBS with 0.1% Tween-20 and 3% BSA for 1 hr at room temperature. After that, membranes were incubated with the primary antibodies: polyclonal rabbit anti-Psq aa 453-552 (1:2000) and polyclonal rabbit anti-PsqBTB aa 92-106 (1:2000), (both designed in the laboratory of Dr. María Domínguez and synthetized by SDIX company using SDIX Genomic Antibody Technology® and Eurogentec), a-FLAG (Sigma, ref. #F3165, 1:1000), a-actin (Sigma, ref. #A2066, 1:500), a- GFP (Abcam, ref#ab290), mouse a-Chromator (1:1000) (a gift from laboratory of Dr. Kristen Johansen), mouse anti-CyCA (1:2000, DSHB Ref #A12) and rat a-Mod(mdg4)2.2 (1:2000), rabbit a-CP190 (1:2000) and rabbit a-Su(Hw) (1:2000) a gift from the laboratory of Dr. Victor Corces; all diluted in PBS with 0.1% Tween-20 and 3% BSA. After overnight incubation at 4ºC, membranes were incubated during 1 hr at room temperature with secondary antibodies: HRP-conjugated rabbit a-IgG (Sigma, ref. #A9169, 1:10000), HRP-conjugated mouse a-IgG (Jackson, ref. #115-035-062, 1:5000) or HRP-conjugated Rat a-IgG (Jackson

REF# 712-035-153); all diluted in PBS with 0.1% Tween-20 and 3% BSA. Proteins were detected using the chemiluminescent substrate ECL (Pierce, ref. #32209), the detector LAS-100 (Fujifilm) and the Image Reader LAS-1000 software (FujiFilm).

8. Immunohistochemistry and microscopy analysis.

miR7 project: Third instar imaginal discs were fixed and stained by standard procedures using the following primary antibodies (dilutions, sources): a-Eyg (guinea pig 1:100, (Junn *et al.*, 2009), a-Elav (mouse 1:100, DSHB Ref# 9F8A9), a-Wg (mouse 1:100, DSHB Ref# 4D4), a-En (mouse 1:100, DSHB Ref# 4D9), a-phospho-H3 (a-PH3; rabbit 1:500, Sigma Ref# H0412), a-GFP (rabbit 1:1000, Invitrogen Ref# A11122), a-β-galactosidase (mouse 1:2000, Cappel), a-Cut (rat 1:5000, DSHB Ref# 2B10), a-DE-cad (rat 1:50, DSHB), a-Dac (mouse 1:100, DSHB Ref# mAbdac2-3), a-Ci (rat 1:5; a gift from Dr. Holgrem), a-luciferase (luci27) (mouse 1:200, Thermo Scientific Ref# 12556) and a-DsRed (rabbit 1:2000, Clontech Ref# 632496). The secondary antibodies used were conjugated to AlexaFluor-488, -555, -647 (Molecular Probes), and diluted at 1:400. Discs were mounted in Fluoromount G (Southern Biotechnology) and the images were captured on a Leica TCS-NT Confocal microscope.

Pipsqueak project: Third instar imaginal discs, ovaries and guts, were fixed and stained by standard procedures using the following primary antibodies (dilutions, sources): a-Psq total (Rabbit 1:200, Dr. María Dominguez), a-PsqBTB (Rabbit 1:200, Dr. María Dominguez), 6H11 (Mouse 6H11 a-Chromator 1:200, Dr. Kristen Johansen), a-tubulin (Rabbit 1:200, Abcam Ref# ab15246), a-CID (Chicken the *Drosophila* homologue of the CENP-A centromere-specific H3-like proteins 1:200, Abcam Ref# ab10887), a-phospho-H3 (Rabbit 1:500, Sigma Ref# H0412), a-Mod(mdg4)2.2 (Rabbit 1:200, Dr. Victor Corces).

For polytene chromosomes immunostaining 3rd instar larvae were dissected in 0,7% NaCl and salivary glands were placed immediately in fixative solution (3,7% formaldehyde + 45% acetic acid in PBT). After 2min they were transferred to a drop of 45% acetic acid diluted in water on Poly-L-Lysine coated slide with a coverslip on top. A hammer was used to “squash” the chromosomes. After checking their integrity under a phase microscope, slides were frozen in liquid nitrogen and the coverslip was removed with a razor blade. The subsequent immunofluorescence was done using standard procedures. The primary antibodies used were (rabbit anti-Psq total 1:200, and mouse 6H11 a-Chromator 1:200, Dr. Kristen Johansen).

To perform immunohistochemistry of cells in culture, we placed over night a million of cells over a small coverslip inside a 24-plate well with complete medium. Afterwards, cells were washed twice with PBS and fixed with new prepared 4% PFA, during 20 minutes at room temperature. After washing twice with PBS we blocked cells for 1 hr with PBT+3%of PSA, and treated with primary antibodies for 1 hr. After washing twice with PBS, secondary antibodies were added (1hr) and the coverslip was then flipped and placed over a slip and sealed with nail varnish.

Adult wings were dissected and mounted in a drop of glycerol over a slip after rinse them first in ethanol 100% and then in glycerol+ethanol 70%.

9. Image capture and processing

Drosophila images (eyes and wings) were captured with light microscope ZEISS Axiophot using the software *CoolSnap*. Images 3D coupling was performed using *Automontage Essentials* software. Image analysis (area calculation, density profiles and cell countering) was performed using ImageJ software (Rasband, W.S., ImageJ, U. S. National Institutes of Health, Bethesda, Maryland, USA, http://rsb.info.nih.gov/ij/, 1997-2005).

10. RNA extraction, retrotranscription, and quantitative PCR

Total RNA from S2, Kc167, PC3 and PNT1A cells or larval tissue disrupted by TissueLyser LT - QIAGEN (all tissue samples were stored in RNAlaterTissueProtect Tubes (Qiagen) until used), was isolated using the RNeasy Mini Kit (Quiagen, ref.# 74106) according to the manufacturer's protocol. RNA samples were treated with DNase (TURBO DNA-free Kit, Applied Biosystems, ref.# AM1907) to eliminate the remaining DNA from the samples, as indicated in the manufacturer's protocol. 1 µg of RNA was reverse-transcribed using SuperScript III Reverse Transcriptase (Invitrogen, ref.# 18080-093) and Oligo(dT) Primers (Invitrogen, ref# 18418-020). Quantitative PCRs were performed using Power SYBR Green PCR Master Mix (Applied Biosystems, ref# 4367659), 10 ng of template cDNA, and gene-specific primers (222 nM) (Table S4 Appendix), under the following conditions: 10 minutes at 95°C, and then 40 cycles of 15 seconds at 95°C and 40 seconds at 60°C. Real-time PCR reactions were performed using a 7500 Real-Time PCR system (Applied Biosystems), according to the manufacturer's recommendations. The results were normalized to endogenous Rp49 (*Drosophila*) or GAPDH (human) expression levels. Three separate samples were collected from each condition and triplicate measurements were conducted. Primers were designed using the Primer Quest online tool (http://eu.idtdna.com/PrimerQuest/Home/Index). Data are presented as mean ± standard error of the mean; statistical analyses were performed using two tailed Student's t-test.

To assess the levels of mature microRNA, specific primer sets were obtained from Applied Biosystems. Products were amplified from 10 ng of total RNA (extracted from cultured cells using miRNeasy-Mini Kit, Quiagen) with the "TaqMan MicroRNA Assay". cDNA was synthesized using an oligo-dT primer and SuperScript RTIII (Invitrogen). Mature microRNA levels were normalized to U14 snRNA.

11. ChIP-seq

Chromatin immunoprecipitation was performed using the protocol follow in the laboratory of Dr. Victor Corces:

$80x10^6$cells/ChIP were collected in 12ml of cultured media. 333µl of 37% the PFA stock was added and incubated on rotator for 10 min at room temperature. Cells were quenched for 5min by adding 1,2ml of 1,25M glycine to final concentration of 0,125M. After spinning down the cells 3-4min at 4ºC 2000rpm cells were resuspended in 2ml cell lysis buffer plus protease inhibitors (PIPES

pH8 5mM, NaCl 85mM, Nonidet P40 0,5%, 1mM PMSF and 1x cOmplete Mini EDTAfree) and incubated for 15min. After collecting them 4000rpm 8min 4ºC they were resuspended in 1,5ml of **lysis buffer 3** (EDTA 1mM, EGTA 0,5mM, Tris-HCl;pH8 10mM, NaCl 100mM, Na-Deoxycholate 0,1%, N-lauroyl sarcosine 0,5%,1mM PMSF and 1x cOmplete Mini EDTAfree) plus protease inhibitors and incubated for 20 min. Crosslinked cells were sonicated in the Biorruptor Diagenode with temperature controller at 4ºC, 30sec on/30 sec off 25 cycles, maximum power. Tryton was added to a final concentration of 1%. To pellet cellular debris we centrifuged at maximum speed in mircocentrifuge for 10 min at 4ºC. After washing the Protein A or G Dynabeads with lysis buffer 3 30µl of beads were added for preclearing 1-2 hr at 4ºC. After that, beads were removed from the medium. 50µl of the supernatant were taken to test the quality of the sonication (QC) and 5µl of the primary antibody (rabbit a-Psq total and rabbit a-PsqBTB from laboratory of Dr. María Dominguez and mouse a-EcR hybridoma bank Ref# DDA2.7) were added to the total supernatant and incubated over night at 4ºC. Then, 30µl of Protein A or G beads were added and incubated during 3 hr at 4ºC. After that beads were washed:

- 3 times with 1ml Low Salt Wash Buffer (SDS 0,1%, Trition X-100 1%, EDTA.Na_2 pH8 2mM, TrisHCl pH8 20mM and NaCl 150mM) 5 min each on rotation at room temperature.
- 2 times with 1ml High Salt Wash Buffer (SDS 0,1%, Trition X-100 1%, EDTA.Na2 pH8 2mM, TrisHCl pH8 20mM and NaCl 500mM) as above.
- 2 times with 1ml of LiCl buffer (TrisHCl pH8 10mM, EDTANa_2 pH8 1mM, LiCl 0,25M, NP40 1% and sodium deoxycholate SDC or deoxycholic acid DOC 1%) as above.
- 1 time with 1ml of TE buffer (TrisHCl pH8 10mM and EDTA Na_2 pH8 1mM) as above.

Elution was performed two time with 200µl freshly prepared IP elution Buffer (0,1M $NaHCO_3$ and 1%SDS) 5 min at 50ºC.To revert the crosslink we added 20ul of NaCl 5M, 8µl of EDTA 0,5M, 16µl of TrispH8 1M and incubated overnight at 65ºC (444µl final volume). For QC we added IP dilution buffer (SDS 0,01%, Trition X-100 1.1%, EDTA.Na_2 pH8 1.2mM, TrisHCl pH8 16.7mM and NaCl 167mM) to the 50µl taken before to a final volume of 200µl final volume and also revert the crosslink as above, with half volume of each reactant.

After incubating for 2hr at 50ºC with 8µl of Proteinase K we extracted one time with phenol:chloroform:isoamyl (25:24:1) equal volume and after a top spin centrifugation for 5 min and we added to the top aqueous layer 2µl of 20mg/ml glycogen, 1/10 volume of Sodium Acetate 3M, 2,5 volumes of iced cold ethanol 100% and incubated the samples at -80ºC for 1 hr to overnight. After a spin at 15000rpm in 4ºC we washed once with cold 70% ethanol to remove salts and we let air dry the pellet and finally dissolve it in 25,5µl of Elution Buffer (Tris pH 8,5 10mM).

To generate sequencing libraries, ChIP DNA was prepared for adaptor ligation by end repair (End-It DNA End Repair Kit, Epicenter Cat# ER0720) and addition of ‘‘A’’ base to 39 ends (Klenow 39–59 exo–, NEB Cat# M0212S). Illumina adaptors (Illumina Cat# PE-102-1001) were titrated according to prepared DNA ChIP sample concentration and ligated with T4 ligase (NEB Cat# M0202S). Ligated ChIP samples were PCR-amplified using Illumina primers and Phusion DNA polymerase (NEB Cat# F-530L) and size selected for 200–300 bp by gel extraction. ChIP libraries were sequenced at the HudsonAlpha Institute for Biotechnology, using an Illumina HiSeq 2000.

12. ChIP-seq and bioinformatics analyses

Two biological replicates were used for ChIP-seq experiments, and only peaks found in both replicates were considered for further analyses. Sequences were mapped to the dm_r6.01 genome with Bowtie 0.12.3 (Langmead, 2010) using default settings. Peaks were then called with MACS 1.4.0 alpha2 using equal numbers of unique reads for input and ChIP samples and a P-value cut-off of 1 x 10^{-5} with an equivalent number of reads from sonicated input sequences. ChIP-seq data sets for H3K4me3, H3K4me1 (GSE36374), H3K27me3 (GSE37444) and insulator proteins dCTCF, BEAF-32, Su(Hw) have been described previously (Kellner *et al.*, 2012; Van Bortle *et al.*, 2012; Wood *et al.*, 2011) and all the additional data sets were provided by the laboratory of Dr. Victor Corces . Negative values for ChIP data were set to zero (white colour) due to the fact that only positive values are obtained for ChIP-seq data. ±2 kb from each peak summit was K-means clustered using Cluster 3.0 (de Hoon *et al.*, 2004) and visualized by Java Treeview (Saldanha, 2004). Primary motifs of Psq were identified by MEME-ChIP using default settings (Machanick *et al.*, 2011).

To calculate the pausing index of genes associated with different proteins, we use the peak data from ChIP-seqs of the different proteins, to intersect them (using the Genomic Hyperbrowser) with a list of TSSs. Afterwards, using the R software, we merge this protein-TSSs with a gene file containing the data of all genes (chromosome, start, end, length and gene ID). This merged file is then used to calculate the Pausing index of each gene containing the specific protein. The Pausing index was calculated using ChIP-seq datasets of Pol II in Kc167 cells obtained from modENCODE. Pol II levels at TSS was considered as the mean enrichment of Pol II in the ±200 bp region around each TSS containing the desired protein. Pol II levels at gene bodies was considered as the mean enrichment of Pol II from +200 bp to the end of the corresponding gene.

13. Eye imaginal disc microarray analysis.

Raw data processed with the gcRMA method and differentially expressed genes were detected by SAM (Significance Analysis of Microarrays) with a 0.1378 FDR, and using the Benjamini and Hochberg correction for multiple hypothesis testing. 196 probesets were found to be differentially expressed (46 up and 150 down-regulated). We curated the 46 upregulated probesets, which included probesets against repetitive elements (transposons), non-coding RNA, or multiple isoforms of the same gene, and ended up with 47 transcripts from which coding sequences were obtained in FlyBase (www.flybase.org), batch-translated with EMBOSS Transeq (http://www.ebi.ac.uk/Tools/emboss/transeq/index.html), and submitted to signal peptide analyses using a Neural networks model available in SignalP 3.0 (22). SignalP 3.0 predicted a signal peptide in 21/47 proteins encoded by the upregulated genes, 19 of which were encoded at unique loci (i.e., the Spn4 locus encoded three Spn4 isoforms with predicted signal peptides: isoforms Spn4–PD, -PE, and -PF). List in Table S5 in supplementary materials shows these positive hits ordered by average fold-change (R fold) between tumour and control eye disc samples.

APPENDIX I

Table S1. Identification of candidate tumour-suppressor gene(s) of *Drosophila melanogaster In Silico* predicted miR-7 target genes in the gain of Delta context.

Gene[a]	RNAi Collection[b]	Stock Number	FlyBase ID	FlyBase Genotype	Phenotype [c] ey-Gal4>Dl>dcr2	Incidence (n>50)[d]
5-HT1β	VDRC	46485	FBst0466727	w^{1118}; P(GD17040) v46485/TM3	N.C.	
5-HT1β	BL	25833	FBst0025833	y^1 v^1; P(y[+t7.7]v[+t1.8]=TRiP.JF01851)attP2	N.C.	
aop	BL	34909	FBst0034909	y^1 sc* v^1; P(TRiP.HMS01256)attP2	Early lethal	100%
aop	BL	26759	FBst0026759	y^1 v^1; P(y[+t7.7v[+t1.8]=TRiP.JF02323)attP2/TM3	N.C.	
ato	BL	26316	FBst0026316	y^1 v^1;; P(TRiP.JF02089)attP2	Hypo	100%
BobA	VDRC	29796	FBst0458154	w^{1118}; P(GD15234)v29796	N.C.	
bowl	BL	27074	FBst0027074	y^1 v^1; P(TRiP.JF02419)attP2	Hyper	10%
bowl	VDRC	v102050	FBst0473922	P(KK110520)VIE-260B	T	70%
Cad87A	BL	28716	FBst0028716	y^1 v^1; P(TRiP.JF03143)attP2	N.C.	
Cad87A	VDRC	105901	FBst0477727	P(KK104234)VIE-260B	N.C.	
Cad87A	VDRC	8578	FBst0471146	w^{1118}; P(GD3637)v8578	Hyper	40%
CG10444	VDRC	4722	FBst0467144	w^{1118}; P(GD2104)v4722	N.C.	
CG10444	VDRC	107008	FBst0478831	P(KK101545)VIE-260B	N.C.	
CG11319	VDRC	7621	FBst0470766	w^{1118}; P(GD954)v7621	N.C.	
CG12488	VDRC	105028	FBst0476856	P(KK113020)VIE-260B	N.C.	
CG13908	BL	28645	FBst0028645	y^1 v^1; P(TRiP.JF03060)attP2	N.C.	
CG13908	VDRC	47179	FBst0467118	w^{1118}; P(GD16461)v47179	N.C.	
CG18549	VDRC	107272	FBst0479094	P(KK102196)VIE-260B	N.C.	
CG31472	VDRC	105941	FBst0477767	P(KK107976)VIE-260B	N.C.	
CG32103	VDRC	108078	FBst0479890	P(KK100089)VIE-260B	N.C.	
CG7272	VDRC	8375	FBst0471046	w^{1118}; P(GD2471)v8375	N.C.	
CG9368	BL	28292	FBst0028292	y^1 v^1; P(TRiP.JF02922)attP2	N.C.	
CG9368	VDRC	29786	FBst0458148	w^{1118}; P(GD15225)v29786/CyO	Hyper	60%
cpa	VDRC	100773	FBst0472646	P(KK108554)VIE-260B	Hypo	100%
da	BL	29326	FBst0029326	y^1 v^1; P(TRiP.JF02488)attP2	Hypo	100%
da	VDRC	105258	FBst0477086	P(KK104800)VIE-260B	Hypo	100%
dachs	BL	27664	FBst0027664	y^1 v^1; P(TRiP.JF02743)attP2	N.C.	
dachs	VDRC	102550	FBst0474419	P(KK111964)VIE-260B	N.C.	
da	BL	26319	FBst0026319	y^1 v^1; P(TRiP.JF02092)attP2	Hypo	100%
gho	VDRC	106929	FBst0478752	P(KK102658)VIE-260B	Pupal lethal	100%
h	BL	27738	FBtp0052562	y^1 v^1; P(TRiP.JF02822)attP2	T	100%
HLHm3	BL	25977	FBst0025977	y^1 v^1; P(TRiP.JF01999)attP2	N.C.	
HLHm4	BL	29378	FBst0029378	y^1 v^1; P(TRiP.JF03310)attP2	N.C.	
HLHm5	BL	26201	FBst0026201	y^1 v^1; P(TRiP.JF02099)attP2	N.C.	
HLHm5	VDRC	47124	FBst0467079	w^{1118}; P(GD16281)v47124	N.C.	
HLHm5	VDRC	101948	FBst0473820	P(KK110311)VIE-260B	N.C.	
HLHmγ	BL	25978	FBst0025978	y^1 v^1; P(TRiP.JF02000)attP2	N.C.	
HLHmδ	VDRC	v13077	FBst0450833	w^{1118}; P(GD4458)v13077	Hypo	100%
HLHmδ	VDRC	v100056	FBst0471930	P(KK103234)VIE-260B	T	30%
ihog	VDRC	v29897	FBst0458215	w^{1118}; P(GD14317)v29897	T	80%
ihog	VDRC	v102602	FBst0474471	P(KK112149)VIE-260B	T	100%
jbug	VDRC	102221	FBst0474090	P(KK111138)VIE-260B	N.C.	
jbug	VDRC	28471	FBst0457492	w^{1118}; P(GD13033)v28471	N.C.	
Lama	VDRC	31312	FBst0031312	y^1 v^1; P(TRiP.JF01259)attP2	Hyper	100%
mbc	VDRC	16044	FBst0452122	w^{1118}; P(GD6965)v16044	N.C.	
Rac1	BL	28985	FBst0028985	y^1 v^1; P(TRiP.JF02813)attP2 e*	N.C.	
Ssadh	VDRC	106637	FBst0472903	P(KK106637)VIE-260B	N.C.	
Sucb	VDRC	101554	FBst0473427	P(KK109063)VIE-260B	N.C.	
Teh1	VDRC	46364	FBst0466655	w^{1118}; P(GD2891)v46364	N.C.	

Teh1	*VDRC*	*102816*	*FBst0474681*	*P(KK103880)VIE-260B*	*N.C.*	
Tom	*VDRC*	*v101652*	*FBst0473525*	*P(KK105340)VIE-260B*	*N.C.*	
Tom	*VDRC*	*v36614*	*FBst0461768*	*w^{1118}; P(GD14880)v36614*	*T*	*40%*

[a] *Genes sorted by alphabetic order. Notice that some RNAi lines targeting the same gene showed different phenotype.*

[b] *VDRC: Vienna* Drosophila *RNAi Centre (http://stockcenter.vdrc.at/control/main), BL: Bloomington* Drosophila *Stock Centre (http://fly.bio.indiana.edu/)*

[c] *T: Tumour; Hyper: Hyperplasia; Hypo: Hypoplasia, NC: No Change. Phenotype obtained from the cross between males from the different RNAi lines and females ey>Dl>dcr2.*

[d] *n = total number of eyes counted.*

The list above contains genes that are predicted to be target for D. melanogaster *miR-7 by the following databases: CBIO (http://cbio.mskcc.org/mirnaviewer/), TargetScan (http://www.targetscan.org/fly_11/), PicTar (http:// http://pictar.mdc-berlin.de/cgi-bin/PicTar_fly.cgi?species=fly/) and MirBase (http://microrna.sanger.ac.uk/sequences/).*

Table S2. Direct Inhibition by RNAi Expression of Core Hedgehog Pathway Genes in the Gain of Delta Context

Gene[a]	*RNAi Collection*[b]	*Stock Number*	*FlyBase ID*	*FlyBase Genotype*	*Phenotype*[c] *ey-Gal4>Dl>dcr2*	*Incidence (n>200)*[d]
boi	*VDRC*	*108265*	*FBst0480077*	*P(KK103113)VIE-260B*	*N.C.*	
ci	*VDRC*	*51479*	*FBst0020742*	*w^{1118}; P(GD1403)v51479*	*Hyper*	*100%*
ci	*VDRC*	*105620*	*FBst0026821*	*P(KK100760)VIE-260B*	*T*	*100%*
ci	*BL*	*28984*	*FBst0032272*	*y^1 v^1; P(TRiP.JF01715)attP2*	*Met*	*10%*
hh	*BL*	*25794*	*FBst0025794*	*y^1 v^1; P(TRiP.JF01804)attP2*	*T*	*100%*
hh	*VDRC*	*1402*	*FBst0451269*	*w^{1118}; P(GD193)v1402*	*T*	*30%*
smo	*BL*	*27037*	*FBst0027037*	*y^1 v^1; P(TRiP.JF02363)attP2*	*T*	*78%*
smo	*VDRC*	*9542*	*FBst0471542*	*w^{1118}; P(GD577)v9542*	*T*	*80%*
pka-C1	*VDRC*	*101524*	*FBst0473397*	*P(KK108966)VIE-260B*	*Hypoplasia*	*100%*

[a] *Canonical positive (boi, ci, hh, smo) and negative (pka-C1) Hh pathway genes sorted by alphabetic order. Note that generally the KK lines provoke stronger phenotypes than GD lines.*

[b] *VDRC: Vienna* Drosophila *RNAi Centre (http://stockcenter.vdrc.at/control/main), BL: Bloomington* Drosophila *Stock Centre (http://fly.bio.indiana.edu/)*

[c] *Met: Metastasis; T: Tumour; Hyper: Hyperplasia; NC: No Change. Phenotype obtained from the cross between males from the different RNAi lines and females ey>Dl>dcr2.*

[d] *n = total number of eyes counted.*

Table S3. List of positive clones obtained in the yeast two-hybrid.

The full list of the 154 positive clones identified in the Y2H is presented in the following tables, as well as a table with a description of the Predicted Biological Score (PBS) categories used to assess the interaction reliability of the interactions detected. Clones identifying the same gene are clustered together.

Global PBS (for Interactions represented in the Screen)		Nb	%
A	Very high confidence in the interaction	5	23.8%
B	High confidence in the interaction	3	14.3%
C	Good confidence in the interaction	1	4.8%
D	Moderate confidence in the interaction This category is the most difficult to interpret because it mixes two classes of interactions : - False-positive interactions - Interactions hardly detectable by the Y2H technique (low representation of the mRNA in the library, prey folding, prey toxicity in yeast)	11	52.4%
E	Interactions involving highly connected prey domains, warning of non-specific interaction. The threshold for high connectivity is 10 for screens with Human, Mouse, Drosophila and Arabidopsis and 6 for all other organisms. They can be classified in different categories: - Prey proteins that are known to be highly connected due to their biological function - Proteins with a prey interacting domain that contains a known protein interaction motif or a biochemically promiscuous motif	1	4.8%
F	Experimentally proven technical artifacts	0	0.0%
Non Appliable			
N/A	The PBS is a score that is automatically computed through algorithms and cannot be attributed for the following reasons : - All the fragments of the same reference CDS are antisens - The 5p sequence is missing - All the fragments of the same reference CDS are either all OOF1 or all OOF2 - All the fragments of the same reference CDS lie in the 5' or 3' UTR		

Clone Name	Type Seq	Gene Name (Best Match)	Start..Stop (nt)	Frame	Sens	%Id 5p	%Id 3p	PBS
pB29_A-18	5p/3p	Drosophila melanogaster - Arc70	366..2837	IF		99.0	95.0	B
pB29_A-115	5p	Drosophila melanogaster - Arc70	366	IF		93.6		B
pB29_A-11	5p	Drosophila melanogaster - Arc70	387	IF		96.8		B
pB29_A-82	5p/3p	Drosophila melanogaster - CG10042-PA [Drosophilamelanogaster]	2236..1668	??	N	87.5	89.9	N/A
pB29_A-113	5p/3p	Drosophila melanogaster - CG17090	2256..3068	IF		97.2	91.2	D
pB29_A-61	5p	Drosophila melanogaster - CG2926-PA [Drosophilamelanogaster]	4944..5451	IF		86.9		C
pB29_A-91	5p/3p	Drosophila melanogaster - CG2926-PA [Drosophilamelanogaster]	5103..6121	IF		91.7	79.7	C
pB29_A-87	5p	Drosophila melanogaster - CG7185	2141	??	N	84.6		N/A
pB29_A-121	5p	Drosophila melanogaster - CG7222-PA	764	??	N	68.9		N/A
pB29_A-106	5p	Drosophila melanogaster - Chro	1485	IF		84.4		D
pB29_A-130	5p/3p	Drosophila melanogaster - EDTP	507..-275	??	N	99.4	98.7	N/A
pB29_A-28	5p/3p	Drosophila melanogaster - Eb1	898..405	??	N	94.8	89.6	N/A
pB29_A-15	5p/3p	Drosophila melanogaster - Eno	136..1183	OOF1		93.4	86.0	N/A
pB29_A-152	5p	Drosophila melanogaster - Fer1HCH	-79	IF		85.2		D
pB29_A-2	3p	Drosophila melanogaster - MICAL	..5826	??			98.7	A
pB29_A-19	5p/3p	Drosophila melanogaster - MICAL	4326..5061	IF		96.0	89.8	A
pB29_A-85	5p	Drosophila melanogaster - MICAL	4341	IF		89.8		A
pB29_A-37	5p/3p	Drosophila melanogaster - MICAL	4341..5503	IF		99.3	93.2	A
pB29_A-124	5p/3p	Drosophila melanogaster - MICAL	4341..5503	IF		96.0	94.6	A
pB29_A-105	5p	Drosophila melanogaster - MICAL	4365	IF		94.3		A
pB29_A-146	5p	Drosophila melanogaster - MICAL	4797	IF		96.8		A
pB29_A-78	5p/3p	Drosophila melanogaster - MICAL	4797..5529	IF		87.8	93.9	A
pB29_A-58	5p/3p	Drosophila melanogaster - MICAL	4797..5529	IF		91.3	91.5	A
pB29_A-89	5p	Drosophila melanogaster - MICAL	4797	IF		86.2		A
pB29_A-142	3p	Drosophila melanogaster - PR2	..3987	??			95.0	N/A
pB29_A-24	5p/3p	Drosophila melanogaster - Rbp2	1898..1548	??	N	86.3	88.2	N/A

Clone Name	Type Seq	Gene Name (Best Match)	Start..Stop (nt)	Frame	Sens	%Id 5p	%Id 3p	PBS
pB29_A-186	5p	Drosophila melanogaster - RpS3A	755	??	N	77.9		N/A
pB29_A-86	5p	Drosophila melanogaster - Su(var)2-10	1086	IF		89.7		B
pB29_A-75	5p/3p	Drosophila melanogaster - Su(var)2-10	1086..1805	IF		87.4	77.0	B
pB29_A-170	5p	Drosophila melanogaster - Su(var)2-10	1086	IF		98.3		B
pB29_A-109	5p	Drosophila melanogaster - Su(var)2-10	1224	IF		96.5		B
pB29_A-41	5p/3p	Drosophila melanogaster - Taf8	-41..836	OOF2		97.2	84.5	N/A
pB29_A-21	5p/3p	Drosophila melanogaster - Xbp1	484..1034 ✕	OOF1		89.1	93.6	N/A
pB29_A-161	5p	Drosophila melanogaster - abs	738	IF		96.4		B
pB29_A-126	5p/3p	Drosophila melanogaster - abs	738..1874 ✕	IF		90.2	79.9	B
pB29_A-165	5p/3p	Drosophila melanogaster - abs	738..1874 ✕	IF		93.5	94.0	B
pB29_A-20	5p/3p	Drosophila melanogaster - abs	739..1874 ✕	OOF1		92.7	100.0	B
pB29_A-25	5p/3p	Drosophila melanogaster - bip2	957..3046	IF		87.4	98.0	A
pB29_A-168	5p	Drosophila melanogaster - bip2	1515	IF		99.7		A
pB29_A-73	5p	Drosophila melanogaster - bip2	1515	IF		99.7		A
pB29_A-127	5p/3p	Drosophila melanogaster - bip2	1782..3053	IF		90.9	89.3	A
pB29_A-163	5p	Drosophila melanogaster - bip2	1818	IF		77.7		A
pB29_A-62	5p/3p	Drosophila melanogaster - bip2	1920..3198	IF		98.3	86.7	A
pB29_A-98	5p/3p	Drosophila melanogaster - bip2	1920..3198	IF		91.8	75.5	A
pB29_A-80	5p	Drosophila melanogaster - bip2	1920	IF		96.6		A
pB29_A-131	5p	Drosophila melanogaster - bip2	1920	IF		96.5		A
pB29_A-38	5p/3p	Drosophila melanogaster - bip2	1923..2634	IF		93.0	86.1	A
pB29_A-185	5p	Drosophila melanogaster - bip2	1941	IF		87.4		A
pB29_A-77	5p/3p	Drosophila melanogaster - bip2	1941..3192	IF		93.1	82.8	A
pB29_A-64	5p	Drosophila melanogaster - bip2	2262	IF		90.3		A
pB29_A-30	5p/3p	Drosophila melanogaster - bip2	2262..3945	IF		97.2	86.5	A
pB29_A-39	5p/3p	Drosophila melanogaster - bip2	2421..4209	IF		98.6	76.8	A
pB29_A-40	5p/3p	Drosophila melanogaster - bip2	2424..3252	IF		87.4	77.7	A
pB29_A-53	5p/3p	Drosophila melanogaster - bip2	2424..3252	IF		91.2	85.2	A
pB29_A-16	5p/3p	Drosophila melanogaster - bip2	2424..3252	IF		83.2	84.7	A
pB29_A-35	5p/3p	Drosophila melanogaster - bip2	2424..3252	IF		95.9	91.6	A
pB29_A-84	5p	Drosophila melanogaster - bip2	2448	IF		99.5		A
pB29_A-60	5p	Drosophila melanogaster - bip2	2520	IF		95.4		A
pB29_A-76	5p	Drosophila melanogaster - bip2	2520	IF		81.6		A
pB29_A-166	5p/3p	Drosophila melanogaster - bol	636..-136	??	N	89.1	82.3	N/A
pB29_A-34	5p/3p	Drosophila melanogaster - crm	267..683	IF		97.6	97.2	D
pB29_A-160	5p	Drosophila melanogaster - dCG6923-PA [Drosophilamelanogaster]	735	IF		90.5		D
pB29_A-176	5p	Drosophila melanogaster - ed	3172	??	N	86.0		N/A
pB29_A-79	5p	Drosophila melanogaster - hdc	2301	??	N	71.9		N/A
pB29_A-104	5p/3p	Drosophila melanogaster - lolal	-95..561 ✻ ✕	OOF2		89.9	82.6	N/A
pB29_A-42	5p/3p	Drosophila melanogaster - lolal	-95..486 ✻ ✕	OOF2		90.5	79.4	N/A
pB29_A-172	5p/3p	Drosophila melanogaster - lolal	-80..506 ✻ ✕	OOF2		97.3	90.6	N/A
pB29_A-66	5p/3p	Drosophila melanogaster - lolal	-77..865 ✻ ✕	OOF2		96.5	72.5	N/A
pB29_A-139	5p	Drosophila melanogaster - lolal	-71..571 ✻ ✕	OOF2		91.9		N/A
pB29_A-81	5p/3p	Drosophila melanogaster - lolal	-71..573 ✻ ✕	OOF2		90.4	88.9	N/A
pB29_A-156	5p	Drosophila melanogaster - lolal	-71	OOF2		95.5		N/A
pB29_A-43	5p/3p	Drosophila melanogaster - lolal	-71..573 ✻ ✕	OOF2		95.4	85.1	N/A
pB29_A-112	5p/3p	Drosophila melanogaster - lolal	-71..1016 ✻ ✕	OOF2		98.0	99.6	N/A

Clone Name	Type Seq	Gene Name (Best Match)	Start..Stop (nt)	Frame	Sens	%Id 5p	%Id 3p	PBS
pB29_A-4	5p/3p	Drosophila melanogaster - lolal	-65	OOF2		90.3	74.3	N/A
pB29_A-96	5p	Drosophila melanogaster - lolal	-56	OOF2		89.8		N/A
pB29_A-188	5p/3p	Drosophila melanogaster - mam	1989..1061	??	N	94.4	96.9	N/A
pB29_A-46	5p/3p	Drosophila melanogaster - ovo	2331..1603	??	N	83.1	80.0	N/A
pB29_A-8	5p	Drosophila melanogaster - psq	-23	OOF2		96.1		A
pB29_A-90	5p	Drosophila melanogaster - psq	-15	OOF1		82.5		A
pB29_A-6	5p/3p	Drosophila melanogaster - rdx	-21..373	OOF1		92.2	96.5	N/A
pB29_A-33	5p/3p	Drosophila melanogaster - ry	3461..3071	??	N	96.9	80.9	N/A
pB29_A-181	5p	Drosophila melanogaster - sca	2431	??	N	79.7		N/A
pB29_A-29	3p	Drosophila melanogaster - sta	..252	??	N		91.7	N/A
pB29_A-175	5p	Drosophila melanogaster - tou	1854	IF		94.0		E
pB29_A-71	5p/3p	Drosophila melanogaster - tou	1857..2961	IF		85.8	98.3	E
pB29_A-17	5p/3p	Drosophila melanogaster - tou	1857..2961	IF		95.3	95.5	E
pB29_A-97	5p/3p	Drosophila melanogaster - tou	2052..3135	IF		93.6	88.9	E
pB29_A-114	5p	Drosophila melanogaster - tou	2052	IF		95.5		E
pB29_A-65	5p	Drosophila melanogaster - tou	2130	IF		91.9		E
pB29_A-70	5p	Drosophila melanogaster - tou	2136	IF		80.4		E
pB29_A-14	5p	Drosophila melanogaster - tou	2136	IF		80.6		E
pB29_A-184	5p	Drosophila melanogaster - tou	2136	IF		77.8		E
pB29_A-119	5p/3p	Drosophila melanogaster - tou	2136..2699	IF		99.1	78.7	E
pB29_A-110	5p	Drosophila melanogaster - tou	2136..2701	IF		96.4		E
pB29_A-47	5p/3p	Drosophila melanogaster - tou	2136..2699	IF		93.2	90.8	E
pB29_A-88	5p	Drosophila melanogaster - tou	2136	IF		80.9		E
pB29_A-144	5p	Drosophila melanogaster - tou	2136	IF		99.2		E
pB29_A-49	5p	Drosophila melanogaster - tou	2136	IF		99.2		E
pB29_A-55	5p/3p	Drosophila melanogaster - tou	2157..3132	IF		85.3	95.3	E
pB29_A-99	5p/3p	Drosophila melanogaster - tou	2157..3132	IF		84.1	87.6	E
pB29_A-32	5p	Drosophila melanogaster - tou	2157	IF		90.6		E
pB29_A-48	5p	Drosophila melanogaster - tou	2157	IF		99.8		E
pB29_A-103	5p	Drosophila melanogaster - tou	2157	IF		100.0		E
pB29_A-182	5p/3p	Drosophila melanogaster - tou	2184..2985	IF		88.8	83.7	E
pB29_A-167	5p	Drosophila melanogaster - tou	2184	IF		87.4		E
pB29_A-155	5p	Drosophila melanogaster - tou	2205..2722	IF		94.8		E
pB29_A-143	5p	Drosophila melanogaster - tou	2205	IF		93.1		E
pB29_A-83	5p/3p	Drosophila melanogaster - tou	2205..2720	IF		96.1	99.8	E
pB29_A-187	5p/3p	Drosophila melanogaster - tou	2205..2720	IF		94.6	85.7	E
pB29_A-27	5p/3p	Drosophila melanogaster - tou	2205..2720	IF		92.6	95.7	E
pB29_A-164	5p	Drosophila melanogaster - tou	2205	IF		84.2		E
pB29_A-74	5p	Drosophila melanogaster - tou	2205	IF		90.8		E
pB29_A-56	5p	Drosophila melanogaster - tou	2205	IF		88.3		E
pB29_A-94	5p/3p	Drosophila melanogaster - CG1472	1677..2250	IF		88.6	94.2	D
pB29_A-177	5p/3p	Drosophila melanogaster - CG14438	7048..5754	??	N	96.8	97.7	N/A
pB29_A-95	3p	Drosophila melanogaster - CG1244	..3410	??			96.4	A
pB29_A-134	5p	Drosophila melanogaster - CG1244	630	IF		95.2		A
pB29_A-92	5p/3p	Drosophila melanogaster - CG1244	630..1439	IF		94.1	93.5	A
pB29_A-3	5p	Drosophila melanogaster - CG1244	2346	IF		97.0		A
pB29_A-133	5p	Drosophila melanogaster - CG1244	2472	IF		93.0		A
pB29_A-189	5p/3p	Drosophila melanogaster - CG1244	2502..3859	IF		96.1	83.2	A
pB29_A-137	5p	Drosophila melanogaster - CG1244	2502	IF		95.3		A
pB29_A-93	5p/3p	Drosophila melanogaster - CG1244	2547..3247	IF		91.5	88.8	A
pB29_A-140	5p	Drosophila melanogaster - CG1244	2547	IF		91.5		A

Clone Name	Type Seq	Gene Name (Best Match)	Start..Stop (nt)	Frame	Sens	%Id 5p	%Id 3p	PBS
pB29_A-45	5p/3p	Drosophila melanogaster - CG1244	2547..3247	IF		91.5	98.1	A
pB29_A-101	5p/3p	Drosophila melanogaster - CG1244	2577..3550	IF		87.5	94.5	A
pB29_A-51	5p	Drosophila melanogaster - CG1244	2577	IF		92.8		A
pB29_A-5	5p/3p	Drosophila melanogaster - CG1244	2577..3550	IF		94.7	99.8	A
pB29_A-138	5p	Drosophila melanogaster - CG1244	2601	IF		94.0		A
pB29_A-107	5p	Drosophila melanogaster - CG1244	2601	IF		96.0		A
pB29_A-129	5p/3p	Drosophila melanogaster - CG1244	2724..3686	IF		97.5	94.4	A
pB29_A-13	5p	Drosophila melanogaster - CG32046	3667	??	N	93.3		N/A
pB29_A-67	5p	Drosophila melanogaster - CG3252	1938	??	N	97.4		N/A
pB29_A-162	5p	Drosophila melanogaster - CG14991	271	??	N	97.7		N/A
pB29_A-154	5p/3p	Drosophila melanogaster - CG5708	93..800	IF		88.7	88.1	D
pB29_A-31	3p	Drosophila melanogaster - CG10712	..1915	??			97.1	A
pB29_A-111	5p	Drosophila melanogaster - CG10712	1266	IF		97.0		A
pB29_A-183	5p	Drosophila melanogaster - CG10712	1266	IF		83.7		A
pB29_A-141	5p	Drosophila melanogaster - CG10712	1266	IF		93.3		A
pB29_A-44	5p	Drosophila melanogaster - CG10712	1266	IF		93.8		A
pB29_A-52	5p/3p	Drosophila melanogaster - CG10712	1284..1929	IF		90.6	88.9	A
pB29_A-120	5p	Drosophila melanogaster - CG10712	1404	IF		87.5		A
pB29_A-69	5p	Drosophila melanogaster - CG10712	1428	IF		85.5		A
pB29_A-12	5p/3p	Drosophila melanogaster - CG10712	1428..2102	IF		99.0	89.6	A
pB29_A-63	5p	Drosophila melanogaster - CG12505	1625..1946	OOF2		97.5		N/A
pB29_A-153	3p	Drosophila melanogaster - CG8332	..-15	??	N		88.7	N/A
pB29_A-158	5p	Drosophila melanogaster - CG17295	-18..220	OOF1		99.2		N/A
pB29_A-148	5p	Drosophila melanogaster - CG12207	614	??	N	92.4		N/A
pB29_A-128	5p	Drosophila melanogaster - CG17612	-30	OOF1		95.8		N/A
pB29_A-151	5p	Drosophila melanogaster - CG4019	75..374	IF		98.0		D
pB29_A-26	5p/3p	Drosophila melanogaster - GenMatch GID: 8573373	-1..943	IF		95.8	99.2	D
pB29_A-132	5p	Drosophila melanogaster - GenMatch GID: 113194865	-1	IF		100.0		D
pB29_A-100	5p/3p	Drosophila melanogaster - GenMatch GID: 210062745	-1..342	IF		96.9	90.1	D
pB29_A-50	3p	Drosophila melanogaster - GenMatch GID: 113194556	..413	??			100.0	N/A

Table S4. Primer list:

Primer sequences	*Primer name*	*Use*
5'-GGCTATGTCTGTATGGTCGATTC-3'	*Gli3 For*	*qRT-PCR*
5'-GTCCGTCCCTTCTCTCTAACT-3'	*Gli3 Rev*	*qRT-PCR*
5'-CTGAGCGGCCGCTTTTGAAACACCACCTCTCA-3'	*3'UTR BOC For*	*subcloning*
5'-ACGTGCGGCCGCAAGAAAATGCTGACTCACA-3'	*3'UTR BOC Rev*	*subcloning*
5'-TCCCAAAGTGCGAGGATTAC-3'	*CDON For*	*qRT-PCR*
5'-CGTCAGCCAGGTCTGTTATT-3'	*CDON Rev*	*qRT-PCR*
5'-CCTAAGATGCCCATGAGAACAG-3'	*BOC For*	*qRT-PCR*
5'-CAGAGATATGTTGCCACGGATTA-3'	*BOC Rev*	*qRT-PCR*
5'-CTAGCGGCCGCTCCAAAAGCATTGTGGTTCA-3'	*3'UTR CDON For*	*subcloning*
5'-CTTGCGGCCGCCCAAGATCCTGCTCCTTCAG-3'	*3'UTR CDON Rev*	*subcloning*
5'-AAACACTGTAACTTCTAAATAAATGTTTAGACATGCCTGTAACCTTCAAACTGAGTCA-3'	*BOC mut For*	*Directed mutagenesis*
5'-TGACTCAGTTTGAAGGTTACAGGCATGTCTAAACATTTATTTAGAAGTTACAGTGTTT-3'	*BOC mut Rev*	*Directed mutagenesis*
5'-AGCTCTGCTTATGACTTCGACATGCTGAGGTCCACATTTCTCCCC-3'	*CDON mut 1 For*	*Directed mutagenesis*
5'-GGGGAGAAATGTGGACCTCAGCATGTCGAAGTCATAAGCAGAGCT-3'	*CDON mut 1 Rev*	*Directed mutagenesis*

5'-GTGATTGGGGTGGGCGAATGACATGCTCTGAAATTCTTTGGAACC-3'	CDON mut 2 For	Directed mutagenesis
5'-GGTTCCAAAGAATTTCAGAGCATGTCATTCGCCCACCCCAATCAC-3'	CDON mut 2 Rev	Directed mutagenesis
5'-GAA GCA CCT CCG GAA CCT -3'	hHes1 For	qRT-PCR
5'-GTC ACC TCG TTC ATG CAC TC -3'	hHes1 Rev	qRT-PCR
5'-GTC CCC ACT GCC TTT GAG -3'	h HERP3 For	qRT-PCR
5'-ACC GTC ATC TGC AAG ACC TC -3'	h HERP3 Rev	qRT-PCR
5'-CAG GCA CTT ACG AAA CAC GA -3'	hHey2 For	qRT-PCR
5'-CCA GCA GTG CAT CAG TAT GTC -3'	hHey2 Rev	qRT-PCR
5'-AGCCACATCGCTCAGACAC-3'	GAPDH For	qRT-PCR
5'-GCCCAATACGACCAAATCC-3'	GAPDH Rev	qRT-PCR
5'-TCAGTCTAAAATCCCATAATAAGTGC-3'	Ihog For	qRT-PCR
5'-AAACCGGAATTGCTTCGAG-3'	Ihog Rev	qRT-PCR
5'-TGCCTAAAGAGACGGGAAAA-3'	Boi For	qRT-PCR
5'-ATGTGTTCCAATTGCGGTTT-3'	BoiRev	qRT-PCR
5'- TGTCCTTCCAGCTTCAAGATGACCATC-3'	Rp49 For	qRT-PCR
5'-CTTGGGCTTGCGCCATTTGTG-3'	Rp49 Rev	qRT-PCR

Table S5: List of genes up-regulated (blue) and down-regulated (red) in the tumour condition compared to the control *ey>Dl>GS88A8* versus *>Dl,GS88A8* (Garelli *et al.*, 2012):

probeset_id	accnum	symbol	R.fold	rawp
1641174_at	CG7361-RA	RFeSP	32.56	4.47E-05
1632525_at	CG9925-RA	CG9925	25.66	1.79E-05
1625664_at	CG14059-RA	CG14059	13.39	1.88E-04
1633959_s_at	TRANSPOSON	NA	7.26	8.93E-06
1627936_s_at	TRANSPOSON	NA	5.36	1.60E-03
1636658_at	CG6955-RA	Lcp65Ad	4.74	9.82E-05
1624269_at	CG8825-RA	gkt	4.62	1.25E-04
1631349_s_at	TRANSPOSON	NA	4.54	5.36E-05
1633998_s_at	TRANSPOSON	NA	4.48	8.93E-05
1640975_at	CG10534-RA	Lcp65Ag2	3.80	1.59E-03
1637945_at	RE67734	NA	3.29	4.11E-04
1636758_s_at	CG11205-RA	phr	3.06	2.32E-04
1640733_at	CG14321-RA	CG14321	2.91	1.43E-03
1623349_x_at	TRANSPOSON	NA	2.90	7.14E-05
1639181_at	CG14598-RA	CG14598	2.73	5.45E-04
1628835_at	CG14534-RA	TwdlE	2.65	4.20E-04
1626934_a_at	CG15288-RA	wb	2.64	4.73E-04
1630621_at	CG15212-RA	CG15212	2.62	2.23E-04
1640104_at	CG7014-RA	RpS5b	2.55	2.14E-04
1626142_at	CG10533-RA	Lcp65Af	2.48	1.20E-03
1624543_s_at	TRANSPOSON	NA	2.46	1.66E-03
1639902_at	CG33200-RA	ventrally-expressed-protein-D	2.40	2.50E-04
1639694_s_at	CG10102-RA	CR10102	2.39	1.09E-03

1626850_s_at	CG31953-RA	CG31953	2.34	5.18E-04
1629083_at	CG16704-RA	CG16704	2.12	1.54E-03
1624859_at	CG4319-RA	rpr	2.08	1.00E-03
1639042_at	CG6414-RA	CG6414	2.04	2.95E-04
1639597_at	CG2297-RA	Obp44a	1.97	4.64E-04
1638783_at	CG17642-RA	mRpL48	1.96	6.43E-04
1623776_s_at	CG11094-RB	dsx	1.95	1.71E-03
1633383_at	CG10704-RA	toe	1.92	1.21E-03
1623459_at	CG9453-RC	Spn4	1.89	1.68E-03
1641282_at	CG6536-RB	mthl4	1.84	5.00E-04
1633809_at	CG13046-RA	CG13046	1.84	5.27E-04
1635109_at	CG5888-RA	CG5888	1.83	4.29E-04
1636925_at	CG31477-RA	CG31477	1.83	1.52E-03
1628275_at	CG9343-RB	Trl	1.76	1.05E-03
1633843_at	CG31672-RA	CG31672	1.76	1.14E-03
1633094_a_at	CG11186-RB	toy	1.75	7.86E-04
1637654_at	CG10566-RA	CG10566	1.72	3.57E-04
1624763_at	CG2556-RA	CG2556	1.58	1.65E-03
1623036_a_at	CG10249-RC	CG10249	1.54	1.29E-03
1633299_at	CG1689-RA	lz	1.53	9.56E-04
1634372_at	CG9490-RA	Ddr	1.53	1.38E-03
1635336_at	CG7554-RA	comm2	1.45	1.19E-03
1635163_at	CG5731-RA	CG5731	1.37	1.75E-03
1636865_at	CG3250-RA	Os-C	0.76	2.44E-03
1628235_at	CG7203-RA	CG7203	0.07	1.61E-04
1638505_at	CG12120-RA	t	0.07	8.04E-05
1630761_at	CG11854-RA	CG11854	0.15	2.41E-04
1633607_at	CG2444-RA	CG2444	0.16	8.66E-04
1631053_at	CG18087-RA	Sgs7	0.17	1.86E-03
1641746_at	CG2555-RA	Cpr11B	0.19	1.34E-04
1639401_at	CG8696-RA	Mal-A1	0.19	2.86E-04
1634115_a_at	CG4791-RA	Cpr31A	0.19	7.68E-04
1632650_at	CG5867-RA	CG5867	0.23	2.68E-04
1636268_at	CG10570-RA	CG10570	0.25	4.38E-04
1628950_at	CG10178-RA	CG10178	0.26	1.55E-03
1635266_at	CG12023-RB	GV1	0.27	3.57E-05
1631252_a_at	CG12023-RB	GV1	0.48	9.38E-04
1626287_at	CG12023-RA	GV1	0.51	1.77E-03
1625616_at	CG14566-RA	CG14566	0.27	4.02E-04
1641729_at	CG13043-RA	CG13043	0.29	2.05E-04
1625255_at	CG11029-RA	CG11029	0.29	1.26E-03
1631561_s_at	CG4607-RA	CG4607	0.29	6.25E-04
1623327_at	S	NA	0.30	1.03E-03
1622946_at	CG6908-RA	CG6908	0.31	5.63E-04
1635817_at	CG11131-RA	CG11131	0.32	1.96E-04

1630067_a_at	CG7052-RA	TepII	0.33	3.84E-04
1623971_at	CG9150-RA	CG9150	0.33	2.51E-03
1641062_at	CG1851-RA	Ady43A	0.33	1.43E-04
1626088_at	CG2177-RA	CG2177	0.34	1.33E-03
1638477_at	CG13403-RA	CG13403	0.34	3.66E-04
1627568_at	CG14109-RA	CG14109	0.34	1.07E-04
1624732_at	CG17527-RA	GstE5	0.35	7.06E-04
1638240_s_at	CG8785-RA	CG8785	0.35	9.29E-04
1640004_at	CG9726-RA	PH4alphaMP	0.35	2.23E-03
1627855_at	CG9792-RA	yellow-e	0.35	1.16E-04
1628052_at	CG10241-RA	Cyp6a17	0.36	3.30E-04
1629346_at	CG1443-RA	CG1443	0.36	8.40E-04
1640377_s_at	CG2849-RB	Rala	0.37	5.89E-04
1633443_s_at	CG2082-RA	CG2082	0.37	2.66E-03
1623364_at	CG4250-RA	CG4250	0.37	9.02E-04
1631394_at	CG31324-RA	CG31324	0.37	1.62E-03
1632527_at	CG13705-RA	CG13705	0.38	2.28E-03
1634084_at	CG4213-RA	CG4213	0.38	2.90E-03
1629906_s_at	CG33045-RA	Kaz1-ORFB	0.38	1.06E-03
1640170_at	CG10311-RA	CG10311	0.38	3.24E-03
1630653_a_at	CG1743-RB	Gs2	0.39	9.65E-04
1627000_s_at	CG6231-RC	CG6231	0.39	2.62E-03
1632633_at	CG6514-RA	TpnC25D	0.39	1.01E-03
1640553_at	CG13063-RA	CG13063	0.40	1.38E-03
1635494_at	CG5779-RA	proPO-A1	0.40	1.47E-03
1637631_at	CG15427-RC	tutl	0.40	3.13E-04
1634636_at	CG6426-RA	CG6426	0.40	1.52E-04
1631701_a_at	CG8502-RC	Cpr49Ac	0.41	9.82E-04
1640675_at	HDC02560	CG34165	0.41	1.79E-04
1635227_at	CG10160-RA	ImpL3	0.41	6.70E-04
1639439_at	CG2471-RA	Sclp	0.41	4.55E-04
1636879_at	CG14356-RA	CG14356	0.42	3.39E-04
1633582_at	CG8585-RA	Ih	0.42	1.37E-03
1623060_at	CG15757-RA	Cpr12A	0.42	1.95E-03
1636603_a_at	CG9297-RA	CG9297	0.42	1.07E-03
1633592_a_at	CG5413-RB	CREG	0.42	5.81E-04
1637353_at	CG3318-RA	Dat	0.43	5.98E-04
1632432_at	CG9850-RA	CG9850	0.43	8.13E-04
1624362_at	CG15361-RA	Nplp4	0.43	3.04E-04
1623522_at	CG11668-RA	CG11668	0.43	9.73E-04
1633703_s_at	CG1668-RA	Pbprp2	0.43	5.54E-04
1630020_at	CG13041-RA	CG13041	0.44	1.83E-03
1630968_at	CG13907-RA	CG13907	0.45	6.88E-04
1632648_at	CG32922-RA	CG14681	0.45	4.82E-04
1635838_at	CG13545-RA	CG13545	0.45	1.70E-03

1626196_at	CG5809-RA	CaBP1	0.46	1.35E-03
1628536_s_at	CG11880-RA	CG11880	0.46	1.18E-03
1628678_at	CG13920-RA	CG13920	0.47	1.46E-03
1640057_at	CG9192-RA	CG9192	0.47	1.15E-03
1632852_s_at	CG2718-RB	Gs1	0.47	2.59E-04
1626109_a_at	CG9023-RA	Drip	0.47	1.71E-03
1637414_at	CG4455-RA	CG4455	0.47	3.22E-04
1633048_at	CG8193-RA	CG8193	0.48	1.44E-03
1637113_s_at	CG15105-RB	abba	0.48	2.72E-03
1625658_at	CG5181-RA	CG5181	0.49	1.36E-03
1636668_at	CG9972-RA	spz5	0.49	8.93E-04
1638818_at	CG33149-RA	Mlp60A	0.50	1.50E-03
1635073_at	CG17108-RA	CG17108	0.50	7.32E-04
1631635_at	CG7294-RA	CG7294	0.50	6.07E-04
1634440_s_at	LP01487	Eip74EF	0.50	1.23E-03
1636392_at	CT36057	CG15785	0.51	1.45E-03
1628884_at	CG11709-RA	PGRP-SA	0.51	6.97E-04
1629903_at	CG30359-RA	Mal-A5	0.52	6.52E-04
1626910_at	CG15282-RA	CG15282	0.53	1.70E-04
1631432_at	CG15786-RA	CG15786	0.53	9.47E-04
1631779_s_at	CG2841-RB	ptr	0.53	9.91E-04
1639660_s_at	CG10550-RB	CG10550	0.53	1.88E-03
1627759_at	CG30080-RA	CG30080	0.53	4.47E-04
1623900_a_at	CG14935-RA	Mal-B2	0.53	8.84E-04
1623092_at	CG3440-RA	Pcp	0.54	3.48E-04
1632685_at	CG32603-RA	CG32603	0.54	2.06E-03
1635792_a_at	CG7021-RA	Ela	0.54	7.50E-04
1625185_at	CG6906-RA	CAH2	0.55	2.77E-04
1627647_at	CG3940-RA	CG3940	0.56	7.77E-04
1625894_at	CG11370-RA	CG11370	0.56	1.49E-03
1627430_at	CG8888-RA	CG8888	0.56	7.41E-04
1631217_a_at	CG7930-RA	TpnC73F	0.56	6.61E-04
1634669_at	CG32333-RA	CG32333	0.56	2.12E-03
1629383_a_at	CG6416-RG	Zasp66	0.57	9.20E-04
1632121_a_at	CG6416-RE	Zasp66	0.62	1.13E-03
1641508_s_at	CG12844-RA	Tsp42Eh	0.58	8.48E-04
1634296_s_at	CG17646-RB	CG17646	0.58	2.64E-03
1624363_at	CG15201-RA	CG15201	0.58	1.63E-03
1630084_at	CG10205-RA	CG10205	0.59	1.51E-03
1635272_a_at	CG10205-RB	CG10205	0.63	2.82E-03
1633481_at	CG14394-RA	CG14394	0.59	1.88E-03
1629674_s_at	CG10999-RA	CG10999	0.59	1.02E-03
1628888_at	CG7180-RA	CG7180	0.59	1.91E-03
1641476_a_at	CG6281-RA	Timp	0.60	1.21E-03
1632533_at	CG6281-RB	Timp	0.65	1.56E-03

1640181_at	CG13044-RA	CG13044	0.60	2.97E-03
1630256_at	CG2958-RA	lectin-24Db	0.60	3.25E-03
1630418_s_at	CG31374-RB	sals	0.60	6.16E-04
1635975_s_at	RE54004	NA	0.61	1.42E-03
1626616_at	CG7465-RA	CG7465	0.61	1.98E-03
1627844_at	CG2060-RA	Cyp4e2	0.61	8.75E-04
1624969_s_at	CG17041-RA	CG42319	0.61	4.91E-04
1640642_at	CG5192-RB	Rh6	0.62	1.46E-03
1624057_at	CG16713-RA	CG16713	0.62	8.22E-04
1623342_at	CG8369-RA	CG8369	0.62	1.29E-03
1635460_a_at	CG17927-RG	Mhc	0.63	2.10E-03
1631222_at	CG11641-RA	pdm3	0.63	2.46E-03
1634978_at	CG13117-RA	CG13117	0.63	1.72E-03
1628927_at	CG17914-RA	yellow-b	0.63	1.89E-03
1625279_a_at	CG10619-RA	tup	0.63	1.08E-03
1641259_at	CG5210-RA	Chit	0.64	1.84E-03
1636174_at	CG10091-RA	GstD9	0.64	2.22E-03
1633483_a_at	CG14207-RA	CG14207	0.64	2.81E-03
1640202_at	CG4475-RA	Idgf2	0.64	1.13E-03
1639287_at	CG9877-RA	CG9877	0.64	2.87E-03
1628188_at	S	NA	0.65	6.79E-04
1623094_at	CG12843-RA	Tsp42Ei	0.65	1.22E-03
1641325_s_at	CG4843-RA	Tm2	0.65	3.26E-03
1625950_a_at	CG7777-RA	CG7777	0.65	1.63E-03
1626984_at	CG1152-RA	Gld	0.66	1.74E-03
1623016_at	CG1299-RA	CG1299	0.67	1.55E-03
1638697_at	CG5597-RA	CG5597	0.67	2.76E-03
1639532_at	CG5391-RA	CG5391	0.67	2.47E-03
1625833_at	CG9896-RA	CG9896	0.68	2.05E-03
1630509_at	CG4696-RA	Mp20	0.68	1.76E-03
1626416_a_at	CG4533-RB	l(2)efl	0.68	2.01E-03
1635584_s_at	CG4898-RB	Tm1	0.68	1.94E-03
1623883_at	CG18661-RA	CG18661	0.68	2.42E-03
1626439_at	CG15353-RA	CG15353	0.69	7.23E-04
1640462_at	CG14716-RA	Ho	0.69	2.93E-03
1638405_at	CG9338-RA	CG9338	0.71	2.70E-03
1629235_s_at	CG7178-RA	wupA	0.73	2.79E-03
1638869_at	CG10112-RA	Cpr51A	0.73	2.88E-03

APPENDIX II

UNIVERSITAS
Miguel
Hernández

OPEN ACCESS Freely available online

PLOS BIOLOGY

Dampening the Signals Transduced through Hedgehog via MicroRNA miR-7 Facilitates Notch-Induced Tumourigenesis

Vanina G. Da Ros, Irene Gutierrez-Perez, Dolors Ferres-Marco, Maria Dominguez*

Instituto de Neurociencias, CSIC-UMH, Alicante, Spain

Abstract

Fine-tuned Notch and Hedgehog signalling pathways via attenuators and dampers have long been recognized as important mechanisms to ensure the proper size and differentiation of many organs and tissues. This notion is further supported by identification of mutations in these pathways in human cancer cells. However, although it is common that the Notch and Hedgehog pathways influence growth and patterning within the same organ through the establishment of organizing regions, the cross-talk between these two pathways and how the distinct organizing activities are integrated during growth is poorly understood. Here, in an unbiased genetic screen in the *Drosophila melanogaster* eye, we found that tumour-like growth was provoked by cooperation between the microRNA miR-7 and the Notch pathway. Surprisingly, the molecular basis of this cooperation between miR-7 and Notch converged on the silencing of Hedgehog signalling. In mechanistic terms, miR-7 silenced the *interference hedgehog* (ihog) Hedgehog receptor, while Notch repressed expression of the *brother of ihog* (boi) Hedgehog receptor. Tumourigenesis was induced co-operatively following Notch activation and reduced Hedgehog signalling, either via overexpression of the microRNA or through specific down-regulation of *ihog*, *hedgehog*, *smoothened*, or *cubitus interruptus* or via overexpression of the *cubitus interruptus* repressor form. Conversely, increasing Hedgehog signalling prevented eye overgrowth induced by the microRNA and Notch pathway. Further, we show that blocking Hh signal transduction in clones of cells mutant for *smoothened* also enhance the organizing activity and growth by Delta-Notch signalling in the wing primordium. Together, these findings uncover a hitherto unsuspected tumour suppressor role for the Hedgehog signalling and reveal an unanticipated cooperative antagonism between two pathways extensively used in growth control and cancer.

Citation: Da Ros VG, Gutierrez-Perez I, Ferres-Marco D, Dominguez M (2013) Dampening the Signals Transduced through Hedgehog via MicroRNA miR-7 Facilitates Notch-Induced Tumourigenesis. PLoS Biol 11(5): e1001554. doi:10.1371/journal.pbio.1001554

Academic Editor: Matthew P. Scott, Stanford University, United States of America

Received August 1, 2012; **Accepted** March 25, 2013; **Published** May 7, 2013

Funding: We acknowledge the funding received from the Ministerio de Ciencia e Innovación (BFU2009-09074 and MEC-CONSOLIDER CSD2007-00023), the Botin Foundation, the Asociación Española Contra el Cáncer (AECC), Generalitat Valenciana (PROMETEO-2008/134) and a European Union Research Grant UE-HEALH-F2-2008-201666. I.G.P. is a Spanish FPI fellow. The funders had no role in study design, data collection and analysis, decision to publish, or preparation of the manuscript.

Competing Interests: The authors have declared that no competing interests exist.

Abbreviations: anti-luc, antibody against Luciferase protein; AP, anterior-posterior; Bdx-Gal4, Beadex-Gal4; BL, Bloomington *Drosophila* Stock Center; boi, brother of ihog; ci, cubitus interruptus; Dac, Dacshund; *DE*-cad, *DE*-cadherin; Dl, Delta; DV, dorsal-ventral; eGFP, enhanced Green Fluorescent Protein; Elav, Embryonic lethal abnormal visual system; en-Gal4, engrailed-Gal4; Eq-Z, Equatorial (eyegone)-lacZ; ey-Flp, eyeless-Flippase; eyeless-Gal4, ey-Gal4; fng-Z, fringe-lacZ; FRT, Flippase Recognition Target; Hh, Hedgehog; hsp70-Flp, heat shock promoter 70-Flippase; ihog, interference hedgehog; IR, interference RNA; MF, morphogenetic furrow; mirr-Z, mirror-lacZ; PH3, phopho histone H3; Ptc-Z, Patched-lacZ; qRT-PCR, quantitative reverse transcription polymerase chain reaction; RNAi, RNA interference; s.e.m., standard error of the mean; Ser-Z, Serrate-lacZ; smo, smoothened; Tub-Gal4, αTubulin84B promoter -Gal4; Tub-Gal80, αTubulin84B promoter -Gal80; UAS, Upstream Activation Sequences; UTR, untraslated region; VDRC, Vienna *Drosophila* RNAi Center; Wg, Wingless; wt, wild type

* E-mail: m.dominguez@umh.es

Introduction

A fundamental question in biology is what instructs cells to stop growing when the proper size is attained to commence terminal differentiation. Indeed, this issue is relevant not only to size regulation but also to cancer. One strategy that organisms use to promote the growth of organs involves the establishment of spatially confined domains called organizers, conserved signalling centres established along the dorsal-ventral (DV) and anterior-posterior (AP) axes of the organs, often involving members of the Notch (DV organizers) and Hedgehog (Hh) (AP organizers) families. Organizers act as a source of graded signals (e.g., Wingless/Wnts, and BMP/Dpp) that promote global organ growth and subsequently, or concurrently, cell fate specification along the DV or AP axes [1,2]. Although how individual organizing pathways promote growth has been studied comprehensively (e.g., [3–5]), our understanding of how orthogonal organizers are integrated and of the cross-talk between them remains limited. Tumourigenesis may occur if the finely balanced growth-promotion and termination is disrupted. Yet little attention has been paid to the issue of how growth by organizers is terminated.

To discover mechanisms of Notch-induced tumourigenesis in an *in vivo* context, we used the fruit fly *Drosophila melanogaster* compound eye. This tissue provides a particularly powerful tool to define novel oncogenes and tumour suppressor networks via unbiased genome-wide screens. Particularly, the early stages of eye development seem to recapitulate molecular mechanisms in

Author Summary

Growth control mechanisms ensure that organs attain the correct final size, generally averting tumour growth. This control is often linked to spatially confined domains known as organizers (conserved signalling centres), established along the dorsal-ventral and anterior-posterior axes of the organ by the Notch and Hedgehog pathways, respectively. The organizers emit signals that dictate growth, cell fate specification, and differentiation. However, how the distinct organizing signals received are integrated by cells within a growing organ remains a mystery. By studying how Delta-Notch signalling drives tumorigenesis, we identified the conserved microRNA miR-7 as a co-operative element in tumorigenesis mediated by Delta. We found that the cooperation between the microRNA and Delta-Notch pathway converged on the silencing of two obligatory and functionally redundant Hedgehog receptors, interference hedgehog and brother of ihog. Downregulation of other *hedgehog* pathway genes via RNA interference or genetic mosaics revealed a tumour suppressor role for Hedgehog signalling in the context of the oncogenic Notch pathway. Given the conservation of miR-7, as well as of the Notch and Hedgehog pathways, the conclusions we have drawn from these studies on *Drosophila* may be applicable to some human cancers.

human NOTCH1-induced oncogenesis (e.g., [6–10]). Human NOTCH1 can function either as an oncogene or a tumour suppressor depending on the cellular context, which often reflects the physiological role of NOTCH1 in the particular stage or cell type. During early development of the fly eye, the pleiotropic Notch pathway plays a predominant role in growth promotion. Consequently, this tissue and stage is useful to identify contextual factors that may synergize with Notch to foster benign and/or invasive tumour growth *in vivo*.

The growth in the compound eye, which is derived from the centre of the eye imaginal disc, depends on a conserved DV Notch-mediated growth-promoting organizer, which is established early in the second larval instar by the asymmetric activation of the Notch receptor by its ligands Delta and Serrate (DLL1,2,4, and JAG1,2 in humans) along the DV boundary (reviewed in [11]). Downstream of the organizer, *eyegone* (*eyg*) gene is expressed specifically in the organizer cells and it controls global eye size [12,13]. A similar DV organizer has been found in a variety of contexts, including the fly and vertebrate limbs, although the expression of *eyg* is restricted to the fly eye. Eyg is functionally related to the human PAX6(5a) oncogene [13] and acts as a transcriptional repressor [14,15] though complementary patterns of expression of the organizer in developing eyes have never been reported.

Growth and retinal differentiation in the eye field is spatially and temporally coordinated. Retinal differentiation depends on a separate organizer, the AP organizer, which is associated with the morphogenetic furrow (MF). The MF begins to form at the posterior margin of the early third instar eye disc, and as it moves in an anterior direction, it leaves differentiated retinal cells in its wake. Just anterior to the MF, eye cells arrest in G1 of the cell cycle prior to the start of differentiation, and most cells then go through a synchronous round of cell division before they terminally exit the cell cycle [16]. The initiation and progression of the MF, and of G1 arrest, is positively regulated by Hh [17–24]. Though the initiation and progression of the MF in the developing eye disc follows that of the DV organizer [25], the expression of *hh* gene starts earlier in second instar [19] and hence overlaps in time with the DV growth-promoting organizer (Figure S1). Early studies of ectopic Hh signalling led to the idea that this signal ultimately contributes to retinal patterning and also directly regulate eye growth [18], although more recently it has been shown that when the Hh pathway is constitutively activated (via inactivation of downstream repressors) in cells confined to a clone, the surrounding wild-type cells overproliferate but the cells within the clone show growth disadvantage and eventually are eliminated by apoptosis [26]. The influence of Hh on growth in Notch-mediated growth regulation needs to be investigated by loss-of-function approaches in the appropriate context.

In both flies and humans, Hh signalling relieves the inhibition exerted by Patched (PTCH1 in humans) on the intermediate pathway component Smoothened (Smo/SMO), allowing Smo to stabilize full-length Cubitus interruptus (Ci), which acts as a transcriptional activator (Ci-155: Gli2,3 in mammals) and inhibiting the processing of Ci-155 to the truncated transcriptional repressor (Ci-75, in flies) [27]. In addition to these core components, two related members of the immunoglobulin/fibronectin type III–like superfamily have recently been identified as Hh co-receptors in *Drosophila*, with functionally overlapping roles: Interference hedgehog (Ihog) and Brother of Ihog (Boi) [28–32]. Indeed, the human counterparts of these proteins, CDO (named after CAM-related/down-regulated by oncogenes) and BOC (Brother of CDO), also act as obligatory co-receptors for Hh signalling [28,32–41]. While overactive Hh signalling is unreservedly oncogenic, making Hh a prime target for therapeutic interventions, there is evidence that loss-of-function of some components of the Hh pathway may exert a tumour-suppressor role. A notable example is that of CDO and BOC, which were initially isolated on the basis of their downregulation by RAS oncogenes in transformed cells, and that were shown to act as tumour suppressors in vitro [42]. More recently, recurrent somatic mutations in the sonic Hh pathway were identified in human pancreatic cancers through global genomic studies, affecting GLI1, GLI3, and BOC [43]. However, the role of these mutations in cancer remains untested.

Here, we describe the identification of the conserved microRNA (miRNA) miR-7 as a gene that enhances Notch pathway-induced eye overgrowth in *D. melanogaster*. miRNAs are small noncoding RNAs that negatively regulate gene expression by binding to "seed" sequences in the untranslated regions (UTRs) and/or in the open reading frame of target messenger RNAs, thereby inhibiting translation and, at times, indirectly driving mRNA degradation. Although miRNAs are in the front line of cancer research, their role in cancer is often unconfirmed *in vivo*. We identified the *ihog* gene as a functionally relevant, direct target of miR-7 in Notch-mediated tumourigenesis *in vivo*. Further, we provide evidence that the microRNA *mir*-7 and Notch pathway cooperatively dampen Hh signal transduction via down-regulation of its receptors *ihog* and *boi*, respectively. As a consequence, we hypothesize that tumours form by the cooperation between the gain of Dl-Notch signalling and a deficiency to transduce Hh signal. We validated this hypothesis by showing that the inhibition of endogenous Hh core components similarly enhanced Dl-Notch-mediated organizing activity resulting in severe overgrowth both in the eye disc and the wing disc. Conversely, increasing Hh signal transduction pathway suppressed eye tumour-like growth by Dl and the microRNA. Given the conservation of these pathways, similar cooperative antagonistic interactions between oncogenic Notch and loss of Hh signalling might play a role in human cancers.

Results

MicroRNA miR-7 Cooperates with Delta to Trigger Severe Overgrowth in *Drosophila* Eye

To identify endogenous genetic determinants that may limit Notch-driven tumourigenesis *in vivo*, we carried out an unbiased (genome-wide) gain-of-expression screen for loci that converted Dl-induced mild eye overgrowth into severe overgrowths (benign tumour-like growth: eye tissue is overgrown and folded) or metastatic tumours (provoke secondary eye growths throughout the body). A Gene Search (GS) transposon system was employed to systematically generate gain-of-expression mutations as in [44], using the *eyeless* (*ey*)-*Gal4* to drive expression of UAS-containing transgenes and the GS lines in the imaginal disc cells of the growing eye (the precursors of the adult fly eye; Figure 1A–B). In this way, we identified a *GS* line (*GS(2)518ND2*) that converted *Dl*-induced modest eye overgrowth (Figure 1C; adult eyes are 130% bigger than control wild type eyes) into severely overgrown and folded eye tissue (*ey-Gal4 UAS-Dl GS(2)518ND2*, hereafter *ey>Dl>GS(2)518*) (250%–320% larger than wild-type eyes; 54% penetrance, $n = 200$ eyes; Figure 1D). Differentiation and growth defects of third instar eye discs of *ey>Dl>GS(2)518* are shown in Figure S3. In the absence of *Dl* overexpression, the overexpression or misexpression of the gene(s) affected by *GS(2)518ND2* did not increase eye size (*ey>GS(2)518*; Figure 1E).

The *GS(2)518ND2* line carried an insertion 3.1 kb upstream of the *mir-7* miRNA gene (Figure 1F), which is transcribed from an internal promoter within a 3′ intron of the *bancal/heterogeneous nuclear ribonucleoprotein K* (*bl/hnRNP-K*) gene [45]. A set of *EP* elements in the vicinity of *GS(2)518ND2* has been previously described to cause *mir-7* overexpression, and to induce proximal fusion of longitudinal (L) veins 3 and 4, as well as distal wing notching or bristle tufting [45–47]. Indeed, expressing *GS(2)518ND2* along the AP compartment boundary in the wing imaginal disc using *patched* (*ptc*)-*Gal4* caused similar L3–L4 fusion as that reported following *mir-7* overexpression in this domain (*ptc>GS(2)518*; Figure 1G). Conversely, the direct overexpression of *mir-7* together with *Dl* (hereafter, *ey>Dl>mir-7*), using a *mir-7* transgene that does not contain any *bl* sequences (*UAS-mir-7*), provoked overgrown larval eye discs *ey>Dl>mir-7* (Figure 1H; compare with sibling wild type eye discs, Figure 1I) associated with significant increased cell proliferation (Figure 1J and Figure S4C–D,H), resulting in adult overgrown and folded eyes similar to that in the *GS(2)518ND2* flies (70% of adult *ey>Dl>mir-7* animals displayed eye benign tumour-like growth, $n = 200$; Figure 1K and Figure S2A–C). There was no increase in eye size when *UAS-mir-7* alone was overexpressed by *ey-Gal4* (*ey>mir-7*; Figure 1L).

Identification of Candidate Tumour Suppressor Targets of miR-7 by in Vivo RNAi Screening in the Delta Overexpression Model

In the wing disc, the miR-7 microRNA is thought to silence target genes of the Notch pathway [47,48]. However, downregulation of Notch signalling alone might not explain the synergism between *mir-7* and *Dl* overexpression in eye overgrowth as we did not detect reduction of the organizing signalling by Dl-Notch in these discs (Figure S3). Therefore, we sought to identify miR-7 target gene(s) that might be relevant to the cooperation with Dl-Notch signalling in eye overgrowth and tumourigenesis. As such, we systematically assayed a set of 39 *D. melanogaster* genes predicted to be miR-7 targets in silico (Table S1, [49]). We used RNA interference (RNAi) UAS-driven transgenes (UAS-IR) to down-regulate candidate and previously validated miR-7 target genes *in vivo*. The *UAS-IR* transgenes silence specific mRNA transcripts by provoking their degradation, which is triggered by the generation of double-stranded RNA fragments complementary to the transcript driven by GAL4/UAS system [50,51]. Here, we employed *ey-Gal4* to drive simultaneously the overexpression of the *UAS-IR* and the *UAS-Dl* transgene (Table S1).

We hypothesized that *mir-7* overexpression would be mimicked by endogenous downregulation of the functional relevant target gene(s) in the context of *Dl* overexpression. The assay would not, however, distinguish between a *bona fide* miR-7 target gene and those genes that are required normally for restricting tissue growth. To identify the former, we considered that a *bona fide* miR-7 target gene would not produce any effect when downregulated in the context of normal Notch signalling. Nevertheless, we took into consideration that RNAi silences mRNA more efficiently than microRNAs, and thus, we considered that UAS-IR lines of bona fide candidate genes would produce phenotypes similar to those of miR-7, or more severe. We tested candidate target genes predicted by several algorithms ([52]; see Materials and Methods) and that contain the conserved *Drosophila* miR-7 binding sites, which normally reduces the number of false positive target predictions.

Of the 39 candidate target genes assayed in conjunction with *Dl* overexpression, only reduction of two genes robustly cooperated with Dl-Notch signalling to provoke severely overgrown and folded eyes. A previously validated target of miR-7, *hairy* [48] was capable of converting *Dl*-induced mild overgrowth into tumour-like growth (Table S1). However, since miR-7 only very subtly reduces the expression of endogenous *hairy* and a GFP-3′UTR hairy sensor [48], we focused our interest on the gene, *interference hedgehog* (*ihog*), that when downregulated in *Dl*-overexpressing cells provoked robust overgrowth (Figure 2, Figure S4E–F,H, and Table S1).

Although not previously characterized as a target gene of miR-7, the downregulation of *ihog* by RNAi concomitant with the gain of *Dl* function consistently produced enlarged eye discs (Figure S4E–F) similar to that in eye discs co-expressing *Dl* and *mir-7* (Figure S3I–J), resulting in adults with overgrown and folded eyes (*ey>Dl>ihog-IR*: 80% of severe overgrown eyes, $n = 200$; Figure 2B and Table S1). This phenotype was seen with the two independently generated *ihog-IR* transgenic lines available, both yielding identical results. Moreover, the expression of *ihog* RNAi alone during eye development did not alter the size or retinal patterning of this organ (*ey>ihog-IR*; Figure 2C). We confirmed that the *ihog-IR* transgenes inhibited *ihog* transcription 10-fold by quantitative reverse transcription-polymerase chain reaction (qRT-PCR; Figure S5A). Furthermore, the mRNA levels of *brother of ihog* (*boi*) were unaffected by these *ihog-IR* lines (Figure S5B). Thus, specific down-regulation of endogenous *ihog*, a predicted target of miR-7, facilitates overgrowth by *Dl* overexpression similar to those that develop when *mir-7* is overexpressed in this context (Figure 1, Figure 2, and Figure S4H).

Validation of *Interference Hedgehog* as a Direct Target of miR-7 in Vitro and in Vivo

Since the *ihog* gene encodes a receptor of Hh in the embryo, including the imaginal eye disc [30], we assessed whether it is directly regulated by miR-7 in luciferase reporter-based cellular assays in vitro and in vivo (Figure 2). There is a single conserved miR-7 binding site in the 3′UTR of *ihog* (Figure 2D) and in *Drosophila* Schneider (S2) cells overexpressing *mir-7*, there was 45% less activity of a luciferase reporter containing the full-length *ihog* 3′ UTR downstream of the firefly luciferase coding region driven by the α-tubulin promoter (*tub-luc::ihog-3′UTR* Figure 2E and Figure S5C). By contrast, when the *ihog* 3′UTR construct carried point mutations in the miR-7 binding site (*tub-luc::ihog(mut)-3′UTR*),

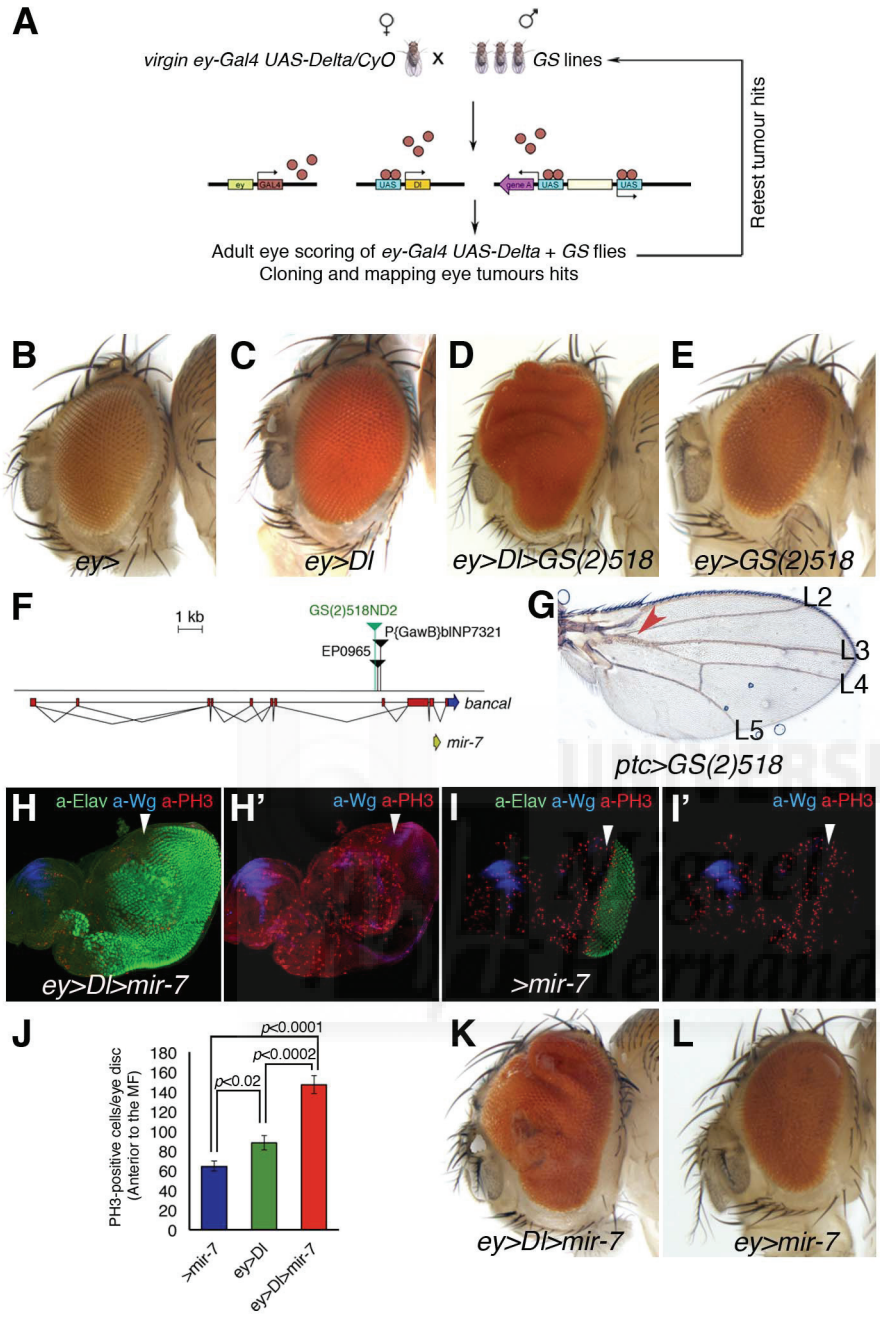

Figure 1. The Conserved MicroRNA miR-7 co-operates with Notch in *D. melanogaster* oncogenesis. (A) A schematic outline of the *Gene Search* (*GS*) gain-of-expression screen for Notch co-operating oncogenes in the developing *Drosophila* eye. (B–E and K–L) Adult heads of control female *ey-Gal4* wild-type eye size (B) and combinations between GS line, UAS transgenes, and *ey-Gal4* are shown. (C) *Dl* expression under the control of *ey-Gal4* results in a mild overgrowth in the eye (130% larger than wild type size). (D) Introducing the *GS(2)518ND2* line enhanced overgrowth by *Dl* (>320%, see also Figure S2). (E) The overexpression of gene(s) affected by the *GS(2)518ND2* line alone causes no overt eye overgrowth. (F) Scheme of the *GS(2)518ND2* insertion. (G) Overexpression of the *GS(2)518ND2* line driven by *ptc-Gal4* showed the typical wing vein L3–L4 fusion. (H–I') Confocal images of third instar eye-antennal discs stained for the mitotic marker PH3 (red), Wg (blue) to define the DV axis, and the neuronal marker Elav (green) of the indicated genotypes. White arrowheads indicate the position of the MF. The co-expression of *UAS-mir-7* with *UAS-Dl* causes eye disc overgrowth and a front of retinal differentiation highly disorganized (H, compare with control sibling eye disc in I). (J) Quantification of mitotic cells labelled by PH3 anterior to the MF of the genotypes: *ey>Dl>mir-7* (red bar), *ey>Dl* (green bar), and wild-type sibling discs +/*UAS-mir7* (>*mir-7*, blue bar). Data shown represent the mean ± s.e.m. of total PH3 measurement in 20 eye discs per genotype. *P* values were calculated by the unpaired Student's *t* test. (K–L) Adult heads overexpressing *mir-7* driven by *ey-Gal4* in the presence (K) or the absence (L) of the *UAS-Dl* transgene. See also Figures S2 to S4 for supplementary data.
doi:10.1371/journal.pbio.1001554.g001

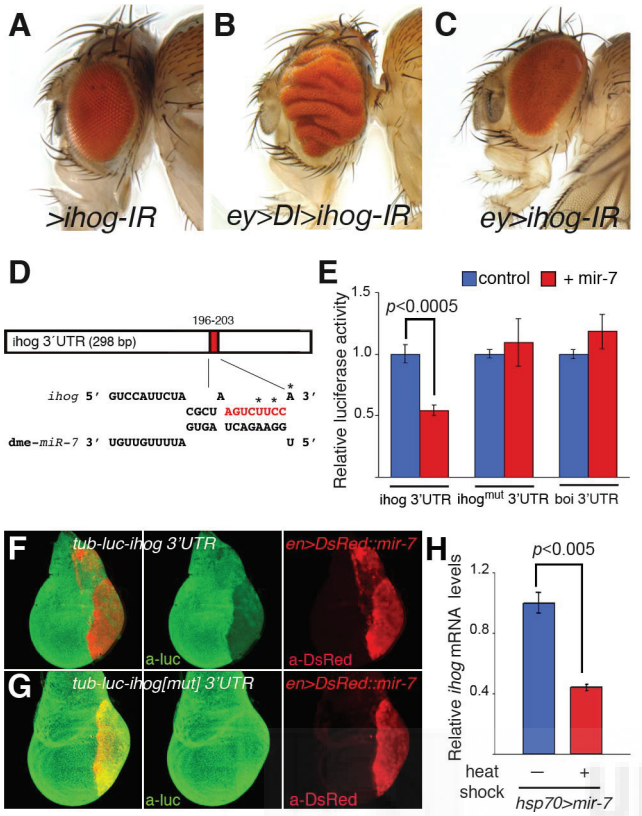

Figure 2. Tumourigenesis promoted by miR-7 via direct repression of *interference hedgehog* (*ihog*). (A–C) Adult heads of female control *UAS-ihog-IR* (A) and combinations of *UAS-ihog-IR* and *ey-Gal4* in the presence (B) or the absence (C) of the *Dl* transgene. (D) Computer predicted consequential pairing of *ihog* target region (top) and miRNA (bottom). The conserved seed match (8 mer) in the 3′UTR of *ihog* is in red. (E) Luciferase assay in *Drosophila* Schneider (S2) cells co-transfected with *mir-7* (red bars) or the empty vector (blue bars), together with a firefly luciferase vector containing the *ihog*3′UTR (*ihog*3′UTR), or the luciferase vector with mutations in the seed sequence (asterisks in *D*, *ihog*^{mut}*3′UTR*) or control *boi*3′UTR (*boi*3′UTR). Firefly luciferase activity was measured 48 h after transfection and normalized against *Renilla* luciferase. The values represent the mean ± s.e.m. of three or four independent experiments. Differences in *ihog(mut)* and *boi* luciferase levels were not statistically significant between treatments. (F–G) Confocal images of mid third instar wing discs carrying the *tub-luc::ihog-3′UTR* (F) or the *tub-luc::ihog*^{mut}*3′UTR* sensor (G) and overexpression of *mir-7* by *en-Gal4* (*en>DsRed::mir-7*, red) and stained with anti-luciferase antibody (green). (H) Differences in *ihog* mRNA levels assessed by RT-qPCR between *hsp70>mir-7* larvae subjected to heat shock treatment (red bar) or not (blue bar). Values represent the mean ± s.e.m. of three independent experiments. *P* values were calculated by the unpaired Student's *t* test.
doi:10.1371/journal.pbio.1001554.g002

luciferase activity was the same as in control cells (Figure 2E). In addition, luciferase activity was unaffected by *mir*-7 overexpression in a control *tub-luc::boi-3′UTR* construct, indicative that the functional similar *boi* was not a target of miR-7 (Figure 2E).

In addition to the direct regulation of the *ihog* mRNA 3′UTR by miR-7 in vitro, there was specific in vivo repression of the *tub-luc::ihog-3′UTR* construct but not the *ihog* 3′UTR construct that carried the mutations in the seed sequence (Figure 2FG) and of an *ihog* 3′UTR eGFP sensor (*tub-eGFP::ihog-3′UTR*) but not a similar *boi* 3′UTR eGFP sensor (*tub-eGFP::boi-3′UTR*) (Figure S6AB) in the posterior compartment cells of third instar wing discs overexpressing *mir-7* driven by *engrailed* (*en*)*-Gal4*. Finally, we demonstrated that endogenous *ihog* mRNA was inhibited by miR-7 in vivo as heat shock induction of mature *mir-7* overexpression (*hsp70-Gal4 UAS-mir-7*) provoked a 55% reduction in *ihog* mRNA transcripts in larvae when assayed by qRT-PCR (Figure 2H and Figure S2D). Overall, these data provide convincing evidence that miR-7 is capable of directly repressing *ihog*, both in vitro and in vivo. Thus, the synergism between miR-7 and the Dl-Notch pathway activity in eye overgrowth would appear to be largely due to the silencing of *ihog*.

brother of ihog Is Negatively Regulated by Notch Signalling during Eye Growth

Although *boi* mRNA expression was not affected in the *ihog-IR* lines and Boi does not appear to be a target of miR-7, there is a well-documented functional overlap in the roles of Ihog and Boi. Moreover, genetic inactivation of both the *boi* and *ihog* genes is typically required to induce *hh* loss-of-function phenotypes [28,30,32]. However, unlike *ihog-IR*, we found that expressing an RNAi transgene against *boi* (*boi-IR* effectively reduces *boi* but not *ihog* mRNA levels by 65%; $p = 0.0005$; Figure S5A–B) did not enhance *Dl*-induced eye overgrowth (*ey>Dl>boi-IR*; Figure 3A–B and Table S2). Since only the concomitant loss of both *ihog* and *boi* leads to a loss of eye tissue [30], we reasoned that a similar situation might occur with respect to the *ihog-IR*-induced severe eye overgrowth (Figure 2B). Consequently, we verified the status of *boi* transcription in relation to eye disc growth. Interestingly, the spatial domain of *boi* in the developing eye disc in vivo using a ß-galactosidase enhancer trap inserted in *boi* (*P*-lacW stock *10111*; Figure 3C) unveiled that *boi* is expressed nonuniformly in the region anterior to the MF with a weakest expression within the DV organizer (Figure 3D–E,H: the MF is denoted by an arrow in H). Indeed, in eye discs double labelled with anti-Eyg (a DV organizer-specific response gene and an obligatory Notch's effector in eye growth [13,53]) and anti-ß-galactosidase (*boi-lacZ* in green), we found that the expression of Eyg precisely borders the "negative" domain of *boi* (Figure 3E–F). This led us to speculate that expression of *boi* is negatively regulated by Notch-Eyg at the growth-promoting organizer, which we investigated by monitoring the spatial domain of *boi-lacZ* in mutants of the DV organizer and by assessing *boi* mRNA levels by qRT-PCR analyses.

We assayed the ubiquitous expression of the Notch DV organizer transcriptional effector Eyg, which provokes a wider DV organizer domain [13,53] and observed an extended domain lacking *boi-lacZ* expression under these conditions (Figure 3G). Conversely, the ubiquitous expression of the modulator *fringe* (*fng*) causes defective Notch receptor activation by its ligands and results in the thinning or loss of the DV organizer [53–55]. Under these conditions, the expression of *boi* was uniform throughout the eye disc due to the absence of the "central domain" that represses this gene in wild-type eye discs (Figure 3I). Thus, *boi* is negatively regulated by Notch's organizer activity or it at least reflects this activity negatively. Since Eyg encodes a transcriptional repressor [14,15], it may directly repress *boi* transcription. This Hh co-receptor does contain a consensus Eyg-binding site for repression (TCACTGA [14]) at position chrX: 2.359.784, although we could not validate the direct binding of Eyg to the *boi* promoter region by chromatin immunoprecipitation (unpublished data). Nevertheless, it is possible that Eyg might bind through other nonconsensus sites. Furthermore, qRT-PCR analyses confirmed downregulated *boi* but not *ihog* transcripts in eye discs overexpressing *Dl* transgene alone by *ey-Gal4* (ey>*Dl*; left in Figure 3J). Importantly, both *boi* and *ihog* mRNA levels were downregulated in eye discs that co-expressed *Dl* with the microRNA *mir-7* (*ey>Dl>mir-7*; Figure 3J). *boi* and *ihog* RNA was isolated from whole eye-antennal disc

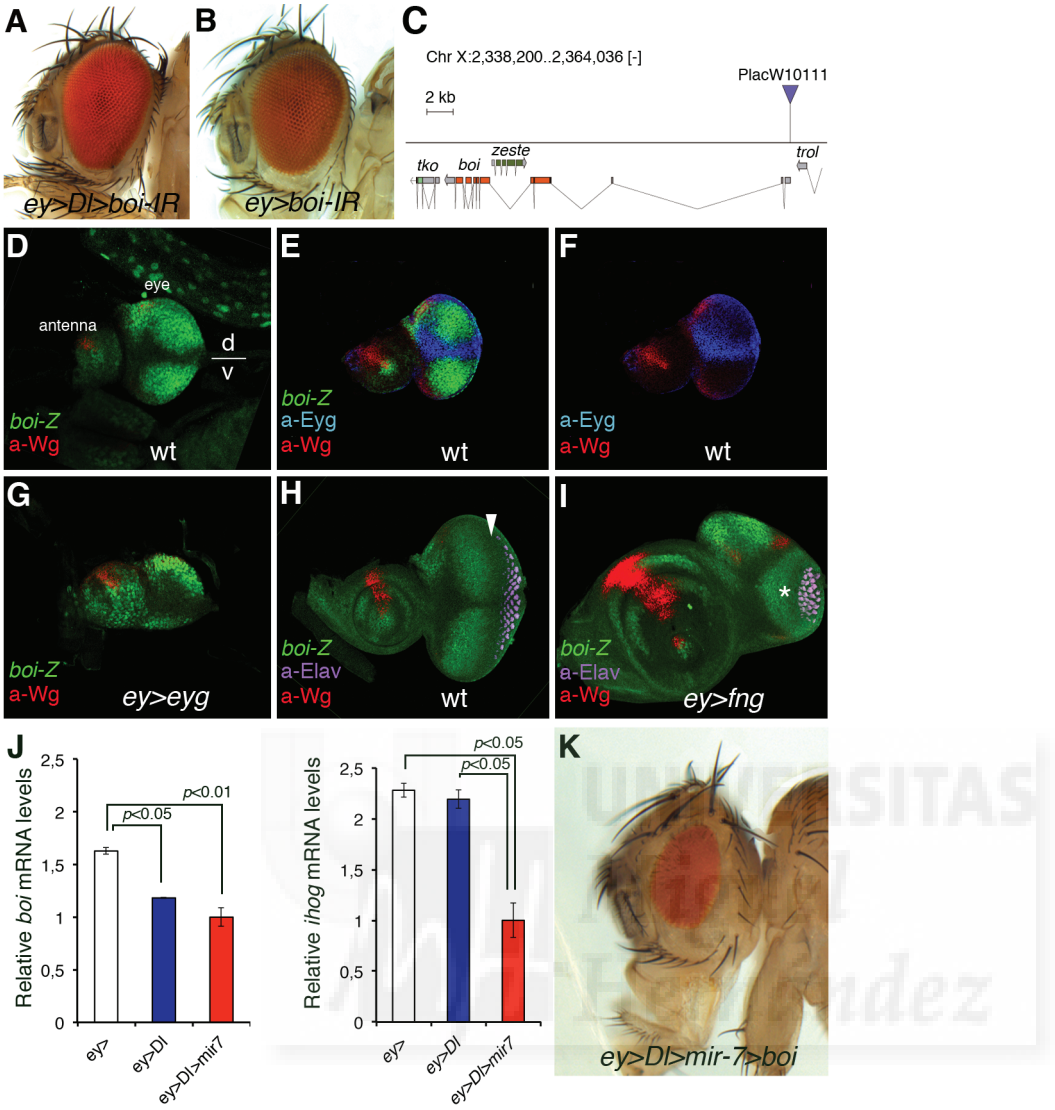

Figure 3. Notch signalling represses *brother of ihog* (*boi*) expression in the dorsal-ventral growth organizer in *Drosophila* eye. (A–B) Adult heads of female flies overexpressing *UAS-Dl* and/or *UAS-boi-IR* and *ey-Gal4*. (C) Map of *PlacW10111 P*-element insertion (triangle) into the *boi* locus. (D–I) *boi* expression in wild-type (D, E, F, and H) and Notch pathway mutant (G and I) eye-antennal discs. The patterning gene wingless (a-Wg, in red) serves to orient the eye disc in the dorsal (D)/ventral (V) axis. Expression of Boi (green) Hh co-receptor at the early third larval stage is repressed along the DV organizer (D and E), as defined by the expression of the DV organizer gene *eyg* (blue, E and F). Retinal differentiation (neuronal marker a-Elav, magenta) is first detected at the posterior end of the eye disc (to the right) and progresses in an anterior direction (H). The arrow points to the MF. (G and I) Expression of *boi-lacZ* (*boi-Z*, green) and wingless (a-Wg, red) in *ey>eyg* (G) and *ey>fng* (I) eye discs. The discs in (H) and (I) are from the same stage and magnification. The enlarged antennal disc in (I) is an effect of the undergrowth of the eye disc, caused in part by defective Notch activation in the D/V organizer due to *fng* overexpression. (J) qRT-PCR analyses of *boi* (left) and *ihog* (right) in *ey-Gal4* (white bar), *ey>Dl* (blue bar), and *ey>Dl>mir-7* (red bar) late third instar eye discs. Two independent experiments of three replicates are shown in each case. Data were normalized to *rp49*. mRNA isolated from 50 pairs of eye-antennal discs per genotype. Data analysed by a two-tailed unpaired *t* test. Error bars represent s.e.m. of three replicates. (K) Adult fly head showing no eye overgrown induced by *Dl* and *mir-7* when *boi* is overexpressed by a transgene (*UAS-boi*, 100% penetrance of rescue).
doi:10.1371/journal.pbio.1001554.g003

complexes; thus, the mRNA levels are the sum of all regions of the discs, including the antenna, which is not affected by *ey*>Dl or *ey*>*mir*-7. Hence expression differences with control may be significant underestimations of the actual differences of each gene in the eye disc parts in the different genotypes. Nevertheless, the qRT-PCR comparisons between the different genotypes showed a trend in *boi* and *ihog* expression response to Dl overexpression that explains the cooperation between the miR-7 and *Dl* signalling, since there is the concomitant downregulation of the two functionally redundant Hh receptor genes, *ihog* and *boi*.

Animals homozygous for mutations in *ihog* and *boi* exhibit a phenotype typical of the loss of *hh* function (e.g., [30]). The defect in $ihog^{-}$ boi^{-} animals can be rescued by expressing a *UAS-ihog::myc* transgene with weak constitutive expression in the absence of Gal4 activity [30]. Surprisingly, we could not overcome overgrowth by *mir-7*/*Dl* using this transgene (unpublished data). This may perhaps reflect that the elevated levels of Ihog expected by Gal4-induced expression of the transgene may exert a dominant negative effect on Hh signalling [31]. A *boi* transgene (*UAS-boi*) [56] fully suppressed the overgrowth induced by the combination

of *mir-7/Dl* (Figure 3K, 100% penetrance, $n = 100$). The same result was obtained using the *EP(X)1447(boi)* that misexpresses endogenous *boi* gene (unpublished data).

Blocking Core Hedgehog Signalling Components or Expressing Ci/GLI Repressor Mimics the Effect of the MicroRNA in Delta-Induced Tumourigenesis

To confirm that silencing Hh signal transduction facilitates a tumorigenic response to Dl-Notch overactivation, we next assayed the effects of directly downregulating core Hh signalling elements with RNAi transgenes driven by *ey-Gal4*, including *smo*, *ci*, and *hh* itself. As noted above, Gal4 drives expression throughout early eye disc development anterior to the MF, a region of undifferentiated proliferating eye cells that act on signals from the Notch-mediated DV organizer, and Gal4 expression terminates before cells exit the cell cycle at the MF [54]. We down-regulated each of these Hh signalling components by RNAi, assaying several independent lines in which the use of *ey-Gal4* avoided the possible effects of a loss of Hedgehog signal transduction on retinal differentiation that might confound the results (Table S2).

The downregulation of *smo* (80% flies exhibited eye tumour-like growth, $n > 200$), *ci* (100%, $n > 200$), or *hh* (30%–100%, $n > 200$) in conjunction with *Dl* overexpression provoked a tumour phenotype similar to that of RNAi of *ihog* but stronger than the overexpression of *mir-7* (compare Figure 1 and Figure 2 with Figure 4B–D; see also Table S2). Furthermore, downregulation of *ci* by RNAi (*ci-IR*) by *ey-Gal4* stimulated a metastatic overproliferation of eye tissue in the context of the *Dl* gain of function, resulting in flies with secondary eye growths within the thorax and abdomen (Figure 4F–G and Table S2). This invasive overgrowth is also observed when *Dl* and the *ci* RNAi transgene are expressed in the wing imaginal discs by the *dpp*-Gal4 (Figure S7). Like the *mir-7* and *ihog-IR* lines (Figure 1L and Figure 2C), none of the above RNAi lines were capable of inducing overgrowth by themselves.

In all contexts, in the absence of Hh signal or its reception, the transcription factors of the Ci/Gli family (in *Drosophila*, full-length Ci-155) can be proteolytically processed into a truncated (N-terminal 75 kDa in *Drosophila*—Ci-75) transcriptional repressor of the Hh pathway (Ci, Gli3, and to a lesser extent Gli2) (Figure 4A). The bifunctional nature of Ci [57–59], and of the mammalian homologues Gli2 and Gli3, could fulfil oncogenic or tumour suppressor roles in function of the status of the Hh signalling. As *ci-IR* downregulates both activator and repressor forms, we next assessed the contribution of the truncated Ci repressor that forms in the absence of Hh signalling, testing the effect of overexpressing *Dl* with a transgene of the constitutive Ci repressor form (*UAS-ci-75*). Co-overexpression of *Dl* and *ci-75* induced eye tumour-like growth in 75% of fly eyes (*ey>Dl>ci75*; $n = 100$; Figure 4H), in

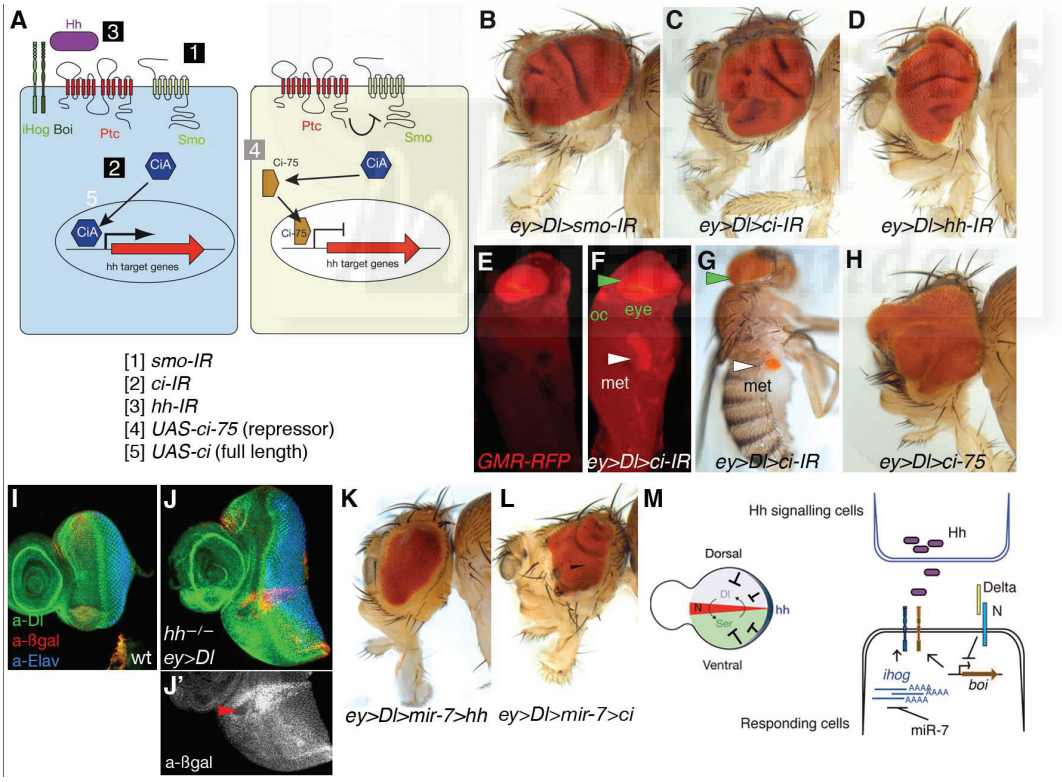

Figure 4. Downregulation of elements in the Hh pathway or overexpression of the repressor form of *ci* co-operates with *Dl* overexpression to trigger tumour growth in the *Drosophila* eye. (A) Schematic representation of Hh signalling and the *UAS* transgenes used to downregulate by RNAi (IR) or activate Hh pathway components. (B–D, H, and K–L) Representative adult heads of female flies of combinations of the indicated *UAS* transgenes and *ey-Gal4* are shown. (E–F) Fluorescent images of *Drosophila* pupae of sibling control (*ey>Dl*, E) or *ey>Dl>ci-IR* (F). (G) Adult fly of *ey>Dl>ci-IR* with a metastatic (met) growth in the abdomen. Eye tissue in the endogenous site (green arrowheads) and distant site (white arrowheads) is labelled by the retinal-specific GMR-myrRFP marker (E, F) or the retinal-specific red pigments (G). (I–J') Third instar wild type of sized eye disc (I) and *ey>Dl* eye disc carrying clones of hh^{AC} labelled by the absence of *arm-lacZ* (ßgal, red in J and grey in J'). Arrowhead points to a clone and its associated twin spot (high red staining). (M) Model of antagonistic interaction between Hh and Notch signalling in normal eye imaginal disc (left) and model of regulatory interactions among the microRNA, Notch pathway, and the Hh receptors *ihog* and *boi* (right). Genotype in (J) is: *yw ey-Flp; ey-Gal4 UAS-Dl/+; FRT82B* hh^{AC}*/FRT82B arm-lacZ*.
doi:10.1371/journal.pbio.1001554.g004

contrast to the overexpression of Ci full length (*UAS-ci*) that acts as an activator in Hh receiving cells and did not provoke eye tumour (unpublished data).

To further verify these findings with the RNAi transgenes, we generated marked clones of cells homozygous for hh^{AC} (a null allele) in the *ey>Dl* background (hh^{AC}/hh^{AC} *ey>Dl*; Figure 4J). Eye discs carrying small patches of hh^{AC} cells were 170% larger than control wild-type eye discs (Figure 4I) and 126% larger than *ey>*Dl without hh^{AC} clones eye discs (see Figure S4B). Using the MARCM technique [60], we also examined GFP-labelled clones of cells overexpressing *Dl* and homozygous for smo^3 (an amorphic allele) (smo^3/smo^3*tub>Dl>GFP*; Figure S8). Whereas clones of smo^3 do not delay the MF [61] and clones of *Dl*-expressing cells normally cause autonomous advancement of the MF [62], we found that clones of smo^3 *Dl*-expressing cells led to advancement of the MF also in surrounding wild-type cells (Figure S8B) and the disc was overall overgrown (unpublished data). The advanced MF is seen in *ey>Dl* eye discs with downregulation of Hh signalling via overexpression of *mir-7* or direct downregulation via RNAi transgenes (Figures S3 and S4). Thus, interfering with Hh signalling exacerbates the organizing activity of Dl-Notch signalling in eye imaginal discs and can foster invasive tumour growth (Figure 4F–G, Figure S7C–D, and Table S2).

Increasing Hedgehog Signal Prevents Tumourigenesis by Delta and miR-7

In normal early eye development, when the Notch organizer induces a dramatic increase in cell proliferation in the disc, *hh* gene is expressed in a thin line of cells along the eye disc margin ([19,20,25]; see Figure S1). Previously, it has been shown that clones of eye disc cells lacking PKA, Ptc, or Cos2 proteins that normally prevent the inappropriate activation of Hh signal transduction exhibit within the clone a growth-disadvantage and are eliminated by apoptosis [26]. This negative influence of Hh signal was also hinted at by the small eye defect associated with overexpression of *UAS-hh* by *ey-Gal4* [25] and is complementary to our findings.

The Ihog/Boc family proteins normally enhance Hh binding to Ptc, the 12-pass transmembrane protein involved in sensing extracellular Hh concentrations. Binding of Hh to Ptc relieves inhibition of Smo by Ptc and blocks the production of Ci repressor. Hence, the downregulation of *ihog/boi* levels by Dl/miR-7 (see Figure 3J) might reduce the interactions of Hh with Ptc. We therefore investigated whether increasing Hh signal via a *UAS-hh* transgene to counterbalance *ihog/boi* deficit could rescue the overgrowth by *Dl/mir-7*. Indeed, we detected significant reduction in eye size in flies *ey>Dl>mir-7>hh* (Figure 4K; 100% rescue, $n>100$; see Figure S9 for scheme of genetic test for rescuing experiment) and also in flies that expressed Ci full length (*ey>Dl>mir-7>ci*; Figure 4L). Note that when Ci full length is expressed in the context of *Dl* and *mir-7* overexpression, although many eyes are substantially reduced in size they still exhibit abnormal patterned growth (see Figure 4L) and other exhibited enhanced tumorigenesis. We interpret these findings as Ci full length can be converted into the repressor form owing to the reduced Hh signalling caused by Dl and miR-7 depletion of *ihog* and *boi*.

Hh signal stimulates the maturation of Ci full length into a short-lived nuclear activator, while the PKA negative regulator opposes this event and when mutated results in constitutive Hh pathway activity. The undergrowth defect of knock-down of *pka* by RNAi expression in the *Dl* overexpressing eye discs (*ey>Dl>pka-IR*; Table S2) further support the tumour suppressor activity of Hh pathway in the context of gain of Dl-Notch signalling in the context of the eye primordium. We suggest here that in healthy flies the release of Hh by these eye disc marginal cells sets eye size in conjunction with the Dl-Notch organizer (Figure 4M, left scheme), and thereby dampening Hh signalling in the context of Dl overexpression (Figure 4M, right) fosters the developing eye tumours or overgrowth beyond the normal eye size.

Hedgehog Signal Transduction Also Attenuates Delta Signalling and Overgrowth in the Wing

Wing disc growth and patterning is also organized by Hh and Notch-mediated organizers [2], with Hh secreted by cells in the posterior (P) compartment inducing short-range targets in anterior (A) cells near the AP boundary (e.g., *ptc*, blue staining in Figure 5A) [63,64]. Notch signalling is activated locally along the DV boundary by its ligands Dl and Serrate (Ser), and it induces symmetric expression of targets in boundary cells (e.g., *wg*, red staining in Figure 5A; reviewed in [2]). Hence, we investigated whether the antagonistic interaction between loss of Hh and gain of Notch apparent in the eye imaginal discs can also be applied to the wing discs.

Dl-expressing clones in the wing induce ectopic *wg* expression in D cells, where the *fringe* gene is expressed, whereas ventrally situated clones did not activate *wg* (e.g., [65–69]). Enhancing Dl activity by co-expressing *Dl* with the E3 ubiquitin ligase *Neuralized*, which promotes the endocytosis and signalling activity of Dl, can induce *wg* in ventrally situated clones [69]. Hence, we assayed ectopic induction of *wg* to examine *Dl* activity in smo^3/smo^3 clones. As shown in Figure 5, we found that ventrally situated A cells homozygous for smo^3 and expressing *Dl* expressed high levels of Wg, similar to the levels of Wg induced by dorsally situated clones, in contrast with most smo^3 *Dl*-expressing clones situated ventrally in P cells away from the boundary (Figure 5B–C) or clones of smo^3 cells that do not overexpressed *Dl* (Figure 5A). Nonautonomous overgrowth is also evident in ventrally situated clones of smo^3/smo^3 *Dl*-expressing (Figure S8C). Clones of smo^3 cells abutting the AP boundary often sort to the P compartment territory [70,71]. MARCM clones do not label the twin spot (smo^+/smo^+); therefore, the inference that the clones at the AP boundary (asterisks in Figure 5A″–B′) are of anterior origin is supported by the finding that they retain anterior features (low levels of Ci protein). Loss of *smo* activity in A cells at the boundary fail to up-regulate Ci expression and do not induce *ptc* transcription. These clones cause an anterior shift in the distribution of *ptc* and up-regulated Ci non-cell-autonomously [64]. We occasionally found ambiguously positioned clones of smo^3/smo^3 *tub>Dl* cells in which the anterior part of the clone exhibited ectopic *wg* expression while the posterior of the clone did not (Figure S8D). Taken together, these findings show that *Dl*-expressing cells unable to transduce the Hh signal behave as they express hyperactivated Dl. Coupled with the analysis of RNAi transgenes, these results confirm that the loss of Hh signalling enhances Dl-Notch signalling activity.

Loss of Hedgehog Signalling in miR-7 Overexpression in the Wing

microRNAs are thought to regulate multiple target genes; however, often when tested in vivo, it is a subset or a given target that function as the major effector of the activity of the microRNAs in a given cellular context. We asked whether our identification of *ihog* as a key target of miR-7 during Dl-mediated tumorigenesis in the eye might reflect endogenous roles of the microRNA in other tissues. Previously, misexpression of *mir-7* driven by *ptc-Gal4* (*ptc>mir-7*) produces wing margin notches, and a reduction of the space between vein L3 and L4 ([48]; see [72]). Both of these phenotypes have been attributed to defects in Notch signalling

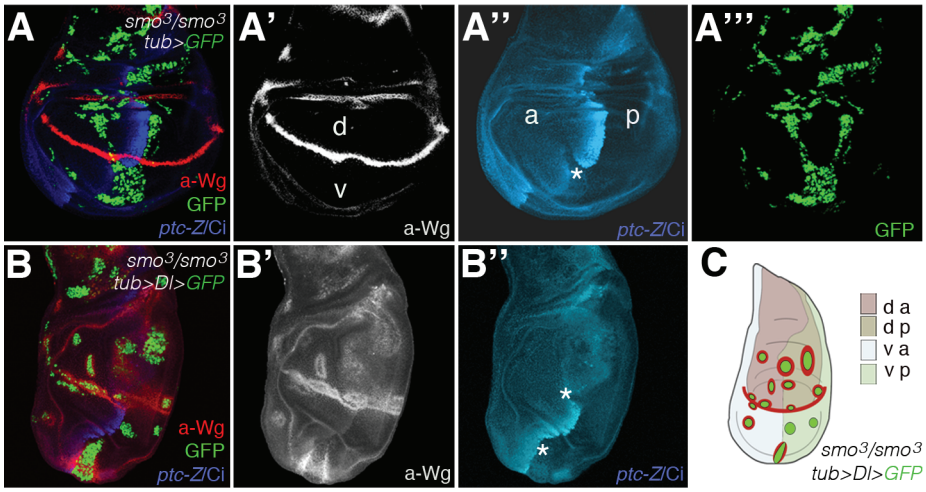

Figure 5. Failure to transduce the Hh signal due to mutations in smoothened enhances Dl-Notch signalling activity in the wing. (A–B″) Confocal images of wing discs bearing MARCM GFP (green)-labelled clones homozygous for *smo*^{3} without (A) or with (B) *Dl* overexpression. Single channel images are also shown. Mosaic discs were stained for Wg (red in A and B, and grey in A′ and B′), and Ci (blue) and Ptc-lacZ (Ptc-Z, blue). (C) A schematic summary of clones in (B). Asterisks in (A″) and (B″) point to "posteriorly" situated clones that were of anterior origin as denoted by the failure to induce Ptc and the low levels of Ci protein (white line delineates the AP boundary in the discs in B). Clones were generated at 24–42 h after egg laying (AEL) by a 1 h heat shock at 37°C ($n = 60$ clones analysed). Genotypes: (A) *yw hsp70-Flp tub-G4 UAS-GFP; tub-Gal80 FRT40A/smo*^{3} *FRT40A ptc-lacZ* and (B) *yw hsp70-Flp Tub-G4 UAS-GFP; Tub-Gal80 FRT40A/smo*^{3} *FRT40A ptc-lacZ; UAS-Dl/+*.
doi:10.1371/journal.pbio.1001554.g005

[48,73], although we noted that L3–L4 fusion is very reminiscent to the phenotype produced by *hh* loss-of-function mutations, including that associated with the ci^{Cell} mutation that produces a truncated form of Ci, which behaves as a constitutive repressor [59]. Indeed, we observed a clear downregulation of Ci protein levels in cells in *ptc>mir-7* (Figure 6A–B″), which are precisely the cells receiving endogenous Hh signals and that upon normal Hh reception stabilize Ci protein levels and prevent the conversion of Ci-155 into truncated Ci repressor. Plots of fluorescence intensity profiles from the wild-type and *ptc>mir-7* discs are shown in Figure 6A′ and B″. The weak downregulation of Ci by mild RNAi expression using *ptc-Gal4* mimicked the L3–L4 fusion defect of *ptc>mir7* (Figure 6C–D). Depleting *ihog* by RNAi driven by *ptc-Gal4* did not produce a defect as *mir-7* overexpression (Figure 6E). The lack of effect of *ihog* RNAi is almost certainly due to the activity of the other Hh co-receptor, *boi*, which is expressed at high levels in the wing margin and in the presumptive L3 vein territory (*boi-lacZ* in green; Figure 6F). These results raised the possibility that like *ihog*, *ci* is also a direct target of miR-7. Indeed, *ci* mRNA does contain a presumptive miR-7 binding site in the *ci* 3′UTR, although this site is not conserved across *Drosophila* species. Thus, the Ci low protein levels in *ptc>mir-7* wing discs could reflect the direct repression of *ci* by the microRNA or the dampening of Hh signalling response by the miR-7-mediated downregulation of *ihog* or both. More consistently with indirect regulation of Ci by miR-7, we observed no change in Ci protein levels in wing discs ectopically expressing the *mir-7* away from the normal Hh secreting cells (the P compartment cells marked by the absence of Ci (green) in Figure 6G). In this experiment, we used the *Beadex* (*Bx*)*-Gal4* driver, with the Bx domain labelled by DsRed because of the *UAS-DsRed::mir-7* transgene (Figure 6G). Therefore, either Ci is not a target of miR-7 or this regulation is context dependent. It is generally considered that when an individual miRNA affects the expression of various proteins in the same pathway, it does so in a rather mild manner [74]. Thus, the relevance of co-regulation of *ihog* and *ci* by miR-7 in Hh receiving cells deserves further analysis given that the human counterparts of these genes (CDO, BOC, and Gli3) also contain binding sites for human miR-7.

Discussion

A challenge to understand oncogenesis produced by pleiotropic signalling pathways, such as Notch, Hh, and Wnts, is to unveil the complex cross-talk, cooperation, and antagonism of these signalling pathways in the appropriate contexts. Studies in flies, mice, and in human cell cultures have provided critical insights into the contribution of Notch to tumourigenesis. These studies highlighted that Notch when acting as an oncogene needs additional mutations or genes to initiate tumourigenesis and for tumour progression, identifying several determinants for such co-operation (e.g., [7,8,10,24,44,75–79]). The identification of these co-operative events has often been knowledge-driven, although unbiased genetic screens also identified known unanticipated tumour-suppressor functions. In this sense, we describe here a conserved microRNA that cooperates with Notch-induced overproliferation and tumour-like overgrowth in the *D. melanogaster* eye, miR-7. Alterations in microRNAs have been implicated in the initiation or progression of human cancers (e.g., [80–84]), although such roles of microRNAs have rarely been demonstrated in vivo (e.g., [85–88]). In addition, by identifying and validating functionally relevant targets of miR-7 in tumourigenesis, we also exposed a hitherto unsuspected tumour suppressor role for the Hh signalling pathway in the context of the oncogenic Notch pathway. Given the conservation of the Notch and Hh pathways, and the recurrent alteration of microRNAs in human cancers, we speculate that the genetic configuration of miR-7, Notch, and Hh is likely to participate in the development of certain human tumours.

In human cancer cells, miR-7 has been postulated to have an oncogene [89,90] or a tumour suppressor functions [91–96] that may reflect the participation of the microRNA in distinct

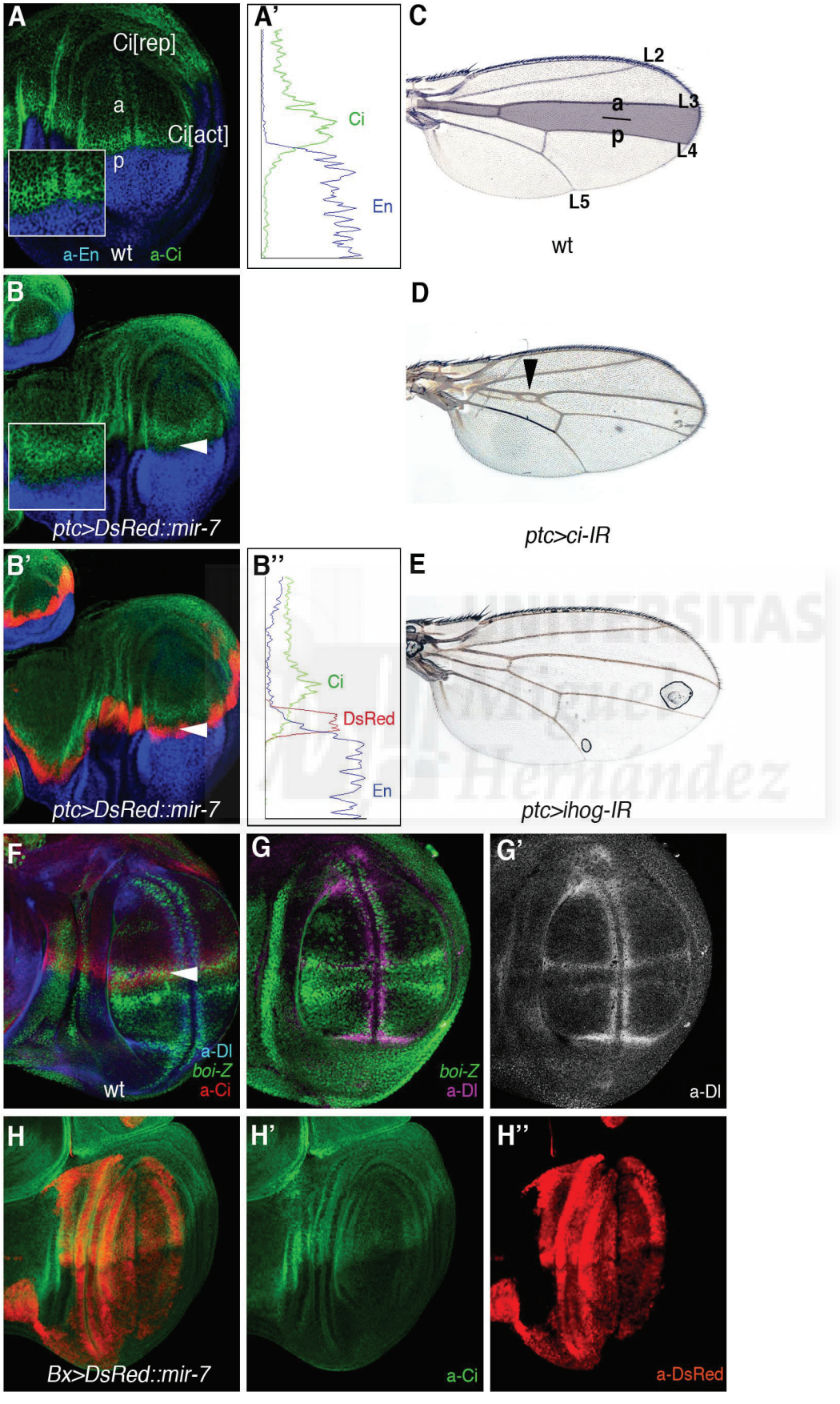
A
Ci[rep]
a
Ci[act]
p
a-En wt a-Ci
A'
Ci
En
C
L2
a
L3
p
L4
L5
wt
B
ptc>DsRed::mir-7
D
ptc>ci-IR
B'
ptc>DsRed::mir-7
B''
Ci
DsRed
En
E
ptc>ihog-IR
F
a-Dl
boi-Z
wt
a-Ci
G
boi-Z
a-Dl
G'
a-Dl
H
Bx>DsRed::mir-7
H'
a-Ci
H''
a-DsRed

Figure 6. miR-7 silencing of Hh signalling explains the L3–L4 fusion defects in the wing. (A) Ci protein (green) is distributed across the entire anterior (A) compartment of the discs. Hh signals from posterior (P) cells induce high levels of Ci in cells along the AP border, and they block Ci proteolysis into the repressor form (Ci[rep]), thereby allowing the Ci activator (C[act]) to accumulate. (B–B′) Overexpression of *mir-7* denoted by red labelling (*UAS-DsRed::mir-7*) driven by *patched (ptc)-Gal4* downregulates Hh signalling as visualized by low Ci levels (green; white arrowhead). Insets show magnifications. Engrailed (En) staining in blue serves to mark the P compartment in (A–B″). Plots of fluorescence intensity profiles of the anterior-posterior compartments from the WT (A) and *ptc>DsRed::mir-7* (B′) discs are shown in (A′) and (B″), respectively. Green trace, Ci; blue trace, En; red trace, DsRed. (C) Adult wild-type wing. The shaded area denotes the domain of expression of the *ptc-Gal4* reporter. (D) *ci-IR* expression by *ptc-Gal4* mimicking the L3–L4 fusion defect seen in adult wings that is caused by *mir-7* overexpression (compare with Figure 1G). (E) Adult wing expressing *ihog-IR* driven by *ptc-Gal4*. (F–F″) The expression of *boi-lacZ* (green) defines all longitudinal veins (L2–L5). Note the high *boi*-lacZ (green in F) expression along L3, marked by high Ci (red in F) and Dl (magenta in F″). (G–G″) Overexpression of *mir-7* (in red) by *Bx-Gal4* did not alter Ci protein levels (green, white arrowhead).
doi:10.1371/journal.pbio.1001554.g006

pathways, due to the regulation of discrete target genes in different cell types, such as *Fos* [97] in mouse, and *Pak1* [91], *IRS-2* [92], *EGFR* [92,93], *Raf-1* [93], α*-synuclein* [98], *CD98* [99], *IGFR1* [94], *bcl-2* [100], PI3K/AKT [101,102], and *YY1* [103] in humans.

In *Drosophila*, multiple, cell-specific, targets for miR-7 have been previously validated via luciferase or in vivo eGFP-reporter sensors or less extensively via functional studies [47,49,73,104–107]. Although microRNAs are thought to regulate multiple target genes, when tested in vivo it is a subset or a given target that predominates in a given cellular context. Indeed, of the 39 predicted miR-7 target genes tested by direct RNAi, only downregulating *ihog* with several RNAi transgenes (*UAS-ihog-IR*) fully mimicked the effect of miR-7 overexpression in the transformation of *Dl*-induced mild overgrowth into severe overgrowth and even tumour-like growth. Moreover, we confirmed that endogenous *ihog* is directly silenced by miR-7 and that this silencing involves direct binding of the microRNA to sequences in the 3′UTR of *ihog* both in vivo and in vitro.

Nevertheless, other miR-7 target genes may contribute to the cooperation with Dl-Notch pathway along with *ihog*, such as *hairy* and *Tom*. While miR-7 can directly silence *hairy* in the wing, this effect has been shown to be very modest [48], and thus, we consider that while *hairy* may contribute to such effects, it is unlikely to be instrumental in this tumour model. Indeed, the loss of *hairy* is inconsequential in eye development [108], although retinal differentiation is accelerated by genetic mosaicism of loss of *hairy* and *extramacrochaetae* [108]. *hairy* is a target of Hh [18,21] that negatively sets the pace of MF progression. It is unclear how Hairy might contribute to Dl-induced tumourigenesis.

The RNAi against *Tom* produced overgrowth with the gain of *Dl* albeit inconsistently and with weak penetrance, where one RNAi line did not modify the Dl-induced overgrowth and the other RNAi line caused tumours in less than 40% of the progeny (Table S1). Tom is required to counteract the activity of the ubiquitin ligase Neuralized in regulating the Notch extracellular domain, and Dl in the signal emitting cells. These interactions are normally required to activate Notch signalling in the receiving cells through lateral inhibition and cell fate allocation [109]. However, although it remains to be shown whether similar interactions are active during cell proliferation and growth, the moderate enhancement of *Dl* that is induced when *Tom* is downregulated by RNAi suggests that miR-7-mediated repression of *Tom* may contribute to the oncogenic effects of miR-7 in the context of *Dl* gain of function, along with other targets such as *ihog*.

Conversely, while the target genes of the Notch pathway, *E(spl)m3* and *E(spl)m4* [48] as well as *E(spl)mγ*, *Bob*, *E(spl)m5*, and *E(spl)mδ* [60], have been identified as direct targets of miR-7 in the normal wing disc via analysis of 3′UTR sensors, there was no evidence that *HLHm3*, *HLHm4*, *HLHm5*, *Bob*, and *HLHmγ* are biological relevant targets of miR-7 in the Dl overexpression context. *HLHmδ* RNAi produced inconsistent phenotypes in the two RNAi transgenic lines available, causing tumour-like growth at very low frequency in only one of the lines (Table S1). We also did not obtain evidence that miR-7 provoked overgrowth by targeting the ETS transcription factor in the EGFR pathway AOP/Yan (Table S1), a functionally validated target of the microRNA miR-7 during retinal differentiation [47]. Neither had we obtained evidence that RNAi of *atonal* provoked eye tumours with Dl overexpression (Table S1), although a strong inhibition via expression of a fusion protein Atonal::EN that converts Atonal into a transcriptional repressor has been shown to be sufficient to trigger tumorigenesis together with Dl [24]. Thus, we reasoned that given that microRNA influenced target genes only subtly (even when using ectopic expression), it is possible that downregulation of *atonal* contributes to the phenotype along with the other targets.

In conclusion, we have identified cooperation between the microRNA miR-7 and Notch in the *D. melanogaster* eye and identified and validated *ihog* as a direct target of the miR-7 in this context and have identified *boi* as a target of Notch-mediated activity at the DV eye organizer, although it remains whether this regulation is direct or indirect. We also uncovered a hitherto unanticipated tumour suppressor activity of the endogenous Hh signalling pathway in the context of gain of Dl-Notch signalling (Figure 4) that is also apparent during wing development (Figure 5).

Hh tumour suppressor role is revealed when components of the Hh pathway were lost in conjunction with a gain of Dl expression in both the eye (Figure 4) and wing (Figure 5 and Figure S8) discs. Hh and Notch establish signalling centres along the AP and DV axes, respectively, of the disc to organize global growth and patterning. Where the organizer domains meet, the Hh and Notch conjoined activities specify the position of the MF in the eye disc and the proximodistal patterning in the wing disc [25,47,48]. We unveil here that in addition antagonistic interaction between the Hh and Notch signalling might help to ensure correct disc growth. Thus, we show that Hh signalling limits the organizing activity of Dl-Notch signalling (Figure 4, Figure 5, and Figure S8). Although it is often confounded whether Dl-Notch signalling instructs overgrowth by autonomous or nonautonomous (i.e., DV organizers) mechanisms, our findings uncover that loss of Hh signalling enhances a noncell autonomous oncogenic role of Dl-Notch pathway (Figure 4J and Figure S8D).

To date, Hh has not yet to be perceived as a tumour suppressor, although it is noteworthy that human homologs of ihog, CDO, and BOC were initially identified as tumour suppressors [42]. Importantly, both CDO and BOC are downregulated by RAS oncogenes in transformed cells [42] and their overexpression can inhibit tumour cell growth in vitro [42,110,111]. Since human RAS regulates tumourigenesis in the lung by overexpressing miR-7 in an ERK-dependent manner [90], it is possible that RAS represses CDO and BOC via this microRNA. Indeed, the 3′UTR of both *CDO* and *BOC* like *Drosophila ihog* contains predicted binding sites for miR-7 (www.targetscan.org). There is additional clinical and experimental evidence connecting elements of the Hedgehog pathway with tumour-suppression. The function of

Growth arrest specific gene 1 (*GAS1*), a Hh ligand-binding factor, overlaps that of *CDO* and *BOC* [39,41] and its downregulation is positively associated with cancer cells [94] and melanoma metastasis [112], while its overexpression inhibits tumour growth [113]. More speculative is the association of some cancer cells with the absence of cilium, a structure absolutely required for Hh signal transduction in vertebrate cells [27].

Given the pleiotropic nature of Notch, Wnts, BMP/TGFß, Ras, and Hh signalling pathways in normal development in vivo, we speculate that competitive interplay as that described here between Notch and Hh may not be uncommon among core growth control and cancer pathways that act within the same cells at the same or different time to exert multiple outputs (such as growth and cell differentiation). Moreover, context-dependent tumour suppressor roles could explain the recurrent, unexplained, identification of somatic mutations in Hh pathway in human cancer samples (e.g., [43]). Indeed, our findings stimulate a re-evaluation of the signalling pathways previously considered to be exclusively oncogenic, such as the Hh pathway.

Materials and Methods

Drosophila Husbandry

The *GS(2)518ND2* line was isolated in a genetic screen for enhancers or suppressors of a mild overgrown eye phenotype induced by *Dl* overexpression when driven by the eye-specific *ey-Gal4* driver (*ey-Gal4 UAS-Dl*). The *PlacWP1O111* stock was a generous gift from Dr. C. Klambt (Munster University, Munster, Germany), and the other *Drosophila* stocks used here were: *UAS-mir-7* and *UAS-DsRed::mir-7* [47], *UAS-boi* [56], *UAS-ci* [57], and *UAS-ci-75* [58,59]. A detailed description of the stocks and transgenic flies used in this study can be found at http://flybase.org/ for *ey-Gal4*, *ptc-Gal4*, *en-Gal4*, *hsp70-Gal4*, *Bx-Gal4*, *UAS-Dl*, *UAS-fng*, *UAS-hh*, *UAS-eyg*, *EP(X)1447 (boi)*, hh^{AC}, and smo^{3}or at http://flystocks.bio.indiana.edu/ and http://stockcenter.vdrc.at/control/main for the BDSC and VDRC RNAi stocks, respectively. Clones of hh^{AC} surrounded by *Dl*-expressing tissue (Figure 4J) were generated by the ey-Flp in eye-antennal imaginal discs of the genotype: *yw ey-Flp; ey-Gal4 UAS-Dl/+; FRT82B* hh^{AC}*/FRT82B arm-lacZ*. In Figure S8, the MARCM GFP-labelled clones of smo^{3}/smo^{3} only or smo^{3}/smo^{3}*tub-Gal4 UAS-Dl* cells were induced by 1 h heat shock at 37°C at 48–72 h AEL in larvae: *y w tub-Gal4 UAS-GFP hsp70-FLP122;* smo^{3} *FRT40A ptc-lacZ/tub-Gal80 FRT40A* and *y w tub-Gal4 UAS-GFP hsp70-FLP122;* smo^{3} *FRT40A ptc-lacZ/tub-Gal80 FRT40A; UAS-Dl/+*, respectively.

All the combinations of *Gal4*, *GS*, and the different *UAS* transgenic lines and mutants were raised at 26.5°C.

GS-Element and PlacW Mapping

Genomic DNA flanking the *P*-element insertion in the *GS(2)518ND2* and the *PlacWP1O111*stock were recovered by inverse PCR using the Pwht1/Plac1 and Plw3-1/Pry 4 primers, respectively (http://www.fruitfly.org/about/methods/inverse.pcr.html), and they were subsequently sequenced. A BLAST search with the sequence produced perfect matches to the genomic region on chr2R:16491078 for *GS(2)518ND2* and on chrX: 2364036 for *PlacWP1O111*.

Quantitative Reverse Transcriptase PCR (qRT-PCR)

To assess the levels of *ihog* or *boi* mRNA when the *mir-7* or RNAi lines were activated by Gal4, we performed qRT-PCR experiments using RNA isolated from wandering third instar larvae of the *hsp70-Gal4* genotype crossed with transgenic lines (*UAS-mir-7*, *UAS-ihog-IR*, or *UAS-boi-IR*) directly or following heat shock (an hour at 37°C followed by 6 h at 25°C). Total RNA from 50 pairs of eye-antennal discs was extracted for experiments in Figure 3J. All tissue samples were stored in RNAlaterTissueProtect Tubes (Qiagen) until used and mature *mir-7*, *ihog*, or *boi* mRNA levels were assessed by qRT-PCR. Note that RNA was isolated from whole eye-antennal disc complexes; thus, the levels of *boi* and *ihog* mRNA expression are the sum of all regions of the discs, including the antennal disc part that might not be unaffected by the expression of *ey-Gal4*. Thus, expression differences between the control and *Dl* and/or *mir-7* overexpressing eye-antennal disc complexes may be significant underestimations of the actual differences in the relevant eye disc part in each genotype. To analyse mature *mir-7* expression, we used *mir-7*-specific primers from the TaqMan MicroRNA Assays (Applied Biosystems), together with the TaqMan MicroRNA Reverse Transcription Kit (Applied Biosystems) and TaqMan Universal PCR Master Mix (Applied Biosystems). The *mir-7* levels were normalized to *U14* snRNA. To determine *ihog* and *boi* mRNA levels, we used SuperScript First-Strand Synthesis System for RT–PCR (Invitrogen) and SYBR Green PCR Master kit (Applied Biosystems), according to the manufacturer's instructions. The cDNAs were amplified using specific primers designed using the ProbeFinder software by Roche Applied Science, and *rp49* was used as a house-keeping gene for normalization.

Primer sequences used in this study include the following: *ihog*, forward primer 5′-TCAGTCTAAAATCCCATAATAAGTGC-3, reverse primer 5′-AAACCGGAATTGCTTCGAG-3′; *boi*, forward primer 5′-TGCCTAAAGAGACGGGAAAA-3′, reverse primer 5′-ATGTGTTCCAATTGCGGTTT-3′; and *rp49*, forward primer 5′-TGTCCTTCCAGCTTCAAGATGACCATC-3′, reverse primer 5′-CTTGGGCTTGCGCCATTTGTG-3′.

In all cases, samples were tested in triplicate and qPCR reactions were run on a 7500 Real-Time PCR System (Applied Biosystems) following the manufacturer's protocol. The data shown are the mean ± s.e.m. of three experiments, and the relative expression was calculated using the comparative C_t method. The qPCR data were analysed by a two-tailed unpaired *t* test.

Immunofluorescence Staining

Third instar imaginal discs were fixed and stained by standard procedures using the following primary antibodies (dilutions, sources): anti-Eyg (1:100, [98]), anti-Elav (1:100, DSHB: Developmental Studies Hybridoma Bank), 4D4 (anti-Wg, 1:100, DSHB), 4D9 (anti-En, 1:100, DSHB), anti-phospho-H3 (anti-PH3; 1:500, Sigma), anti-GFP (1:1,000, Invitrogen), anti-β-galactosidase (1:2,000, Cappel), anti-Cut (1:5,000, DSHB), anti-*D*E-cad (1.50, DSHB), anti-Dac (1:100, DSHB), anti-Ci (1:5; a gift from Dr. Holgrem), anti-luciferase (luci27) (1:200, Thermo Scientific), and anti-DsRed (1:2,000, Clontech). The secondary antibodies used were conjugated to AlexaFluor-488, -555, -647 (Molecular Probes), and diluted at 1:400. Discs were mounted in Fluoromount G (Southern Biotechnology), and the images were captured on a Leica TCS-NT Confocal microscope. The RGB Profile Plot function of ImageJ was employed for the intensity profile plots in Figure 6A′ and B″.

Construction of Sensor Transgenes

The *tub-luc::ihog3′UTR* or *tub-luc::boi3′UTR* constructs were generated by cloning the full-length 3′ UTR of the *Drosophila ihog* or *boi* genes into the 3′ end of the *tub-firefly luciferase* plasmid. To construct the *tub-luc::ihog*^{mut}*3′UTR* reporter, three nucleotides of the predicted binding site for miR-7 in the *ihog* 3′UTR were mutated (AGTCTTCCA to AGTCATGCT) using the QuickChange Site-Directed Mutagenesis kit (Agilent Technologies Inc.). The *tub-eGFP::ihog3′UTR* or *tub-eGFP::boi3′UTR* constructs were

generated by cloning the full-length 3′UTR of *ihog* or *boi* genes into the 3′ end of the *tub-eGFP* reporter vector (a gift from Dr. Cohen). The final constructs were verified by sequencing. Transgenic eGFP and luciferase sensor flies were generated on a w^{1118} background by standard transformation into *Drosophila* embryos (BestGene Inc.).

Luciferase Reporter Assays

For *Drosophila* S2 cell luciferase assays, cells were co-transfected in 24-well plates as described previously [7] with the *Renilla* luciferase plasmid (75 ng) for normalization and different combinations of the following plasmids: *actin-Gal4* (400 ng), *pUAS-mir-7* or empty *pUAST* (400 ng; [48]), *tub-luc::ihog3′UTR*, *tub-luc::boi3′UTR*, or *tub-luc::ihog^{mut}3′UTR* (25 ng). The relative luciferase activity was measured 48 h after transfection using the Dual-Glo Luciferase Reporter Assay system (Promega) according to the manufacturer's instructions. The data shown are the mean ± s.e.m. of three independent experiments, which was analysed by a two-tailed unpaired *t* test.

Measurement of PH3 Positive Cells

Female virgin *w; ey-Gal4 UAS-Dl/Cy0-GFP* were crossed to males *w; +/+; UAS-DsRed::mir-7* and their F1 progeny larvae (*w; ey-Gal4, UAS-Dl/+; UAS-DsRed::mir-7/+*) were selected by *DsRed* labelling in the pair of eye-antennal discs. The particle analysis function of ImageJ software was used to count PH3-positive nuclei of the confocal images of third instar imaginal discs to generate the data shown in Figure 1J. The analyses of the area of eye disc and antennal disc parts in Figure S4H was done using ImageJ, and data represent mean values of area of eye discs normalized against the antennal disc part in at least six discs *per* genotype.

Supporting Information

Figure S1 Hh signal along the disc AP axis and Notch-mediated DV growth promoting organizer starts long before the initiation of retinal differentiation. (A) Mid second larval instar (LII) eye disc carrying the enhancer trap line *hh^{P30}-lacZ* and stained for ßgalactosidase (hh-Z, green), Wg (red), and Elav (blue). The absence of blue staining denotes that the MF has not yet initiated in this disc. (B) Mid-late LII eye disc carrying the *eyg-lacZ* enhancer trap line and stained for ßgal (blue) and Wg (red). Notch signalling target Eyg expression labels the growth organizer. Disc as in Figure 3F.
(TIF)

Figure S2 The conserved MicroRNA miR-7 and Dl-Notch pathway cooperatively induce eye overgrowth. (A–C) Illustrative images of adult eyes overexpressing *Dl* with the *GS(2)518* line (A) or the *UAS-mir-7* transgene (B–C) with *ey-Gal4*. (A) The overgrown, folded eye tissue often present areas of undifferentiated or poorly differentiated outgrowths (arrowhead) (10%, $n = 200$ in A). The undifferentiated outgrowths are seen also in flies co-expressing *Dl* with the *UAS-mir-7* transgene (B and C). (D) Quantification of relative mature *mir-7* RNA levels in larvae carrying *hsp70>mir-7* after heat shock (red bar) or not (blue bar). *P* was calculated using the Student *t* test, and values represented the mean ± sem. of three independent experiments.
(TIF)

Figure S3 Overgrowth and abnormal neuronal differentiation progression in eye discs co-expressing *Dl* and the *GS(2)518* line. Confocal images of eye discs of control wild type (*ey>*, A, C, E, and G) and eye discs overexpressing *Dl* and *mir-7* by *ey-Gal4* (*ey>Dl>GS(2)518*: B, D, F, H–J) and carrying the indicated enhancer trap lines to monitor DV patterning: expression of D marker *mirror-lacZ* (*mirr-Z*), ventral marker *fringe-lacZ* (*fng-Z*), DV organizer-specific marker *Serrate-lacZ* (*Ser-Z*), and *eyegone-lacZ* (*Eq-Z*). Eye discs are stained for ßgalactosidase (green), neuronal marker Elav (blue), or Wg (red). (I–J′) Eye discs are stained for Dac (pink) or *D*E-cadherin (*D*E-cad, green in I and J and grey in I′ and J′) to highlight the morphology of the front of retinal differentiation (MF) and cell shape changes the accompanied neuronal differentiation, respectively. Although it has been postulated that the microRNA mir-7 silences Notch signalling, the overexpression of *mir-7* with *Dl* causes eye disc overgrowth associated with enhanced Dl-Notch signalling as detected by the misexpression of DV organizer-specific markers (F and H). Seldom the pattern of retinal differentiation is highly disrupted in the overgrown discs (F and H) and often the front of neuronal differentiation (arrowhead, I′) is highly irregular or advanced in discs co-expressing *Dl* and *GS(2)518* line. Anterior is to the left. Scale bar, 2 mm.
(TIF)

Figure S4 Overgrowth and abnormal neuronal differentiation progression in eye discs co-expressing *Dl* and the microRNA *mir-7* or the *ihog-IR* or *ci-IR* transgenes. Confocal images of mitotic marker PH3 (blue in A–E; pink in F and green in G), neuronal marker Elav (green, A–F and red in G), and Wg (red, A–D and pink in F) staining of third instar eye-antennal imaginal discs of wild-type *ey-Gal4* (*ey>*, A–A′), *ey-Gal4 UAS-Dl* (*ey>Dl*, B–B′), *ey-Gal4 UAS-Dl/+*; *UAS-mir-7/+* (*ey>Dl>mir-7*, C–D′), *ey-Gal4UAS-Dl/+*; *UAS-ihog-IR/+* (*ey>Dl>ihog-IR*, E–F), and *ey-Gal4 UAS-Dl/+*; *UAS-ci-IR/+* (*ey>Dl>ci-IR*, G). The asterisks point to undifferentiated outgrowth of the eye discs (C, F, and G). Disc in (C) is as in Figure 1H. Note that eye disc overgrowth is also accompanied by advanced or disorganized front of retinal differentiation. The *ey-Gal4* transgene drives expression anterior to the MF (white arrowhead in A), where eye disc cells proliferate asynchronously. Posterior to the MF, subsets of cells start differentiating into photoreceptor neurons visualized by the neuronal marker Elav (green, A) and the remaining cells divide one last time synchronously (row of PH3 cells behind the MF). (H) Quantitation of the eye imaginal disc size of the indicated genotypes. The area for each disc was calculated in pixel using ImageJ and values were normalized with those of the corresponding antennal disc part. As expected, co-expressing *Dl* with the RNAi against *ihog* or *ci* with *ey-Gal4* provoked overgrowth similar, but stronger than the misexpression of the *mir-7*. Anterior is to the left in all images, and dorsal is up.
(TIF)

Figure S5 Quantification of *ihog* and *boi* mRNAs and mature *mir-7* levels. (A) Relative *ihog* mRNA levels in larvae. (B) Relative *boi* mRNA levels in larvae. (C) Relative miR-7 levels in S2 cells transfected with *actGal5* plasmid and with (red bar) or without (blue bar) the *UAS mir-7* plasmid. The values represented the mean ± s.e.m. of at least three independent experiments. Data analysed by a two-tailed unpaired *t* test.
(TIF)

Figure S6 Overexpression of *DsRed::mir-7* by *en-Gal4* in the wing disc also caused reproducible in vivo downregulation of *eGFP* in a *tub-eGFP::ihog-3′UTR* (A) but not in a *tub-eGFP::boi-3′UTR* sensor (B).
(TIF)

Figure S7 Invasive growth caused by co-expressing *Dl* and *ci-IR* in the wing primordium. (A) Wild-type third instar wing imaginal discs. Dpp-GAL4 (*dpp>*) drives expression of *UAS-GFP* (gree) in a narrow band of anterior cells along the AP compartment

boundary. Expression of mitotic marker PH3 (blue) and En (red) are also shown. (B) Expression of the RNAi transgene against *ci* (*dpp>ci-IR*) led to anterior expansion of the *dpp* domain visualized by GFP (green) and ectopic P cells (grey in B′) in the A territory at the DV boundary, but the disc is not overgrown. (C, D) Co-expression of *Dl* along with *ci-IR* led to extensive overgrowths. Note that mutant A cells mix with wild-type P (En, positive) cells (arrowheads) in some parts, reminiscent of malignant growth. Expression of Ci (grey in the inset) is also shown in (D).
(TIF)

Figure S8 Blocking Hh signal transduction due to mutations in smoothened enhances organizing activity by Dl-Notch signalling in the mosaic eye and wing discs. (A) Control eye discs carrying MARCM *GFP*(green)-labelled smo^3 clones and (B) GFP-labelled clones of smo^3 that overexpress *Dl* and stained for *ptc-lacZ* (Ptc-Z, blue) and Ci (blue). Note that the smo^3/smo^3*tub-Gal4 UAS-Dl* clones cause nonautonomously advancement of the MF denoted by up-regulated Ci levels, similar to the effect seen in eye discs co-expressing *Dl* with the *mir-7*. (A′) and (B′) show single channel confocal images. (C) Wing discs carrying MARCM *GFP*-labelled clones of smo^3 cells and staining for Wg (red, C and C″) and clones of smo3 that overexpress Dl (smo^3/smo^3 *tub>Dl*, D–D″). In (D–D″), arrowheads point to ventrally situated clones of anterior origin (visualized by *ptc-lacZ*, not shown). The asterisk points to a clone of ambiguous A origin with weak ectopic Wg only in the anterior portion of the clone. DAPI counterstaining (pink, C‴ and D‴) is shown to illustrate the stimulation of growth of the surrounding tissue by the *smo3 tub-Dl* clones. Genotype in (A and C) is *yw tub-Gal4 UAS-GFP hsp70-Flp;* smo^3 *FRT40A ptc-lacZ/tub-Gal80 FRT40A* and in (B and D) is *yw tub-Gal4 UAS-GFP hsp70-Flp;* smo^3 *FRT40A ptc-lacZ/tub-Gal80 FRT40A; UAS-Dl/+*.
(TIF)

Figure S9 General genetic scheme of crosses for rescuing experiments in Figure 4. Similar genetic schemes were following the rescue by the UAS-boi transgene in Figure 3J. Larvae carrying both the chromosomes with the transgenes *ey-Gal4 UAS-Dl* (2nd) and *UAS-DsRed::mir-7* (3rd) were selected under a fluorescence binocular (MZFLIII, Leica) for expression of DsRed in the eye under the control of Gal4. The resulting adult males were crossed to female virgins of the genotype *UAS-hh/CyO*. Larvae resulting from the cross were again selected and the DsRed-positive were transferred to a new tube, and the eyes of the resulting non-CyO adults eyes (males and females) were analysed.
(DOCX)

Table S1 Identification of candidate tumour-suppressor gene(s) of *Drosophila* in silico predicted miR-7 target genes in the gain of Dl context.
(DOCX)

Table S2 Direct inhibition by RNAi expression of core Hedgehog pathway genes in the gain of Dl context.
(DOCX)

Acknowledgments

We thank Dr. R. Carthew, Dr. C. Klambt, Dr. A.M. O'Reilly, the Bloomington Stock Center, and the Vienna Drosophila Research Centre for fly stocks; Dr. N. Aspiazu for the anti-Eyg antibody; and Dr. Carthew and Dr. S. Cohen for the *pUAS-mir-7* and the *tub::eGFP* plasmids, respectively. We also thank members of the lab for helpful comments, and I. Gutierrez-García and E. Ballesta-Illan for technical assistance.

Author Contributions

The author(s) have made the following declarations about their contributions: Conceived and designed the experiments: VDR MD. Performed the experiments: VDR IGP DFM MD. Analyzed the data: VDR MD. Contributed reagents/materials/analysis tools: VDR IGP DFM. Wrote the paper: VDR MD.

References

1. Day SJ, Lawrence PA (2000) Measuring dimensions: the regulation of size and shape. Development 127: 2977–2987.
2. Irvine KD, Rauskolb C (2001) Boundaries in development: formation and function. Annu Rev Cell Dev Biol 17: 189–214. doi:10.1146/annurev.cellbio.17.1.189.
3. Crickmore MA, Mann RS (2006) Hox control of organ size by regulation of morphogen production and mobility. Science 313: 63–68. doi:10.1126/science.1128650.
4. Affolter M, Basler K (2007) The Decapentaplegic morphogen gradient: from pattern formation to growth regulation. Nat Rev Genet 8: 663–674. doi:10.1038/nrg2166.
5. Wartlick O, Mumcu P, Kicheva A, Bittig T, Seum C, et al. (2011) Dynamics of Dpp signaling and proliferation control. Science 331: 1154–1159. doi:10.1126/science.1200037.
6. Efstratiadis A, Szabolcs M, Klinakis A (2007) Notch, Myc and breast cancer. Cell Cycle 6: 418–429.
7. Vallejo DM, Caparros E, Dominguez M (2011) Targeting Notch signalling by the conserved miR-8/200 microRNA family in development and cancer cells. EMBO J 30: 756–769. doi:10.1038/emboj.2010.358.
8. Fre S, Pallavi SK, Huyghe M, Laé M, Janssen K-P, et al. (2009) Notch and Wnt signals cooperatively control cell proliferation and tumorigenesis in the intestine. Proc Natl Acad Sci USA 106: 6309–6314. doi:10.1073/pnas.0900427106.
9. Palomero T, Sulis ML, Cortina M, Real PJ, Barnes K, et al. (2007) Mutational loss of PTEN induces resistance to NOTCH1 inhibition in T-cell leukemia. Nat Med 13: 1203–1210. doi:10.1038/nm1636.
10. Ntziachristos P, Tsirigos A, Van Vlierberghe P, Nedjic J, Trimarchi T, et al. (2012) Genetic inactivation of the polycomb repressive complex 2 in T cell acute lymphoblastic leukemia. Nat Med 18: 298–301. doi:10.1038/nm.2651.
11. Dominguez M, Casares F (2005) Organ specification-growth control connection: new in-sights from the Drosophila eye-antennal disc. Dev Dyn 232: 673–684. doi:10.1002/dvdy.20311.
12. Chao JL (2004) Localized Notch signal acts through eyg and upd to promote global growth in Drosophila eye. Development 131: 3839–3847. doi:10.1242/dev.01258.
13. Dominguez M, Ferres-Marco D, Gutierrez-Aviño FJ, Speicher SA, Beneyto M (2004) Growth and specification of the eye are controlled independently by Eyegone and Eyeless in Drosophila melanogaster. Nat Genet 36: 31–39. doi:10.1038/ng1281.
14. Yao J-G, Sun YH (2005) Eyg and Ey Pax proteins act by distinct transcriptional mechanisms in Drosophila development. EMBO J 24: 2602–2612. doi:10.1038/sj.emboj.7600725.
15. Salvany L, Requena D, Azpiazu N (2012) Functional association between Eyegone and HP1a mediates wingless transcriptional repression during development. Mol Cell Biol 32: 2407–2415. doi:10.1128/MCB.06311-11.
16. Baker NE (2007) Patterning signals and proliferation in Drosophila imaginal discs. Curr Opin Genet Dev 17: 287–293. doi:10.1016/j.gde.2007.05.005.
17. Ma C, Zhou Y, Beachy PA, Moses K (1993) The segment polarity gene hedgehog is required for progression of the morphogenetic furrow in the developing Drosophila eye. Cell 75: 927–938.
18. Heberlein U, Singh CM, Luk AY, Donohoe TJ (1995) Growth and differentiation in the Drosophila eye coordinated by hedgehog. Nature 373: 709–711. doi:10.1038/373709a0.
19. Dominguez M, Hafen E (1997) Hedgehog directly controls initiation and propagation of retinal differentiation in the Drosophila eye. Genes Dev 11: 3254–3264.
20. Borod ER, Heberlein U (1998) Mutual regulation of decapentaplegic and hedgehog during the initiation of differentiation in the Drosophila retina. Dev Biol 197: 187–197. doi:10.1006/dbio.1998.8888.
21. Pappu KS, Chen R, Middlebrooks BW, Woo C, Heberlein U, et al. (2003) Mechanism of hedgehog signaling during Drosophila eye development. Development 130: 3053–3062.
22. Firth LC, Baker NE (2005) Extracellular signals responsible for spatially regulated proliferation in the differentiating Drosophila eye. Dev Cell 8: 541–551. doi:10.1016/j.devcel.2005.01.017.

23. Roignant J-Y, Treisman JE (2009) Pattern formation in the Drosophila eye disc. Int J Dev Biol 53: 795–804. doi:10.1387/ijdb.072483jr.
24. Bossuyt W, De Geest N, Aerts S, Leenaerts I, Marynen P, et al. (2009) The atonal proneural transcription factor links differentiation and tumor formation in Drosophila. Plos Biol 7: e40. doi:10.1371/journal.pbio.1000040.
25. Cavodeassi F, Diez Del Corral R, Campuzano S, Dominguez M (1999) Compartments and organising boundaries in the Drosophila eye: the role of the homeodomain Iroquois proteins. Development 126: 4933–4942.
26. Christiansen AE, Ding T, Bergmann A (2012) Ligand-independent activation of the Hedgehog pathway displays non-cell autonomous proliferation during eye development in Drosophila. Mech Dev 129: 98–108. doi:10.1016/j.mod.2012.05.009.
27. Ingham PW (2012) Hedgehog signaling. Cold Spring Harbor Perspectives in Biology 4. doi:10.1101/cshperspect.a011221.
28. Yao S, Lum L, Beachy P (2006) The Ihog cell-surface proteins bind hedgehog and mediate pathway activation. Cell 125: 343–357. doi:10.1016/j.cell.2006.02.040.
29. McLellan JS, Yao S, Zheng X, Geisbrecht BV, Ghirlando R, et al. (2006) Structure of a heparin-dependent complex of Hedgehog and Ihog. Proc Natl Acad Sci USA 103: 17208–17213. doi:10.1073/pnas.0606738103.
30. Camp D, Currie K, Labbé A, van Meyel DJ, Charron F (2010) Ihog and Boi are essential for Hedgehog signaling in Drosophila. Neural Dev 5: 28. doi:10.1186/1749-8104-5-28.
31. Yan D, Wu Y, Yang Y, Belenkaya TY, Tang X, et al. (2010) The cell-surface proteins Dally-like and Ihog differentially regulate Hedgehog signaling strength and range during development. Development 137: 2033–2044. doi:10.1242/dev.045740.
32. Zheng X, Mann RK, Sever N, Beachy PA (2010) Genetic and biochemical definition of the Hedgehog receptor. Genes Dev 24: 57–71. doi:10.1101/gad.1870310.
33. Okada A, Charron F, Morin S, Shin DS, Wong K, et al. (2006) Boc is a receptor for sonic hedgehog in the guidance of commissural axons. Nature 444: 369–373. doi:10.1038/nature05246.
34. Tenzen T, Allen BL, Cole F, Kang J-S, Krauss RS, et al. (2006) The cell surface membrane proteins Cdo and Boc are components and targets of the Hedgehog signaling pathway and feedback network in mice. Dev Cell 10: 647–656. doi:10.1016/j.devcel.2006.04.004.
35. McLellan JS, Zheng X, Hauk G, Ghirlando R, Beachy PA, et al. (2008) The mode of Hedgehog binding to Ihog homologues is not conserved across different phyla. Nature 455: 979–983. doi:10.1038/nature07358.
36. Cohen MM (2010) Hedgehog signaling update. Am J Med Genet A 152A: 1875–1914. doi:10.1002/ajmg.a.32909.
37. Kavran JM, Ward MD, Oladosu OO, Mulepati S, Leahy DJ (2010) All mammalian Hedgehog proteins interact with cell adhesion molecule, down-regulated by oncogenes (CDO) and brother of CDO (BOC) in a conserved manner. J Biol Chem 285: 24584–24590. doi:10.1074/jbc.M110.131680.
38. Beachy PA, Hymowitz SG, Lazarus RA, Leahy DJ, Siebold C (2010) Interactions between Hedgehog proteins and their binding partners come into view. Genes Dev 24: 2001–2012. doi:10.1101/gad.1951710.
39. Izzi L, Lévesque M, Morin S, Laniel D, Wilkes BC, et al. (2011) Boc and Gas1 each form distinct Shh receptor complexes with Ptch1 and are required for Shh-mediated cell proliferation. Dev Cell 20: 788–801. doi:10.1016/j.devcel.2011.04.017.
40. Zhang W, Hong M, Bae G-U, Kang J-S, Krauss RS (2011) Boc modifies the holoprosencephaly spectrum of Cdo mutant mice. Dis Model Mech 4: 368–380. doi:10.1242/dmm.005744.
41. Allen BL, Song JY, Izzi L, Althaus IW, Kang J-S, et al. (2011) Overlapping roles and collective requirement for the coreceptors GAS1, CDO, and BOC in SHH pathway function. Dev Cell 20: 775–787. doi:10.1016/j.devcel.2011.04.018.
42. Kang JS, Gao M, Feinleib JL, Cotter PD, Guadagno SN, et al. (1997) CDO: an oncogene-, serum-, and anchorage-regulated member of the Ig/fibronectin type III repeat family. J Cell Biol 138: 203–213.
43. Jones S, Zhang X, Parsons DW, Lin JC-H, Leary RJ, et al. (2008) Core signaling pathways in human pancreatic cancers revealed by global genomic analyses. Science 321: 1801–1806. doi:10.1126/science.1164368.
44. Ferres-Marco D, Gutierrez-Garcia I, Vallejo DM, Bolivar J, Gutierrez-Aviño FJ, et al. (2006) Epigenetic silencers and Notch collaborate to promote malignant tumours by Rb silencing. Nature 439: 430–436. doi:10.1038/nature04376.
45. Aboobaker AA, Tomancak P, Patel N, Rubin GM, Lai EC (2005) Drosophila microRNAs exhibit diverse spatial expression patterns during embryonic development. Proc Natl Acad Sci USA 102: 18017–18022. doi:10.1073/pnas.0508823102.
46. Charroux B, Freeman M, Kerridge S, Baonza A (2006) Atrophin contributes to the negative regulation of epidermal growth factor receptor signaling in Drosophila. Dev Biol 291: 278–290. doi:10.1016/j.ydbio.2005.12.012.
47. Li X, Carthew RW (2005) A microRNA mediates EGF receptor signaling and promotes photoreceptor differentiation in the Drosophila eye. Cell 123: 1267–1277. doi:10.1016/j.cell.2005.10.040.
48. Stark A, Brennecke J, Russell RB, Cohen SM (2003) Identification of Drosophila MicroRNA targets. Plos Biol 1: E60. doi:10.1371/journal.pbio.0000060.
49. Li X, Cassidy JJ, Reinke CA, Fischboeck S, Carthew RW (2009) A MicroRNA imparts robustness against environmental fluctuation during development. Cell 137: 273–282. doi:10.1016/j.cell.2009.01.058.
50. Dietzl G, Chen D, Schnorrer F, Su K-C, Barinova Y, et al. (2007) A genome-wide transgenic RNAi library for conditional gene inactivation in Drosophila. Nature 448: 151–156. doi:10.1038/nature05954.
51. Ni J-Q, Zhou R, Czech B, Liu L-P, Holderbaum L, et al. (2011) A genome-scale shRNA resource for transgenic RNAi in Drosophila. Nat Meth 8: 405–407. doi:10.1038/nmeth.1592.
52. Mazière P, Enright AJ (2007) Prediction of microRNA targets. Drug Discov Today 12: 452–458. doi:10.1016/j.drudis.2007.04.002.
53. Tsai Y-C, Sun YH (2004) Long-range effect of upd, a ligand for Jak/STAT pathway, on cell cycle in Drosophila eye development. Genesis 39: 141–153. doi:10.1002/gene.20035.
54. Dominguez M, de Celis JF (1998) A dorsal/ventral boundary established by Notch controls growth and polarity in the Drosophila eye. Nature 396: 276–278. doi:10.1038/24402.
55. Gutierrez-Aviñon FJ, Ferres-Marco D, Dominguez M (2009) The position and function of the Notch-mediated eye growth organizer: the roles of JAK/STAT and four-jointed. EMBO Rep 10: 1051–1058. doi:10.1038/embor.2009.140.
56. Hartman TR, Zinshteyn D, Schofield HK, Nicolas E, Okada A, et al. (2010) Drosophila Boi limits Hedgehog levels to suppress follicle stem cell proliferation. J Cell Biol 191: 943–952. doi:10.1083/jcb.201007142.
57. Dominguez M, Brunner M, Hafen E, Basler K (1996) Sending and receiving the hedgehog signal: control by the Drosophila Gli protein Cubitus interruptus. Science 272: 1621–1625.
58. Aza-Blanc P, Ramírez-Weber FA, Laget MP, Schwartz C, Kornberg TB (1997) Proteolysis that is inhibited by hedgehog targets Cubitus interruptus protein to the nucleus and converts it to a repressor. Cell 89: 1043–1053.
59. Méthot N, Basler K (1999) Hedgehog controls limb development by regulating the activities of distinct transcriptional activator and repressor forms of Cubitus interruptus. Cell 96: 819–831.
60. Lee T, Luo L (2001) Mosaic analysis with a repressible cell marker (MARCM) for Drosophila neural development. Trends Neurosci 24: 251–254.
61. Dominguez M (1999) Dual role for Hedgehog in the regulation of the proneural gene atonal during ommatidia development. Development 126: 2345–2353.
62. Baonza AA, Freeman MM (2001) Notch signalling and the initiation of neural development in the Drosophila eye. Development 128: 3889–3898.
63. Tabata T, Kornberg TB (1994) Hedgehog is a signaling protein with a key role in patterning Drosophila imaginal discs. Cell 76: 89–102.
64. Chen Y, Struhl G (1996) Dual roles for patched in sequestering and transducing Hedgehog. Cell 87: 553–563.
65. Baonza A, Freeman M (2005) Control of cell proliferation in the Drosophila eye by notch signaling. Dev Cell 8: 529–539. doi:10.1016/j.devcel.2005.01.019.
66. Doherty D, Feger G, Younger-Shepherd S, Jan LY, Jan YN (1996) Delta is a ventral to dorsal signal complementary to Serrate, another Notch ligand, in Drosophila wing formation. Genes Dev 10: 421–434. doi:10.1101/gad.10.4.421.
67. de Celis JF, Garcia-Bellido A, Bray SJ (1996) Activation and function of Notch at the dorsal-ventral boundary of the wing imaginal disc. Development 122: 359–369.
68. de Celis JFJ, Bray SS (1997) Feed-back mechanisms affecting Notch activation at the dorsoventral boundary in the Drosophila wing. Development 124: 3241–3251.
69. Pitsouli C, Delidakis C (2005) The interplay between DSL proteins and ubiquitin ligases in Notch signaling. Development 132: 4041–4050. doi:10.1242/dev.01979.
70. Rodriguez I, Basler K (1997) Control of compartmental affinity boundaries by hedgehog. Nature 389: 614–618. doi:10.1038/39343.
71. Blair SS, Ralston A (1997) Smoothened-mediated Hedgehog signalling is required for the maintenance of the anterior-posterior lineage restriction in the developing wing of Drosophila. Development 124: 4053–4063.
72. Bejarano F, Bortolamiol-Becet D, Dai Q, Sun K, Saj A, et al. (2012) A genome-wide transgenic resource for conditional expression of Drosophila microRNAs. Development 139: 2821–2831. doi:10.1242/dev.079939.
73. Lai EC, Tam B, Rubin GM (2005) Pervasive regulation of Drosophila Notch target genes by GY-box-, Brd-box-, and K-box-class microRNAs. Genes Dev 19: 1067–1080. doi:10.1101/gad.1291905.
74. Uhlmann S, Mannsperger H, Zhang JD, Horvat E-Á, Schmidt C, et al. (2012) Global microRNA level regulation of EGFR-driven cell-cycle protein network in breast cancer. Mol Syst Biol 8: 570. doi:10.1038/msb.2011.100.
75. Vidal M, Cagan RL (2006) Drosophila models for cancer research. Curr Opin Genet Dev 16: 10–16. doi:10.1016/j.gde.2005.12.004.
76. Liefke R, Oswald F, Alvarado C, Ferres-Marco D, Mittler G, et al. (2010) Histone demethylase KDM5A is an integral part of the core Notch-RBP-J repressor complex. Genes Dev 24: 590–601. doi:10.1101/gad.563210.
77. Herz H-M, Madden LD, Chen Z, Bolduc C, Buff E, et al. (2010) The H3K27me3 demethylase dUTX is a suppressor of Notch- and Rb-dependent tumors in Drosophila. Mol Cell Biol 30: 2485–2497. doi:10.1128/MCB.01633-09.
78. Weng AP, Millholland JM, Yashiro-Ohtani Y, Arcangeli ML, Lau A, et al. (2006) c-Myc is an important direct target of Notch1 in T-cell acute

lymphoblastic leukemia/lymphoma. Genes Dev 20: 2096–2109. doi:10.1101/gad.1450406.
79. Pallavi SK, Ho DM, Hicks C, Miele L, Artavanis-Tsakonas S (2012) Notch and Mef2 synergize to promote proliferation and metastasis through JNK signal activation in Drosophila. EMBO J 31: 2895–2907 doi:10.1038/emboj.2012.129.
80. Calin GA, Croce CM (2006) MicroRNA signatures in human cancers. Nat Rev Cancer 6: 857–866. doi:10.1038/nrc1997.
81. Cho WC (2007) OncomiRs: the discovery and progress of microRNAs in cancers. Mol Cancer 6: 60. doi:10.1186/1476-4598-6-60.
82. Iorio MV, Visone R, Di Leva G, Donati V, Petrocca F, et al. (2007) MicroRNA signatures in human ovarian cancer. Cancer Res 67: 8699–8707. doi:10.1158/0008-5472.CAN-07-1936.
83. Ma L, Weinberg RA (2008) Micromanagers of malignancy: role of microRNAs in regulating metastasis. Trends Genet 24: 448–456. doi:10.1016/j.tig.2008.06.004.
84. Lee YS, Dutta A (2009) MicroRNAs in cancer. Annu Rev Pathol Mech Dis 4: 199–227. doi:10.1146/annurev.pathol.4.110807.092222.
85. He L, Thomson JM, Hemann MT, Hernando-Monge E, Mu D, et al. (2005) A microRNA polycistron as a potential human oncogene. Nature 435: 828–833. doi:10.1038/nature03552.
86. Voorhoeve PM, le Sage C, Schrier M, Gillis AJM, Stoop H, et al. (2006) A genetic screen implicates miRNA-372 and miRNA-373 as oncogenes in testicular germ cell tumors. Cell 124: 1169–1181. doi:10.1016/j.cell.2006.02.037.
87. Nolo R, Morrison CM, Tao C, Zhang X, Halder G (2006) The bantam MicroRNA is a target of the hippo tumor-suppressor pathway. Curr Biol 16: 1895–1904. doi:10.1016/j.cub.2006.08.057.
88. Thompson BJ, Cohen SM (2006) The hippo pathway regulates the bantam microRNA to control cell proliferation and apoptosis in Drosophila. Cell 126: 767–774. doi:10.1016/j.cell.2006.07.013.
89. Foekens JA, Sieuwerts AM, Smid M, Look MP, de Weerd V, et al. (2008) Four miRNAs associated with aggressiveness of lymph node-negative, estrogen receptor-positive human breast cancer. Proc Natl Acad Sci USA 105: 13021–13026. doi:10.1073/pnas.0803304105.
90. Chou Y-T, Lin H-H, Lien Y-C, Wang Y-H, Hong C-F, et al. (2010) EGFR promotes lung tumorigenesis by activating miR-7 through a Ras/ERK/Myc pathway that targets the Ets2 transcriptional repressor ERF. Cancer Res 70: 8822–8831. doi:10.1158/0008-5472.CAN-10-0638.
91. Reddy SDN, Ohshiro K, Rayala SK, Kumar R (2008) MicroRNA-7, a homeobox D10 target, inhibits p21-activated kinase 1 and regulates its functions. Cancer Res 68: 8195–8200. doi:10.1158/0008-5472.CAN-08-2103.
92. Kefas B, Godlewski J, Comeau L, Li Y, Abounader R, et al. (2008) microRNA-7 inhibits the epidermal growth factor receptor and the Akt pathway and is down-regulated in glioblastoma. Cancer Res 68: 3566–3572. doi:10.1158/0008-5472.CAN-07-6639.
93. Webster RJ, Giles KM, Price KJ, Zhang PM, Mattick JS, et al. (2009) Regulation of epidermal growth factor receptor signaling in human cancer cells by microRNA-7. J Biol Chem 284: 5731–5741. doi:10.1074/jbc.M804280200.
94. Jiang L, Liu X, Chen Z, Jin Y, Heidbreder CE, et al. (2010) MicroRNA-7 targets IGF1R (insulin-like growth factor 1 receptor) in tongue squamous cell carcinoma cells. Biochem J 432: 199–205. doi:10.1042/BJ20100859.
95. Erkan EP, Breakefield XO, Saydam O (2011) miRNA signature of schwannomas: possible role(s) of "tumor suppressor" miRNAs in benign tumors. Oncotarget 2: 265–270.
96. Skalsky RL, Cullen BR (2011) Reduced expression of brain-enriched microRNAs in glioblastomas permits targeted regulation of a cell death gene. PLoS ONE 6: e24248. doi:10.1371/journal.pone.0024248.
97. Lee H-J, Palkovits M, Young WS (2006) miR-7b, a microRNA up-regulated in the hypothalamus after chronic hyperosmolar stimulation, inhibits Fos translation. Proc Natl Acad Sci USA 103: 15669–15674. doi:10.1073/pnas.0605781103.
98. Junn E, Lee K-W, Jeong BS, Chan TW, Im J-Y, et al. (2009) Repression of alpha-synuclein expression and toxicity by microRNA-7. Proc Natl Acad Sci USA 106: 13052–13057. doi:10.1073/pnas.0906277106.
99. Nguyen HTT, Dalmasso G, Yan Y, Laroui H, Dahan S, et al. (2010) MicroRNA-7 modulates CD98 expression during intestinal epithelial cell differentiation. J Biol Chem 285: 1479–1489. doi:10.1074/jbc.M109.057141.
100. Xiong S, Zheng Y, Jiang P, Liu R, Liu X, et al. (2011) MicroRNA-7 inhibits the growth of human non-small cell lung cancer A549 cells through targeting BCL-2. Int J Biol Sci 7: 805–814.
101. Fang YX, Xue J-L, Shen Q, Chen J, Tian L (2012) miR-7 inhibits tumor growth and metastasis by targeting the PI3K/AKT pathway in hepatocellular carcinoma. Hepatology 55: 1852–1862. doi:10.1002/hep.25576.
102. Xu L, Wen Z, Zhou Y, Liu Z, Li Q, et al. (2013) MicroRNA-7 regulated TLR9 signaling enhanced growth and metastatic potential of human lung cancer cells by altering PIK3R3/Akt pathway. Mol Biol Cell 24: 42–55. doi:10.1091/mbc.E12-07-0519.
103. Zhang N, Li X, Wu CW, Dong Y, Cai M, et al. (2012) microRNA-7 is a novel inhibitor of YY1 contributing to colorectal tumorigenesis. Oncogene. doi:10.1038/onc.2012.526.
104. Stark A, Brennecke J, Bushati N, Russell RB, Cohen SM (2005) Animal MicroRNAs confer robustness to gene expression and have a significant impact on 3′UTR evolution. Cell 123: 1133–1146. doi:10.1016/j.cell.2005.11.023.
105. Yu JY, Reynolds SH, Hatfield SD, Shcherbata HR, Fischer KA, et al. (2009) Dicer-1-dependent Dacapo suppression acts downstream of Insulin receptor in regulating cell division of Drosophila germline stem cells. Development 136: 1497–1507. doi:10.1242/dev.025999.
106. Tokusumi T, Tokusumi Y, Hopkins DW, Shoue DA, Corona L, et al. (2011) Germ line differentiation factor Bag of Marbles is a regulator of hematopoietic progenitor maintenance during Drosophila hematopoiesis. Development 138: 3879–3884. doi:10.1242/dev.069336.
107. Pek JW, Lim AK, Kai T (2009) Drosophila maelstrom ensures proper germline stem cell lineage differentiation by repressing microRNA-7. Dev Cell 17: 417–424. doi:10.1016/j.devcel.2009.07.017.
108. Brown NL, Sattler CA, Paddock SW, Carroll SB (1995) Hairy and emc negatively regulate morphogenetic furrow progression in the Drosophila eye. Cell 80: 879–887.
109. De Renzis S, Yu J, Zinzen R, Wieschaus E (2006) Dorsal-ventral pattern of Delta trafficking is established by a Snail-Tom-Neuralized pathway. Dev Cell 10: 257–264. doi:10.1016/j.devcel.2006.01.011.
110. Kang J-S, Mulieri PJ, Hu Y, Taliana L, Krauss RS (2002) BOC, an Ig superfamily member, associates with CDO to positively regulate myogenic differentiation. EMBO J 21: 114–124. doi:10.1093/emboj/21.1.114.
111. Kang J-S, Feinleib JL, Knox S, Ketteringham MA, Krauss RS (2003) Promyogenic members of the Ig and cadherin families associate to positively regulate differentiation. Proc Natl Acad Sci USA 100: 3989–3994. doi:10.1073/pnas.0736565100.
112. Gobeil S, Zhu X, Doillon CJ, Green MR (2008) A genome-wide shRNA screen identifies GAS1 as a novel melanoma metastasis suppressor gene. Genes Dev 22: 2932–2940. doi:10.1101/gad.1714608.
113. López-Ornelas A, Mejía-Castillo T, Vergara P, Segovia J (2011) Lentiviral transfer of an inducible transgene expressing a soluble form of Gas1 causes glioma cell arrest, apoptosis and inhibits tumor growth. Cancer Gene Ther 18: 87–99. doi:10.1038/cgt.2010.54.

REFERENCES

Aboobaker, A. A., Tomancak, P., Patel, N., Rubin, G. M., and Lai, E. C. (2005). Drosophila microRNAs exhibit diverse spatial expression patterns during embryonic development. Proc Natl Acad Sci U S A *102*, 18017-18022.

Albagli, O., Dhordain, P., Deweindt, C., Lecocq, G., and Leprince, D. (1995). The BTB/POZ domain: a new protein-protein interaction motif common to DNA- and actin-binding proteins. Cell Growth Differ *6*, 1193-1198.

Altschul, S. F., Madden, T. L., Schaffer, A. A., Zhang, J., Zhang, Z., Miller, W., and Lipman, D. J. (1997). Gapped BLAST and PSI-BLAST: a new generation of protein database search programs. Nucleic Acids Res *25*, 3389-3402.

Allen, B. L., Song, J. Y., Izzi, L., Althaus, I. W., Kang, J. S., Charron, F., Krauss, R. S., and Mcmahon, A. P. (2011). Overlapping roles and collective requirement for the coreceptors GAS1, CDO, and BOC in SHH pathway function. Dev Cell *20*, 775-787.

Ambros, V. (2004). The functions of animal microRNAs. Nature *431*, 350-355.

Amin, A., Li, Y., and Finkelstein, R. (1999). Hedgehog activates the EGF receptor pathway during Drosophila head development. Development *126*, 2623-2630.

Anand, A., Villella, A., Ryner, L. C., Carlo, T., Goodwin, S. F., Song, H. J., Gailey, D. A., Morales, A., Hall, J. C., Baker, B. S., and Taylor, B. J. (2001). Molecular genetic dissection of the sex-specific and vital functions of the Drosophila melanogaster sex determination gene fruitless. Genetics *158*, 1569-1595.

Andersson, E. R., Sandberg, R., and Lendahl, U. (2011). Notch signaling: simplicity in design, versatility in function. Development *138*, 3593-3612.

Aparicio, R., Simoes Da Silva, C. J., and Busturia, A. (2015). MicroRNA miR-7 contributes to the control of Drosophila wing growth. Dev Dyn *244*, 21-30.

Arnold, C. D., Gerlach, D., Stelzer, C., Boryn, L. M., Rath, M., and Stark, A. (2013). Genome-wide quantitative enhancer activity maps identified by STARR-seq. Science *339*, 1074-1077.

Artavanis-Tsakonas, S. (1988). The molecular biology of the Notch locus and the fine tuning of differentiation in Drosophila. Trends Genet *4*, 95-100.

Artavanis-Tsakonas, S., Rand, M. D., and Lake, R. J. (1999). Notch signaling: cell fate control and signal integration in development. Science *284*, 770-776.

Aster, J. C. (2005). Deregulated NOTCH signaling in acute T-cell lymphoblastic leukemia/lymphoma: new insights, questions, and opportunities. Int J Hematol *82*, 295-301.

Averof, M., and Cohen, S. M. (1997). Evolutionary origin of insect wings from ancestral gills. Nature *385*, 627-630.

Aza-Blanc, P., Ramirez-Weber, F. A., Laget, M. P., Schwartz, C., and Kornberg, T. B. (1997). Proteolysis that is inhibited by hedgehog targets Cubitus interruptus protein to the nucleus and converts it to a repressor. Cell *89*, 1043-1053.

Banerji, J., Rusconi, S., and Schaffner, W. (1981). Expression of a beta-globin gene is enhanced by remote SV40 DNA sequences. Cell *27*, 299-308.

Baonza, A., and Freeman, M. (2005). Control of cell proliferation in the Drosophila eye by Notch signaling. Dev Cell *8*, 529-539.

Bardwell, V. J., and Treisman, R. (1994). The POZ domain: a conserved protein-protein interaction motif. Genes Dev *8*, 1664-1677.

Barski, A., Cuddapah, S., Cui, K., Roh, T. Y., Schones, D. E., Wang, Z., Wei, G., Chepelev, I., and Zhao, K. (2007). High-resolution profiling of histone methylations in the human genome. Cell *129*, 823-837.

Bartel, D. P. (2004). MicroRNAs: genomics, biogenesis, mechanism, and function. Cell *116*, 281-297.

Basler, K., and Struhl, G. (1994). Compartment boundaries and the control of Drosophila limb pattern by hedgehog protein. Nature *368*, 208-214.

Bate, M., and Arias, A. M. (1991). The embryonic origin of imaginal discs in Drosophila. Development *112*, 755-761.

Beachy, P. A., Hymowitz, S. G., Lazarus, R. A., Leahy, D. J., and Siebold, C. (2010). Interactions between Hedgehog proteins and their binding partners come into view. Genes Dev *24*, 2001-2012.

Bejarano, F., Bortolamiol-Becet, D., Dai, Q., Sun, K., Saj, A., Chou, Y. T., Raleigh, D. R., Kim, K., Ni, J. Q., Duan, H., Yang, J. S., Fulga, T. A., Van Vactor, D., Perrimon, N., and Lai, E. C. (2012). A genome-wide transgenic resource for conditional expression of Drosophila microRNAs. Development *139*, 2821-2831.

Bejarano, F., and Busturia, A. (2004). Function of the Trithorax-like gene during Drosophila development. Dev Biol *268*, 327-341.

Belozerov, V. E., Majumder, P., Shen, P., and Cai, H. N. (2003). A novel boundary element may facilitate independent gene regulation in the Antennapedia complex of Drosophila. EMBO J *22*, 3113-3121.

Bender, M., Imam, F. B., Talbot, W. S., Ganetzky, B., and Hogness, D. S. (1997). Drosophila ecdysone receptor mutations reveal functional differences among receptor isoforms. Cell *91*, 777-788.

Biehs, B., Sturtevant, M. A., and Bier, E. (1998). Boundaries in the Drosophila wing imaginal disc organize vein-specific genetic programs. Development *125*, 4245-4257.

Biggin, M. D., and Tjian, R. (1988). Transcription factors that activate the Ultrabithorax promoter in developmentally staged extracts. Cell *53*, 699-711.

Blackman, R. K., Sanicola, M., Raftery, L. A., Gillevet, T., and Gelbart, W. M. (1991). An extensive 3' cis-regulatory region directs the imaginal disk expression of decapentaplegic, a member of the TGF-beta family in Drosophila. Development *111*, 657-666.

Blair, S. S. (1993). Mechanisms of compartment formation: evidence that non-proliferating cells do not play a critical role in defining the D/V lineage restriction in the developing wing of Drosophila. Development *119*, 339-351.

Blair, S. S., and Ralston, A. (1997). Smoothened-mediated Hedgehog signalling is required for the maintenance of the anterior-posterior lineage restriction in the developing wing of Drosophila. Development *124*, 4053-4063.

Blankenberg, D., Von Kuster, G., Coraor, N., Ananda, G., Lazarus, R., Mangan, M., Nekrutenko, A., and Taylor, J. (2010). Galaxy: a web-based genome analysis tool for experimentalists. Curr Protoc Mol Biol *Chapter 19*, Unit 19 10 11-21.

Bonchuk, A., Denisov, S., Georgiev, P., and Maksimenko, O. (2011). Drosophila BTB/POZ domains of "ttk group" can form multimers and selectively interact with each other. J Mol Biol *412*, 423-436.

Bonora, G., Plath, K., and Denholtz, M. (2014). A mechanistic link between gene regulation and genome architecture in mammalian development. Curr Opin Genet Dev *27*, 92-101.

Borod, E. R., and Heberlein, U. (1998). Mutual regulation of decapentaplegic and hedgehog during the initiation of differentiation in the Drosophila retina. Dev Biol *197*, 187-197.

Bossuyt, W., De Geest, N., Aerts, S., Leenaerts, I., Marynen, P., and Hassan, B. A. (2009). The atonal proneural transcription factor links differentiation and tumor formation in Drosophila. PLoS Biol *7*, e40.

Bracken, A. P., Dietrich, N., Pasini, D., Hansen, K. H., and Helin, K. (2006). Genome-wide mapping of Polycomb target genes unravels their roles in cell fate transitions. Genes Dev *20*, 1123-1136.

Bracken, A. P., Pasini, D., Capra, M., Prosperini, E., Colli, E., and Helin, K. (2003). EZH2 is downstream of the pRB-E2F pathway, essential for proliferation and amplified in cancer. EMBO J *22*, 5323-5335.

Brand, A. H., and Perrimon, N. (1993). Targeted gene expression as a means of altering cell fates and generating dominant phenotypes. Development *118*, 401-415.

Bray, S. J. (2006). Notch signalling: a simple pathway becomes complex. Nat Rev Mol Cell Biol *7*, 678-689.

Brookes, E., De Santiago, I., Hebenstreit, D., Morris, K. J., Carroll, T., Xie, S. Q., Stock, J. K., Heidemann, M., Eick, D., Nozaki, N., Kimura, H., Ragoussis, J., Teichmann, S. A., and Pombo, A. (2012). Polycomb associates genome-wide with a specific RNA polymerase II variant, and regulates metabolic genes in ESCs. Cell Stem Cell *10*, 157-170.

Brou, C., Logeat, F., Gupta, N., Bessia, C., Lebail, O., Doedens, J. R., Cumano, A., Roux, P., Black, R. A., and Israel, A. (2000). A novel proteolytic cleavage involved in Notch signaling: the role of the disintegrin-metalloprotease TACE. Mol Cell *5*, 207-216.

Brown, N. L., Sattler, C. A., Paddock, S. W., and Carroll, S. B. (1995). Hairy and emc negatively regulate morphogenetic furrow progression in the Drosophila eye. Cell *80*, 879-887.

Bruckner, A., Polge, C., Lentze, N., Auerbach, D., and Schlattner, U. (2009). Yeast two-hybrid, a powerful tool for systems biology. Int J Mol Sci *10*, 2763-2788.

Brumby, A. M., and Richardson, H. E. (2005). Using Drosophila melanogaster to map human cancer pathways. Nat Rev Cancer *5*, 626-639.

Brutlag, D. L. (1980). Molecular arrangement and evolution of heterochromatic DNA. Annu Rev Genet *14*, 121-144.

Buchner, K., Roth, P., Schotta, G., Krauss, V., Saumweber, H., Reuter, G., and Dorn, R. (2000). Genetic and molecular complexity of the position effect variegation modifier mod(mdg4) in Drosophila. Genetics *155*, 141-157.

Bulger, M., and Groudine, M. (2010). Enhancers: the abundance and function of regulatory sequences beyond promoters. Dev Biol *339*, 250-257.

Burtis, K. C., Thummel, C. S., Jones, C. W., Karim, F. D., and Hogness, D. S. (1990). The Drosophila 74EF early puff contains E74, a complex ecdysone-inducible gene that encodes two ets-related proteins. Cell *61*, 85-99.

Busturia, A., Lloyd, A., Bejarano, F., Zavortink, M., Xin, H., and Sakonju, S. (2001). The MCP silencer of the Drosophila Abd-B gene requires both Pleiohomeotic and GAGA factor for the maintenance of repression. Development *128*, 2163-2173.

Buszczak, M., and Spradling, A. C. (2006). Searching chromatin for stem cell identity. Cell *125*, 233-236.

Buttitta, L., Mo, R., Hui, C. C., and Fan, C. M. (2003). Interplays of Gli2 and Gli3 and their requirement in mediating Shh-dependent sclerotome induction. Development *130*, 6233-6243.

Cai, H. N., and Shen, P. (2001). Effects of cis arrangement of chromatin insulators on enhancer-blocking activity. Science *291*, 493-495.

Calin, G. A., and Croce, C. M. (2006). MicroRNA signatures in human cancers. Nat Rev Cancer *6*, 857-866.

Calin, G. A., Dumitru, C. D., Shimizu, M., Bichi, R., Zupo, S., Noch, E., Aldler, H., Rattan, S., Keating, M., Rai, K., Rassenti, L., Kipps, T., Negrini, M., Bullrich, F., and Croce, C. M. (2002). Frequent deletions and down-regulation of micro- RNA genes miR15 and miR16 at 13q14 in chronic lymphocytic leukemia. Proc Natl Acad Sci U S A *99*, 15524-15529.

Camp, D., Currie, K., Labbe, A., Van Meyel, D. J., and Charron, F. (2010). Ihog and Boi are essential for Hedgehog signaling in Drosophila. Neural Dev *5*, 28.

Capelson, M., and Corces, V. G. (2005). The ubiquitin ligase dTopors directs the nuclear organization of a chromatin insulator. Mol Cell *20*, 105-116.

Cavodeassi, F., Diez Del Corral, R., Campuzano, S., and Dominguez, M. (1999). Compartments and organising boundaries in the Drosophila eye: the role of the homeodomain Iroquois proteins. Development *126*, 4933-4942.

Cimmino, A., Calin, G. A., Fabbri, M., Iorio, M. V., Ferracin, M., Shimizu, M., Wojcik, S. E., Aqeilan, R. I., Zupo, S., Dono, M., Rassenti, L., Alder, H., Volinia, S., Liu, C. G., Kipps, T. J., Negrini, M., and Croce, C. M. (2005). miR-15 and miR-16 induce apoptosis by targeting BCL2. Proc Natl Acad Sci U S A *102*, 13944-13949.

Cohen, B., Wimmer, E. A., and Cohen, S. M. (1991). Early development of leg and wing primordia in the Drosophila embryo. Mech Dev *33*, 229-240.

Cohen, M. M., Jr. (2010). Hedgehog signaling update. Am J Med Genet A *152A*, 1875-1914.

Colland, F., and Daviet, L. (2004). Integrating a functional proteomic approach into the target discovery process. Biochimie *86*, 625-632.

Comet, I., Savitskaya, E., Schuettengruber, B., Negre, N., Lavrov, S., Parshikov, A., Juge, F., Gracheva, E., Georgiev, P., and Cavalli, G. (2006). PRE-mediated bypass of two Su(Hw) insulators targets PcG proteins to a downstream promoter. Dev Cell *11*, 117-124.

Core, L. J., Waterfall, J. J., Gilchrist, D. A., Fargo, D. C., Kwak, H., Adelman, K., and Lis, J. T. (2012). Defining the status of RNA polymerase at promoters. Cell Rep *2*, 1025-1035.

Core, L. J., Waterfall, J. J., and Lis, J. T. (2008). Nascent RNA sequencing reveals widespread pausing and divergent initiation at human promoters. Science *322*, 1845-1848.

Creyghton, M. P., Cheng, A. W., Welstead, G. G., Kooistra, T., Carey, B. W., Steine, E. J., Hanna, J., Lodato, M. A., Frampton, G. M., Sharp, P. A., Boyer, L. A., Young, R. A., and Jaenisch, R. (2010). Histone H3K27ac separates active from poised enhancers and predicts developmental state. Proc Natl Acad Sci U S A *107*, 21931-21936.

Croston, G. E., Kerrigan, L. A., Lira, L. M., Marshak, D. R., and Kadonaga, J. T. (1991). Sequence-specific antirepression of histone H1-mediated inhibition of basal RNA polymerase II transcription. Science *251*, 643-649.

Czerny, T., Schaffner, G., and Busslinger, M. (1993). DNA sequence recognition by Pax proteins: bipartite structure of the paired domain and its binding site. Genes Dev *7*, 2048-2061.

Chambers, A. F., Groom, A. C., and Macdonald, I. C. (2002). Dissemination and growth of cancer cells in metastatic sites. Nat Rev Cancer *2*, 563-572.

Chang, C. J., and Hung, M. C. (2012). The role of EZH2 in tumour progression. Br J Cancer *106*, 243-247.

Charroux, B., Freeman, M., Kerridge, S., and Baonza, A. (2006). Atrophin contributes to the negative regulation of epidermal growth factor receptor signaling in Drosophila. Dev Biol *291*, 278-290.

Chawla, A., Repa, J. J., Evans, R. M., and Mangelsdorf, D. J. (2001). Nuclear receptors and lipid physiology: opening the X-files. Science *294*, 1866-1870.

Chen, Y., and Struhl, G. (1996). Dual roles for patched in sequestering and transducing Hedgehog. Cell *87*, 553-563.

Cherbas, L., Willingham, A., Zhang, D., Yang, L., Zou, Y., Eads, B. D., Carlson, J. W., Landolin, J. M., Kapranov, P., Dumais, J., Samsonova, A., Choi, J. H., Roberts, J., Davis, C. A., Tang, H., Van Baren, M. J., Ghosh, S., Dobin, A., Bell, K., Lin, W., Langton, L., Duff, M. O., Tenney, A. E., Zaleski, C., Brent, M. R., Hoskins, R. A., Kaufman, T. C., Andrews, J., Graveley, B. R., Perrimon, N., Celniker, S. E., Gingeras, T. R., and Cherbas, P. (2011). The transcriptional diversity of 25 Drosophila cell lines. Genome Res *21*, 301-314.

Cho, K. O., and Choi, K. W. (1998). Fringe is essential for mirror symmetry and morphogenesis in the Drosophila eye. Nature *396*, 272-276.

Cho, W. C. (2007). OncomiRs: the discovery and progress of microRNAs in cancers. Mol Cancer *6*, 60.

Chou, Y. T., Lin, H. H., Lien, Y. C., Wang, Y. H., Hong, C. F., Kao, Y. R., Lin, S. C., Chang, Y. C., Lin, S. Y., Chen, S. J., Chen, H. C., Yeh, S. D., and Wu, C. W. (2010). EGFR promotes lung tumorigenesis by activating miR-7 through a Ras/ERK/Myc pathway that targets the Ets2 transcriptional repressor ERF. Cancer Res *70*, 8822-8831.

Da Ros, V. G., Gutierrez-Perez, I., Ferres-Marco, D., and Dominguez, M. (2013). Dampening the signals transduced through hedgehog via microRNA miR-7 facilitates notch-induced tumourigenesis. PLoS Biol *11*, e1001554.

De Celis, J. F., and Bray, S. (1997). Feed-back mechanisms affecting Notch activation at the dorsoventral boundary in the Drosophila wing. Development *124*, 3241-3251.

De Celis, J. F., and Garcia-Bellido, A. (1994). Roles of the Notch gene in Drosophila wing morphogenesis. Mech Dev *46*, 109-122.

De Celis, J. F., Garcia-Bellido, A., and Bray, S. J. (1996). Activation and function of Notch at the dorsal-ventral boundary of the wing imaginal disc. Development *122*, 359-369.

De Hoon, M. J., Imoto, S., Nolan, J., and Miyano, S. (2004). Open source clustering software. Bioinformatics *20*, 1453-1454.

De Renzis, S., Yu, J., Zinzen, R., and Wieschaus, E. (2006). Dorsal-ventral pattern of Delta trafficking is established by a Snail-Tom-Neuralized pathway. Dev Cell *10*, 257-264.

De Strooper, B., Annaert, W., Cupers, P., Saftig, P., Craessaerts, K., Mumm, J. S., Schroeter, E. H., Schrijvers, V., Wolfe, M. S., Ray, W. J., Goate, A., and Kopan, R. (1999). A presenilin-1-dependent gamma-secretase-like protease mediates release of Notch intracellular domain. Nature *398*, 518-522.

Decoville, M., Giacomello, E., Leng, M., and Locker, D. (2001). DSP1, an HMG-like protein, is involved in the regulation of homeotic genes. Genetics *157*, 237-244.

Delattre, M., Tatout, C., and Coen, D. (2000). P-element transposition in Drosophila melanogaster: influence of size and arrangement in pairs. Mol Gen Genet *263*, 445-454.

Delloye-Bourgeois, Céline, Gibert, Benjamin, Rama, Nicolas, Delcros, Jean-Guy, Gadot, Nicolas, Scoazec, Jean-Yves, Krauss, Robert, Bernet, Agnès, and Mehlen, Patrick (2013). Sonic Hedgehog Promotes Tumor Cell Survival by Inhibiting CDON Pro-Apoptotic Activity. PLoS Biol *11*, e1001623.

Demir, E., and Dickson, B. J. (2005). fruitless splicing specifies male courtship behavior in Drosophila. Cell *121*, 785-794.

Devaiah, B. N., Lewis, B. A., Cherman, N., Hewitt, M. C., Albrecht, B. K., Robey, P. G., Ozato, K., Sims, R. J., 3rd, and Singer, D. S. (2012). BRD4 is an atypical kinase that phosphorylates serine2 of the RNA polymerase II carboxy-terminal domain. Proc Natl Acad Sci U S A *109*, 6927-6932.

Diaz-Benjumea, F. J., and Cohen, S. M. (1993). Interaction between dorsal and ventral cells in the imaginal disc directs wing development in Drosophila. Cell *75*, 741-752.

Diaz-Benjumea, F. J., and Cohen, S. M. (1995). Serrate signals through Notch to establish a Wingless-dependent organizer at the dorsal/ventral compartment boundary of the Drosophila wing. Development *121*, 4215-4225.

Dietzl, G., Chen, D., Schnorrer, F., Su, K. C., Barinova, Y., Fellner, M., Gasser, B., Kinsey, K., Oppel, S., Scheiblauer, S., Couto, A., Marra, V., Keleman, K., and Dickson, B. J. (2007). A genome-wide transgenic RNAi library for conditional gene inactivation in Drosophila. Nature *448*, 151-156.

Ding, Q., Motoyama, J., Gasca, S., Mo, R., Sasaki, H., Rossant, J., and Hui, C. C. (1998). Diminished Sonic hedgehog signaling and lack of floor plate differentiation in Gli2 mutant mice. Development *125*, 2533-2543.

Djiane, A., Krejci, A., Bernard, F., Fexova, S., Millen, K., and Bray, S. J. (2013). Dissecting the mechanisms of Notch induced hyperplasia. EMBO J *32*, 60-71.

Doggett, K., Turkel, N., Willoughby, L. F., Ellul, J., Murray, M. J., Richardson, H. E., and Brumby, A. M. (2015). BTB-Zinc Finger Oncogenes Are Required for Ras and Notch-Driven Tumorigenesis in Drosophila. PLoS One *10*, e0132987.

Doherty, D., Feger, G., Younger-Shepherd, S., Jan, L. Y., and Jan, Y. N. (1996). Delta is a ventral to dorsal signal complementary to Serrate, another Notch ligand, in Drosophila wing formation. Genes Dev *10*, 421-434.

Dominguez, M. (1999). Dual role for Hedgehog in the regulation of the proneural gene atonal during ommatidia development. Development *126*, 2345-2353.

Dominguez, M. (2014). Oncogenic programmes and Notch activity: an 'organized crime'? Semin Cell Dev Biol *28*, 78-85.

Dominguez, M., Brunner, M., Hafen, E., and Basler, K. (1996). Sending and receiving the hedgehog signal: control by the Drosophila Gli protein Cubitus interruptus. Science *272*, 1621-1625.

Dominguez, M., and De Celis, J. F. (1998). A dorsal/ventral boundary established by Notch controls growth and polarity in the Drosophila eye. Nature *396*, 276-278.

Dominguez, M., Ferres-Marco, D., Gutierrez-Avino, F. J., Speicher, S. A., and Beneyto, M. (2004). Growth and specification of the eye are controlled independently by Eyegone and Eyeless in Drosophila melanogaster. Nat Genet *36*, 31-39.

Dominguez, M., and Hafen, E. (1997). Hedgehog directly controls initiation and propagation of retinal differentiation in the Drosophila eye. Genes Dev *11*, 3254-3264.

Dorn, R., Krauss, V., Reuter, G., and Saumweber, H. (1993). The enhancer of position-effect variegation of Drosophila, E(var)3-93D, codes for a chromatin protein containing a conserved domain common to several transcriptional regulators. Proc Natl Acad Sci U S A *90*, 11376-11380.

Dorsett, D. (1993). Distance-independent inactivation of an enhancer by the suppressor of Hairy-wing DNA-binding protein of Drosophila. Genetics *134*, 1135-1144.

Duncan, I. W., and Kaufman, T. C. (1975). Cytogenic analysis of chromosome 3 in Drosophila melanogaster: mapping of the proximal portion of the right arm. Genetics *80*, 733-752.

Ebert, M. S., and Sharp, P. A. (2010). Emerging roles for natural microRNA sponges. Curr Biol *20*, R858-861.

Ebert, M. S., and Sharp, P. A. (2010). MicroRNA sponges: progress and possibilities. RNA *16*, 2043-2050.

Eggert, H., Gortchakov, A., and Saumweber, H. (2004). Identification of the Drosophila interband-specific protein Z4 as a DNA-binding zinc-finger protein determining chromosomal structure. J Cell Sci *117*, 4253-4264.

Ellisen, L. W., Bird, J., West, D. C., Soreng, A. L., Reynolds, T. C., Smith, S. D., and Sklar, J. (1991). TAN-1, the human homolog of the Drosophila notch gene, is broken by chromosomal translocations in T lymphoblastic neoplasms. Cell *66*, 649-661.

Enright, A. J., John, B., Gaul, U., Tuschl, T., Sander, C., and Marks, D. S. (2003). MicroRNA targets in Drosophila. Genome Biol 5, R1.

Epstein, J. A., Glaser, T., Cai, J., Jepeal, L., Walton, D. S., and Maas, R. L. (1994). Two independent and interactive DNA-binding subdomains of the Pax6 paired domain are regulated by alternative splicing. Genes Dev 8, 2022-2034.

Erkan, E. P., Breakefield, X. O., and Saydam, O. (2011). miRNA signature of schwannomas: possible role(s) of "tumor suppressor" miRNAs in benign tumors. Oncotarget 2, 265-270.

Escalante, R., Wessels, D., Soll, D. R., and Loomis, W. F. (1997). Chemotaxis to cAMP and slug migration in Dictyostelium both depend on migA, a BTB protein. Mol Biol Cell 8, 1763-1775.

Esquela-Kerscher, A., and Slack, F. J. (2006). Oncomirs - microRNAs with a role in cancer. Nat Rev Cancer 6, 259-269.

Fang, Yuxiang, Xue, Jing-Lun, Shen, Qi, Chen, Jinzhong, and Tian, Ling (2012). MicroRNA-7 inhibits tumor growth and metastasis by targeting the phosphoinositide 3-kinase/Akt pathway in hepatocellular carcinoma. Hepatology 55, 1852-1862.

Farkas, G., Gausz, J., Galloni, M., Reuter, G., Gyurkovics, H., and Karch, F. (1994). The Trithorax-like gene encodes the Drosophila GAGA factor. Nature 371, 806-808.

Faucheux, M., Roignant, J. Y., Netter, S., Charollais, J., Antoniewski, C., and Theodore, L. (2003). batman Interacts with polycomb and trithorax group genes and encodes a BTB/POZ protein that is included in a complex containing GAGA factor. Mol Cell Biol 23, 1181-1195.

Feaver, W. J., Gileadi, O., and Kornberg, R. D. (1991). Purification and characterization of yeast RNA polymerase II transcription factor b. J Biol Chem 266, 19000-19005.

Fehon, R. G., Kooh, P. J., Rebay, I., Regan, C. L., Xu, T., Muskavitch, M. A., and Artavanis-Tsakonas, S. (1990). Molecular interactions between the protein products of the neurogenic loci Notch and Delta, two EGF-homologous genes in Drosophila. Cell 61, 523-534.

Ferguson, E. L., and Horvitz, H. R. (1985). Identification and characterization of 22 genes that affect the vulval cell lineages of the nematode Caenorhabditis elegans. Genetics 110, 17-72.

Ferrando, A. A. (2009). The role of NOTCH1 signaling in T-ALL. Hematology Am Soc Hematol Educ Program, 353-361.

Ferres-Marco, D., Gutierrez-Garcia, I., Vallejo, D. M., Bolivar, J., Gutierrez-Avino, F. J., and Dominguez, M. (2006). Epigenetic silencers and Notch collaborate to promote malignant tumours by Rb silencing. In Nature, pp. 430-436.

Fischer, J. A., Giniger, E., Maniatis, T., and Ptashne, M. (1988). GAL4 activates transcription in Drosophila. Nature 332, 853-856.

Fleming, R. J., Gu, Y., and Hukriede, N. A. (1997). Serrate-mediated activation of Notch is specifically blocked by the product of the gene fringe in the dorsal compartment of the Drosophila wing imaginal disc. Development *124*, 2973-2981.

Foekens, J. A., Sieuwerts, A. M., Smid, M., Look, M. P., De Weerd, V., Boersma, A. W., Klijn, J. G., Wiemer, E. A., and Martens, J. W. (2008). Four miRNAs associated with aggressiveness of lymph node-negative, estrogen receptor-positive human breast cancer. Proc Natl Acad Sci U S A *105*, 13021-13026.

Formstecher, E., Aresta, S., Collura, V., Hamburger, A., Meil, A., Trehin, A., Reverdy, C., Betin, V., Maire, S., Brun, C., Jacq, B., Arpin, M., Bellaiche, Y., Bellusci, S., Benaroch, P., Bornens, M., Chanet, R., Chavrier, P., Delattre, O., Doye, V., Fehon, R., Faye, G., Galli, T., Girault, J. A., Goud, B., De Gunzburg, J., Johannes, L., Junier, M. P., Mirouse, V., Mukherjee, A., Papadopoulo, D., Perez, F., Plessis, A., Rosse, C., Saule, S., Stoppa-Lyonnet, D., Vincent, A., White, M., Legrain, P., Wojcik, J., Camonis, J., and Daviet, L. (2005). Protein interaction mapping: a Drosophila case study. Genome Res *15*, 376-384.

Fre, S., Pallavi, S. K., Huyghe, M., Lae, M., Janssen, K. P., Robine, S., Artavanis-Tsakonas, S., and Louvard, D. (2009). Notch and Wnt signals cooperatively control cell proliferation and tumorigenesis in the intestine. Proc Natl Acad Sci U S A *106*, 6309-6314.

Freeman, M. (1997). Cell determination strategies in the Drosophila eye. Development *124*, 261-270.

Frigerio, G., Burri, M., Bopp, D., Baumgartner, S., and Noll, M. (1986). Structure of the segmentation gene paired and the Drosophila PRD gene set as part of a gene network. Cell *47*, 735-746.

Fromont-Racine, M., Rain, J. C., and Legrain, P. (1997). Toward a functional analysis of the yeast genome through exhaustive two-hybrid screens. Nat Genet *16*, 277-282.

Fuda, N. J., and Lis, J. T. (2013). A new player in Pol II pausing. EMBO J *32*, 1796-1798.

Gailey, D. A., Billeter, J. C., Liu, J. H., Bauzon, F., Allendorfer, J. B., and Goodwin, S. F. (2006). Functional conservation of the fruitless male sex-determination gene across 250 Myr of insect evolution. Mol Biol Evol *23*, 633-643.

Gan, M., Moebus, S., Eggert, H., and Saumweber, H. (2011). The Chriz-Z4 complex recruits JIL-1 to polytene chromosomes, a requirement for interband-specific phosphorylation of H3S10. J Biosci *36*, 425-438.

Garcia-Bellido, A., Ripoll, P., and Morata, G. (1973). Developmental compartmentalisation of the wing disk of Drosophila. Nat New Biol *245*, 251-253.

Garcia-Bellido, A., Ripoll, P., and Morata, G. (1976). Developmental compartmentalization in the dorsal mesothoracic disc of Drosophila. Dev Biol *48*, 132-147.

Garelli, A., Gontijo, A. M., Miguela, V., Caparros, E., and Dominguez, M. (2012). Imaginal discs secrete insulin-like peptide 8 to mediate plasticity of growth and maturation. Science *336*, 579-582.

Gaszner, M., and Felsenfeld, G. (2006). Insulators: exploiting transcriptional and epigenetic mechanisms. Nat Rev Genet *7*, 703-713.

Gauhar, Z., Sun, L. V., Hua, S., Mason, C. E., Fuchs, F., Li, T. R., Boutros, M., and White, K. P. (2009). Genomic mapping of binding regions for the Ecdysone receptor protein complex. Genome Res *19*, 1006-1013.

Gdula, D. A., Gerasimova, T. I., and Corces, V. G. (1996). Genetic and molecular analysis of the gypsy chromatin insulator of Drosophila. Proc Natl Acad Sci U S A *93*, 9378-9383.

Gerasimova, T. I., Gdula, D. A., Gerasimov, D. V., Simonova, O., and Corces, V. G. (1995). A Drosophila protein that imparts directionality on a chromatin insulator is an enhancer of position-effect variegation. Cell *82*, 587-597.

Gerasimova, T. I., Lei, E. P., Bushey, A. M., and Corces, V. G. (2007). Coordinated control of dCTCF and gypsy chromatin insulators in Drosophila. Mol Cell *28*, 761-772.

Geyer, P. K., and Corces, V. G. (1992). DNA position-specific repression of transcription by a Drosophila zinc finger protein. Genes Dev 6, 1865-1873.

Geyer, P. K., Spana, C., and Corces, V. G. (1986). On the molecular mechanism of gypsy-induced mutations at the yellow locus of Drosophila melanogaster. EMBO J 5, 2657-2662.

Ghosh, D., Gerasimova, T. I., and Corces, V. G. (2001). Interactions between the Su(Hw) and Mod(mdg4) proteins required for gypsy insulator function. EMBO J *20*, 2518-2527.

Giardine, B., Riemer, C., Hardison, R. C., Burhans, R., Elnitski, L., Shah, P., Zhang, Y., Blankenberg, D., Albert, I., Taylor, J., Miller, W., Kent, W. J., and Nekrutenko, A. (2005). Galaxy: a platform for interactive large-scale genome analysis. Genome Res *15*, 1451-1455.

Gil, J., Bernard, D., and Peters, G. (2005). Role of polycomb group proteins in stem cell self-renewal and cancer. DNA Cell Biol *24*, 117-125.

Gilbert, S. F. (1996). Cellular dialogues in organogenesis. Birth Defects Orig Artic Ser *30*, 1-12.

Giniger, E., Tietje, K., Jan, L. Y., and Jan, Y. N. (1994). lola encodes a putative transcription factor required for axon growth and guidance in Drosophila. Development *120*, 1385-1398.

Gobeil, S., Zhu, X., Doillon, C. J., and Green, M. R. (2008). A genome-wide shRNA screen identifies GAS1 as a novel melanoma metastasis suppressor gene. Genes Dev *22*, 2932-2940.

Godt, D., Couderc, J. L., Cramton, S. E., and Laski, F. A. (1993). Pattern formation in the limbs of Drosophila: bric a brac is expressed in both a gradient and a wave-like pattern and is required for specification and proper segmentation of the tarsus. Development *119*, 799-812.

Goecks, J., Nekrutenko, A., and Taylor, J. (2010). Galaxy: a comprehensive approach for supporting accessible, reproducible, and transparent computational research in the life sciences. Genome Biol *11*, R86.

Golovnin, A. K., Shapovalov, I. S., Kostyuchenko, M. V., Shamsutdinov, M. F., Georgiev, P. G., and Melnikova, L. S. (2014). Chromator protein directly interacts with the common part of the Drosophila melanogaster Mod(mdg4) family proteins. Dokl Biochem Biophys *454*, 21-24.

Golovnin, A., Volkov, I., and Georgiev, P. (2012). SUMO conjugation is required for the assembly of Drosophila Su(Hw) and Mod(mdg4) into insulator bodies that facilitate insulator complex formation. J Cell Sci *125*, 2064-2074.

Gómez-Díaz, Elena, and Corces, Victor G. (2014). Architectural proteins: regulators of 3D genome organization in cell fate. Trends in Cell Biology *24*, 703-711.

Grillo, M., Furriols, M., Casanova, J., and Luschnig, S. (2011). Control of germline torso expression by the BTB/POZ domain protein pipsqueak is required for embryonic terminal patterning in Drosophila. Genetics *187*, 513-521.

Gupta, G. P., and Massague, J. (2006). Cancer metastasis: building a framework. Cell *127*, 679-695.

Gurudatta, B. V., and Corces, V. G. (2009). Chromatin insulators: lessons from the fly. Brief Funct Genomic Proteomic *8*, 276-282.

Gutierrez-Avino, F. J., Ferres-Marco, D., and Dominguez, M. (2009). The position and function of the Notch-mediated eye growth organizer: the roles of JAK/STAT and four-jointed. EMBO Rep *10*, 1051-1058.

Hagstrom, K., Muller, M., and Schedl, P. (1997). A Polycomb and GAGA dependent silencer adjoins the Fab-7 boundary in the Drosophila bithorax complex. Genetics *146*, 1365-1380.

Hammond, S. M. (2006). RNAi, microRNAs, and human disease. Cancer Chemother Pharmacol *58 Suppl 1*, s63-68.

Hanahan, D., and Weinberg, R. A. (2011). Hallmarks of cancer: the next generation. Cell *144*, 646-674.

Hansen, T. B., Jensen, T. I., Clausen, B. H., Bramsen, J. B., Finsen, B., Damgaard, C. K., and Kjems, J. (2013). Natural RNA circles function as efficient microRNA sponges. Nature *495*, 384-388.

Hartman, T. R., Zinshteyn, D., Schofield, H. K., Nicolas, E., Okada, A., and O'reilly, A. M. (2010). Drosophila Boi limits Hedgehog levels to suppress follicle stem cell proliferation. J Cell Biol *191*, 943-952.

Hatfield, S. D., Shcherbata, H. R., Fischer, K. A., Nakahara, K., Carthew, R. W., and Ruohola-Baker, H. (2005). Stem cell division is regulated by the microRNA pathway. Nature *435*, 974-978.

Hayashita, Y., Osada, H., Tatematsu, Y., Yamada, H., Yanagisawa, K., Tomida, S., Yatabe, Y., Kawahara, K., Sekido, Y., and Takahashi, T. (2005). A polycistronic microRNA cluster, miR-17-92, is overexpressed in human lung cancers and enhances cell proliferation. Cancer Res *65*, 9628-9632.

He, L., and Hannon, G. J. (2004). MicroRNAs: small RNAs with a big role in gene regulation. Nat Rev Genet *5*, 522-531.

Heberlein, U., Borod, E. R., and Chanut, F. A. (1998). Dorsoventral patterning in the Drosophila retina by wingless. Development *125*, 567-577.

Heberlein, U., Singh, C. M., Luk, A. Y., and Donohoe, T. J. (1995). Growth and differentiation in the Drosophila eye coordinated by hedgehog. Nature *373*, 709-711.

Heberlein, U., Wolff, T., and Rubin, G. M. (1993). The TGF beta homolog dpp and the segment polarity gene hedgehog are required for propagation of a morphogenetic wave in the Drosophila retina. Cell *75*, 913-926.

Heger, Peter, George, Rebecca, and Wiehe, Thomas (2013). Successive Gain of Insulator Proteins in Arthropod Evolution. Evolution; International Journal of Organic Evolution *67*, 2945-2956.

Heintzman, N. D., Hon, G. C., Hawkins, R. D., Kheradpour, P., Stark, A., Harp, L. F., Ye, Z., Lee, L. K., Stuart, R. K., Ching, C. W., Ching, K. A., Antosiewicz-Bourget, J. E., Liu, H., Zhang, X., Green, R. D., Lobanenkov, V. V., Stewart, R., Thomson, J. A., Crawford, G. E., Kellis, M., and Ren, B. (2009). Histone modifications at human enhancers reflect global cell-type-specific gene expression. Nature *459*, 108-112.

Heintzman, N. D., and Ren, B. (2009). Finding distal regulatory elements in the human genome. Curr Opin Genet Dev *19*, 541-549.

Heintzman, N. D., Stuart, R. K., Hon, G., Fu, Y., Ching, C. W., Hawkins, R. D., Barrera, L. O., Van Calcar, S., Qu, C., Ching, K. A., Wang, W., Weng, Z., Green, R. D., Crawford, G. E., and Ren, B. (2007). Distinct and predictive chromatin signatures of transcriptional promoters and enhancers in the human genome. Nat Genet *39*, 311-318.

Hendrix, D. A., Hong, J. W., Zeitlinger, J., Rokhsar, D. S., and Levine, M. S. (2008). Promoter elements associated with RNA Pol II stalling in the Drosophila embryo. Proc Natl Acad Sci U S A *105*, 7762-7767.

Herranz, H., Weng, R., and Cohen, S. M. (2014). Crosstalk between epithelial and mesenchymal tissues in tumorigenesis and imaginal disc development. Curr Biol *24*, 1476-1484.

Herz, H. M., Madden, L. D., Chen, Z., Bolduc, C., Buff, E., Gupta, R., Davuluri, R., Shilatifard, A., Hariharan, I. K., and Bergmann, A. (2010). The H3K27me3 demethylase dUTX is a suppressor of Notch- and Rb-dependent tumors in Drosophila. Mol Cell Biol *30*, 2485-2497.

Hodgson, J. W., Argiropoulos, B., and Brock, H. W. (2001). Site-specific recognition of a 70-base-pair element containing d(GA)(n) repeats mediates bithoraxoid polycomb group response element-dependent silencing. Mol Cell Biol *21*, 4528-4543.

Horard, B., Tatout, C., Poux, S., and Pirrotta, V. (2000). Structure of a polycomb response element and in vitro binding of polycomb group complexes containing GAGA factor. Mol Cell Biol *20*, 3187-3197.

Hori, K., Sen, A., and Artavanis-Tsakonas, S. (2013). Notch signaling at a glance. J Cell Sci *126*, 2135-2140.

Horowitz, H., and Berg, C. A. (1995). Aberrant splicing and transcription termination caused by P element insertion into the intron of a Drosophila gene. Genetics *139*, 327-335.

Horowitz, H., and Berg, C. A. (1996). The Drosophila pipsqueak gene encodes a nuclear BTB-domain-containing protein required early in oogenesis. Development *122*, 1859-1871.

Houbaviy, H. B., Murray, M. F., and Sharp, P. A. (2003). Embryonic stem cell-specific MicroRNAs. Dev Cell *5*, 351-358.

Huang, D. H., and Chang, Y. L. (2004). Isolation and characterization of CHRASCH, a polycomb-containing silencing complex. Methods Enzymol *377*, 267-282.

Huang, D. H., Chang, Y. L., Yang, C. C., Pan, I. C., and King, B. (2002). pipsqueak encodes a factor essential for sequence-specific targeting of a polycomb group protein complex. Mol Cell Biol *22*, 6261-6271.

Huang, Y. C., Smith, L., Poulton, J., and Deng, W. M. (2013). The microRNA miR-7 regulates Tramtrack69 in a developmental switch in Drosophila follicle cells. Development *140*, 897-905.

Hui, C. C., and Joyner, A. L. (1993). A mouse model of greig cephalopolysyndactyly syndrome: the extra-toesJ mutation contains an intragenic deletion of the Gli3 gene. Nat Genet *3*, 241-246.

Hurlbut, G. D., Kankel, M. W., Lake, R. J., and Artavanis-Tsakonas, S. (2007). Crossing paths with Notch in the hyper-network. Curr Opin Cell Biol *19*, 166-175.

Ingham, P. W. (2012). Hedgehog signaling. Cold Spring Harb Perspect Biol *4*.

Iorio, M. V., Visone, R., Di Leva, G., Donati, V., Petrocca, F., Casalini, P., Taccioli, C., Volinia, S., Liu, C. G., Alder, H., Calin, G. A., Menard, S., and Croce, C. M. (2007). MicroRNA signatures in human ovarian cancer. Cancer Res *67*, 8699-8707.

Irvine, K. D., and Rauskolb, C. (2001). Boundaries in development: formation and function. Annu Rev Cell Dev Biol *17*, 189-214.

Ito, H., Fujitani, K., Usui, K., Shimizu-Nishikawa, K., Tanaka, S., and Yamamoto, D. (1996). Sexual orientation in Drosophila is altered by the satori mutation in the sex-determination gene fruitless that encodes a zinc finger protein with a BTB domain. Proc Natl Acad Sci U S A *93*, 9687-9692.

Ivaldi, M. S., Karam, C. S., and Corces, V. G. (2007). Phosphorylation of histone H3 at Ser10 facilitates RNA polymerase II release from promoter-proximal pausing in Drosophila. Genes Dev *21*, 2818-2831.

Izzi, L., Levesque, M., Morin, S., Laniel, D., Wilkes, B. C., Mille, F., Krauss, R. S., Mcmahon, A. P., Allen, B. L., and Charron, F. (2011). Boc and Gas1 each form distinct Shh receptor complexes with Ptch1 and are required for Shh-mediated cell proliferation. Dev Cell *20*, 788-801.

Janiszewska, M., and Polyak, K. (2015). Clonal evolution in cancer: a tale of twisted twines. Cell Stem Cell *16*, 11-12.

Janknecht, R., Sander, C., and Pongs, O. (1991). (HX)n repeats: a pH-controlled protein-protein interaction motif of eukaryotic transcription factors? FEBS Lett *295*, 1-2.

Januschke, J., and Gonzalez, C. (2008). Drosophila asymmetric division, polarity and cancer. Oncogene *27*, 6994-7002.

Jiang, L., Liu, X., Chen, Z., Jin, Y., Heidbreder, C. E., Kolokythas, A., Wang, A., Dai, Y., and Zhou, X. (2010). MicroRNA-7 targets IGF1R (insulin-like growth factor 1 receptor) in tongue squamous cell carcinoma cells. Biochem J *432*, 199-205.

Jin, Y., Wang, Y., Walker, D. L., Dong, H., Conley, C., Johansen, J., and Johansen, K. M. (1999). JIL-1: a novel chromosomal tandem kinase implicated in transcriptional regulation in Drosophila. Mol Cell *4*, 129-135.

Johnson, D. S., Mortazavi, A., Myers, R. M., and Wold, B. (2007). Genome-wide mapping of in vivo protein-DNA interactions. Science *316*, 1497-1502.

Johnson, S. M., Grosshans, H., Shingara, J., Byrom, M., Jarvis, R., Cheng, A., Labourier, E., Reinert, K. L., Brown, D., and Slack, F. J. (2005). RAS is regulated by the let-7 microRNA family. Cell *120*, 635-647.

Jones, S., Zhang, X., Parsons, D. W., Lin, J. C., Leary, R. J., Angenendt, P., Mankoo, P., Carter, H., Kamiyama, H., Jimeno, A., Hong, S. M., Fu, B., Lin, M. T., Calhoun, E. S., Kamiyama, M., Walter, K., Nikolskaya, T., Nikolsky, Y., Hartigan, J., Smith, D. R., Hidalgo, M., Leach, S. D., Klein, A. P., Jaffee, E. M., Goggins, M., Maitra, A., Iacobuzio-Donahue, C., Eshleman, J. R., Kern, S. E., Hruban, R. H., Karchin, R., Papadopoulos, N., Parmigiani, G., Vogelstein, B., Velculescu, V. E., and Kinzler, K. W. (2008). Core signaling pathways in human pancreatic cancers revealed by global genomic analyses. Science *321*, 1801-1806.

Joost, S., Almada, L. L., Rohnalter, V., Holz, P. S., Vrabel, A. M., Fernandez-Barrena, M. G., Mcwilliams, R. R., Krause, M., Fernandez-Zapico, M. E., and Lauth, M. (2012). GLI1 inhibition promotes epithelial-to-mesenchymal transition in pancreatic cancer cells. Cancer Res *72*, 88-99.

Jun, S., Wallen, R. V., Goriely, A., Kalionis, B., and Desplan, C. (1998). Lune/eye gone, a Pax-like protein, uses a partial paired domain and a homeodomain for DNA recognition. Proc Natl Acad Sci U S A *95*, 13720-13725.

Jung, C., Mittler, G., Oswald, F., and Borggrefe, T. (2013). RNA helicase Ddx5 and the noncoding RNA SRA act as coactivators in the Notch signaling pathway. Biochim Biophys Acta *1833*, 1180-1189.

Jung, H. R., Pasini, D., Helin, K., and Jensen, O. N. (2010). Quantitative mass spectrometry of histones H3.2 and H3.3 in Suz12-deficient mouse embryonic stem cells reveals distinct, dynamic post-translational modifications at Lys-27 and Lys-36. Mol Cell Proteomics *9*, 838-850.

Junn, E., Lee, K. W., Jeong, B. S., Chan, T. W., Im, J. Y., and Mouradian, M. M. (2009). Repression of alpha-synuclein expression and toxicity by microRNA-7. Proc Natl Acad Sci U S A *106*, 13052-13057.

Kang, J. S., Feinleib, J. L., Knox, S., Ketteringham, M. A., and Krauss, R. S. (2003). Promyogenic members of the Ig and cadherin families associate to positively regulate differentiation. Proc Natl Acad Sci U S A *100*, 3989-3994.

Kang, J. S., Gao, M., Feinleib, J. L., Cotter, P. D., Guadagno, S. N., and Krauss, R. S. (1997). CDO: an oncogene-, serum-, and anchorage-regulated member of the Ig/fibronectin type III repeat family. J Cell Biol *138*, 203-213.

Kang, J. S., Mulieri, P. J., Hu, Y., Taliana, L., and Krauss, R. S. (2002). BOC, an Ig superfamily member, associates with CDO to positively regulate myogenic differentiation. EMBO J *21*, 114-124.

Karanu, F. N., Murdoch, B., Gallacher, L., Wu, D. M., Koremoto, M., Sakano, S., and Bhatia, M. (2000). The notch ligand jagged-1 represents a novel growth factor of human hematopoietic stem cells. J Exp Med *192*, 1365-1372.

Karlin, S., and Burge, C. (1996). Trinucleotide repeats and long homopeptides in genes and proteins associated with nervous system disease and development. Proc Natl Acad Sci U S A *93*, 1560-1565.

Kasinathan, S., Orsi, G. A., Zentner, G. E., Ahmad, K., and Henikoff, S. (2014). High-resolution mapping of transcription factor binding sites on native chromatin. Nat Methods *11*, 203-209.

Kassis, J. A., and Brown, J. L. (2013). Polycomb group response elements in Drosophila and vertebrates. Adv Genet *81*, 83-118.

Katokhin, A. V., Pindiurin, A. V., Fedorova, E. V., and Baricheva, E. M. (2001). [Molecular genetic analysis of Thrithorax-like gene encoded transcriptional factor GAGA in Drosophila melanogaster]. Genetika *37*, 467-474.

Kavran, J. M., Ward, M. D., Oladosu, O. O., Mulepati, S., and Leahy, D. J. (2010). All mammalian Hedgehog proteins interact with cell adhesion molecule, down-regulated by oncogenes (CDO) and brother of CDO (BOC) in a conserved manner. J Biol Chem *285*, 24584-24590.

Kefas, B., Godlewski, J., Comeau, L., Li, Y., Abounader, R., Hawkinson, M., Lee, J., Fine, H., Chiocca, E. A., Lawler, S., and Purow, B. (2008). microRNA-7 inhibits the epidermal growth factor receptor and the Akt pathway and is down-regulated in glioblastoma. Cancer Res *68*, 3566-3572.

Kellner, W. A., Ramos, E., Van Bortle, K., Takenaka, N., and Corces, V. G. (2012). Genome-wide phosphoacetylation of histone H3 at Drosophila enhancers and promoters. Genome Res *22*, 1081-1088.

Kent, O. A., and Mendell, J. T. (2006). A small piece in the cancer puzzle: microRNAs as tumor suppressors and oncogenes. Oncogene *25*, 6188-6196.

Kerrigan, L. A., Croston, G. E., Lira, L. M., and Kadonaga, J. T. (1991). Sequence-specific transcriptional antirepression of the Drosophila Kruppel gene by the GAGA factor. J Biol Chem *266*, 574-582.

Kim, T. K., Hemberg, M., Gray, J. M., Costa, A. M., Bear, D. M., Wu, J., Harmin, D. A., Laptewicz, M., Barbara-Haley, K., Kuersten, S., Markenscoff-Papadimitriou, E., Kuhl, D., Bito, H., Worley, P. F., Kreiman, G., and Greenberg, M. E. (2010). Widespread transcription at neuronal activity-regulated enhancers. Nature *465*, 182-187.

King-Jones, K., and Thummel, C. S. (2005). Nuclear receptors--a perspective from Drosophila. Nat Rev Genet *6*, 311-323.

Kinzler, K. W., and Vogelstein, B. (1990). The GLI gene encodes a nuclear protein which binds specific sequences in the human genome. Mol Cell Biol *10*, 634-642.

Kirmizis, A., Bartley, S. M., and Farnham, P. J. (2003). Identification of the polycomb group protein SU(Z)12 as a potential molecular target for human cancer therapy. Mol Cancer Ther *2*, 113-121.

Kleer, C. G., Cao, Q., Varambally, S., Shen, R., Ota, I., Tomlins, S. A., Ghosh, D., Sewalt, R. G., Otte, A. P., Hayes, D. F., Sabel, M. S., Livant, D., Weiss, S. J., Rubin, M. A., and Chinnaiyan, A. M. (2003). EZH2 is a marker of aggressive breast cancer and promotes neoplastic transformation of breast epithelial cells. Proc Natl Acad Sci U S A *100*, 11606-11611.

Klymenko, T., and Muller, J. (2004). The histone methyltransferases Trithorax and Ash1 prevent transcriptional silencing by Polycomb group proteins. EMBO Rep *5*, 373-377.

Koelle, M. R., Talbot, W. S., Segraves, W. A., Bender, M. T., Cherbas, P., and Hogness, D. S. (1991). The Drosophila EcR gene encodes an ecdysone receptor, a new member of the steroid receptor superfamily. Cell *67*, 59-77.

Koonin, E. V., Senkevich, T. G., and Chernos, V. I. (1992). A family of DNA virus genes that consists of fused portions of unrelated cellular genes. Trends Biochem Sci *17*, 213-214.

Kopan, R., and Ilagan, M. X. (2009). The canonical Notch signaling pathway: unfolding the activation mechanism. Cell *137*, 216-233.

Kovall, R. A. (2008). More complicated than it looks: assembly of Notch pathway transcription complexes. Oncogene *27*, 5099-5109.

Kozlova, T., and Thummel, C. S. (2002). Spatial patterns of ecdysteroid receptor activation during the onset of Drosophila metamorphosis. Development *129*, 1739-1750.

Krek, A., Grun, D., Poy, M. N., Wolf, R., Rosenberg, L., Epstein, E. J., Macmenamin, P., Da Piedade, I., Gunsalus, K. C., Stoffel, M., and Rajewsky, N. (2005). Combinatorial microRNA target predictions. Nat Genet *37*, 495-500.

Lai, E. C., Tam, B., and Rubin, G. M. (2005). Pervasive regulation of Drosophila Notch target genes by GY-box-, Brd-box-, and K-box-class microRNAs. Genes Dev *19*, 1067-1080.

Laird, P. W. (2005). Cancer epigenetics. Hum Mol Genet *14 Spec No 1*, R65-76.

Langmead, B. (2010). Aligning short sequencing reads with Bowtie. Curr Protoc Bioinformatics *Chapter 11*, Unit 11 17.

Lanzuolo, C., and Orlando, V. (2012). Memories from the polycomb group proteins. Annu Rev Genet *46*, 561-589.

Lawrence, P. A., and Struhl, G. (1996). Morphogens, compartments, and pattern: lessons from drosophila? Cell *85*, 951-961.

Le Borgne, R., Bardin, A., and Schweisguth, F. (2005). The roles of receptor and ligand endocytosis in regulating Notch signaling. Development *132*, 1751-1762.

Lecuit, T., Brook, W. J., Ng, M., Calleja, M., Sun, H., and Cohen, S. M. (1996). Two distinct mechanisms for long-range patterning by Decapentaplegic in the Drosophila wing. Nature *381*, 387-393.

Lee, C., Li, X., Hechmer, A., Eisen, M., Biggin, M. D., Venters, B. J., Jiang, C., Li, J., Pugh, B. F., and Gilmour, D. S. (2008). NELF and GAGA factor are linked to promoter-proximal pausing at many genes in Drosophila. Mol Cell Biol *28*, 3290-3300.

Lee, H. J., Palkovits, M., and Young, W. S., 3rd (2006). miR-7b, a microRNA up-regulated in the hypothalamus after chronic hyperosmolar stimulation, inhibits Fos translation. Proc Natl Acad Sci U S A *103*, 15669-15674.

Lee, K. H., Lee, J. K., Choi, D. W., Do, I. G., Sohn, I., Jang, K. T., Jung, S. H., Heo, J. S., Choi, S. H., and Lee, K. T. (2015). Postoperative Prognosis Prediction of Pancreatic Cancer With Seven MicroRNAs. Pancreas.

Lee, R. C., Feinbaum, R. L., and Ambros, V. (1993). The C. elegans heterochronic gene lin-4 encodes small RNAs with antisense complementarity to lin-14. Cell *75*, 843-854.

Lehmann, M., Siegmund, T., Lintermann, K. G., and Korge, G. (1998). The pipsqueak protein of Drosophila melanogaster binds to GAGA sequences through a novel DNA-binding domain. J Biol Chem *273*, 28504-28509.

Leong, K. G., and Karsan, A. (2006). Recent insights into the role of Notch signaling in tumorigenesis. Blood *107*, 2223-2233.

Leong, K. G., Niessen, K., Kulic, I., Raouf, A., Eaves, C., Pollet, I., and Karsan, A. (2007). Jagged1-mediated Notch activation induces epithelial-to-mesenchymal transition through Slug-induced repression of E-cadherin. J Exp Med *204*, 2935-2948.

Lewis, B. P., Burge, C. B., and Bartel, D. P. (2005). Conserved seed pairing, often flanked by adenosines, indicates that thousands of human genes are microRNA targets. Cell *120*, 15-20.

Li, H. B., Ohno, K., Gui, H., and Pirrotta, V. (2013). Insulators target active genes to transcription factories and polycomb-repressed genes to polycomb bodies. PLoS Genet *9*, e1003436.

Li, L., Lyu, X., Hou, C., Takenaka, N., Nguyen, H. Q., Ong, C. T., Cubenas-Potts, C., Hu, M., Lei, E. P., Bosco, G., Qin, Z. S., and Corces, V. G. (2015). Widespread rearrangement of 3D chromatin organization underlies polycomb-mediated stress-induced silencing. Mol Cell *58*, 216-231.

Li, X., and Carthew, R. W. (2005). A microRNA mediates EGF receptor signaling and promotes photoreceptor differentiation in the Drosophila eye. Cell *123*, 1267-1277.

Li, X., Cassidy, J. J., Reinke, C. A., Fischboeck, S., and Carthew, R. W. (2009). A microRNA imparts robustness against environmental fluctuation during development. Cell *137*, 273-282.

Lieber, T., Kidd, S., and Young, M. W. (2002). kuzbanian-mediated cleavage of Drosophila Notch. Genes Dev *16*, 209-221.

Liefke, R., Oswald, F., Alvarado, C., Ferres-Marco, D., Mittler, G., Rodriguez, P., Dominguez, M., and Borggrefe, T. (2010). Histone demethylase KDM5A is an integral part of the core Notch-RBP-J repressor complex. Genes Dev *24*, 590-601.

Lohe, A. R., Hilliker, A. J., and Roberts, P. A. (1993). Mapping simple repeated DNA sequences in heterochromatin of Drosophila melanogaster. Genetics *134*, 1149-1174.

Lopez-Ornelas, A., Mejia-Castillo, T., Vergara, P., and Segovia, J. (2011). Lentiviral transfer of an inducible transgene expressing a soluble form of Gas1 causes glioma cell arrest, apoptosis and inhibits tumor growth. Cancer Gene Ther *18*, 87-99.

Lowell, S., Jones, P., Le Roux, I., Dunne, J., and Watt, F. M. (2000). Stimulation of human epidermal differentiation by delta-notch signalling at the boundaries of stem-cell clusters. Curr Biol *10*, 491-500.

Lu, H., Zawel, L., Fisher, L., Egly, J. M., and Reinberg, D. (1992). Human general transcription factor IIH phosphorylates the C-terminal domain of RNA polymerase II. Nature *358*, 641-645.

Lupien, M., Eeckhoute, J., Meyer, C. A., Wang, Q., Zhang, Y., Li, W., Carroll, J. S., Liu, X. S., and Brown, M. (2008). FoxA1 translates epigenetic signatures into enhancer-driven lineage-specific transcription. Cell *132*, 958-970.

Ma, L., and Weinberg, R. A. (2008). Micromanagers of malignancy: role of microRNAs in regulating metastasis. Trends Genet *24*, 448-456.

Macdonald, N., Welburn, J. P., Noble, M. E., Nguyen, A., Yaffe, M. B., Clynes, D., Moggs, J. G., Orphanides, G., Thomson, S., Edmunds, J. W., Clayton, A. L., Endicott, J. A., and Mahadevan, L. C. (2005). Molecular basis for the recognition of phosphorylated and phosphoacetylated histone h3 by 14-3-3. Mol Cell *20*, 199-211.

Macdonald, P. M., Ingham, P., and Struhl, G. (1986). Isolation, structure, and expression of even-skipped: a second pair-rule gene of Drosophila containing a homeo box. Cell *47*, 721-734.

Machanick, P., and Bailey, T. L. (2011). MEME-ChIP: motif analysis of large DNA datasets. Bioinformatics *27*, 1696-1697.

Madden, K., Crowner, D., and Giniger, E. (1999). LOLA has the properties of a master regulator of axon-target interaction for SNb motor axons of Drosophila. Dev Biol *213*, 301-313.

Maeda, R. K., and Karch, F. (2006). The ABC of the BX-C: the bithorax complex explained. Development *133*, 1413-1422.

Mallin, D. R., Myung, J. S., Patton, J. S., and Geyer, P. K. (1998). Polycomb group repression is blocked by the Drosophila suppressor of Hairy-wing [su(Hw)] insulator. Genetics *148*, 331-339.

Mangelsdorf, D. J., and Evans, R. M. (1995). The RXR heterodimers and orphan receptors. Cell *83*, 841-850.

Marshall, N. F., Peng, J., Xie, Z., and Price, D. H. (1996). Control of RNA polymerase II elongation potential by a novel carboxyl-terminal domain kinase. J Biol Chem *271*, 27176-27183.

Martinez, A. M., Colomb, S., Dejardin, J., Bantignies, F., and Cavalli, G. (2006). Polycomb group-dependent Cyclin A repression in Drosophila. Genes Dev *20*, 501-513.

Matise, M. P., Epstein, D. J., Park, H. L., Platt, K. A., and Joyner, A. L. (1998). Gli2 is required for induction of floor plate and adjacent cells, but not most ventral neurons in the mouse central nervous system. Development *125*, 2759-2770.

Maurel-Zaffran, C., and Treisman, J. E. (2000). pannier acts upstream of wingless to direct dorsal eye disc development in Drosophila. Development *127*, 1007-1016.

Maziere, P., and Enright, A. J. (2007). Prediction of microRNA targets. Drug Discov Today *12*, 452-458.

Mcbrayer, Z., Ono, H., Shimell, M., Parvy, J. P., Beckstead, R. B., Warren, J. T., Thummel, C. S., Dauphin-Villemant, C., Gilbert, L. I., and O'connor, M. B. (2007). Prothoracicotropic hormone regulates developmental timing and body size in Drosophila. Dev Cell *13*, 857-871.

Mcdermott, A., Gustafsson, M., Elsam, T., Hui, C. C., Emerson, C. P., Jr., and Borycki, A. G. (2005). Gli2 and Gli3 have redundant and context-dependent function in skeletal muscle formation. Development *132*, 345-357.

Mclellan, J. S., Yao, S., Zheng, X., Geisbrecht, B. V., Ghirlando, R., Beachy, P. A., and Leahy, D. J. (2006). Structure of a heparin-dependent complex of Hedgehog and Ihog. Proc Natl Acad Sci U S A *103*, 17208-17213.

Mclellan, J. S., Zheng, X., Hauk, G., Ghirlando, R., Beachy, P. A., and Leahy, D. J. (2008). The mode of Hedgehog binding to Ihog homologues is not conserved across different phyla. Nature *455*, 979-983.

Melfi, R., Palla, F., Di Simone, P., Alessandro, C., Cali, L., Anello, L., and Spinelli, G. (2000). Functional characterization of the enhancer blocking element of the sea urchin early histone gene cluster reveals insulator properties and three essential cis-acting sequences. J Mol Biol *304*, 753-763.

Melnick, A., Carlile, G., Ahmad, K. F., Kiang, C. L., Corcoran, C., Bardwell, V., Prive, G. G., and Licht, J. D. (2002). Critical residues within the BTB domain of PLZF and Bcl-6 modulate interaction with corepressors. Mol Cell Biol *22*, 1804-1818.

Melnikova, L., Juge, F., Gruzdeva, N., Mazur, A., Cavalli, G., and Georgiev, P. (2004). Interaction between the GAGA factor and Mod(mdg4) proteins promotes insulator bypass in Drosophila. Proc Natl Acad Sci U S A *101*, 14806-14811.

Memczak, S., Jens, M., Elefsinioti, A., Torti, F., Krueger, J., Rybak, A., Maier, L., Mackowiak, S. D., Gregersen, L. H., Munschauer, M., Loewer, A., Ziebold, U., Landthaler, M., Kocks, C., Le Noble, F., and Rajewsky, N. (2013). Circular RNAs are a large class of animal RNAs with regulatory potency. Nature *495*, 333-338.

Merlo, L. M., Pepper, J. W., Reid, B. J., and Maley, C. C. (2006). Cancer as an evolutionary and ecological process. Nat Rev Cancer *6*, 924-935.

Methot, N., and Basler, K. (1999). Hedgehog controls limb development by regulating the activities of distinct transcriptional activator and repressor forms of Cubitus interruptus. Cell *96*, 819-831.

Michael, M. Z., Sm, O' Connor, Van Holst Pellekaan, N. G., Young, G. P., and James, R. J. (2003). Reduced accumulation of specific microRNAs in colorectal neoplasia. Mol Cancer Res *1*, 882-891.

Miele, L., Golde, T., and Osborne, B. (2006). Notch signaling in cancer. Curr Mol Med *6*, 905-918.

Mikkelsen, T. S., Ku, M., Jaffe, D. B., Issac, B., Lieberman, E., Giannoukos, G., Alvarez, P., Brockman, W., Kim, T. K., Koche, R. P., Lee, W., Mendenhall, E., O'donovan, A., Presser, A., Russ, C., Xie, X., Meissner, A., Wernig, M., Jaenisch, R., Nusbaum, C., Lander, E. S., and Bernstein, B. E. (2007). Genome-wide maps of chromatin state in pluripotent and lineage-committed cells. Nature *448*, 553-560.

Minoguchi, S., Taniguchi, Y., Kato, H., Okazaki, T., Strobl, L. J., Zimber-Strobl, U., Bornkamm, G. W., and Honjo, T. (1997). RBP-L, a transcription factor related to RBP-Jkappa. Mol Cell Biol *17*, 2679-2687.

Mishra, K., Chopra, V. S., Srinivasan, A., and Mishra, R. K. (2003). Trl-GAGA directly interacts with lola like and both are part of the repressive complex of Polycomb group of genes. Mech Dev *120*, 681-689.

Mishra, R. K., Mihaly, J., Barges, S., Spierer, A., Karch, F., Hagstrom, K., Schweinsberg, S. E., and Schedl, P. (2001). The iab-7 polycomb response element maps to a nucleosome-free region of chromatin and requires both GAGA and pleiohomeotic for silencing activity. Mol Cell Biol *21*, 1311-1318.

Modolell, J., Bender, W., and Meselson, M. (1983). Drosophila melanogaster mutations suppressible by the suppressor of Hairy-wing are insertions of a 7.3-kilobase mobile element. Proc Natl Acad Sci U S A *80*, 1678-1682.

Mohr, O. L. (1919). Character Changes Caused by Mutation of an Entire Region of a Chromosome in Drosophila. Genetics *4*, 275-282.

Morata, G., and Lawrence, P. A. (1975). Control of compartment development by the engrailed gene in Drosophila. Nature *255*, 614-617.

Mousavi, K., Zare, H., Wang, A. H., and Sartorelli, V. (2012). Polycomb protein Ezh1 promotes RNA polymerase II elongation. Mol Cell *45*, 255-262.

Mraz, M., and Pospisilova, S. (2012). MicroRNAs in chronic lymphocytic leukemia: from causality to associations and back. Expert Rev Hematol *5*, 579-581.

Mraz, M., Pospisilova, S., Malinova, K., Slapak, I., and Mayer, J. (2009). MicroRNAs in chronic lymphocytic leukemia pathogenesis and disease subtypes. Leuk Lymphoma *50*, 506-509.

Muller, J., and Kassis, J. A. (2006). Polycomb response elements and targeting of Polycomb group proteins in Drosophila. Curr Opin Genet Dev *16*, 476-484.

Mumm, J. S., and Kopan, R. (2000). Notch signaling: from the outside in. Dev Biol *228*, 151-165.

Muravyova, E., Golovnin, A., Gracheva, E., Parshikov, A., Belenkaya, T., Pirrotta, V., and Georgiev, P. (2001). Loss of insulator activity by paired Su(Hw) chromatin insulators. Science *291*, 495-498.

Nechaev, S., and Adelman, K. (2011). Pol II waiting in the starting gates: Regulating the transition from transcription initiation into productive elongation. Biochim Biophys Acta *1809*, 34-45.

Negre, N., Brown, C. D., Ma, L., Bristow, C. A., Miller, S. W., Wagner, U., Kheradpour, P., Eaton, M. L., Loriaux, P., Sealfon, R., Li, Z., Ishii, H., Spokony, R. F., Chen, J., Hwang, L., Cheng, C., Auburn, R. P., Davis, M. B., Domanus, M., Shah, P. K., Morrison, C. A., Zieba, J., Suchy, S., Senderowicz, L., Victorsen, A., Bild, N. A., Grundstad, A. J., Hanley, D., Macalpine, D. M., Mannervik, M., Venken, K., Bellen, H., White, R., Gerstein, M., Russell, S., Grossman, R. L., Ren, B., Posakony, J. W., Kellis, M., and White, K. P. (2011). A cis-regulatory map of the Drosophila genome. Nature *471*, 527-531.

Nellen, D., Burke, R., Struhl, G., and Basler, K. (1996). Direct and long-range action of a DPP morphogen gradient. Cell *85*, 357-368.

Neumann, C. J., and Cohen, S. M. (1996). A hierarchy of cross-regulation involving Notch, wingless, vestigial and cut organizes the dorsal/ventral axis of the Drosophila wing. Development *122*, 3477-3485.

Nguyen, D. X., Bos, P. D., and Massague, J. (2009). Metastasis: from dissemination to organ-specific colonization. Nat Rev Cancer 9, 274-284.

Nguyen, H. T., Dalmasso, G., Yan, Y., Laroui, H., Dahan, S., Mayer, L., Sitaraman, S. V., and Merlin, D. (2010). MicroRNA-7 modulates CD98 expression during intestinal epithelial cell differentiation. J Biol Chem 285, 1479-1489.

Ni, J. Q., Zhou, R., Czech, B., Liu, L. P., Holderbaum, L., Yang-Zhou, D., Shim, H. S., Tao, R., Handler, D., Karpowicz, P., Binari, R., Booker, M., Brennecke, J., Perkins, L. A., Hannon, G. J., and Perrimon, N. (2011). A genome-scale shRNA resource for transgenic RNAi in Drosophila. Nat Methods 8, 405-407.

Nora, E. P., Lajoie, B. R., Schulz, E. G., Giorgetti, L., Okamoto, I., Servant, N., Piolot, T., Van Berkum, N. L., Meisig, J., Sedat, J., Gribnau, J., Barillot, E., Bluthgen, N., Dekker, J., and Heard, E. (2012). Spatial partitioning of the regulatory landscape of the X-inactivation centre. Nature 485, 381-385.

Nowak, S. J., and Corces, V. G. (2000). Phosphorylation of histone H3 correlates with transcriptionally active loci. Genes Dev 14, 3003-3013.

Ntziachristos, P., Tsirigos, A., Van Vlierberghe, P., Nedjic, J., Trimarchi, T., Flaherty, M. S., Ferres-Marco, D., Da Ros, V., Tang, Z., Siegle, J., Asp, P., Hadler, M., Rigo, I., De Keersmaecker, K., Patel, J., Huynh, T., Utro, F., Poglio, S., Samon, J. B., Paietta, E., Racevskis, J., Rowe, J. M., Rabadan, R., Levine, R. L., Brown, S., Pflumio, F., Dominguez, M., Ferrando, A., and Aifantis, I. (2012). Genetic inactivation of the polycomb repressive complex 2 in T cell acute lymphoblastic leukemia. Nat Med 18, 298-301.

Nusslein-Volhard, C., and Wieschaus, E. (1980). Mutations affecting segment number and polarity in Drosophila. Nature 287, 795-801.

O'donnell, K. H., and Wensink, P. C. (1994). GAGA factor and TBF1 bind DNA elements that direct ubiquitous transcription of the Drosophila alpha 1-tubulin gene. Nucleic Acids Res 22, 4712-4718.

O'meara, M. M., and Simon, J. A. (2012). Inner workings and regulatory inputs that control Polycomb repressive complex 2. Chromosoma 121, 221-234.

Ohsako, T., Horiuchi, T., Matsuo, T., Komaya, S., and Aigaki, T. (2003). Drosophila lola encodes a family of BTB-transcription regulators with highly variable C-terminal domains containing zinc finger motifs. Gene 311, 59-69.

Ohtsuki, S., and Levine, M. (1998). GAGA mediates the enhancer blocking activity of the eve promoter in the Drosophila embryo. Genes Dev 12, 3325-3330.

Okada, A., Charron, F., Morin, S., Shin, D. S., Wong, K., Fabre, P. J., Tessier-Lavigne, M., and Mcconnell, S. K. (2006). Boc is a receptor for sonic hedgehog in the guidance of commissural axons. Nature 444, 369-373.

Oliver, D., Sheehan, B., South, H., Akbari, O., and Pai, C. Y. (2010). The chromosomal association/dissociation of the chromatin insulator protein Cp190 of Drosophila melanogaster is mediated by the BTB/POZ domain and two acidic regions. BMC Cell Biol *11*, 101.

Oswald, F., Kostezka, U., Astrahantseff, K., Bourteele, S., Dillinger, K., Zechner, U., Ludwig, L., Wilda, M., Hameister, H., Knochel, W., Liptay, S., and Schmid, R. M. (2002). SHARP is a novel component of the Notch/RBP-Jkappa signalling pathway. EMBO J *21*, 5417-5426.

Pagans, S., Ortiz-Lombardia, M., Espinas, M. L., Bernues, J., and Azorin, F. (2002). The Drosophila transcription factor tramtrack (TTK) interacts with Trithorax-like (GAGA) and represses GAGA-mediated activation. Nucleic Acids Res *30*, 4406-4413.

Pai, C. Y., Lei, E. P., Ghosh, D., and Corces, V. G. (2004). The centrosomal protein CP190 is a component of the gypsy chromatin insulator. Mol Cell *16*, 737-748.

Palomero, T., Sulis, M. L., Cortina, M., Real, P. J., Barnes, K., Ciofani, M., Caparros, E., Buteau, J., Brown, K., Perkins, S. L., Bhagat, G., Agarwal, A. M., Basso, G., Castillo, M., Nagase, S., Cordon-Cardo, C., Parsons, R., Zuniga-Pflucker, J. C., Dominguez, M., and Ferrando, A. A. (2007). Mutational loss of PTEN induces resistance to NOTCH1 inhibition in T-cell leukemia. Nat Med *13*, 1203-1210.

Pallavi, S. K., Ho, D. M., Hicks, C., Miele, L., and Artavanis-Tsakonas, S. (2012). Notch and Mef2 synergize to promote proliferation and metastasis through JNK signal activation in Drosophila. EMBO J *31*, 2895-2907.

Pan, Y., and Wang, B. (2007). A novel protein-processing domain in Gli2 and Gli3 differentially blocks complete protein degradation by the proteasome. J Biol Chem *282*, 10846-10852.

Pan, Y., Wang, C., and Wang, B. (2009). Phosphorylation of Gli2 by protein kinase A is required for Gli2 processing and degradation and the Sonic Hedgehog-regulated mouse development. Dev Biol *326*, 177-189.

Panin, V. M., Papayannopoulos, V., Wilson, R., and Irvine, K. D. (1997). Fringe modulates Notch-ligand interactions. Nature *387*, 908-912.

Papayannopoulos, V., Tomlinson, A., Panin, V. M., Rauskolb, C., and Irvine, K. D. (1998). Dorsal-ventral signaling in the Drosophila eye. Science *281*, 2031-2034.

Pappu, K. S., Chen, R., Middlebrooks, B. W., Woo, C., Heberlein, U., and Mardon, G. (2003). Mechanism of hedgehog signaling during Drosophila eye development. Development *130*, 3053-3062.

Parnell, T. J., and Geyer, P. K. (2000). Differences in insulator properties revealed by enhancer blocking assays on episomes. EMBO J *19*, 5864-5874.

Pasini, D., Bracken, A. P., Jensen, M. R., Lazzerini Denchi, E., and Helin, K. (2004). Suz12 is essential for mouse development and for EZH2 histone methyltransferase activity. EMBO J *23*, 4061-4071.

Pasini, D., Malatesta, M., Jung, H. R., Walfridsson, J., Willer, A., Olsson, L., Skotte, J., Wutz, A., Porse, B., Jensen, O. N., and Helin, K. (2010). Characterization of an antagonistic switch between histone H3 lysine 27

methylation and acetylation in the transcriptional regulation of Polycomb group target genes. Nucleic Acids Res *38*, 4958-4969.

Pasquinelli, A. E., Reinhart, B. J., Slack, F., Martindale, M. Q., Kuroda, M. I., Maller, B., Hayward, D. C., Ball, E. E., Degnan, B., Muller, P., Spring, J., Srinivasan, A., Fishman, M., Finnerty, J., Corbo, J., Levine, M., Leahy, P., Davidson, E., and Ruvkun, G. (2000). Conservation of the sequence and temporal expression of let-7 heterochronic regulatory RNA. Nature *408*, 86-89.

Pauler, F. M., Sloane, M. A., Huang, R., Regha, K., Koerner, M. V., Tamir, I., Sommer, A., Aszodi, A., Jenuwein, T., and Barlow, D. P. (2009). H3K27me3 forms BLOCs over silent genes and intergenic regions and specifies a histone banding pattern on a mouse autosomal chromosome. Genome Res *19*, 221-233.

Pek, J. W., Lim, A. K., and Kai, T. (2009). Drosophila maelstrom ensures proper germline stem cell lineage differentiation by repressing microRNA-7. Dev Cell *17*, 417-424.

Perez-Torrado, R., Yamada, D., and Defossez, P. A. (2006). Born to bind: the BTB protein-protein interaction domain. Bioessays *28*, 1194-1202.

Pignoni, F., and Zipursky, S. L. (1997). Induction of Drosophila eye development by decapentaplegic. Development *124*, 271-278.

Pirrotta, V., and Li, H. B. (2012). A view of nuclear Polycomb bodies. Curr Opin Genet Dev *22*, 101-109.

Pitsouli, C., and Delidakis, C. (2005). The interplay between DSL proteins and ubiquitin ligases in Notch signaling. Development *132*, 4041-4050.

Poux, S., Horard, B., Sigrist, C. J., and Pirrotta, V. (2002). The Drosophila trithorax protein is a coactivator required to prevent re-establishment of polycomb silencing. Development *129*, 2483-2493.

Raab, J. R., and Kamakaka, R. T. (2010). Insulators and promoters: closer than we think. Nat Rev Genet *11*, 439-446.

Raaphorst, F. M., Otte, A. P., Van Kemenade, F. J., Blokzijl, T., Fieret, E., Hamer, K. M., Satijn, D. P., and Meijer, C. J. (2001). Distinct BMI-1 and EZH2 expression patterns in thymocytes and mature T cells suggest a role for Polycomb genes in human T cell differentiation. J Immunol *166*, 5925-5934.

Rada-Iglesias, A., Bajpai, R., Swigut, T., Brugmann, S. A., Flynn, R. A., and Wysocka, J. (2011). A unique chromatin signature uncovers early developmental enhancers in humans. Nature *470*, 279-283.

Raff, J. W., Kellum, R., and Alberts, B. (1994). The Drosophila GAGA transcription factor is associated with specific regions of heterochromatin throughout the cell cycle. EMBO J *13*, 5977-5983.

Ranganathan, P., Weaver, K. L., and Capobianco, A. J. (2011). Notch signalling in solid tumours: a little bit of everything but not all the time. Nat Rev Cancer *11*, 338-351.

Rangarajan, A., Talora, C., Okuyama, R., Nicolas, M., Mammucari, C., Oh, H., Aster, J. C., Krishna, S., Metzger, D., Chambon, P., Miele, L., Aguet, M., Radtke, F., and Dotto, G. P. (2001). Notch signaling is a direct determinant of keratinocyte growth arrest and entry into differentiation. EMBO J *20*, 3427-3436.

Rath, U., Ding, Y., Deng, H., Qi, H., Bao, X., Zhang, W., Girton, J., Johansen, J., and Johansen, K. M. (2006). The chromodomain protein, Chromator, interacts with JIL-1 kinase and regulates the structure of Drosophila polytene chromosomes. J Cell Sci *119*, 2332-2341.

Rath, U., Wang, D., Ding, Y., Xu, Y. Z., Qi, H., Blacketer, M. J., Girton, J., Johansen, J., and Johansen, K. M. (2004). Chromator, a novel and essential chromodomain protein interacts directly with the putative spindle matrix protein skeletor. J Cell Biochem *93*, 1033-1047.

Ready, D. F., Hanson, T. E., and Benzer, S. (1976). Development of the Drosophila retina, a neurocrystalline lattice. Dev Biol *53*, 217-240.

Reddy, S. D., Ohshiro, K., Rayala, S. K., and Kumar, R. (2008). MicroRNA-7, a homeobox D10 target, inhibits p21-activated kinase 1 and regulates its functions. Cancer Res *68*, 8195-8200.

Reinhart, B. J., Slack, F. J., Basson, M., Pasquinelli, A. E., Bettinger, J. C., Rougvie, A. E., Horvitz, H. R., and Ruvkun, G. (2000). The 21-nucleotide let-7 RNA regulates developmental timing in Caenorhabditis elegans. Nature *403*, 901-906.

Rewitz, K. F., Yamanaka, N., Gilbert, L. I., and O'connor, M. B. (2009). The insect neuropeptide PTTH activates receptor tyrosine kinase torso to initiate metamorphosis. Science *326*, 1403-1405.

Richards, G. (1981). INSECT HORMONES IN DEVELOPMENT. Biological Reviews *56*, 501-549.

Richards, G. (1981). The radioimmune assay of ecdysteroid titres in Drosophila melanogaster. Mol Cell Endocrinol *21*, 181-197.

Richly, H., Aloia, L., and Di Croce, L. (2011). Roles of the Polycomb group proteins in stem cells and cancer. Cell Death Dis *2*, e204.

Richly, H., Lange, M., Simboeck, E., and Di Croce, L. (2010). Setting and resetting of epigenetic marks in malignant transformation and development. Bioessays *32*, 669-679.

Richter, C., Oktaba, K., Steinmann, J., Muller, J., and Knoblich, J. A. (2011). The tumour suppressor L(3)mbt inhibits neuroepithelial proliferation and acts on insulator elements. Nat Cell Biol *13*, 1029-1039.

Riddiford, L. M. (1993). Hormone receptors and the regulation of insect metamorphosis. Receptor *3*, 203-209.

Riddiford, L. M., Cherbas, P., and Truman, J. W. (2000). Ecdysone receptors and their biological actions. Vitam Horm *60*, 1-73.

Ringrose, L. (2006). Polycomb, trithorax and the decision to differentiate. Bioessays *28*, 330-334.

Ringrose, L., and Paro, R. (2004). Epigenetic regulation of cellular memory by the Polycomb and Trithorax group proteins. Annu Rev Genet *38*, 413-443.

Robertson, G., Hirst, M., Bainbridge, M., Bilenky, M., Zhao, Y., Zeng, T., Euskirchen, G., Bernier, B., Varhol, R., Delaney, A., Thiessen, N., Griffith, O. L., He, A., Marra, M., Snyder, M., and Jones, S. (2007). Genome-wide profiles of STAT1 DNA association using chromatin immunoprecipitation and massively parallel sequencing. Nat Methods *4*, 651-657.

Rodriguez, I., and Basler, K. (1997). Control of compartmental affinity boundaries by hedgehog. Nature *389*, 614-618.

Rorth, P. (1996). A modular misexpression screen in Drosophila detecting tissue-specific phenotypes. Proc Natl Acad Sci U S A *93*, 12418-12422.

Ryner, L. C., Goodwin, S. F., Castrillon, D. H., Anand, A., Villella, A., Baker, B. S., Hall, J. C., Taylor, B. J., and Wasserman, S. A. (1996). Control of male sexual behavior and sexual orientation in Drosophila by the fruitless gene. Cell *87*, 1079-1089.

Saldanha, A. J. (2004). Java Treeview--extensible visualization of microarray data. Bioinformatics *20*, 3246-3248.

Salvany, L., Requena, D., and Azpiazu, N. (2012). Functional association between eyegone and HP1a mediates wingless transcriptional repression during development. Mol Cell Biol *32*, 2407-2415.

Santagata, S., Demichelis, F., Riva, A., Varambally, S., Hofer, M. D., Kutok, J. L., Kim, R., Tang, J., Montie, J. E., Chinnaiyan, A. M., Rubin, M. A., and Aster, J. C. (2004). JAGGED1 expression is associated with prostate cancer metastasis and recurrence. Cancer Res *64*, 6854-6857.

Sanyal, A., Lajoie, B. R., Jain, G., and Dekker, J. (2012). The long-range interaction landscape of gene promoters. Nature *489*, 109-113.

Sasaki, H., Hui, C., Nakafuku, M., and Kondoh, H. (1997). A binding site for Gli proteins is essential for HNF-3beta floor plate enhancer activity in transgenics and can respond to Shh in vitro. Development *124*, 1313-1322.

Schmitges, F. W., Prusty, A. B., Faty, M., Stutzer, A., Lingaraju, G. M., Aiwazian, J., Sack, R., Hess, D., Li, L., Zhou, S., Bunker, R. D., Wirth, U., Bouwmeester, T., Bauer, A., Ly-Hartig, N., Zhao, K., Chan, H., Gu, J., Gut, H., Fischle, W., Muller, J., and Thoma, N. H. (2011). Histone methylation by PRC2 is inhibited by active chromatin marks. Mol Cell *42*, 330-341.

Schnepp, B., Grumbling, G., Donaldson, T., and Simcox, A. (1996). Vein is a novel component in the Drosophila epidermal growth factor receptor pathway with similarity to the neuregulins. Genes Dev *10*, 2302-2313.

Schnetz, M. P., Handoko, L., Akhtar-Zaidi, B., Bartels, C. F., Pereira, C. F., Fisher, A. G., Adams, D. J., Flicek, P., Crawford, G. E., Laframboise, T., Tesar, P., Wei, C. L., and Scacheri, P. C. (2010). CHD7 targets active gene enhancer elements to modulate ES cell-specific gene expression. PLoS Genet 6, e1001023.

Schoborg, T., and Labrador, M. (2014). Expanding the roles of chromatin insulators in nuclear architecture, chromatin organization and genome function. Cell Mol Life Sci *71*, 4089-4113.

Schuettengruber, B., and Cavalli, G. (2013). Polycomb domain formation depends on short and long distance regulatory cues. PLoS One *8*, e56531.

Schuettengruber, Bernd, Martinez, Anne-Marie, Iovino, Nicola, and Cavalli, Giacomo (2011). Trithorax group proteins: switching genes on and keeping them active. Nat Rev Mol Cell Biol *12*, 799-814.

Schumacher, A., and Magnuson, T. (1997). Murine Polycomb- and trithorax-group genes regulate homeotic pathways and beyond. Trends Genet *13*, 167-170.

Schwartz, Y. B., Linder-Basso, D., Kharchenko, P. V., Tolstorukov, M. Y., Kim, M., Li, H. B., Gorchakov, A. A., Minoda, A., Shanower, G., Alekseyenko, A. A., Riddle, N. C., Jung, Y. L., Gu, T., Plachetka, A., Elgin, S. C., Kuroda, M. I., Park, P. J., Savitsky, M., Karpen, G. H., and Pirrotta, V. (2012). Nature and function of insulator protein binding sites in the Drosophila genome. Genome Res *22*, 2188-2198.

Schwartz, Y. B., and Pirrotta, V. (2007). Polycomb silencing mechanisms and the management of genomic programmes. Nat Rev Genet *8*, 9-22.

Schweinsberg, S., Hagstrom, K., Gohl, D., Schedl, P., Kumar, R. P., Mishra, R., and Karch, F. (2004). The enhancer-blocking activity of the Fab-7 boundary from the Drosophila bithorax complex requires GAGA-factor-binding sites. Genetics *168*, 1371-1384.

Schwendemann, A., and Lehmann, M. (2002). Pipsqueak and GAGA factor act in concert as partners at homeotic and many other loci. Proc Natl Acad Sci U S A 99, 12883-12888.

Segraves, W. A., and Hogness, D. S. (1990). The E75 ecdysone-inducible gene responsible for the 75B early puff in Drosophila encodes two new members of the steroid receptor superfamily. Genes Dev *4*, 204-219.

Serizawa, H., Makela, T. P., Conaway, J. W., Conaway, R. C., Weinberg, R. A., and Young, R. A. (1995). Association of Cdk-activating kinase subunits with transcription factor TFIIH. Nature *374*, 280-282.

Sexton, T., Yaffe, E., Kenigsberg, E., Bantignies, F., Leblanc, B., Hoichman, M., Parrinello, H., Tanay, A., and Cavalli, G. (2012). Three-dimensional folding and functional organization principles of the Drosophila genome. Cell *148*, 458-472.

Shellenbarger, D. L., and Mohler, J. D. (1978). Temperature-sensitive periods and autonomy of pleiotropic effects of l(1)Nts1, a conditional notch lethal in Drosophila. Dev Biol 62, 432-446.

Siegel, V., Jongens, T. A., Jan, L. Y., and Jan, Y. N. (1993). pipsqueak, an early acting member of the posterior group of genes, affects vasa level and germ cell-somatic cell interaction in the developing egg chamber. Development *119*, 1187-1202.

Sigrist, C. J., and Pirrotta, V. (1997). Chromatin insulator elements block the silencing of a target gene by the Drosophila polycomb response element (PRE) but allow trans interactions between PREs on different chromosomes. Genetics *147*, 209-221.

Simon, J. A., and Kingston, R. E. (2013). Occupying chromatin: Polycomb mechanisms for getting to genomic targets, stopping transcriptional traffic, and staying put. Mol Cell *49*, 808-824.

Skalsky, R. L., and Cullen, B. R. (2011). Reduced expression of brain-enriched microRNAs in glioblastomas permits targeted regulation of a cell death gene. PLoS One *6*, e24248.

Smith, P. A., and Corces, V. G. (1992). The suppressor of Hairy-wing binding region is required for gypsy mutagenesis. Mol Gen Genet *233*, 65-70.

Soeller, W. C., Oh, C. E., and Kornberg, T. B. (1993). Isolation of cDNAs encoding the Drosophila GAGA transcription factor. Mol Cell Biol *13*, 7961-7970.

Soshnev, A. A., Baxley, R. M., Manak, J. R., Tan, K., and Geyer, P. K. (2013). The insulator protein Suppressor of Hairy-wing is an essential transcriptional repressor in the Drosophila ovary. Development *140*, 3613-3623.

Soshnikova, N., and Duboule, D. (2009). Epigenetic regulation of vertebrate Hox genes: a dynamic equilibrium. Epigenetics *4*, 537-540.

Stark, A., Brennecke, J., Bushati, N., Russell, R. B., and Cohen, S. M. (2005). Animal MicroRNAs confer robustness to gene expression and have a significant impact on 3'UTR evolution. Cell *123*, 1133-1146.

Stark, A., Brennecke, J., Russell, R. B., and Cohen, S. M. (2003). Identification of Drosophila MicroRNA targets. PLoS Biol *1*, E60.

Steelman, L. S., Stadelman, K. M., Chappell, W. H., Horn, S., Basecke, J., Cervello, M., Nicoletti, F., Libra, M., Stivala, F., Martelli, A. M., and Mccubrey, J. A. (2008). Akt as a therapeutic target in cancer. Expert Opin Ther Targets *12*, 1139-1165.

Steffen, P. A., and Ringrose, L. (2014). What are memories made of? How Polycomb and Trithorax proteins mediate epigenetic memory. Nat Rev Mol Cell Biol *15*, 340-356.

Stock, J. K., Giadrossi, S., Casanova, M., Brookes, E., Vidal, M., Koseki, H., Brockdorff, N., Fisher, A. G., and Pombo, A. (2007). Ring1-mediated ubiquitination of H2A restrains poised RNA polymerase II at bivalent genes in mouse ES cells. Nat Cell Biol *9*, 1428-1435.

Stott, K., Blackburn, J. M., Butler, P. J., and Perutz, M. (1995). Incorporation of glutamine repeats makes protein oligomerize: implications for neurodegenerative diseases. Proc Natl Acad Sci U S A *92*, 6509-6513.

Stratton, M. R., Campbell, P. J., and Futreal, P. A. (2009). The cancer genome. Nature *458*, 719-724.

Strigini, M., and Cohen, S. M. (1999). Formation of morphogen gradients in the Drosophila wing. Semin Cell Dev Biol *10*, 335-344.

Struhl, G., and Basler, K. (1993). Organizing activity of wingless protein in Drosophila. Cell *72*, 527-540.

Strutt, H., Cavalli, G., and Paro, R. (1997). Co-localization of Polycomb protein and GAGA factor on regulatory elements responsible for the maintenance of homeotic gene expression. EMBO J *16*, 3621-3632.

Suh, M. R., Lee, Y., Kim, J. Y., Kim, S. K., Moon, S. H., Lee, J. Y., Cha, K. Y., Chung, H. M., Yoon, H. S., Moon, S. Y., Kim, V. N., and Kim, K. S. (2004). Human embryonic stem cells express a unique set of microRNAs. Dev Biol *270*, 488-498.

Tabata, T., and Kornberg, T. B. (1994). Hedgehog is a signaling protein with a key role in patterning Drosophila imaginal discs. Cell *76*, 89-102.

Tang, C., Mei, L., Pan, L., Xiong, W., Zhu, H., Ruan, H., Zou, C., Tang, L., Iguchi, T., and Wu, X. (2015). Hedgehog signaling through GLI1 and GLI2 is required for epithelial-mesenchymal transition in human trophoblasts. Biochim Biophys Acta *1850*, 1438-1448.

Tenzen, T., Allen, B. L., Cole, F., Kang, J. S., Krauss, R. S., and Mcmahon, A. P. (2006). The cell surface membrane proteins Cdo and Boc are components and targets of the Hedgehog signaling pathway and feedback network in mice. Dev Cell *10*, 647-656.

Terradot, L., Durnell, N., Li, M., Li, M., Ory, J., Labigne, A., Legrain, P., Colland, F., and Waksman, G. (2004). Biochemical characterization of protein complexes from the Helicobacter pylori protein interaction map: strategies for complex formation and evidence for novel interactions within type IV secretion systems. Mol Cell Proteomics *3*, 809-819.

Thiery, J. P., Acloque, H., Huang, R. Y., and Nieto, M. A. (2009). Epithelial-mesenchymal transitions in development and disease. Cell *139*, 871-890.

Thummel, C. S. (1995). From embryogenesis to metamorphosis: the regulation and function of Drosophila nuclear receptor superfamily members. Cell *83*, 871-877.

Thummel, C. S. (1996). Flies on steroids--Drosophila metamorphosis and the mechanisms of steroid hormone action. Trends Genet *12*, 306-310.

Thummel, C. S. (2001). Molecular mechanisms of developmental timing in C. elegans and Drosophila. Dev Cell *1*, 453-465.

Thummel, C. S., Burtis, K. C., and Hogness, D. S. (1990). Spatial and temporal patterns of E74 transcription during Drosophila development. Cell *61*, 101-111.

Tie, F., Banerjee, R., Saiakhova, A. R., Howard, B., Monteith, K. E., Scacheri, P. C., Cosgrove, M. S., and Harte, P. J. (2014). Trithorax monomethylates histone H3K4 and interacts directly with CBP to promote H3K27 acetylation and antagonize Polycomb silencing. Development *141*, 1129-1139.

Tie, F., Banerjee, R., Stratton, C. A., Prasad-Sinha, J., Stepanik, V., Zlobin, A., Diaz, M. O., Scacheri, P. C., and Harte, P. J. (2009). CBP-mediated acetylation of histone H3 lysine 27 antagonizes Drosophila Polycomb silencing. Development *136*, 3131-3141.

Toba, G., Ohsako, T., Miyata, N., Ohtsuka, T., Seong, K. H., and Aigaki, T. (1999). The gene search system. A method for efficient detection and rapid molecular identification of genes in Drosophila melanogaster. Genetics *151*, 725-737.

Tokusumi, T., Tokusumi, Y., Hopkins, D. W., Shoue, D. A., Corona, L., and Schulz, R. A. (2011). Germ line differentiation factor Bag of Marbles is a regulator of hematopoietic progenitor maintenance during Drosophila hematopoiesis. Development *138*, 3879-3884.

Tomlinson, A. (1985). The cellular dynamics of pattern formation in the eye of Drosophila. J Embryol Exp Morphol *89*, 313-331.

Tomlinson, A., and Ready, D. F. (1987). Cell fate in the Drosophila ommatidium. Dev Biol *123*, 264-275.

Tomlinson, A., and Ready, D. F. (1987). Neuronal differentiation in Drosophila ommatidium. Dev Biol *120*, 366-376.

Triezenberg, S. J. (1995). Structure and function of transcriptional activation domains. Curr Opin Genet Dev *5*, 190-196.

Tsai, Y. C., and Sun, Y. H. (2004). Long-range effect of upd, a ligand for Jak/STAT pathway, on cell cycle in Drosophila eye development. Genesis *39*, 141-153.

Tsukiyama, T., Becker, P. B., and Wu, C. (1994). ATP-dependent nucleosome disruption at a heat-shock promoter mediated by binding of GAGA transcription factor. Nature *367*, 525-532.

Uhlmann, S., Mannsperger, H., Zhang, J. D., Horvat, E. A., Schmidt, C., Kublbeck, M., Henjes, F., Ward, A., Tschulena, U., Zweig, K., Korf, U., Wiemann, S., and Sahin, O. (2012). Global microRNA level regulation of EGFR-driven cell-cycle protein network in breast cancer. Mol Syst Biol *8*, 570.

Usui-Aoki, K., Ito, H., Ui-Tei, K., Takahashi, K., Lukacsovich, T., Awano, W., Nakata, H., Piao, Z. F., Nilsson, E. E., Tomida, J., and Yamamoto, D. (2000). Formation of the male-specific muscle in female Drosophila by ectopic fruitless expression. Nat Cell Biol *2*, 500-506.

Valk-Lingbeek, M. E., Bruggeman, S. W., and Van Lohuizen, M. (2004). Stem cells and cancer; the polycomb connection. Cell *118*, 409-418.

Vallejo, D. M., Caparros, E., and Dominguez, M. (2011). Targeting Notch signalling by the conserved miR-8/200 microRNA family in development and cancer cells. EMBO J *30*, 756-769.

Van Bortle, K., and Corces, V. G. (2012). Nuclear organization and genome function. Annu Rev Cell Dev Biol *28*, 163-187.

Van Bortle, K., and Corces, V. G. (2013). The role of chromatin insulators in nuclear architecture and genome function. Curr Opin Genet Dev *23*, 212-218.

Van Bortle, K., Nichols, M. H., Li, L., Ong, C. T., Takenaka, N., Qin, Z. S., and Corces, V. G. (2014). Insulator function and topological domain border strength scale with architectural protein occupancy. Genome Biol *15*, R82.

Van Bortle, K., Ramos, E., Takenaka, N., Yang, J., Wahi, J. E., and Corces, V. G. (2012). Drosophila CTCF tandemly aligns with other insulator proteins at the borders of H3K27me3 domains. Genome Res *22*, 2176-2187.

Van Heyningen, V., and Williamson, K. A. (2002). PAX6 in sensory development. Hum Mol Genet *11*, 1161-1167.

Varambally, S., Dhanasekaran, S. M., Zhou, M., Barrette, T. R., Kumar-Sinha, C., Sanda, M. G., Ghosh, D., Pienta, K. J., Sewalt, R. G., Otte, A. P., Rubin, M. A., and Chinnaiyan, A. M. (2002). The polycomb group protein EZH2 is involved in progression of prostate cancer. Nature *419*, 624-629.

Vasudevan, S., Tong, Y., and Steitz, J. A. (2007). Switching from repression to activation: microRNAs can up-regulate translation. Science *318*, 1931-1934.

Viatour, P., Ehmer, U., Saddic, L. A., Dorrell, C., Andersen, J. B., Lin, C., Zmoos, A. F., Mazur, P. K., Schaffer, B. E., Ostermeier, A., Vogel, H., Sylvester, K. G., Thorgeirsson, S. S., Grompe, M., and Sage, J. (2011). Notch signaling inhibits hepatocellular carcinoma following inactivation of the RB pathway. J Exp Med *208*, 1963-1976.

Vidal, M., and Cagan, R. L. (2006). Drosophila models for cancer research. Curr Opin Genet Dev *16*, 10-16.

Vogelmann, J., Le Gall, A., Dejardin, S., Allemand, F., Gamot, A., Labesse, G., Cuvier, O., Negre, N., Cohen-Gonsaud, M., Margeat, E., and Nollmann, M. (2014). Chromatin insulator factors involved in long-range DNA interactions and their role in the folding of the Drosophila genome. PLoS Genet *10*, e1004544.

Vogelstein, B., and Kinzler, K. W. (2004). Cancer genes and the pathways they control. Nat Med *10*, 789-799.

Vojtek, A. B., and Hollenberg, S. M. (1995). Ras-Raf interaction: two-hybrid analysis. Methods Enzymol *255*, 331-342.

Voorhoeve, P. M., Le Sage, C., Schrier, M., Gillis, A. J., Stoop, H., Nagel, R., Liu, Y. P., Van Duijse, J., Drost, J., Griekspoor, A., Zlotorynski, E., Yabuta, N., De Vita, G., Nojima, H., Looijenga, L. H., and Agami, R. (2007). A

genetic screen implicates miRNA-372 and miRNA-373 as oncogenes in testicular germ cell tumors. Adv Exp Med Biol *604*, 17-46.

Wang, C., Pan, Y., and Wang, B. (2010). Suppressor of fused and Spop regulate the stability, processing and function of Gli2 and Gli3 full-length activators but not their repressors. Development *137*, 2001-2009.

Wang, C., Ruther, U., and Wang, B. (2007). The Shh-independent activator function of the full-length Gli3 protein and its role in vertebrate limb digit patterning. Dev Biol *305*, 460-469.

Weber, U., Siegel, V., and Mlodzik, M. (1995). pipsqueak encodes a novel nuclear protein required downstream of seven-up for the development of photoreceptors R3 and R4. EMBO J *14*, 6247-6257.

Webster, R. J., Giles, K. M., Price, K. J., Zhang, P. M., Mattick, J. S., and Leedman, P. J. (2009). Regulation of epidermal growth factor receptor signaling in human cancer cells by microRNA-7. J Biol Chem *284*, 5731-5741.

Wei, W., and Brennan, M. D. (2000). Polarity of transcriptional enhancement revealed by an insulator element. Proc Natl Acad Sci U S A *97*, 14518-14523.

Weinberg, R. A. (1995). The retinoblastoma protein and cell cycle control. Cell *81*, 323-330.

Weng, A. P., Ferrando, A. A., Lee, W., Morris, J. P. Th, Silverman, L. B., Sanchez-Irizarry, C., Blacklow, S. C., Look, A. T., and Aster, J. C. (2004). Activating mutations of NOTCH1 in human T cell acute lymphoblastic leukemia. Science *306*, 269-271.

Wharton, K. A., Yedvobnick, B., Finnerty, V. G., and Artavanis-Tsakonas, S. (1985). opa: a novel family of transcribed repeats shared by the Notch locus and other developmentally regulated loci in D. melanogaster. Cell *40*, 55-62.

Wieschaus, E., and Gehring, W. (1976). Clonal analysis of primordial disc cells in the early embryo of Drosophila melanogaster. Dev Biol *50*, 249-263.

Wightman, B., Ha, I., and Ruvkun, G. (1993). Posttranscriptional regulation of the heterochronic gene lin-14 by lin-4 mediates temporal pattern formation in C. elegans. Cell *75*, 855-862.

Wilson, C. W., and Chuang, P. T. (2010). Mechanism and evolution of cytosolic Hedgehog signal transduction. Development *137*, 2079-2094.

Wolpert, L. (1969). Positional information and the spatial pattern of cellular differentiation. J Theor Biol *25*, 1-47.

Wood, A. M., Van Bortle, K., Ramos, E., Takenaka, N., Rohrbaugh, M., Jones, B. C., Jones, K. C., and Corces, V. G. (2011). Regulation of chromatin organization and inducible gene expression by a Drosophila insulator. Mol Cell *44*, 29-38.

Wu, J. Y., and Rao, Y. (1999). Fringe: defining borders by regulating the notch pathway. Curr Opin Neurobiol 9, 537-543.

Wu, L., and Belasco, J. G. (2008). Let me count the ways: mechanisms of gene regulation by miRNAs and siRNAs. Mol Cell 29, 1-7.

Xi, H., Shulha, H. P., Lin, J. M., Vales, T. R., Fu, Y., Bodine, D. M., Mckay, R. D., Chenoweth, J. G., Tesar, P. J., Furey, T. S., Ren, B., Weng, Z., and Crawford, G. E. (2007). Identification and characterization of cell type-specific and ubiquitous chromatin regulatory structures in the human genome. PLoS Genet 3, e136.

Xiong, S., Zheng, Y., Jiang, P., Liu, R., Liu, X., and Chu, Y. (2011). MicroRNA-7 inhibits the growth of human non-small cell lung cancer A549 cells through targeting BCL-2. Int J Biol Sci 7, 805-814.

Xu, K., Wu, Z. J., Groner, A. C., He, H. H., Cai, C., Lis, R. T., Wu, X., Stack, E. C., Loda, M., Liu, T., Xu, H., Cato, L., Thornton, J. E., Gregory, R. I., Morrissey, C., Vessella, R. L., Montironi, R., Magi-Galluzzi, C., Kantoff, P. W., Balk, S. P., Liu, X. S., and Brown, M. (2012). EZH2 oncogenic activity in castration-resistant prostate cancer cells is Polycomb-independent. Science 338, 1465-1469.

Xu, Lin, Wen, Zhenke, Zhou, Ya, Liu, Zhongmin, Li, Qinchuan, Fei, Guangru, Luo, Junmin, and Ren, Tao (2013). MicroRNA-7–regulated TLR9 signaling–enhanced growth and metastatic potential of human lung cancer cells by altering the phosphoinositide-3-kinase, regulatory subunit 3/Akt pathway. Molecular Biology of the Cell 24, 42-55.

Xu, Z., Wei, G., Chepelev, I., Zhao, K., and Felsenfeld, G. (2011). Mapping of INS promoter interactions reveals its role in long-range regulation of SYT8 transcription. Nat Struct Mol Biol 18, 372-378.

Yan, D., Wu, Y., Yang, Y., Belenkaya, T. Y., Tang, X., and Lin, X. (2010). The cell-surface proteins Dally-like and Ihog differentially regulate Hedgehog signaling strength and range during development. Development 137, 2033-2044.

Yang, J., and Weinberg, R. A. (2008). Epithelial-mesenchymal transition: at the crossroads of development and tumor metastasis. Dev Cell 14, 818-829.

Yao, C., Ding, Y., Cai, W., Wang, C., Girton, J., Johansen, K. M., and Johansen, J. (2012). The chromodomain-containing NH(2)-terminus of Chromator interacts with histone H1 and is required for correct targeting to chromatin. Chromosoma 121, 209-220.

Yao, C., Wang, C., Li, Y., Ding, Y., Rath, U., Sengupta, S., Girton, J., Johansen, K. M., and Johansen, J. (2014). The spindle matrix protein, Chromator, is a novel tubulin binding protein that can interact with both microtubules and free tubulin. PLoS One 9, e103855.

Yao, J. G., and Sun, Y. H. (2005). Eyg and Ey Pax proteins act by distinct transcriptional mechanisms in Drosophila development. EMBO J 24, 2602-2612.

Yao, S., Lum, L., and Beachy, P. (2006). The ihog cell-surface proteins bind Hedgehog and mediate pathway activation. Cell 125, 343-357.

Yao, T. P., Forman, B. M., Jiang, Z., Cherbas, L., Chen, J. D., Mckeown, M., Cherbas, P., and Evans, R. M. (1993). Functional ecdysone receptor is the product of EcR and Ultraspiracle genes. Nature *366*, 476-479.

Yilmaz, M., and Christofori, G. (2009). EMT, the cytoskeleton, and cancer cell invasion. Cancer Metastasis Rev *28*, 15-33.

Ying, M., and Chen, D. (2012). Tudor domain-containing proteins of Drosophila melanogaster. Dev Growth Differ *54*, 32-43.

Yu, J. Y., Reynolds, S. H., Hatfield, S. D., Shcherbata, H. R., Fischer, K. A., Ward, E. J., Long, D., Ding, Y., and Ruohola-Baker, H. (2009). Dicer-1-dependent Dacapo suppression acts downstream of Insulin receptor in regulating cell division of Drosophila germline stem cells. Development *136*, 1497-1507.

Yuan, W., Xu, M., Huang, C., Liu, N., Chen, S., and Zhu, B. (2011). H3K36 methylation antagonizes PRC2-mediated H3K27 methylation. J Biol Chem *286*, 7983-7989.

Yue, D., Li, H., Che, J., Zhang, Y., Tseng, H. H., Jin, J. Q., Luh, T. M., Giroux-Leprieur, E., Mo, M., Zheng, Q., Shi, H., Zhang, H., Hao, X., Wang, C., Jablons, D. M., and He, B. (2014). Hedgehog/Gli promotes epithelial-mesenchymal transition in lung squamous cell carcinomas. J Exp Clin Cancer Res *33*, 34.

Zecca, M., Basler, K., and Struhl, G. (1996). Direct and long-range action of a wingless morphogen gradient. Cell *87*, 833-844.

Zhang, N., Li, X., Wu, C. W., Dong, Y., Cai, M., Mok, M. T., Wang, H., Chen, J., Ng, S. S., Chen, M., Sung, J. J., and Yu, J. (2013). microRNA-7 is a novel inhibitor of YY1 contributing to colorectal tumorigenesis. Oncogene *32*, 5078-5088.

Zhang, W., Hong, M., Bae, G. U., Kang, J. S., and Krauss, R. S. (2011). Boc modifies the holoprosencephaly spectrum of Cdo mutant mice. Dis Model Mech *4*, 368-380.

Zheng, X., Mann, R. K., Sever, N., and Beachy, P. A. (2010). Genetic and biochemical definition of the Hedgehog receptor. Genes Dev *24*, 57-71.

Zitnan, D., Kim, Y. J., Zitnanova, I., Roller, L., and Adams, M. E. (2007). Complex steroid-peptide-receptor cascade controls insect ecdysis. Gen Comp Endocrinol *153*, 88-96.

Zollman, S., Godt, D., Prive, G. G., Couderc, J. L., and Laski, F. A. (1994). The BTB domain, found primarily in zinc finger proteins, defines an evolutionarily conserved family that includes several developmentally regulated genes in Drosophila. Proc Natl Acad Sci U S A *91*, 10717-10721.